National Library
of Canada

Acquisitions and
Bibliographic Services Branch

395 Wellington Street
Ottawa, Ontario
K1A 0N4

Bibliothèque nationale
du Canada

Direction des acquisitions et
des services bibliographiques

395, rue Wellington
Ottawa (Ontario)
K1A 0N4

Your file Votre référence

Our file Notre référence

NOTICE

The quality of this microform is heavily dependent upon the quality of the original thesis submitted for microfilming. Every effort has been made to ensure the highest quality of reproduction possible.

If pages are missing, contact the university which granted the degree.

Some pages may have indistinct print especially if the original pages were typed with a poor typewriter ribbon or if the university sent us an inferior photocopy.

AVIS

La qualité de cette microforme dépend grandement de la qualité de la thèse soumise au microfilmage. Nous avons tout fait pour assurer une qualité supérieure de reproduction.

S'il manque des pages, veuillez communiquer avec l'université qui a conféré le grade.

La qualité d'impression de certaines pages peut laisser à désirer, surtout si les pages originales ont été dactylographiées à l'aide d'un ruban usé ou si l'université nous a fait parvenir une photocopie de qualité inférieure.

Canada

MODELLING OF INDOOR AIR HUMIDITY TRANSIENT BEHAVIOUR: EFFECT ON EXTERIOR WALL MOISTURE PERFORMANCE

Ismail M. Budaiwi

A Thesis

in

The Centre

for

Building Studies

Presented in Partial Fulfilment of the Requirement
for the Degree of Doctor of Philosophy
Concordia University
Montréal, Québec, Canada

March 1994

ISBN 0-315-90821-1

Canada

ABSTRACT

MODELLING OF INDOOR AIR HUMIDITY TRANSIENT BEHAVIOUR: EFFECT ON EXTERIOR WALL MOISTURE PERFORMANCE

Ismail M. Budaiwi

Indoor air humidity is an influential parameter in determining the quality of the indoor environment, building energy consumption as well as the performance of the exterior building envelope. The main objectives of this study are to predict indoor humidity transient behaviour within buildings and to investigate its effect on exterior wall moisture performance. To achieve these objectives, the study incorporates four main developments. First, evaluation of moisture absorption and desorption by interior materials. Second, prediction of air humidity behaviour in single-zone and multi-zone enclosures. Third, theoretical description of multi-layer walls moisture response under transient boundary conditions, and their interaction with the indoor environment. Fourth, development of simulation tools and case studies for theoretical evaluation and analysis. Moisture absorption and desorption processes within buildings can have considerable impact on air humidity. A theoretical model for evaluating moisture absorption and desorption by interior materials is proposed. The model has been incorporated into single-zone and multi-zone indoor humidity evaluation models. Based on these models, computer programs were developed to theoretically study indoor humidity response to the various moisture transport processes in different enclosures. The study has revealed the importance of the involved processes and the wide variation of their influence in determining indoor humidity behaviour. In addition, results have indicated the uniqueness of individual zones air humidity behaviour and its dependence on their relative location along the building air flow path.

Wall moisture response has been modelled by a system of governing equations describing the transient simultaneous heat and moisture transfer through the wall system components.

The governing equations were numerically formulated using the implicit finite-difference scheme, and the resulting heat and mass balance equations were simultaneously solved. Based on these mathematical developments, a computer model was developed and used in conjunction with the indoor air humidity prediction model to evaluate the impact of indoor humidity behaviour on wall moisture performance. Moisture behaviour of non-cavity and cavity wall systems has been theoretically evaluated under different indoor air humidity variational patterns. Results indicate that modifications in indoor humidity behaviour imposed by the air leakage and the indoor moisture generation processes were found to be the most influential. The impact of the other moisture transport processes was found to be relatively less appreciable. The indirect relationships between the seasonal moisture accumulation and the space physical characteristics were studied through a parametric evaluation approach. The relationship between the level of moisture accumulation in the wall components and the air leakage coefficient of the exterior walls was found to be a negative decaying relationship, while it is a positive decaying relationship with the indoor moisture generation rate. Depending on the type of wall and its interaction with the indoor environment, moisture behaviour of the exterior wall can be greatly altered in response to changes in indoor air humidity. Hence, its transient behaviour has to be considered for more accurate and realistic evaluation of wall moisture performance. In addition, modifying indoor humidity behaviour can be seen as a potential measure for improving short term as well as long term moisture performance of exterior walls.

ACKNOWLEDGMENT

Praise be to God for giving me the will and the power to conduct this study.

The author wishes to express his sincere thanks and appreciation to his supervisor, Dr. Ramy El Diasty, for his support, encouragement and continuous effort through out the course of this work. The author is also very grateful to his supervisor Dr. Paul Fazio for his encouragement, help and support.

Special thanks go to my colleagues, Adel Abdou, Dr. Tarek Hegazy, Ahmed Mokhtar and Khaled El-Rayes for their participation with their thoughtful suggestions and for being faithful partners.

For their patience, sacrifice and encouragement, I would like to express my gratitude to my mother, my wife and my children to whom I dedicate this work.

TABLE OF CONTENTS

LIST OF FIGURES

LIST OF TABLES

NOMENCLATURE

A_c= condensation area, m^2

A_m= exposed material area, m^2

A_{oe}= equivalent orifice area, m^2

A_o= apparent area, m^2

A_e= evaporation surface area, m^2

A_w= area of exterior wall, m^2

Bi= Biot number, (dimensionless)

C= flow coefficient (dimensionless)

c_p= air specific heat, $J/kg\,C$

C_p= wind pressure coefficient

c_v= water vapour specific heat, $J/kg\,C$

c_l= water specific heat, $J/kg\,C$

c_{vm}= material specific heat, $J/kg\,C$

c_{vg}= glass specific heat, $J/kg\,C$

C_{VR}= vapour retarder thermal conductance, $W/m^2\,C$

C_m= material moisture capacity, $kg/m^3\,Pa$, slope of moisture equilibrium curve, kg/m^3

C_w= wall leakage coefficient, $m^3/m^2\,Pa^{65}\,s$

D_{va}= coefficient of water vapour diffusion in air, m^2/s

D_v= material vapour diffusion coefficient, $kg/m\,Pa\,s$

D_L= material liquid transport coefficient, $kg/m\,Pa\,s$

D_w= material moisture transfer coefficient, m^2/s

D_T= thermal moisture transfer coefficient, $kg/m\,s\,C$

g= gravitational constant, m/s^2

Gr= Grashof number

g_v= rate of vapour transport, $kg/m^2\,s$

g_l= rate of liquid transport, $kg/m^2\,s$

h= distance from neutral plane, m

H= wall or opening height, m

H_d= door height, m

h_{Di}= mass transfer coefficient at interior surface, $kg/m^2\,s$

h_{Do}= mass transfer coefficient at exterior surface, $kg/m^2\,s$

h_{Dc}= mass transfer coefficient at wall cavity surfaces, $kg/m^2 s$

h_i= interior surface heat transfer coefficient, $W/m^2 C$

h_o= exterior surface heat transfer coefficient, $W/m^2 C$

h_{mc}= surface mass transfer coefficient for condensation process, $kg/m^2 s$

h_{ms}= surface mass transfer coefficient for absorption/desorption processes, $kg/m^2 s$

h_{me}= surface mass transfer coefficient for evaporation process, $kg/m^2 s$

h_c= surface heat transfer coefficient, $W/m^2 C$

H_m= surface mass transfer coefficient, $kg/m^2 Pa s$

h_m= surface mass transfer coefficient (humidity ratio based), $kg/m^2 s$

h_{fg}= latent heat of vaporization, J/kg

h_{rs}= window air space radiative heat transfer coefficient, $W/m^2 C$

h_{ec}= convective heat transfer coefficient for wall cavity surface, $W/m^2 C$

h_{rc}= radiative heat transfer coefficient for wall cavity surface, $W/m^2 C$

I_{bv}= direct solar radiation on vertical surface, W/m^2

I_{dv}= diffused solar radiation on vertical surface, W/m^2

I_{rv}= reflected solar radiation on vertical surface, W/m^2

M= molar weight of water, kg/mol

M_m= amount of absorbed or desorbed moisture, kg

M_{ml}= total lost or gained moisture, kg

mg= rate of indoor moisture generation, kg/s

m_s= rate of moisture absorption at wall surface, $kg/m^2 s$

m_{sc}= mass condensation rate, $kg/m^2 s$

n= flow exponent (dimensionless), as subscript it denotes node number or number of zones

na= number of airflow processes

nc= number of condensation processes

nv= number of evaporation processes

ng= number of moisture generating processes

$ns1$= number of absorption/desorption materials which can be modelled by lumped parameter analysis

$ns2$= number of absorption/desorption materials which can not be modelled by lumped parameter analysis

Nu= Nusselt's number (dimensionless)

K= thermal conductivity, $W/m C$

K_a= air thermal conductivity, $W/m \cdot C$

K_g= glass thermal conductivity, $W/m \cdot C$

L_m= moisture interaction depth, m

L_g= glass pane thickness, m

L_c= wall cavity thickness, m

P= pressure, Pa

P_w= wind pressure, Pa

P_s= thermal induced pressure, Pa

P^e_s= effective stack pressure, Pa

P_{vs}= saturation pressure, Pa

P_{VR}= vapour retarder moisture permeance, $kg/m^2 \cdot Pa \cdot s$

P_m= vapour pressure within material, Pa

P_{mo}= initial vapour pressure within material, Pa

P_{vr}= indoor air vapour pressure, Pa

Pr= Prandtl number

P_R= room reference air pressure, Pa

R= general gas characteristic constant, $J/mol \cdot K$

R_v= water vapour characteristic constant, $J/kg \cdot K$

Q_a= air flow rate, kg/s

Q_{oi}= flow into zone i, kg/s

Q_{io}= flow out of zone i, kg/s

Q_{ic}= air flow between the cavity space and the indoor space, kg/s

Q_{oc}= air flow between the cavity space and the outdoor environment, kg/s

Q_{sp}= rate of supply air, kg/s

q_s= incident solar radiation, W/m^2

t= time, s

t_r= return air temperature, C

t_d= coil surface temperature, C

t_{co}= coil outlet temperature, C

T= temperature, C

T_k= temperature, K

T_∞= ambient air temperature, C

T_i= indoor air temperature, C

T_o= outdoor air temperature, C

T_{si}= interior surface temperature, C

T_{so}= exterior surface temperature, C

T_m= material temperature, K

V= room volume, m^3 or wind speed, m/s

V_m= material volume, m^3

V_c= wall cavity volume, m^3

W= air moisture content, kg/kg

W_∞= ambient air moisture content, kg/kg

W_d= saturation air moisture content at cooling coil dew-point temperature, kg/kg

W_s= saturation air moisture content, kg/kg

W_r= room air moisture content, kg/kg

W_m= material air moisture content, kg/kg

W_{ms}= material surface air moisture content, kg/kg

W_{ro}= initial room air moisture content, kg/kg

W_{mo}= initial material surface air moisture content, kg/kg

W_o= air moisture content outdoors or outside a given space, kg/kg

W_{sc}= saturation air moisture content at condensation surface, kg/kg

W_{se}= saturation air moisture content at the evaporation surface, kg/kg

W_{ra}= time-step average indoor air moisture content, kg/kg

W_{sp}= supply air moisture content, kg/kg

x= length, m

U= material moisture content, kg/kg

Ue= material equilibrium moisture content, kg/kg

U_{hm}= maximum hygroscopic moisture content, kg/kg

$\tau,\tau+1$= denote the start and end of any time interval

τ,η= dimensionless variables

ΔL= partition or wall thickness, m

ρ_{ao}= outdoor air density, kg/m^3

ρ_{ai}= indoor air density, kg/m^3

ρ_v= water vapour density, kg/m^3

ξ= slope of moisture equilibrium curve, *kg/kg*

α_m= material moisture diffusivity, m^2/s

ρ_m= material density, kg/m^3

ρ_g= glass density, kg/m^3

ρ_a= air density, kg/m^3

ϕ = relative humidity

CHAPTER 1

INTRODUCTION

1.1 Background

Indoor air humidity has been recognized as an important environmental parameter affecting building performance in many aspects. It can affect building functional, aesthetical, moisture, thermal comfort and energy performance. For functional reasons, indoor air humidity in some buildings is required to be maintained at a relatively high level. Although air humidity in some humidified buildings is not always maintained at the intended humidity level, there are an increasing number of buildings, such as hospitals, libraries and museums, in which the maintenance of air humidity level is highly desirable at all times and is considered as one of the required functions of the building [1]. The need to maintain air humidity at a relatively high level arises either from comfort and health requirements of the occupants, or from the fact that some interior materials and valuable items are moisture-sensitive and may be subjected to damage when exposed to low air humidity levels. When indoor humidity is not mechanically maintained, it experiences considerable fluctuations determined by the building's functional and physical characteristics as well as the outdoor climatic conditions. In buildings where air ventilation is reduced to achieve a more airtight enclosure, air humidity is expected to be very high when considerable moisture is produced within the space.

In cold climates, internal surface condensation is a likely product of high indoor humidity. Internal surface condensation occurs on cold exterior walls, cold bridges and windows.

Window construction often represents the poorest component of the building enclosure in a thermal sense, even when a double glazed window is used. Hence a glazed window is expected to have the lowest inside surface temperature. The window, therefore, determines the potential for surface condensation and the practical limit of indoor humidity if condensation is to be avoided. Condensation on interior surfaces is a source of many problems in buildings ranging from minor visual discomfort by obstructing the link between the indoor and outdoor environments, to damaging decorative finishes as well as wood and metal sashes. In addition, mould growth is a well known problem associated with the presence of condensation. Moulds are usually most severe in room corners of external uninsulated walls. This is mainly attributed to insufficient ventilation which creates pockets of stagnant air in such corners [2]. Furthermore, in winter, corners and edges tend to be the coldest surfaces of the room which raises the risk of condensation at these locations.

A far more serious product of high indoor humidity is the interstitial condensation because it is invisible and can not be realized until great damage occurs. In multi-layer wall constructions interstitial condensation normally occurs in the layer that presents an effective resistance to heat flow but permits easy movement of water vapour because with the sharp drop in temperature, the dew point can be reached causing condensation to occur. The wall cavity represents an example of such high risk locations within the wall. the consequences of this type of condensation become more serious and more frequent in a wall cavity filled with an insulating material. Interstitial condensation can result in problems of material deterioration, staining, odours and rotting of structural components. In order to reduce the risk of surface and interstitial condensation and their related problems, moisture may have to be mechanically removed from the indoor air.

Although indoor humidity is one of several environmental parameters affecting the exterior wall system moisture performance, it remains the most influential parameter. This influence can be clearly recognized through the surface condensation phenomenon on cold exterior surface, and the interstitial condensation within the exterior wall components. In cold climates, moisture performance of the exterior wall system is an important factor in determining the overall building envelope performance, and hence in determining the performance of the building as a whole. The building exterior envelope's main function is to separate the indoor environment from the outdoor environment by protecting it from direct exposure to undesirable external environmental conditions either through prevention or modification. It cannot, however, act as an absolute separator. Instead it restricts to some degree the transfer of a number of environmental constituents from one environment to another. These functions could vary from one type of climatic conditions to another, and from time to time even for the same climatic conditions. For example, in cold climates, the exterior envelope is required to allow in solar radiation while preventing indoor heat energy loss whether in the conductive, radiative or convective forms. Meanwhile, in hot climates, it is necessary to prevent any form of external heat from passing to the indoor environment while allowing indoor generated heat to escape by increasing the ventilation rate at the appropriate time. In all types of climates, the exterior building envelope is required to keep outdoor pollutants and precipitation out while maintaining a good link with the outdoor environment through windows which serve a number of functions that are intimately tied to the quality of the indoor environment.

In recent years, the desire for reduced energy consumption in buildings has resulted in a greater degree of separation between the indoor and the outdoor environments by reducing air leakage through the building envelope and increasing its thermal resistance.

In spite of the considerable savings in energy achieved by this action, it has prompted many new problems related to durability and maintenance as well as the quality of the indoor air. By separating two different environments, the building exterior envelope endures considerable thermal and moisture stresses across it, resulting from large differences in temperature and vapour pressure between the indoor and the outdoor environments. As the exterior envelope thermal resistance increases and the airflow across it is reduced, these stresses will consequently increase the prospects for premature deterioration of the envelope components, as well as excessive maintenance costs. In order to avoid such problems, it is essential to design the building envelope as a part of inter-dependent systems comprising the building in view of its particular indoor environment that it is intended to preserve.

The level of indoor humidity at any time is determined by the balance between moisture gains and losses within the space. Depending on the building type and its functional characteristics, moisture sources in buildings could include occupants and their moisture generating activities, air infiltration, mechanical ventilation, evaporation from damp materials or free water surfaces, some heating systems (i.g. kerosene heaters), and moisture desorption by interior materials. On the other hand, moisture can be lost from the space by air exfiltration, surface condensation, mechanical exhaust, and moisture absorption by interior hygroscopic materials. Moisture can also be transferred in relatively negligible amounts by diffusions through the building envelope components. Most of the moisture transport processes involved are time-dependent, therefore when indoor humidity is not mechanically controlled, it is expected to behave dynamically with its level being determined by the resulting interaction between the different moisture transport processes. In addition of being a time-dependent parameter, indoor humidity is space-dependent. In

a multi-zone space, the behaviour of air humidity in each zone could be different. The diversity of zonal air humidity behaviour depends on the characteristics of the zones as well as their inter-zonal moisture interaction. Such diversity could result in a diverse zonal moisture and energy performance.

1.2 Importance of Research Topic

1.2.1 Prediction of indoor air humidity behaviour: Indoor air humidity has considerable influence on the quality of the indoor environment and the building energy consumption. It can influence the state of occupants comfort as well as their health. High humidity could affect the quality of the indoor environment due to mould and mildew growth. In addition, it can increase the contamination level and reduce the quality of the indoor air since air borne bacteria and some other indoor contaminants such as formaldehyde have been found to be more active at higher indoor humidity levels [8]. On the other hand, at very low indoor humidity levels, excessive dryness could lead to difficulty in breathing, eye and nose irritation as well as skin irritation and other related problems.

Moisture performance of interior furnishings and building construction components is greatly influenced by the level of indoor humidity. At low humidity levels, cracking and flaking of moisture sensitive materials could occur. In cold climates, high indoor humidity could result in objectionable surface condensation on windows, and damaging interstitial condensation within the building envelope components. In many situations, either for functional or operational reasons, indoor humidity is required to be maintained at a certain constant level. In order to achieve this goal, indoor air has to be continuously humidified or dehumidified resulting in energy consumption. Air humidification can be performed

either by directly adding moisture to the space or by supplying the space with appropriately humidified air through the HVAC system. Similarly, air dehumidification can be performed locally within the space, or by supplying properly dried air into the space. However, more energy is needed to perform the dehumidification process. Depending on the level of indoor humidity and its variational behaviour around the required level, air humidification and dehumidification processes could be performed in an alternating manner. For better assessment of the quality of the building indoor environment and more accurate prediction of energy consumption in buildings, the dynamic nature of indoor air humidity must be considered.

1.2.2 Effect of indoor air humidity behaviour on exterior wall moisture performance:

The exterior wall system constitutes an essential component of the building envelope which determines the building overall performance. Besides its functional importance, the exterior wall could form the larger portion of the building envelope area. Consequently, exterior wall performance will have serious economical as well as functional implications. In cold and hot-humid climates, moisture performance of exterior walls is an essential factor in determining their overall performance.

Moisture performance of the wall system can be defined as its ability to prevent the occurrence of moisture related problems and sustain the intended functional performance even in the presence of unavoidable moisture accumulation. Moisture problems can only arise in the presence of water in its liquid form. Since water vapour exists everywhere within the wall system, the occurrence of condensation, which transfers the water vapour from its harmless form to its problem-causing liquid form, is the first indication of the rising potential of moisture problems. For condensation to occur at any point in the wall system,

the local vapour partial pressure must exceed the saturation vapour pressure corresponding to the temperature at that point. Such conditions can only exist when the wall system separates two environments; one of high vapour pressure, and the other of low air temperature. This could occur either in cold climates when indoor humidity is relatively high, or in hot-humid climates when indoor temperature is kept relatively low. However, the most serious moisture problems are normally encountered in cold climates. The increasing trend towards producing energy efficient buildings have resulted in higher indoor humidity and excessive use of wall insulation. These combined together have increased the prospect of interstitial and surface condensation.

Moisture performance of the exterior wall system is dependent on many factors related to its thermal and moisture characteristics and to a great extent on the prevailing environmental conditions. All outdoor environmental parameters as well as indoor humidity are variable with time. Therefore, for a realistic and more accurate modelling of wall moisture behaviour, the variability of these parameters must be considered. Since variations of outdoor air conditions are mainly seasonal, while indoor humidity could experience considerable fluctuation within a short period of time, therefore, variability of indoor humidity is more crucial. The effect of indoor humidity variations on wall moisture behaviour is determined by the type of moisture transfer mechanisms between the wall system and the indoor environment. Moisture can be transferred into the wall system by vapour diffusion and by convection due to air movement across the wall system. Moisture transfer by convection, which represents the fastest transfer mode, is normally the prevailing moisture transfer mechanism. In this case, wall moisture conditions will quickly respond to any changes in the indoor air humidity. For example a sudden rise in indoor humidity, even for a short period of time, may result in condensation within the wall.

Therefore, with the dynamic behaviour of indoor humidity, a continuous alternation of the wetting and drying processes within the wall system may occur. Such behaviour will result in a unique moisture performance (i.e. moisture accumulation patterns, occurrence of condensation, etc.) over a period of time which would not be recognized by assuming constant indoor humidity level.

There have been considerable effort documented in literature to model wall moisture performance. Available steady state models can be used only to grade the wall performance by checking the potential of interstitial condensation. However, they can neither be used to evaluate the suitability of a certain wall system for a particular environment nor to assess the long-term performance. In certain situations, steady state analysis would indicate that condensation occurs, while transient analysis would indicate that the total moisture level would remain acceptable [3]. The dynamic moisture behaviour of the wall system has been the subject of many studies. Mathematical models for predicting transient simultaneous heat and moisture transfer through multi-layer constructions have been evolving with different degrees of sophistication and practicality. However, the transient nature of the boundary conditions were either neglected or given little attention. In some cases, considerations were given to the variability of the outdoor environmental parameters [3]. Although the dynamic nature of indoor air humidity was neglected, its influence on the wall moisture performance was shown to be significant [3].

1.3 Objectives of Research

The main objectives of the present research can be summarized as following:

i) To theoretically predict air humidity transient behaviour within single-zone and multi-zone enclosures, taking into account the dynamic nature and interaction of

the moisture transport processes in buildings, as well as, the variability of outdoor environmental parameters.

ii) To study the relative influence of some of the indoor humidity determining factors such as, building physical and functional characteristics.

iii) To study the effect of the different moisture transport processes on indoor air humidity behaviour and consequently on building moisture performance pertaining to surface condensation potential as well as humidification and dehumidification requirements.

iv) To evaluate the effect of indoor humidity behaviour, determined by the boundary conditions and the building characteristics, on the moisture performance of the exterior wall system. This will be done by evaluating the moisture content variations and distribution in the materials comprising the wall system both in the presence and absence of convective moisture transfer.

v) To investigate the indirect relationship between the building physical and functional characteristics and the exterior wall moisture behaviour through their effect on indoor humidity.

1.4 Research Approach and Methodology

Evaluation of indoor air humidity behaviour and its effect on exterior wall system moisture performance may be carried out either experimentally or through theoretical modelling. Indoor humidity, however, is a function of many interrelated moisture transport processes

which are dependent on building physical and functional characteristics. Experimental simulation of such processes and their interaction will be extremely difficult and impractical to implement. Although the interaction between indoor humidity and the wall system can be experimentally simulated, it is a relatively slow process in determining the effect of indoor humidity behaviour on wall moisture performance. Consequently theoretical modelling seems to be the only feasible alternative for evaluating indoor humidity behaviour and its influence on wall moisture behaviour. Mathematical modelling of such complicated problems will be a more useful tool for understanding the physical processes involved and their interactions. In addition, mathematical modelling is more comprehensive since it is independent of laboratory conditions and limitations of experimental results. Once it is developed, less effort and time are needed to perform the simulation at different conditions. In this study, indoor humidity behaviour and its interaction with the exterior wall system will be mathematically modelled. The results of the proposed theoretical modelling approaches will be compared with relevant experimental results available in literature. The main components that could or will be included in the mathematical model are shown in Fig. 1.1. The highlighted boxes indicate that further development or modifications of the current knowledge is needed in order to achieve the objectives of this study.

In order to achieve the research objectives, it is necessary to carry out the following tasks:

i) Development of a mathematical model to describe indoor air humidity behaviour and distribution. Such a model should include all relevant moisture transport processes within the space. In addition, the interaction of these moisture transport processes and the behaviour of the corresponding environmental parameters must be considered.

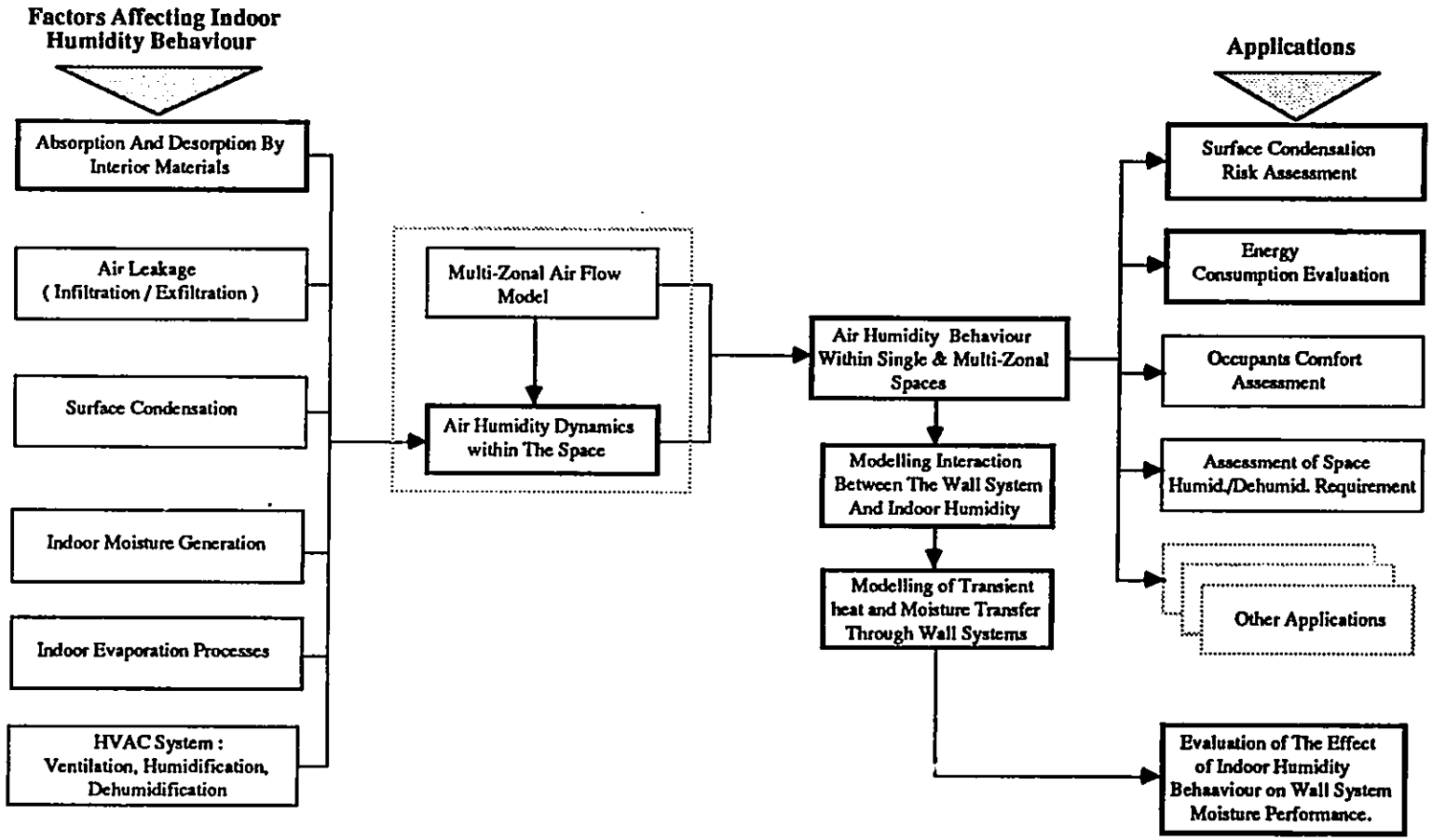

Fig. 1.1 A flow chart illustrating the main research components.

ii) Mathematical modelling of transient simultaneous heat and moisture transfer through exterior wall systems. This model should include a procedure for checking interstitial condensation and evaluating the moisture accumulation within the wall component.

iii) Mathematical description of the moisture interaction between the indoor environment and the different exterior wall systems.

iv) Development of computer programs to simulate indoor air humidity behaviour and wall moisture performance over a period of time under transient boundary conditions.

v) Development of case studies for investigating the inter-dependence among the different moisture transport processes in buildings and their influence on indoor air humidity behaviour within single-zone and multi-zone enclosures.

vi) Development of a case study together with a parametric analysis for evaluating the impact of indoor air humidity behaviour on exterior walls under different modes of moisture transfer mechanisms.

CHAPTER 2

LITERATURE REVIEW

2.1 The Impact and Behaviour of Air Humidity in Buildings: An Overview

2.1.1 Effect on building indoor environment: The role of indoor humidity as an environmental parameter affecting the occupants thermal comfort and health as well as the quality of the indoor environment has been discussed [4-8]. The level of indoor humidity has been found to be a main factor in the growth of certain types of biological organisms [6]. Such an environment will negatively influence occupants health causing respiratory illnesses and allergies and consequently may affect the productivity of occupants [6-7]. For functional reasons, indoor humidity in many situations is required to be maintained at a relatively higher level [1,9]. In cold climates, with the increased air tightness to conserve energy and the increased indoor moisture generating activities, high indoor air humidity level and associated problems are inevitable unless certain measures are implemented [10,11]. Moisture problems associated with high indoor humidity have been the subject of many studies [2,12-17]. Winter moisture condensation whether it appears as surface condensation or as concealed condensation within the building construction is seen as the most common moisture-related problems that affect houses [12]. Problems associated with surface condensation can range from merely obstructing the view through the window to severe damages to the windows framing system and the creation of pools of water that encourages the growth of moulds and fungi [2]. Surface condensation on hygroscopic materials and factors affecting it have also been studied [18]. The mechanism of surface condensation and possible measures to eliminate it or

reduce its effect have been discussed [2,14,16,19]. Concealed condensation, however, has been recognized as the most damaging form of condensation in buildings causing material deterioration and lowering the performance of the building construction components [2,14]. This phenomenon has been extensively investigated and possible remedies have been recommended [2,13-14]. Models for predicting and evaluating interstitial condensation have been available with varying approaches and degrees of analysis [20-22], however, the basic concept behind these models remains the same. In addition to its effect on occupants and the building construction and furnishing components, indoor humidity can influence the building energy consumption.

2.1.2 Effect on building energy consumption: In order to maintain indoor air humidity at a constant level all year round, both humidification and dehumidification processes would be needed. The potential increase in energy consumption due to these processes has been emphasized in literature [8,23]. The effect of moisture transport processes in buildings on energy consumption through their influence on indoor humidity has been the subject of several studies [24-27]. The effect of moisture absorption and desorption by building materials on heating loads of houses has been discussed [28]. It has been found that the hygroscopic effect in building materials often amount to tens of percents of the heating load of well insulated houses. In order to account for the variations in latent heat loads due to different moisture transport processes, indoor humidity has been estimated by applying the concept of moisture mass balance [24]. The effect of hygroscopic moisture storage capacity has been modelled by an exponential decay behaviour, with the characterizing constants of this behaviour determined experimentally. A detailed three-dimensional finite element model for evaluating moisture absorption and desorption rates in buildings has been incorporated with a building energy analysis program [26]. Analysis

of residential cooling loads in humid climates by the integrated program shows that moisture absorption and desorption can have a significant impact on the cooling load and in indoor humidity conditions. The effect of the cyclical moisture absorption/ desorption by building construction and furnishing materials on space latent heat load has been investigated experimentally [25]. Depending on the material moisture capacity, moisture absorption/ desorption alone could represent a significant component of the total latent heat load that would have to be mechanically added or removed from the space. A simple calculation of the dynamic latent heat load represented by the materials in a typical office shows that the latent heat load of the materials can be as much as ten times the latent heat load of the space alone [25]. The effect of walls moisture storage capacity on indoor air humidity behaviour and consequently on energy consumption has been studied by Isetti et. al. [27]. In this study, a time-dependent model has been suggested for predicting the indoor vapour content and its corresponding latent heat within the space. It has been found that the moisture storage capacity of the wall generally exerts a significant damping on the water vapour content of a room and hence could influence its energy requirement. In addition, when air humidity need not to be controlled considerable benefits to cooling equipment sizing and operating costs can be achieved when moisture storage capacity of the walls is considered in the space latent loads calculations. The impact of moisture absorption due to night ventilation on cooling load has been theoretically investigated [29]. It was found that for a typical residence, moisture absorption during the first few hours after resuming operation of the air conditioning system can account for significant increase in the latent cooling load if a large surface area of unpainted hygroscopic material is exposed. On the other hand, the evaporation cooling resulting from moisture desorption at the material surface was found to reduce the sensible heat by almost the same amount.

2.1.3 Behaviour of air humidity in buildings: A study of humidity in Canadian houses [30] has indicated that indoor humidity is subjected to considerable seasonal variations, while indoor air temperature remains almost constant. It mainly follows the trend of the outdoor humidity, especially in summer because of increased ventilation, but also is influenced by seasonal ventilation habits of the occupants and the moisture storage of hygroscopic materials in the house. In winter, the difference between indoor and outdoor humidity reaches a maximum due to the increase in indoor moisture-generating activities and reduced ventilation. Relationship between indoor humidity, air leakage and ventilation has been modelled [31,32], to determine the effect of air exchange rate on indoor humidity level and to examine the effect of other parameters such as occupancy, building characteristics and weather parameters. It has been found that most of these parameters can have a significant impact on indoor humidity behaviour, especially at low air leakage rates. Indoor air humidity evaluation involves several topics which are directly or indirectly related to the determination of air humidity behaviour in buildings. These topics include; air leakage across the building envelope, inter-space airflow in multi-zone buildings, surface condensation and moisture absorption and desorption by building materials.

As the role of indoor air humidity in determining the moisture performance of the building indoor environment and the durability of the construction materials is appreciated, the need for managing it becomes more obvious. Moisture management in buildings through the control of indoor air moisture content has been discussed [23,33-34]. In order to achieve proper moisture control in buildings, the actual moisture behaviour of indoor air humidity must be known. In addition, better understanding and appreciation of moisture requirements as well as its impact on the building construction components are required.

2.2 Literature Related to Indoor Air Humidity Evaluation

2.2.1 Air leakage and inter-space air movement: Air flow across the building enclosure elements can have a great influence on the indoor humidity level and its distribution pattern within the space. Evaluation of air leakage through the building envelope has been the subject of many experimental and theoretical studies [35-41]. Air pressurization and the tracer gas techniques are widely used in evaluating the air leakage characteristics of houses [42]. Although the measured values can accurately describe the leakage characteristics of the tested house, they are of limited use for other houses, since each has its unique air leakage characteristics. Theoretical models [20,38-41] for predicting air leakage are more stable and practical to be implemented. There are various theoretical models with different degrees of complexity ranging from simplified theoretical technique to multi-zone air infiltration and ventilation network [43-44].

Two conventional methods of estimating the rate of air infiltration have been described by ASHRAE [20]. In one method, known as the air leakage method, the estimate of air infiltration is based on an assumed number of air changes per hour for each room depending on the number of windows and doors. In the second method, known as the crack method, air infiltration is estimated based on the leakage characteristics of the exterior building envelope and the pressure difference across it. The crack method is generally considered more accurate when leakage characteristics and the pressure difference can be properly evaluated. However, the accuracy of both these methods are restricted by the limited data on air leakage characteristics of building components and by the difficulty of predicting pressure difference due to variable wind conditions and stack effect. As an alternative to the crack method, leakage characteristics can be expressed

in terms of an equivalent sharp-edge orifice area which will yield the same rate of flow at a particular pressure difference as the element in question [42]. Based on laboratory tests, air leakage values for various wall components are given by ASHRAE [20]. Evaluation of wind and stack pressures have also been discussed by ASHRAE [20], and more detailed evaluation of wind pressures has been discussed in terms of the pressure coefficients [45].

Inter-space air flow normally occurs through large openings connecting different zones with the possibility of opposite flow across it in the presence of a temperature difference between the connected zones. Natural air flow through rectangular openings in vertical and horizontal partitions has been experimentally and theoretically investigated [46,47]. A comprehensive review of previous research work on inter-zone convective heat transfer was carried out [48]. Most researchers have attempted to describe the natural convective heat flow through large openings by a dimensionless correlation using Nusselt's number, Prandtl's number and Grashof's number. Using the orifice equation, it has been shown that heat transfer and the corresponding mass flow predicted by a correlation equation for the two-way flow through a doorway can be expressed through the power law elements [49]. A multi-room air flow model [50] has been developed as part of a model to compute air infiltration and air flow between rooms. The model has been incorporated into a comprehensive loads-predicting computer program. Later the same model has been discussed but with the implementation of an infiltration predicting technique [49]. Simultaneous solution of the air mass balance equations in all rooms is accomplished by a slightly modified Newton's iteration method. A more comprehensive model is suggested [51], by including the HVAC systems. Numerical aspects of an air flow network methods that would provide a verified approach to building air flow calculations have been

discussed. Detailed simulation of indoor air movement has been presented by using the turbulence model [52]. A larger scale air movement prediction model has been developed to simulate air movement in a multi-story building [53]. By applying the mass balance equation for each floor space and shaft, and then solving the resulting set of nonlinear equations simultaneously using the method of successive linear approximation, air movement between different zones as a result of a combination of wind effect, stack effect and operation of air-handling systems has been predicted.

2.2.2 Surface condensation and moisture absorption and desorption by building materials: Condensation on cold interior surfaces and moisture absorption and desorption can greatly affect indoor humidity behaviour . In winter, the internal surface of windows could act as a dehumidifier removing a lot of moisture from the space [2]. Prediction of the rate of surface condensation on windows has been discussed [22,54]. A procedure for estimating superficial mass condensation rate at steady state conditions has been suggested [22]. Calculation of the rate condensation is based on both the heat balance and mass transfer equations. By introducing the latent heat term in the heat balance equation, and solving the resulting equation with the mass transfer equation a relation between the glass temperature and the difference between saturation pressure at the window's temperature and the bulk partial vapour pressure can be obtained. Using this relationship and the relationship between saturated vapour pressure and the window's temperature, two curves can be obtained. The intersection point between these curves is then used to estimate condensation rate. Mathematical formulation of the above procedure has been utilized as part of a numerical solution of the transient heat transfer through windows due to surface condensation [55]. In this formulation, the need for a graphical solution is eliminated with the implementation of the numerical solution. An alternative

approach using the basic concept of the film condensation theory has been suggested [56]. In this approach, Nusselt's theory of film condensation has been modified to account for the presence of a large percentage of a non-condensable gas (i.e. air) to be applicable for atmospheric vapour condensation.

Moisture interaction with materials in general and the building materials in particular has received considerable attention in literature [20,57-63]. Most materials interacts with ambient moisture through absorption and desorption at the material exterior surfaces. One possible explanation of this phenomenon is that there is an imbalance of forces at the material surface giving rise to surface free energy which decreases as more moisture is absorbed [57]. In general, it can be said that the absorption process results from the interaction between a gas and a solid surface which continues until a thermodynamic equilibrium is achieved between the gaseous phase and the adsorbed layer [58]. Inside the material, modes of moisture interaction are determined by the material internal pore structure and the state of the moisture [57-59]. When no more moisture transfer occurs between the material and its surroundings, the material moisture content is called the equilibrium moisture content corresponding to those particular ambient conditions. The equilibrium moisture content for any material is determined by the ambient temperature and the partial vapour pressure. However, for practical reasons, the material equilibrium moisture content is normally expressed in terms of relative humidity [20]. The curves which relate the equilibrium moisture content to the ambient relative humidity are known as isotherms. In addition to the ambient conditions, the equilibrium moisture content is dependent on the material initial moisture conditions. Although with varying degrees, the equilibrium moisture content obtained by absorption when the material is initially dry is always less than that obtained by desorption at the same ambient conditions when the

material is initially wet, except at 0% and 100% relative humidity [57,60]. This phenomenon, which is known as moisture hysteresis, has been the subject of different interpretation. A possible reason for such behaviour is the different conditions at capillary condensation [61,62], which result in different levels of moisture gain by the material. Another explanation for this phenomenon is that in sorption, water vapour can find its way to all pores where it may condense. The desorption, however, is supposed to be a process of displacement by a non-wetting phase (i.e. air), consequently, a pore may not be able to desorb its water content. This phenomenon is called the "ink-bottle" effect [58]. Equilibrium moisture contents at different relative and absolute humidity levels have been evaluated for some commonly used fibres [60]. Moreover, the moisture absorption curves, and in some cases the desorption curves, for many building materials have been evaluated [61-63].

Recently, some theoretical and experimental studies have dealt with modelling moisture absorption and desorption processes in buildings. As part of an indoor humidity calculation model, Kusuda [64], suggested a method to calculate the amount of moisture absorption by the room surfaces, in which he speculates that moisture absorption is limited to a thin film of material which attains instantaneous moisture equilibrium. In this model two parameters; the surface mass transfer coefficient and the room surface average moisture content must be determined experimentally to fit the measured indoor humidity in a particular enclosure so as to be used in indoor humidity calculations. Therefore, these values may not be universally applicable for other situations. However, it has been suggested by Kusuda [64], that the mass transfer coefficient is not as sensitive to room characteristics as the other parameter. Therefore, approximate theoretical relationship, such as Lewis relationship, can be used to evaluate it. Evaluating moisture conditions and

transfer dynamics at the room surfaces is the main part of an absorption /desorption model. Kusuda and Miki [65], have conducted an experimental program for evaluating surface moisture conditions of some building materials at certain ambient conditions using the infrared reflectance technique called "Quadra-Beam" method. These surface moisture conditions results can be implemented in the moisture absorption model described by Kusuda [64], and hence, the amount of moisture absorbed or desorbed by building materials can be calculated without resorting to the unknown values of the average surface moisture content. However, this requires an extensive experimental effort since the moisture conditions of each material must be evaluated at different ambient humidity levels. A mathematical model based on heat and mass transfer equations has been suggested for predicting moisture sorption rates at the interior building surfaces [29]. The model takes into account the temperature gradient across the material and the effect of the latent heat generated by the moisture absorption process.The resulting heat and mass transfer equations were solved numerically by the implicit finite-difference method. Although the model predictions were found to be in good agreement with the experimental results, the node spacing and the time step have to be progressively decreased until model prediction stabilizes. Theoretical results have indicated that the effect of the temperature gradient and the enthalpy on the moisture transfer process is minimal.

Moisture absorption and desorption within heated or cooled spaces are increasingly becoming an important part of the energy analysis models. A theoretical approach has been suggested by Franssen and Koppen [28] in which the unsteady state, one dimensional diffusion equation was solved by assuming instant equilibrium and that the slab is semi-infinite. Although these assumptions were experimentally found to be acceptable for some materials, this may not hold true for other materials at different

conditions and times of exposure. Moreover, the alternation of the absorption and desorption processes, due to fluctuation in indoor humidity, has not been addressed. As part of an energy consumption model, Miller [24] has suggested the use of a simple resistor-capacitor electrical circuit to describe the dynamic moisture behaviour of materials. In this study, two constants, similar to what Kusuda has suggested, had to be determined experimentally. An extensive experimental study was conducted by Martin and Verschoor [25] to investigate the cyclical moisture absorption and desorption of fifteen materials in order to evaluate their latent heat storage effect on cooling energy consumption. The moisture response of most materials has been shown to follow an exponential decay behaviour. However, experimental evaluation of moisture absorption and desorption rates at all possible initial and boundary conditions is an extremely difficult and impractical task.

A detailed three dimensional finite element model has been developed to evaluate moisture absorption and desorption rates in building materials [26]. Assuming that the surface material comes into instant equilibrium with the environment, then by solving a system of differential equations describing heat and mass transfer, the amount of absorbed or desorbed moisture can be determined. However, solving these equations requires the knowledge of several transfer coefficients that are available for a few materials and are difficult to evaluate. Moreover, assuming instantaneous moisture equilibrium can only be justified for some materials at certain conditions. A more simplified moisture absorption and desorption evaluating procedure based on the concept of effective penetration depth has been suggested [66,67]. The objective of this procedure is to match the experimental or detailed theoretical moisture absorption and desorption rate to a simple theoretical model, which is based on lumped analysis, by varying the material dry weight. An effective moisture penetration thickness with uniform moisture

content can then be established to be used in the dynamic modelling of moisture absorption and desorption processes. This approach is not practical in terms of the effort needed to establish the effective moisture penetration thickness, which in itself may not be a reliable parameter in modelling moisture absorption and desorption dynamics in buildings. A major limitation of the effective thickness approach is that the cyclic integral of the total moisture absorption and desorption over a relatively short period of time must be zero because of the limited moisture capacity of the material layer. Consequently, this approach is not applicable for long term moisture storage modelling. In an effort to simulate the dynamic behaviour of indoor air humidity and temperature [68], moisture absorption by interior surfaces and furnishings was modelled by identifying a mass change time constant for each material. The rate change in the moisture content of the material in response to step changes in room humidity is assumed to follow an exponential decay. Although this exponential behaviour has been proven by various studies [24-25], for some interior surfaces a time constant is meaningless because of material and geometrical characteristics. Moreover, when it is impossible to theoretically determine the time constant, considerable effort is needed to evaluate it for one particular material configuration either experimentally or through detailed theoretical analysis. As part of an analytical model for assessing the wall cavity long term moisture behaviour, Cunningham [69-71] assumed that moisture absorption and desorption by the hygroscopic materials within the wall cavity follows an exponential decay. Moisture transfer between the material and the ambient air has been evaluated under periodic boundary conditions using the effective penetration depth concept [72]. In this approach, an effective material thickness which is assumed to represent the moisture transfer resistance is theoretically evaluated. It was found that the effective depth for one-side exposure to be a function of the angular frequency of the driving moisture content as well as the material diffusion coefficient. On

the other hand, the effective depth for the two-side exposure was found to be equal to one-sixth of the material thickness.

2.2.3 Evaluation of indoor air humidity behaviour: There has been an appreciable interest in literature to study moisture behaviour within building enclosures [54,73-75]. Water vapour loss by ventilation, condensation and diffusion through the fabric of the building envelope has been modelled by a vapour flow circuit [54]. Later, a similar procedure in which the flow of moisture by the same mechanisms were expressed in terms of their latent heat flow, and their generating vapour pressures in terms of dew-point temperatures, so as to be implemented in terms of a thermal circuit representation [73]. The influence of moisture absorption by wood on indoor air humidity transient behaviour has been theoretically and experimentally studied [74]. In that study, it was indicated that the dynamic behaviour of moisture sorption by sorptive building materials such as wood plays an important role on the dynamics of the room air humidity. In another study dealing with moisture loads of kitchen and the influence of building materials moisture absorption, it was found that materials having low hygroscopic moisture capacity will have limited impact on indoor air humidity [75]. A time-dependent model based on sinusoidal boundary conditions for predicting indoor vapour content in a room and its corresponding latent heat has been described [27]. The model takes into account the moisture storage capacity of the walls, which has been shown to have a significant effect on the behaviour of indoor humidity variation. In most cases, however, a steady sinusoidal behaviour can not be justified, since many interrelated factors would normally contribute to the indoor environment behaviour. In addition, identifying such boundary conditions across partitions within the space or these separating two different zones may prove to be impossible, especially if inter-zone airflow is taking place. A computer model based on similar

mathematical formulations has been developed to evaluate the exterior wall moisture capacity and its impact on indoor air humidity dynamics [76]. The program can simulate simultaneous heat and moisture transfer through walls and slabs of a room and its effect on indoor temperature and humidity. Simulation results has indicated that moisture storage at building wall and slabs is significant, and if its effect is not taken into account in predicting indoor conditions and evaluating the air-conditioning performance, erroneous results will be obtained. In an effort to investigate the performance of different types of ventilators in maintaining acceptable indoor humidity, a computer program has been developed to predict the variations of air temperature and humidity in buildings [68]. The computer program was based on a mathematical model that incorporate the different moisture transport processes in buildings.

Moisture content of the indoor air is also influenced by the amount and conditions of the HVAC supply air. Using the appropriate mechanical system control, indoor humidity can be maintained within a desirable limit throughout the year. Central humidification and dehumidification by the air-handling system are normally done for commercial and industrial buildings [23]. In residential buildings, indoor humidity is normally controlled by directly adding moisture into the space. In many cases, for economical and practical considerations, only indoor temperature is controlled while air humidity is allowed to fluctuate. When air is supplied to the space for cooling in summer or ventilation in winter, indoor moisture content is automatically regulated according to the supply air conditions. Depending on the system response to varying space loads, considerable fluctuations in indoor humidity may occur [77-79]. When the temperature or flow rate of the supply air is changed in response to changes in space loads, the moisture removing potential of the supply air is changed and consequently affecting the moisture content of the indoor air.

Models for indoor humidity calculations have been developed [64,68,80], however a detailed humidity calculation model has not been available with the same degree of sophistication as that for the heat transfer processes [64]. All available models are based on the mass balance between gained and lost moisture. The simplest model [80], predicts indoor humidity as a function of occupancy and ventilation rate with a simple treatment of the effect of moisture storage in hygroscopic materials. Other models [64,68], have considered more time-dependent mechanisms of moisture transport in an enclosure. In addition, moisture absorption has been treated in more details. However, for these models to be used, material properties which are generally not available or difficult to determine must be known. In related studies, the dynamic long term behaviour of moisture conditions in building cavities has been modelled both without condensation [69], and with condensation [70]. The effect of hygroscopic materials in the cavity under non-steady conditions is considered in both cases. The result is a pair of linear coupled differential equations which can be solved easily to predict long term cavity moisture performance based on two primary time constants. The model was then modified [71] to include the presence of evaporating surfaces within the wall cavity.

2.3 Literature Related to Moisture Performance and Transfer Through Exterior Walls

2.3.1 Heat and moisture transfer through porous building materials and construction components: Moisture in one or more of its forms (i.e., vapour,liquid and solid) can exist in the building porous materials. Knowledge of the moisture transport mechanisms through building materials is the first step towards understanding its impact and interaction with its porous media. Water vapour diffusion being the most common mechanism of moisture transfer in buildings, has received particular attention in literature [20,45]. Mechanisms of water vapour movement in porous materials have been described

and their relevance to practical problems in buildings and other structures have been discussed [81]. In a more comprehensive study [82], both experimental and theoretical approaches were utilized to investigate moisture transport (mainly vapour diffusion) in different building materials. In some building components, especially those exposed directly to the outdoor environment, moisture transport in the liquid form becomes an important mechanism. A series of studies have dealt with water movement and absorption in building materials [83-90]. In practice, full saturation of building materials rarely occurs in building components, hence water flow at lower moisture content is of greater importance. Darcy's equation has been modified to account for unsaturated water flow in building materials by using a moisture content dependent hydraulic conductivity [83]. Water absorption by some building materials has been experimentally and theoretically studied [84,85,89-90]. In addition, evaporation and drying in some building materials and their effect on water movement in the material have been investigated [86,88]. In a more practical and relevant study, the absorption and shedding of rain by exterior building surfaces have been investigated based on the unsaturated flow theory [87].

The practicality of the moisture transport theories is very much dependent on the availability of the corresponding flow coefficients. Building materials properties pertaining to water transport is generally lacking [83], although methods for evaluating these coefficients are available [82,91]. This is partly because such coefficients are highly variable with the moisture content and are difficult to evaluate. The main reason probably is due to the fact that the majority of building components are kept at low moisture content levels at which liquid transport is not important. Furthermore, even for those parts of the building subjected to higher moisture content, these levels will not be retained for long periods of time [92]. For buildings, water vapour theories are more practical because of

their applicability and the relative ease to evaluate the corresponding moisture transport coefficients. Evaluation of vapour diffusion coefficients has been the subject of many studies [82,93-97]. A widely accepted method for evaluating material vapour diffusion coefficient is the cup method which is adopted by ASHRAE [20]. Depending on the boundary conditions and the way the material specimen is exposed to, the cup method is called either dry cup, wet cup or inverted cup test. Apart from the vapour diffusion coefficients, the material equilibrium moisture corresponding to a certain ambient conditions is an important parameter for evaluating transient moisture transfer by vapour diffusion. The curves of the material equilibrium moisture content plotted against ambient relative humidity are known as isotherms. For many building materials, these curves can be found in literature [61-63,98].

Moisture and heat transfer in porous building materials are interdependent and can greatly influence each other. In buildings with the presence of large temperature and vapour pressure gradients across the exterior envelope, accurate assessment of the moisture transport and accumulation requires the consideration of both heat and moisture transfer. Theories for heat and mass transfer in porous materials serve as the fundamental base towards developing a theoretical model for evaluating moisture performance of composite construction systems. Considerable advancements have been achieved in the development of such theories [82,99,100-106]. Detailed theoretical analysis of moisture transfer in its different forms through porous bodies under different driving potentials has been carried out by Luikov [100]. In spite of such advancement, a comprehensive and satisfactory theory is still lacking, and considering the wide range of porous media and their applications, it is even doubtful whether a universal theory can be developed [103].

Heat and mass transfer through some building materials have received special attention [107,108]. Fibrous thermal insulation is an important part of the exterior building envelope, and because of its moisture and thermal characteristics, the interdependence of heat and moisture transfer becomes more pronounced and important for accurate evaluation of the moisture transport process. Analysis of simultaneous heat and moisture transfer in fibrous insulating materials has been the subject of many studies [108-116]. A mathematical model based on empirical expressions for heat and moisture fluxes has been presented to describe simultaneous heat and moisture transport through glass fibre insulation [110]. The same empirical formulation is then used to investigate the effect of hygroscopicity of some insulation materials on moisture and heat transfer [111]. The influence of the moisture transport on the thermal performance of the glass fibre insulation has been experimentally studied [112]. Results have indicated that moisture absorption from air with relative humidity up to 93% in the form of water vapour does not significantly affect the thermal performance of insulation. A more detailed analysis of heat and moisture transfer in porous insulation has been carried out [113]. A steady one-dimensional solution has been presented for the problem of condensation within the insulating material. The analysis includes both the convective and the diffusive transport mechanisms along with phase change. The same problem has been analytically investigated in which the behaviour of condensate and its distribution pattern with time within the material were investigated [115]. Hygroscopic mass transfer through a fibrous media under thermal gradient has been experimentally and theoretically investigated [116]. Results indicated that temperature and relative humidity gradients were approximately linear in the hygroscopic range.

2.3.2 Evaluation of construction components moisture performance: Great attention

has been given in literature to the evaluation of moisture performance of composite building constructions. Both experimental and theoretical techniques have been widely used to assess moisture performance of the exterior building wall components. In some experimental studies a specimen with certain moisture characteristics is placed between two controlled environments for a period of time through which the specimen thermal and moisture behaviour is monitored [117-118], and occasionally theoretical predictions of a specific model are compared with experimental results [82,119]. In other experimental studies, one side of the test specimen is exposed to the outdoor environment while the other side is maintained at constant conditions representing the indoor environment [120-124]. This makes it possible to assess actual moisture behaviour of various components of the building envelope over the course of seasonal weather patterns. Results from such experiments will have a limited value for validating most theoretical models, since some environmental factors, such as precipitation and wind, behave in a random fashion. Moreover, these experimental studies are likely to be limited to a few test conditions because of the effort and time involved in conducting them. The natural alternative to experimental evaluation of wall moisture performance is theoretical modelling. Simultaneous heat and mass transfer through walls has been theoretically described with different levels of details [100,104,125]. Unfortunately, most of these theories are not practically useful, because for their implementation, moisture transfer coefficients of all materials comprising the wall system, which are not available for practical use, must be known. In spite of the tangible progress in evaluating these coefficients for building materials, much more is needed to be done for many building materials.

Wall moisture performance as a whole is normally determined by the moisture conditions of the air cavity and the thermal insulation, because of their thermal and moisture

characteristics. As mentioned in the previous section, many theoretical and experimental studies have been devoted to the analysis of heat and moisture transfer in fibrous thermal insulation. Moreover, thermal insulation has always been part of the wall system being investigated either experimentally or theoretically [104,117,120,125]. Long term moisture behaviour of building cavities has been modelled both in the absence of condensation [69], and in the presence of condensation [70]. Air infiltration, vapour diffusion and material hygroscopicity under non-steady state conditions have been considered. In modelling moisture interaction between the material and the surrounding air, an approximate lumped model is used in which moisture transfer from and to the material is modelled by using a fictitious moisture transfer coefficient representing the surface and diffusive transfer of moisture. This coefficient is a function of material moisture and geometrical characteristics, as well as, the surface mass transfer coefficient and material surface moisture conditions. Some of these determining factors and consequently the moisture transfer coefficient are time-dependent. However, for the purpose of simplifying his model Cunningham [69] has assumed a mean fixed value for the moisture transfer coefficient. Such an assumption can probably be justified when modelling long term moisture behaviour of materials under certain boundary conditions, but it can not be justified in modelling short term moisture transfer problems (i.g. moisture absorption/desorption as part of an indoor air humidity evaluation model). Important moisture performance parameters have been identified to evaluate the long term moisture performance of cavities. Later, the model was extended to allow for evaporating surfaces within the cavity [71]. Comparison with field results shows good agreement with model predictions.

Accurate assessment of wall moisture performance requires that all wall components be included in the model, and their thermal and moisture interaction must be modelled.

Several moisture transport models have been developed with a wide range of complexity and applications. The simplest of these uses one dimensional steady state heat conduction and water vapour diffusion to predict water vapour partial pressure and temperature at any location across the wall. The moisture profile method described by ASHRAE [20] and the Kieper method [126] are examples of such models. Potential condensation is determined by comparing the local vapour pressure and saturation vapour pressure which corresponds to the local temperature. The major advantage of these methods is their relative ease in determining the most likely location of condensation within the wall, and roughly comparing the moisture performance of different walls at different conditions. However, steady state models can not be used to determine the suitability of a certain wall system for a particular environment. In certain situations, steady state analysis would indicate that condensation occurs while transient analysis would indicate that the total moisture level would remain acceptable [3]. Moreover, such methods do not take into account the effect of air leakage, material hygroscopicity, and the transient nature of wall moisture behaviour and the environmental parameters which are critical for evaluating long term moisture performance of the wall. Slight modification of the Kieper method is introduced by incorporating the effect of latent heat released by condensed water on the wall thermal behaviour [126]. Introducing the effect of air leakage [127] has enhanced the model but not necessarily increased its accuracy, because a uniform and steady state air flow through a multi-layer wall will hardly occur.

A simple method for predicting moisture performance of exterior walls in cold climates has been developed [128]. Analysis of concealed condensation was based on average conditions rather than extreme conditions, and seasonal variations were considered when assessing moisture accumulation. Another simple model was proposed to predict annual

moisture cycling behaviour of wall cavities in response to varying weather conditions [3]. Calculations are made from a steady state model and integrated using hourly time steps. This model does not account for the storage capacity of hygroscopic materials and the effect of phase change or heat capacity. Moisture deposition is assumed to occur in the warm side of the cavity (i.e. sheathing), and the effect of air-borne convection on moisture transport has been estimated only for wind induced situations. Similar studies have been carried out to predict moisture behaviour of wood frame walls [129,130]. In these studies, computer models have been developed to predict the moisture behaviour of the outer portions of wood frame walls. The computer program WALLDRY has been developed to respond to external weather conditions including temperature, relative humidity, wind direction and speed, and solar radiation [130]. However, it lacks a detailed model of air flow in the insulating cavity. In addition material moisture storage capacity is ignored and wall interaction with the surroundings was simplified by assuming instantaneous equilibrium with varying environmental parameters. So far, in all of the above mentioned models, indoor humidity is assumed constant.

For accurate modelling of wall moisture behaviour, the dynamic nature of heat and mass flow through composite constructions must be formulated as part of a moisture performance prediction model. Detailed analytical model has been developed [125] to describe transient heat and mass transfer through multi-layer constructions. Constitutive equations for simultaneous heat and mass transfer in porous materials are derived from the integrated mass, momentum and energy balance equations using the volume averaging technique. The boundary layer and the interfacial balance equations are also derived. In spite of its detailed analytical approach, this model requires a formidable experimental program in order to evaluate the transport coefficients needed to solve the

equations for a composite wall. Moreover, the effect of air flow within the wall system has not been modelled. In a more practical model, the problem of coupled heat and moisture transfer through single and multi-layer slabs has been analytically solved [131]. Although the resulting solution can be useful in predicting transient heat and moisture transfer through walls, it can not be used for evaluating wall moisture performance since it is based on the response factor method. In other practical models [132-134], transient moisture and heat transfer were formulated based on conservation of species mass and energy. The resulting equations were solved numerically by the finite-difference technique. The effect of moisture storage capacity has been considered by utilizing the absorption isotherm of the material. Nevertheless, both these studies neither accounted for moisture transport by convection nor for the effect of the variability of environmental parameters. A more general time-dependent finite-difference nodal model for heat and moisture transfer in building structures is described [92]. Non-linear processes such as condensation, radiation and convection are described in terms of an effective conductance at each time step. Moisture performance of a framed structure containing a hygroscopic framing material and a cavity filled with air or insulation has been mathematically modelled [135]. Parameters that characterize the long term moisture performance of the structure have been identified. However, the effect of the model assumptions and approximations on the solution even for long term moisture assessment can be appreciable. Since this model is based on lumped parameter analysis, it can not predict the short term moisture behaviour of the structure which is essential for accurate assessment of its performance especially in cold climates. In a more specific application, moisture diffusion due to temperature and moisture gradient in a homogeneous slab has been analytically solved for periodic boundary conditions [136]. Comparison with numerical solutions have indicated acceptable accuracy.

2.4 Summary

The following findings can be drawn from the literature review:

i) Indoor humidity is a significant environmental factor that affecting the building aesthetical, functional and moisture performance. In addition, it can significantly influence the building energy consumption through the latent heat associated with the humidification and the dehumidification processes.

ii) Accurate indoor air humidity prediction can only be achieved by considering several interrelated time-dependent moisture transport processes. This is particularly true when air humidity in the space is not controlled.

iii) Moisture absorption and desorption by interior building materials can greatly affect indoor humidity conditions and building energy consumptions. However, a practical and a reasonably accurate theoretical model that takes into account the alternating nature of these processes has not been found in literature.

iv) There is a need for a comprehensive model that would predict indoor humidity behaviour and distribution in buildings and takes into account the different moisture transport processes and account for space-envelope interaction.

v) Although the effect of indoor humidity on wall moisture performance has been found to be significant, its variational behaviour has been neglected by assuming constant indoor humidity conditions.

vi) The indirect relationship between building physical and functional characteristics,

such as the air leakage characteristics of the exterior walls and the indoor moisture generation rate, and the moisture performance of the exterior wall system has not been studied.

The above findings drawn from the literature review consolidated the importance and the potential of the present study and will formulate its objectives. One of the main objectives of this study is to mathematically model the transient behaviour of indoor air humidity which will be the subject of a later chapter. In buildings where no humidity control is implemented, indoor humidity behaviour is determined by several time-dependent moisture transport processes. Moisture absorption and desorption by interior materials can have a considerable impact on indoor air humidity, however, a practical theoretical model has not been available. In the next chapter, theoretical modelling of moisture absorption and desorption by building materials, in the hygroscopic range, is discussed.

CHAPTER 3

MODELLING OF MOISTURE ABSORPTION AND DESORPTION IN BUILDINGS

3.1 Introduction

Moisture absorption and desorption by interior materials can play an important role in determining indoor air humidity behaviour in buildings. Until recently, most indoor humidity evaluation models were strictly based on the mass balance between humidity generation rate and humidity dilution by air leakage, ignoring moisture absorption and desorption by interior surfaces. This could lead to considerable inaccuracy in the predicted humidity level since as much as one third of the moisture generated in a room could be absorbed by its surfaces [64]. Moisture absorption and desorption taking place in most residential and commercial buildings are dynamic and alternating processes depending on the level and the variational behaviour of indoor humidity. Therefore, a time-dependent model is required to predict the effect of moisture absorption and desorption on indoor humidity.

Available theoretical models that deal with moisture absorption/ desorption processes in buildings are either too impractical to be implemented or incapable of modelling the actual dynamic moisture behaviour of such processes. For some models to be implemented, certain parameters, which can only be evaluated through an extensive experimental program or detailed theoretical analysis, are required. When the lumped approach is used in modelling both the material moisture conditions and the moisture transfer processes from and to the material, material dynamic moisture behaviour, especially short term behaviour, can not be accurately modelled. In addition, difficulty will arise when evaluating

the model lumped parameters. The main objective of this chapter is to develop a practical theoretical model for evaluating moisture absorption and desorption by interior building materials. In order to evaluate the amount of moisture absorption and desorption by a given material, its surface moisture conditions must be known. The dynamic behaviour of surface moisture conditions (i.e., variations in surface vapour pressure) differs from one material to another depending on its moisture and geometrical characteristics. Therefore, for accurate modelling of moisture absorption/desorption processes inside buildings, where many different materials may exist, the diversity of material moisture behaviour, and hence; the diversity in the modelling approach must be considered. Since material moisture behaviour is mainly determined by its moisture and geometrical characteristics, the Biot number, given in equation 3.1, is used in this study to determine the moisture behaviour of the material by relating its moisture diffusion coefficient D_v to its moisture interaction thickness L_m. Based on the value of the Biot number, the modelling approach is determined. Within the building indoor environment a very low value of Biot number would indicate that moisture conditions across the material thickness is constant and hence the lumped parameter approach can be used. On the other hand, a very high value of the Biot number would reveal that instant moisture equilibrium is reached between the material surface and the ambient air. In the building indoor environment, where the value of the surface mass transfer coefficient H_m is confined to a narrow range, a high value of Biot number will be associated with a very low moisture diffusion coefficient for the material in question. Consequently, its contribution to the moisture absorption/ desorption processes in buildings can be neglected. Most interior materials, however, remain in a state of continuous moisture exchange with the indoor ambient air. These materials, which correspond to moderate values of Biot number, are the most difficult to model since their surface moisture conditions are dependent on the non-linear moisture distribution across

the material thickness. Surface moisture condition of such materials is determined by solving the governing differential equation with the corresponding boundary and non-linear initial conditions using an approximate analytic method called the Moment Method. Comparison with experimental results and numerical solutions has revealed good agreement with the solutions of the proposed model.

3.2 The Underlying Model

Moisture absorption and desorption by interior materials in buildings are continuous and randomly alternating processes. Generally, for materials with large surface area to volume ratio, or materials having a very small equilibrium moisture capacity, the equilibrium moisture content corresponding to the ambient humidity change can immediately be attained. In this case, evaluation of the amount of moisture absorbed or desorbed requires only the knowledge of material weight and its moisture sorption isotherm. However, in most cases moisture absorption and desorption are time-dependent processes. The mathematical modelling approach of these processes is dependent on the moisture behaviour of the material (i.e. behaviour of moisture distribution across the material thickness) which is determined by the boundary conditions and the physical and geometrical characteristics of the material. Material moisture conditions in the building indoor environment are normally kept within the hygroscopic moisture range, hence, it is unlikely that a continuous liquid phase can exist within interior materials. In this case, moisture transport within the material can be described by the vapour diffusion coefficient D_v. The one dimensionless parameter that can relate these factors is the Biot number *Bi*, as given by equation 3.1.

The Biot number can be viewed as the ratio between the material resistance to moisture

$$Bi = \frac{H_m V_m / A_m}{D_v} \tag{3.1}$$

transfer, $(V_m/A_m)/D_v$ to the convective mass transfer resistance, $1/H_m$. The value of *Bi* has a significant physical meaning in relating where the greater resistance to moisture transfer occurs. In this paper, the Biot number is used to categorize the moisture behaviour of the different materials that would normally be available within buildings. Depending on the value of the Biot number, the modelling approach for moisture absorption/desorption processes will be determined. The surface mass transfer coefficient, H_m in equation 3.1 can be expressed in terms of the convective heat transfer coefficient, h_c using Lewis relationship given in equation 3.2.

$$H_m = \frac{h_c}{\rho_a c_p} \cdot \frac{M}{R T_k} \tag{3.2}$$

In the building indoor environment, the value of the surface convective transfer coefficient, h_c is either determined by the natural convective process or the airflow regime within the space. According to Kusuda [64], an average surface convective transfer coefficient of about 0.85 $W/m^2 \cdot C$ can be used in evaluating the surface mass transfer coefficient within the indoor environment. Although this value is relatively small compared to the design values suggested by ASHRAE [20], it must be noted that this value is an average value representing convective transfer over all in. ɔrior surfaces rather than the interior surfaces of the exterior walls or roofs. In a natural convective environment, h_c, will depend on the temperature difference between the material surface and the ambient air. On the other hand, in the presence of air movement within the space, h_c, for a particular surface will be dependent on the air speed and the flow pattern over that surface. For both the natural and forced convection processes, an approximate average value of the surface convective

transfer coefficient within a space can be determined using the appropriate model available in ASHRAE [20]. More accurate evaluation of the surface convective transfer coefficient can be obtained by utilizing the available detailed air movement simulation models. Once the surface convective transfer coefficient h_c is known, the surface mass transfer coefficient H_m can be evaluated by equation 3.2.

The transient moisture behaviour of building materials can be related to the value of *Bi* through the following three cases:

I) Building Materials at High Biot Number (Bi→ ∞)

A large value of *Bi* indicates that the diffusive resistance controls the moisture transfer process, which means that there is more capacity for moisture transfer by convection than by diffusion through material. When the Biot number approaches infinity ($Bi \rightarrow \infty$), the material surface immediately attains moisture equilibrium with the ambient conditions ($P_{ms}=P_{vr}$). In the building indoor environment, a very high value of Biot number can only be attributed to the moisture characteristics of the material in question. The contribution of such materials to moisture absorption and desorption processes is nil or very small such that it can be disregarded since a negligible amount of moisture is transported to or from the material due to its high moisture resistance. For most building materials, moisture equilibrium can not be attained immediately. Hence, surface moisture conditions, which determines the rate of absorption or desorption, are usually different from the ambient conditions.

II) Building Materials at Low Biot Number (Bi→ 0)

A small value of *Bi* represents the case where internal resistance to moisture transfer is

negligibly small and there is more capacity for moisture transfer by diffusion than there is by convection. As *Bi* approaches zero (in practice <= 0.1), the moisture content gradient within the medium gets extremely small, and hence a lumped-parameter analysis can be performed. Assuming a constant temperature and ignoring the effect of hysteresis, the dynamics of the vapour pressure within the material can be described by equation 3.3.

$$P_m(t) = P_{vr} + (P_{mo} - P_{vr})\exp\left(\frac{-H_m A_m}{C_m V_m} t\right) \qquad (3.3)$$

where,

$$C_m = \frac{\xi \rho_m}{P_{vs}} \qquad (kg/m^3.Pa)$$

The amount of moisture absorbed or desorbed during a period of time can be determined by equation 3.4, using the change in the pressure evaluated from equation 3.3 and the moisture isotherms of the material.

$$M_m = V_m C_m \Delta P_m \qquad (3.4)$$

III) Building Materials at Moderate Biot Number (0<Bi<∞)

In most cases, moisture interaction between the ambient air and the materials within the space occurs through a thin layer at the material surface. The amount of moisture transfer is mainly determined by the surface moisture conditions, which depends on the thickness and the moisture conditions of the moisture interaction layer as well as the surface mass transfer coefficient.

The dynamic moisture transfer process in the material can be described by equation 3.5, based on the following assumptions:

- vapour pressure is the only driving force, and the process is one-dimensional.
- the problem is isothermal (i.e. heat generated by moisture sorption at the surface is assumed negligible).
- hysteresis effect is negligible; the absorption isotherm is used to model material moisture capacity, since the moisture capacity of interest is within the hygroscopic range.
- the moisture diffusion coefficient is constant.

$$\frac{\partial U}{\partial t} = \alpha_m \cdot \frac{\partial^2 U}{\partial x^2} \tag{3.5}$$

where,

$$\alpha_m = \frac{D_v}{C_m} \qquad (m^2/s)$$

However, equation 3.5 can not describe the moisture interaction between the material surface and the surroundings, because of the discontinuity of the moisture content as a driving force at the boundaries. Instead, moisture transfer through the material may be expressed in terms of air humidity ratio or vapour pressure as given in equation 3.6.

$$\frac{\partial P_m(x,t)}{\partial t} = \alpha_m \cdot \frac{\partial^2 P_m(x,t)}{\partial x^2} \tag{3.6}$$

In order to solve for vapour pressure at the material surface $P_m(0,t)$, it is essential to identify the boundary conditions, the initial conditions and the interactive thickness of the material. In the present modelling, the ratio of the material volume, V_m to its exposed area, A_m is identified as the moisture interaction thickness, L_m as given by equation 3.7.

$$L_m = \frac{V_m}{A_m} \tag{3.7}$$

The material volume, V_m which determines the moisture capacity of a particular material, is dependent on the ambient air humidity behaviour, as well as, the moisture characteristics of the material. In the building indoor environment where air humidity normally fluctuates around a daily average value, a periodic air humidity behaviour can be assumed when evaluating the material moisture interaction thickness. For a given material, equation 3.6 can be solved numerically for the assumed indoor air humidity behaviour to determine the material interaction depth L_m. At L_m, the material is assumed to be impermeable to vapour flow while convective moisture transfer is taking place at the material surface as illustrated in Fig. 3.1.

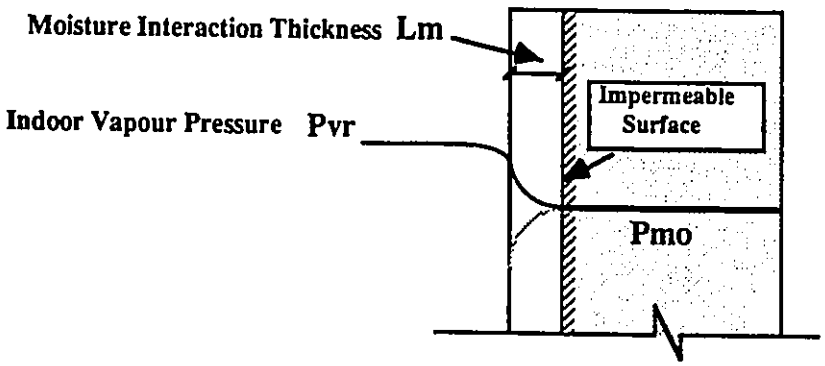

Fig. 3.1 Dynamic moisture interaction between the hygroscopic materials and the ambient air.

Since moisture absorption and desorption in buildings are alternating processes, and because of the relatively large moisture interaction thickness involved in modelling these processes, equation 3.6 must be solved for a nonuniform initial conditions. The governing boundary and initial conditions are given by equations 3.8a-3.8c. The exact solution of the above non-homogeneous mathematical problem can be obtained by splitting it up into a

$$\frac{\partial P_m}{\partial x} = 0 \qquad at \quad x = L_m \qquad (3.8a)$$

$$-D_v \frac{\partial P_m}{\partial x} = H_m \left(P_{vr} - P_m(0,t)\right) \qquad at \quad x = 0 \qquad (3.8b)$$

$$P_m = F(x) \qquad at \quad t = 0 \qquad (3.8c)$$

set of simpler problems that can be solved by the separation of variables method outlined in [137]. Utilizing this procedure, the variation of vapour pressure at the material surface can be expressed by:

$$P_m(0,t) = P_{vr} + \sum_{n=1}^{\infty} \exp(-\alpha_m \beta_n^2\, t).\frac{1}{N(\beta_n)}.\cos\beta_n L_m. \int_0^{L_m} (F(x') - P_{vr}).\cos\beta_n (L_m - x')dx' \qquad (3.9)$$

where,

$$\frac{1}{N(\beta_n)} = 2(\beta_n^2 + H^2)/[L_m(\beta_n^2 + H^2) + H]$$

$$H = H_m / D_v$$

and β_n are the roots of the following equation:

$$\beta_n \tan\beta_n L_m = H$$

The above exact solution involves an infinite series which requires the knowledge of the corresponding eigenvalues in order to evaluate. These eigenvalues are the roots of a transcendental equation which must be solved numerically. Moreover, equation 3.9 involves an integral that requires the knowledge of the initial function *F(x)* which in itself

will involve an infinite series and a similar integral if the solution is to handle a continuously changing boundary conditions. Such a procedure is too impractical and time consuming to be implemented as a part of an indoor moisture absorption/desorption model considering the dynamic and alternating nature of the problem and the number of materials that could be involved. Furthermore, with such a solution, the problem of moisture coupling between the indoor air and the material surface will be difficult to model as will be discussed in the next chapter. An alternative approach for solving equation 3.6 is the numerical analysis, however, by using such an approach, the moisture interaction between the material and the ambient air can not be accurately modelled, especially in a dynamic environment such as the building indoor environment. Moreover, considering the number of materials and the nature of the moisture transfer problem a large amount of computations would be needed. For example, when the finite-difference technique is used, hundreds of nodes could be required to formulate the moisture transfer process through the material. Consequently, hundreds of equations may have to be solved simultaneously at each time interval.

When the exact analytical solutions are difficult to obtain or when the numerical solution can not be justified, approximate analytic solutions are preferable. Considering the assumptions and the uncertainties involved in modelling moisture absorption and desorption in buildings, the use of the approximate analytic methods can be justified. The approximate analytic method that will be used to solve equation 3.6 is called the Moment Method [137]. This method is based on taking various moments of the differential equation of the moisture transfer with respect to a suitable weight function over the finite region of the problem. The mathematical formulation of the present problem can be put in terms of dimensionless variables; τ and η as:

$$\frac{\partial P_m(\eta,\tau)}{\partial \tau} = \frac{\partial^2 P_m(\eta,\tau)}{\partial \eta^2} \tag{3.10}$$

$$\frac{\partial P_m}{\partial \eta} = 0 \qquad at\ \eta = 1\ ,\ \tau > 0 \tag{3.10a}$$

$$-D_v \frac{\partial P_m}{\partial \eta} = H_m L_m \left(P_{vr} - P_m(0,\tau)\right) \qquad at\ \eta = 0\ ,\ \tau > 0 \tag{3.10b}$$

$$P_m(\eta,0) = F(\eta) \qquad at\ \tau = 0 \tag{3.10c}$$

The dimensionless quantities are defined as:

$$\eta = \frac{x}{L_m} \qquad and \qquad \tau = \frac{\alpha_m\, t}{L_m^2}$$

To solve this problem by the Moment Method, the pressure distribution $P_m(\eta,\tau)$ is expressed by a polynomial in the form given in equation 3.11.

$$P_m\,(\eta,\tau) = \sum_{k=0}^{n} a_k(\tau)\ \eta^k \qquad 0 < \eta < 1 \tag{3.11}$$

In order to determine *(n+1)* coefficients *($a_k(\tau)$, k=0,1,...n), (n+1)* relations are required. Two relations can be obtained by utilizing the two boundary conditions (3.10a) and (3.10b). The remaining *(n-1)* relations may be obtained by taking *(n-1)* moments of the differential equation 3.10. By operating the weight functions *$W_i(\eta)$, i= 1,2,...(n-1)*, on both sides of equation 3.10 and substituting in equation 3.11 we obtain the following equation [137]:

$$\sum_{k=2}^{n} \left[k(k-1)\int_{\eta=0}^{1} w_i(\eta)\,\eta^{k-2} d\eta\right] a_k(\tau) = \sum_{k=0}^{n} \left(\int_{\eta=0}^{1} w_i(\eta)\eta^k d\eta\right) \cdot \frac{da_k(\tau)}{d\tau} \tag{3.12}$$

$$i = 1,2,3,\ldots..(n-1)$$

Equation 3.12 provides a system of *(n-1)* ordinary differential equations that could be solved to determine the remaining *(n-1)* coefficients. Solving these equations, however, requires *(n-1)* initial conditions. These initial conditions can be determined by equation 3.13 [137].

$$\sum_{k=0}^{n} \left[\int_{\eta=0}^{1} w_i(\eta)\eta^k \, d\eta \right] a_k(0) = \int_{\eta=0}^{1} w_i(\eta)F(\eta)d\eta \qquad (3.13)$$

$$i=1,2,\ldots.(n-1)$$

3.3 Mathematical Formulations

For the present problem a fourth degree polynomial given by equation 3.11 is assumed.

$$P_m(\eta,\tau) = a_0(\tau) + a_1(\tau)\eta + a_2(\tau)\eta^2 + a_3(\tau)\eta^3 + a_4(\tau)\eta^4 \qquad (3.14)$$

Moisture absorption and desorption in buildings are dynamic and randomly alternating processes, consequently they can not be modelled by the analytic solution of equation 3.10. Instead, a numerical technique in conjunction with the analytic solution of equation 3.10 which describes these processes separately is the only feasible alternative. Through this approach, equation 3.9 with the corresponding boundary and initial conditions has to be solved at each time interval. Hence, the boundary and initial conditions have to be updated continuously.

Moisture absorption and desorption in buildings are long term processes, hence any pressure distribution across the moisture interaction thickness can be assumed as an initial condition for the first time interval of the modelling process. A uniform pressure distribution, as given by equation 3.15a, is assumed to represent the initial moisture status of the material. To insure continuity of the solution, the end conditions of a particular

interval, given by equation 3.15b, is taken as the initial conditions for the subsequent interval.

$$P_m(\eta,0) = P_{mo} \tag{3.15a}$$

$$P_m(\eta,0) = a_0 + a_1\eta + a_2\eta^2 + a_3\eta^3 + a_4\eta^4 \tag{3.15b}$$

In order to solve for the pressure distribution by equation 3.14, the surface pressure as a function of time $P_m(0,\tau)$ must be known. Unfortunately, this function cannot be determined directly because of the integral operations involved in the coefficient $a_0(\tau)$ in equation 3.14. However, since a numerical technique with relatively short time intervals is needed to model the absorption/desorption processes, it can be safely assumed that the surface vapour pressure $P_m(0,\tau)$ is linearly related with time during that time interval, t1.

$$P_m(0,\tau) = P_m(0,0) + \beta_p \tau \tag{3.16}$$

where,

$$\beta_p = \frac{P_m(0,\tau_1) - P_m(0,0)}{\tau_1}$$

$$\tau_1 = \frac{\alpha_m \, t1}{L^2_m}$$

Utilizing the initial conditions given by equations 3.15a-b, and the surface vapour pressure function given by equation 3.16, the time dependent coefficients in equation 3.14 can be determined by the Moment Method as:

$$a_1(\tau) = -Bi[P_d - \beta_p \tau] \tag{3.17}$$

$$a_0(\tau) = [168bl - 1008b2 + 1008b3 - \frac{14}{5}BiP_d - \frac{1}{15}Bi\beta_p]\exp(-52\tau) -$$
$$[217bl - 1302b2 + 1302b3 - \frac{1519}{420}BiP_d - \frac{217}{2520}Bi\beta_p]\exp(-42\tau) +$$
$$[55bl - 320b2 + 315b3 - \frac{13}{12}BiP_d - \frac{Bi}{24}\beta_p]\exp(-10\tau) + \quad (3.18)$$
$$bl + \frac{Bi}{3}P_d + \frac{Bi}{45}\beta_p + BiP_d\tau - \frac{Bi}{2}\beta_p\tau^2 - \frac{Bi}{3}\beta_p\tau$$

$$a_2(\tau) = [-1008bl + 6048b2 - 6048b3 + \frac{84}{5}BiP_d + \frac{2}{5}Bi\beta_p]\exp(-52\tau) +$$
$$[1218bl - 7308b2 + 7308b3 - \frac{203}{10}BiP_d - \frac{29}{60}Bi\beta_p]\exp(-42\tau) -$$
$$[330bl - 1920b2 + 1890b3 - \frac{13}{2}BiP_d - \frac{Bi}{4}\beta_p]\exp(-10\tau) - \quad (3.19)$$
$$\frac{1}{6}Bi\beta_p + \frac{Bi}{2}P_d - \frac{Bi}{2}\beta_p\tau$$

$$a_3(\tau) = \frac{1}{6}Bi\beta_p + \frac{32}{5}[1 - \exp(-10\tau)].$$
$$[-105bl + 630b2 - 630b3 + \frac{7}{4}BiP_d + \frac{Bi}{24}\beta_p]\exp(-42\tau) + \quad (3.20)$$
$$[220bl - 1280b2 + 1260b3 - \frac{13}{3}BiP_d - \frac{Bi}{6}\beta_p]\exp(-10\tau)$$

$$a_4(\tau) = [-105bl + 630b2 - 630b3 + \frac{7}{4}BiP_d + \frac{Bi}{24}\beta_p]\exp(-42\tau) \quad (3.21)$$
$$-\frac{Bi}{24}\beta_p$$

where,

$$P_d = P_{vr} - P_m(0,0)$$

b1, b2, b3 are expressed for the initial interval as:

$$b1 = P_{mo}\ ,\ b2 = \frac{P_{mo}}{2}\ ,\ b3 = \frac{P_{mo}}{3} \tag{3.22a}$$

and for the intermediate intervals as:

$$b1 = a_0(\tau_1) + \frac{a_1(\tau_1)}{2} + \frac{a_2(\tau_1)}{3} + \frac{a_3(\tau_1)}{4} + \frac{a_4(\tau_1)}{5}$$

$$b2 = \frac{a_0(\tau_1)}{2} + \frac{a_1(\tau_1)}{3} + \frac{a_2(\tau_1)}{4} + \frac{a_3(\tau_1)}{5} + \frac{a_4(\tau_1)}{6} \tag{3.22b}$$

$$b3 = \frac{a_0(\tau_1)}{3} + \frac{a_1(\tau_1)}{4} + \frac{a_2(\tau_1)}{5} + \frac{a_3(\tau_1)}{6} + \frac{a_4(\tau_1)}{7}$$

When the moment method is used to solve equation 3.10, difficulty may be experienced in satisfying the initial conditions. Consequently, solutions by this method may not be accurate for short times. The accuracy of the solution depend on the initial conditions, the type of boundary conditions and the degree of polynomial representation used. For uniform or linear initial pressure distribution, a third degree polynomial representation is sufficient to obtain a reasonably accurate solution provided that no convective transfer occurs at the boundaries. Higher polynomial representation is needed to solve for problems with more complicated initial conditions. However, with convective transfer at the boundaries, the accuracy of the solution becomes dependent on the ambient conditions, material surface conditions and the surface mass transfer coefficient. In this case, higher order polynomial representation will not enhance the accuracy in a decisive manner because of the variability of the ambient conditions, instead, solution oscillation may occur

for short time intervals. Although, the solution normally stabilizes with time, this behaviour is not acceptable when modelling short term moisture absorption and desorption problems (i.e., the material surface is suddenly exposed to higher or lower ambient vapour pressure). In order to avoid short term deviation in the solution, the initial conditions may have to be relaxed whenever there is a considerable sudden change in the ambient conditions. The relaxation process is performed by using the coefficients given by equations 3.17-3.21 to modify the values of b1, b2 and b3. These coefficients are recalculated by setting the coefficient a_0 and the surface vapour pressure $P_m(0,\tau_1)$ equals to the surface vapour pressure at the end of the previous interval, while the ambient conditions, P_m are set to its new value. New values of b1,b2 and b3 are then evaluated using equation 3.22b. These values will constitute the initial condition of the new moisture absorption or desorption problem.

The vapour pressure on the material surface at the end of each time interval t1 can be given by:

$$P_m(0,\tau) = \frac{A}{B} \tag{3.23}$$

where

$$\begin{aligned} A = & [-217b1 + 1302b2 - 1302b3 + \frac{1519}{420}BiP_d - \frac{217}{2520}Bi\frac{P_m(0,0)}{\tau_1}]\exp(-42\tau_1) + \\ & [168b1 - 1008b2 + 1008b3 - \frac{14}{5}BiP_d + \frac{Bi}{15}\frac{P_m(0,0)}{\tau_1}]\exp(-52\tau_1) + \\ & [55b1 - 320b2 + 315b3 - \frac{13}{12}BiP_d + \frac{Bi}{24}\frac{P_m(0,0)}{\tau_1}]\exp(-10\tau_1) + \\ & BiP_d\tau_1 + \frac{Bi}{2}P_m(0,0)\ \tau_1 + \frac{Bi}{3}P_m(0,0) + \frac{Bi}{3}P_d - \frac{Bi}{45}\frac{P_m(0,0)}{\tau_1} + b1 \end{aligned} \tag{3.24}$$

and

$$B = 1 + \frac{Bi}{2}\tau_1 + \frac{Bi}{3} - \frac{Bi}{45\tau_1} - \frac{217}{2520}\frac{Bi}{\tau_1}\exp(-42\tau_1) + \frac{Bi}{15\tau_1}\exp(-52\tau_1) + \frac{Bi}{24\tau_1}\exp(-10\tau_1) \quad (3.25)$$

For constant ambient conditions, the amount of moisture absorption or desorption during a time interval, t1 can be approximately given by equation 3.26.

$$M_m = H_m A_m \left(P_{vr} - \frac{P_m(0,\tau 1) + P_m(0,0)}{2}\right).t1 \quad (3.26)$$

The total moisture lost or gained within a room is given by equation 3.27.

$$M_{mi} = H_{ma}\sum_{i=1}^{n} A_{mi}\left(P_{vr} - \frac{P_{mi}(0,\tau 1) + P_{mi}(0,0)}{2}\right).t1 \quad (3.27)$$

where,

H_{ma}= average surface mass transfer coefficient, $kg/m^2 \cdot Pa \cdot s$

n= number of relevant materials in the room

The average surface mass transfer coefficient H_{ma} can be evaluated by Lewis relationship given in equation 3.2 using the average surface convective transfer coefficient.

3.4 Comparisons and Discussions

The proposed theoretical model for evaluating the surface moisture conditions of the material is compared with Kusuda's and Miki's experimental results of an absorption test on a 3 *mm* thick balsa wood specimen [65]. The specimen was exposed to constant ambient conditions of 24 *deg-C* and 70% relative humidity from both sides, thus half the specimen thickness (1.5 *mm*) is theoretically modelled. The material properties used

include; material density, moisture diffusivity, and the moisture equilibrium curve. For balsa wood, a density of 160 kg/m^3, and a moisture diffusivity of 1 10^{-10} m^2/s are used. Since the experiment is conducted within the moisture hygroscopic range of the material, the moisture sorption isotherm for wood, shown in Fig. 3.2, was used in modelling material moisture capacity. Although it is an important parameter in the modelling process, the value of surface mass transfer coefficient, H_m during the experiment is not known and can not be evaluated using Lewis relationship. However, the most likely value of the surface mass transfer coefficient in that particular environment (i.e. environmental chamber) can be determined. According to Kusuda [64], the average mass transfer coefficient in a room is estimated to be 5 10^{-9} $kg/Pa \cdot m^2 \cdot s$. However, in a test environmental chamber, the surface mass transfer coefficient will be dependent on the airflow regime within the space and the degree of exposure of the test specimen. The airflow regime within the test chamber is mainly determined by the method used for maintaining the air temperature and humidity. In an experimental validation program, Thomas and Burch [29], have evaluated the surface mass transfer coefficient within an environmental chamber using the cup method. A value of about 5 10^{-9} $kg/m^2 \cdot Pa \cdot s$ was found to represent the mass transfer coefficient at the specimen surface. Since this value corresponds to an ambient environment similar to Kusuda's test environment, it can be used in modelling the moisture behaviour of the balsa wood specimen. Fig. 3.3 compares the experimental results and the theoretical evaluation of the transient behaviour of the surface moisture conditions of the balsa wood specimen. It can be seen that there is a good agreement between the experimental and the theoretical results. However, a better agreement can be obtained when smaller surface mass transfer coefficient is used, since the theoretical curve will be shifted downward.

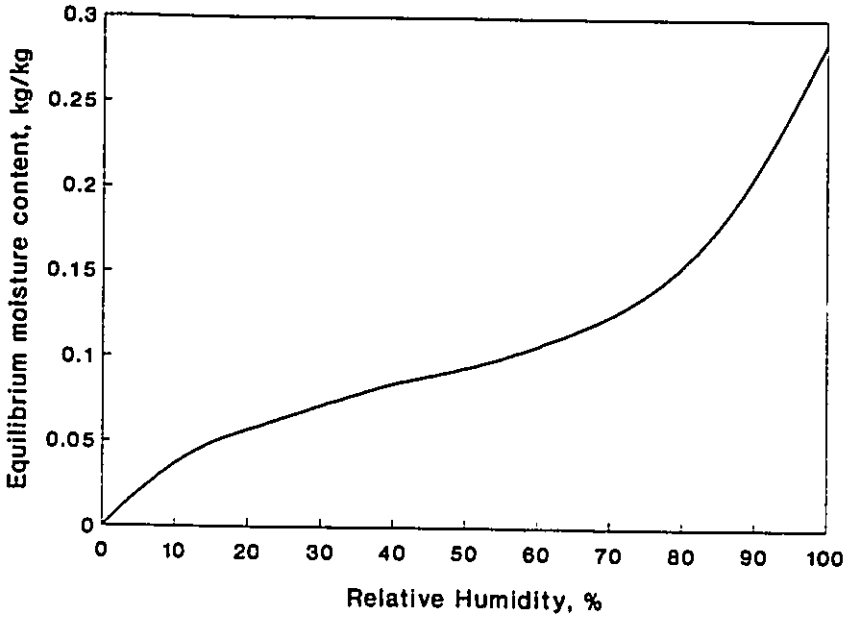

Fig. 3.2 Wood Moisture Absorption Isotherm [67].

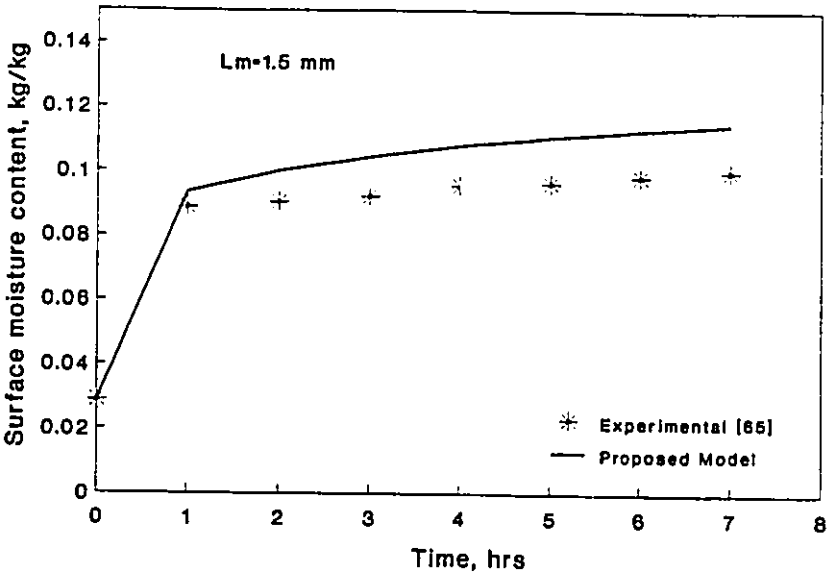

Fig. 3.3 Comparison between experimental results and theoretical prediction of surface moisture content.

The solution of the proposed model is also compared with the experimental results of a desorption test on a 13 mm thick gypsum board specimen [29]. In this experimental work, material moisture and physical characteristics, initial conditions, as well as, the surface mass transfer coefficient are clearly defined. The material moisture capacity is evaluated from its absorption isotherm given in Fig. 3.4. The density of the gypsum board is 670 kg/m^3, and its moisture diffusivity is about $1.8\ 10^{-8}\ m^2/s$. For this particular desorption test, a surface mass transfer coefficient of 0.0044 m/s, which corresponds to a value of $3.2\ 10^{-8}$ $kg/m^2 \cdot Pa \cdot s$, is used. The test specimen has an initial moisture content of .0079 kg/kg, which corresponds to about 74% relative humidity as can be found from Fig. 3.4. By exposing one side of the specimen (0.18 m in diameter), to a new ambient relative humidity of about 26% and regularly weighing the specimen, the desorption rates were determined. Experimental and theoretical evaluations of moisture desorption rates of the gypsum board specimen are shown in Fig. 3.5. It can be seen that the theoretical solution is in satisfactory agreement overall except at the beginning of the process. This can be attributed to measurement uncertainties at the beginning of the experiment and the sensitivity of the mass balance scale used [29].

The proposed model can accurately describe material surface moisture response to varying ambient conditions. Hence, it can be implemented to predict moisture absorption and desorption in buildings. In order to demonstrate the capabilities of the proposed model, its prediction of material surface moisture behaviour is compared with the numerical solutions using the finite-difference implicit formulations under different boundary conditions as illustrated by Fig. 3.6 through Fig. 3.9. The two materials used (i.e., gypsum and wood) represent two common building materials with completely different moisture characteristics. Fig. 3.6 shows the variation of the vapour pressure at the surface of a 2

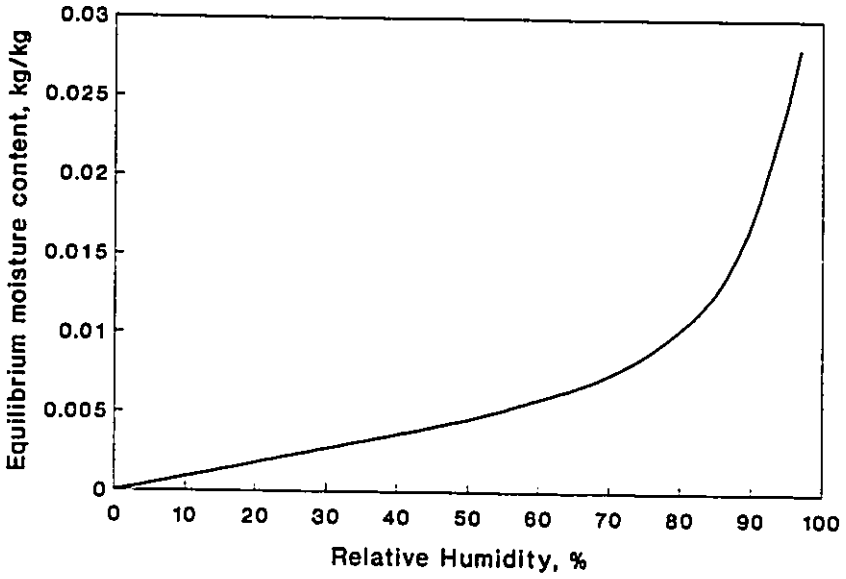

Fig. 3.4 Gypsum Board Absorption Isotherm [29].

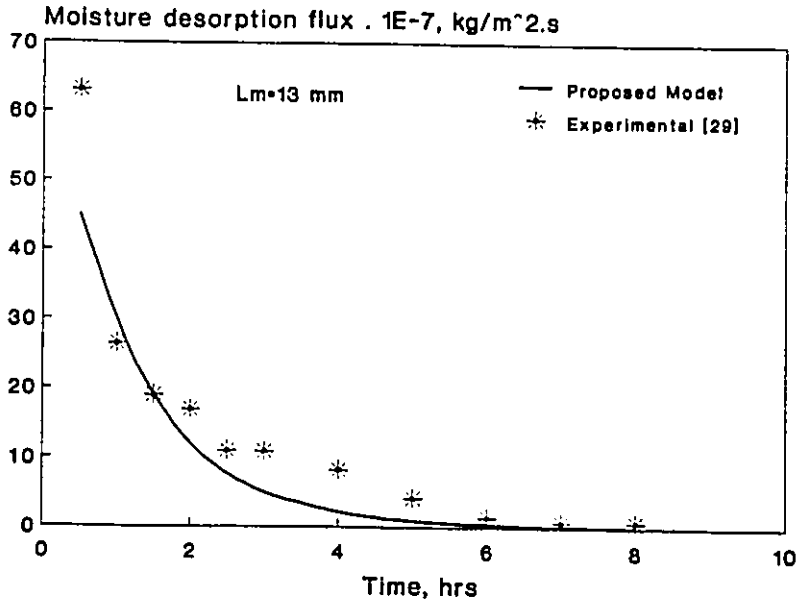

Fig. 3.5 Comparison between experimental results and theoretical prediction of moisture desorption rates.

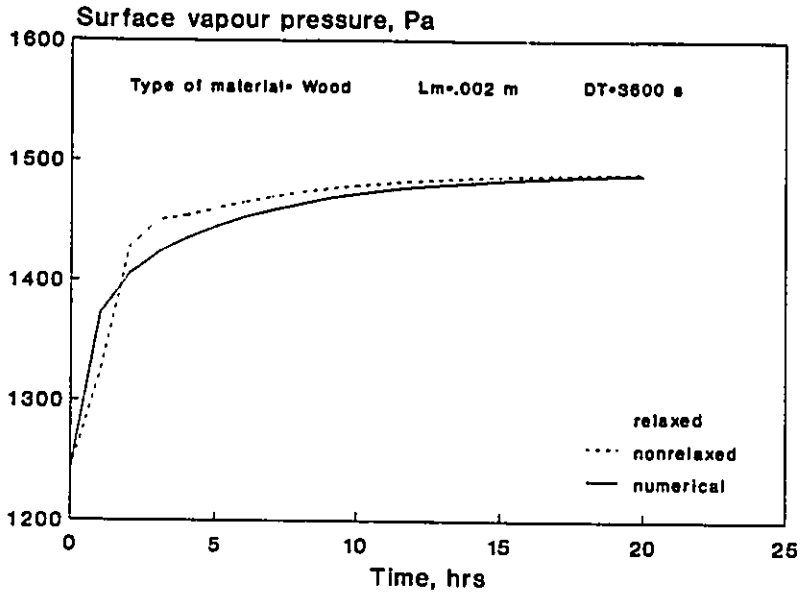

Fig. 3.6 Predicted surface vapour pressure of a wood board using proposed and numerical techniques when ambient conditions are suddenly changed.

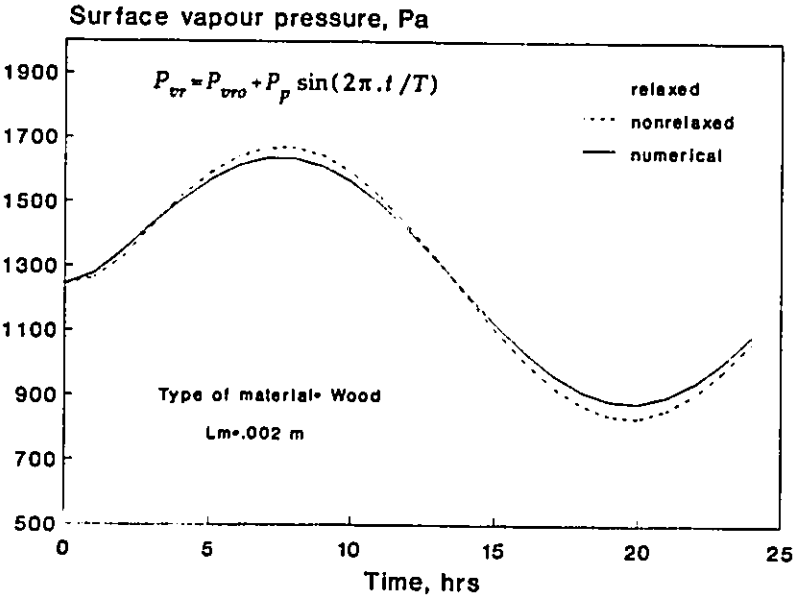

Fig. 3.7 Predicted surface vapour pressure of a wood board using proposed and numerical techniques when periodic ambient conditions are applied.

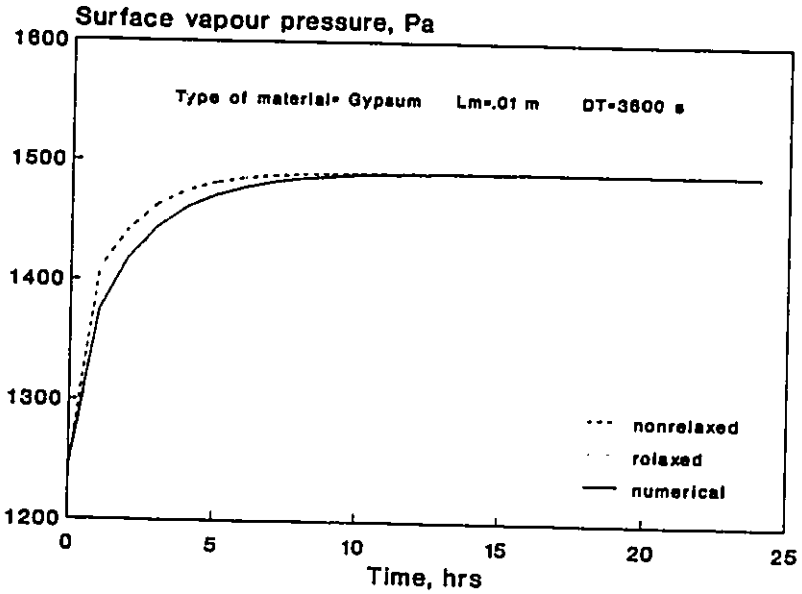

Fig. 3.8 Predicted surface vapour pressure of a gypsum board using proposed and numerical techniques when ambient condition is suddenly changed.

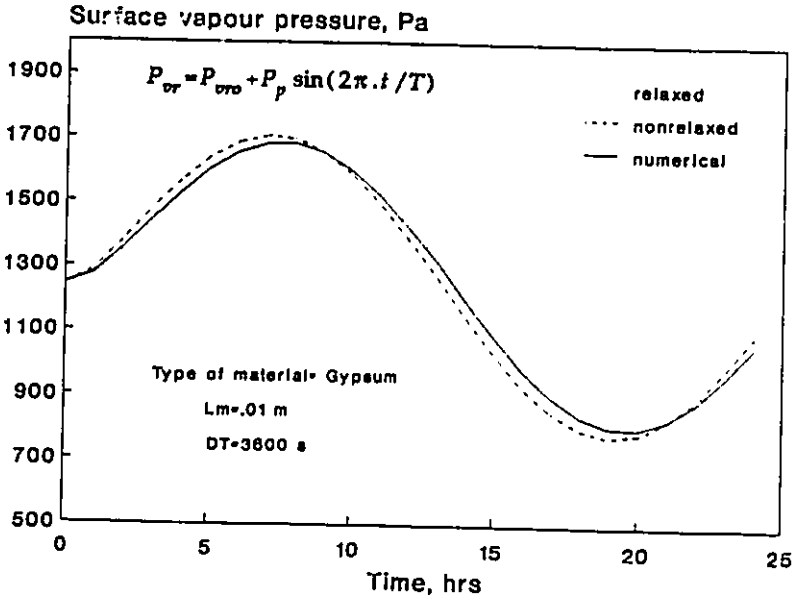

Fig. 3.9 Predicted surface vapour pressure of a gypsum board using proposed and numerical techniques when periodic ambient conditions are applied.

mm thick board when the ambient relative humidity is suddenly changed from 50% to 60%. It can be seen that almost perfect agreement is obtained between the numerical solution and the model prediction when the initial condition is relaxed while poor agreement is obtained at the beginning of the solution when no relaxation is implemented. Similar conclusions can be drawn from Fig. 3.7 when the material is exposed to a daily periodic ambient conditions (P_{vro}=0.5 P_{vs}, P_p=0.1 *Pvs*, *T*=24 *hrs*). The non-relaxed solution does not show considerable deviation from the numerical solution as compared to the case when sudden change in ambient conditions occurs. When similar comparisons are carried out for a 10 *mm* gypsum board, the same kind of responses are obtained for both sudden and periodical variations of ambient conditions as shown in Figures 3.8-3.9.

The moisture interaction thickness, L_m of a particular material depends on its moisture characteristics as well as the type and behaviour of ambient conditions. For materials having high hygroscopic moisture capacity or low moisture diffusivity such as wood, moisture interaction between the material and the ambient air will be limited to a very thin layer at the material surface. On the other hand, moisture penetrates deeper in materials having a relatively high moisture diffusivity such as gypsum which result in larger moisture interaction thickness. The material thickness as used for wood and gypsum in the above discussion are practically reasonable to represent the dynamic moisture interaction between the material and the ambient indoor environment in most buildings. However, for the model to be generally applicable, it must be able to accommodate larger dynamic moisture capacity for different materials. By increasing the moisture interaction thickness of wood to 5 *mm*, the prediction of the proposed model deviates considerably from the numerical solution with and without the implementation of the relaxation strategy as illustrated in Fig. 3.10. However, by reducing the time step, DT from 3600 s to 300 s, the

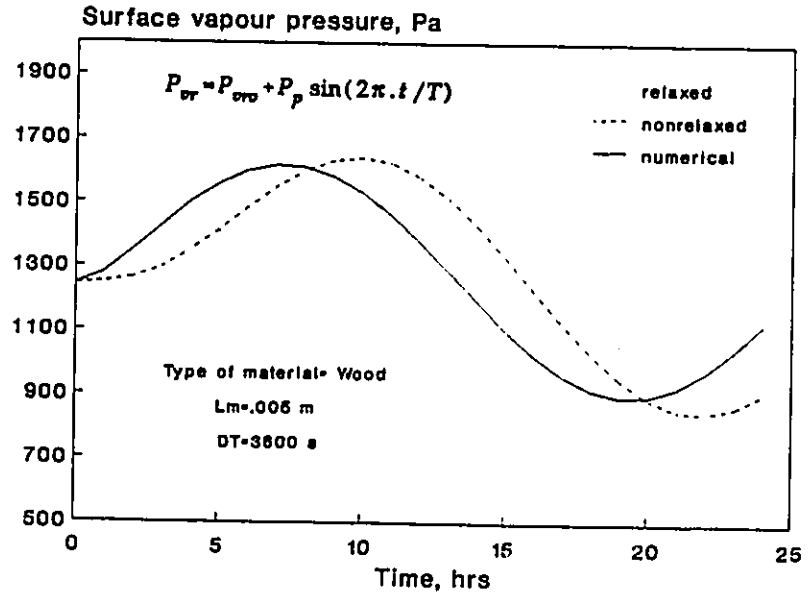

Fig. 3.10 Comparison between numerical and proposed solutions when a time step of 3600 seconds is used.

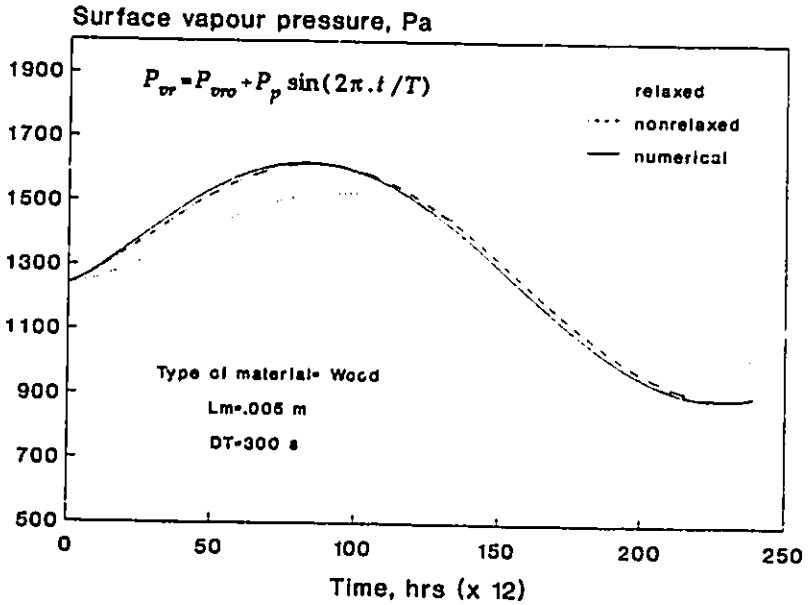

Fig. 3.11 Comparison between numerical and proposed solutions when a time step of 300 seconds is used.

non-relaxed solution is almost identical to the numerical solution while the relaxed solution is still deviating although noticeable improvement is achieved as shown in Fig. 3.11. The non-relaxed solution remains in good agreement with the numerical solution even at much higher moisture interaction thicknesses for both wood and gypsum as shown in Figs. 3.12-3.13 when L_m=20 *mm* for wood and L_m=30 *mm* for gypsum. The accuracy of the solution is improved when a smaller time step is used since smaller corresponding change in ambient conditions is considered for the solution. This means that larger time step can be used, provided no considerable fluctuation occurs during this period. Consequently, the choice of the time step will depend on the expected behaviour of the ambient conditions. In most buildings, short term fluctuations in indoor air humidity are not expected to be substantial, hence the use of a larger time step (i.e., one hour) can be justified. However, it can be generally said that when modelling moisture absorption and desorption in buildings, a smaller time step will always result in better agreement with the numerical solutions.

For the above theoretical modelling of material moisture behaviour, constant values are used to describe material moisture capacity C_m, and material moisture diffusivity α_m. In reality, both vary with the moisture content. The material moisture capacity (which is equivalent to the specific heat in thermal analysis) varies with equilibrium relative humidity according to the slope of the moisture sorption isotherm. In practice, when the relative humidity range in interest is relatively small, or when the slope of the sorption isotherm does not exhibit considerable variations within the range of interest, then a constant moisture capacity can be used in modelling dynamic moisture behaviour of materials. Similarly, when the material moisture content varies within a limited range, such as materials within the building indoor environment, a constant moisture diffusion coefficient

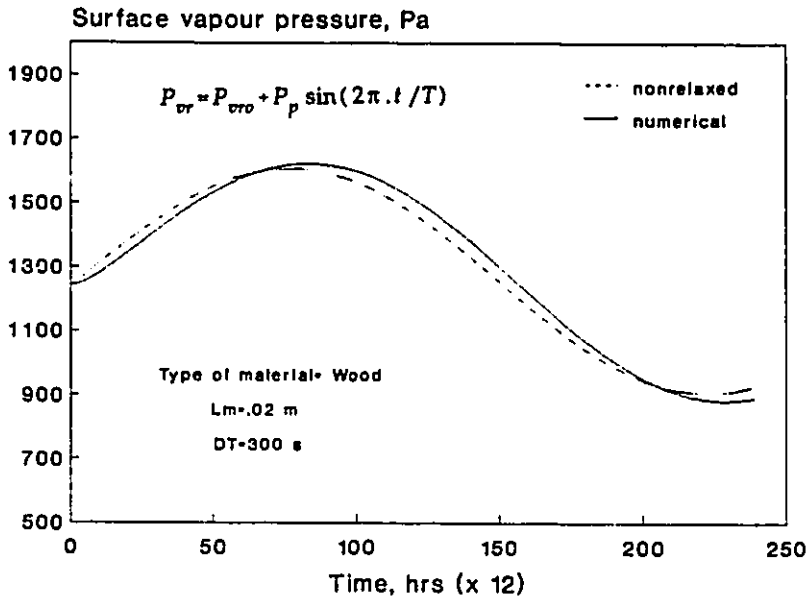

Fig. 3.12 Comparison between numerical and proposed solutions for a relatively larger moisture interaction thickness.

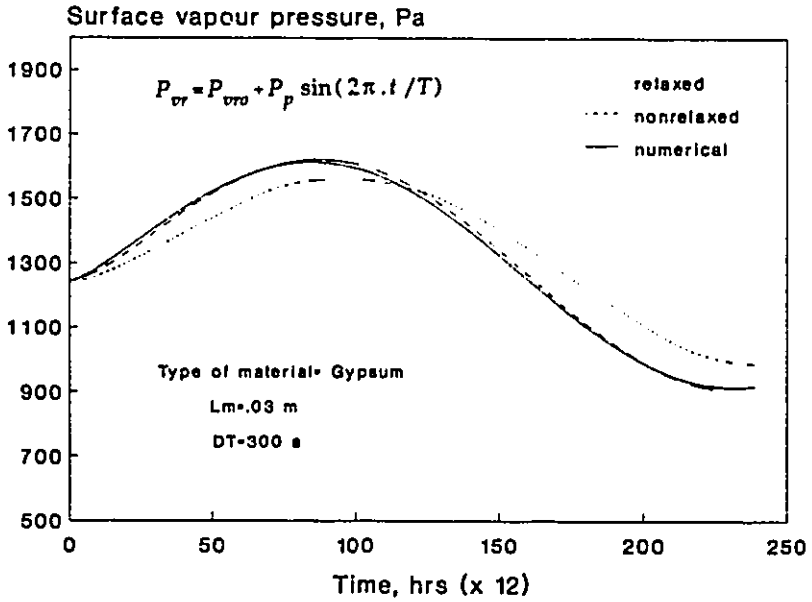

Fig. 3.13 Predicted surface vapour pressure of a gypsum board using proposed and numerical techniques when larger moisture interaction thickness is used.

can be used to describe moisture transfer through the material. However, for more accurate dynamic moisture modelling, the variability of the material moisture capacity and its moisture diffusion coefficient has to be considered whenever it is practically possible.

In order to implement the proposed model for predicting moisture absorption and desorption in buildings, the moisture interaction thickness, L_m must be identified for each interior material. Its value can either be determined by the physical and geometrical characteristics of the material or by the type of behaviour of boundary conditions. In the building indoor environment, however, air humidity normally fluctuates around a daily average in a periodical manner. Such behaviour will limit the penetration of moisture within the material to a certain depth beyond which no significant amount of moisture is stored. Fig. 3.14 shows the variations of the moisture interaction thickness with material moisture characteristics and the mass surface transfer coefficient for a daily periodic boundary condition. It can be seen that the moisture interaction thickness is directly promotional to the material moisture diffusivity and the surface transfer coefficient. For a gypsum board with a moisture diffusivity of 1.8 10^{-8} m^2/s, and a surface transfer coefficient of 3 10^{-9} $kg/m^2 \cdot Pa \cdot s$, the moisture interaction thickness can be found from Fig. 3.9 to be 0.026 m. This thickness will determine the moisture storage capacity of the gypsum board, and hence the moisture interaction between the material and the indoor environment. Fig. 3.15 shows the response of the surface vapour pressure of a gypsum board for different moisture interaction thicknesses, L_m under daily periodic boundary conditions with a maximum relative humidity periodic fluctuation of 20%. It can be seen that there is a relatively noticeable difference in the material surface moisture behaviour when a moisture interaction thickness of 0.02 m is used instead of 0.026 m. On the other hand, for a moisture interaction thickness larger than 0.026 m, the surface moisture responses are

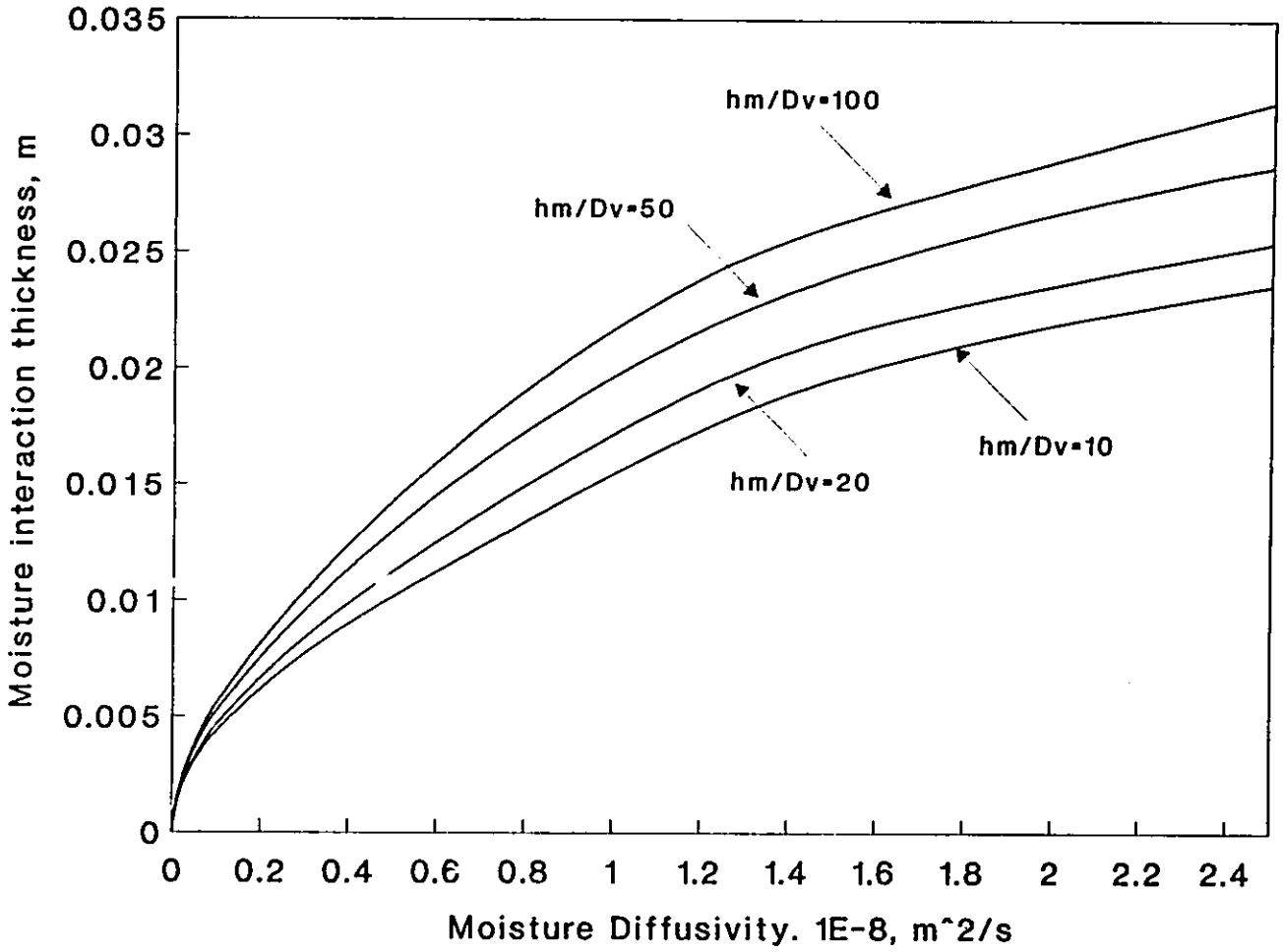

Fig. 3.14 Relationship between moisture interaction thickness and material moisture diffusivity.

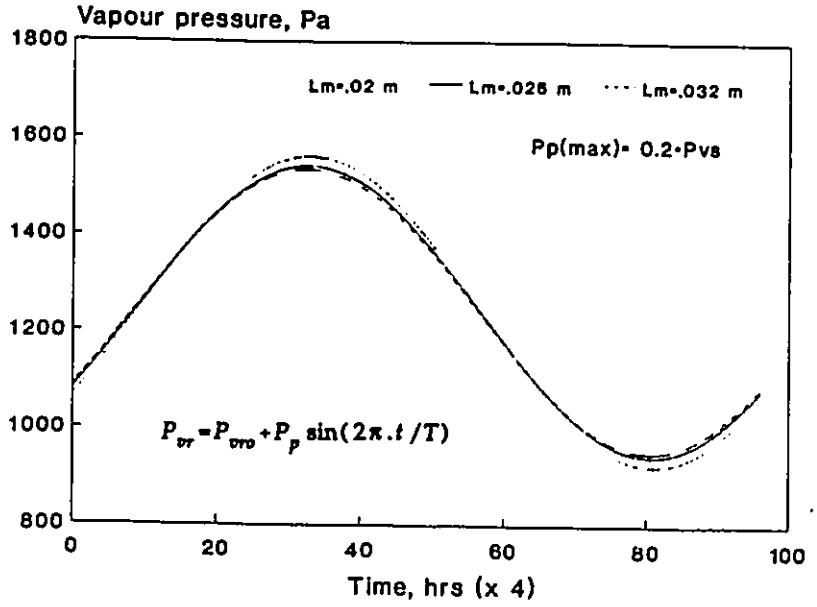

Fig. 3.15 Variation of vapour pressure at material surface due to periodic boundary conditions for different moisture interaction thicknesses.

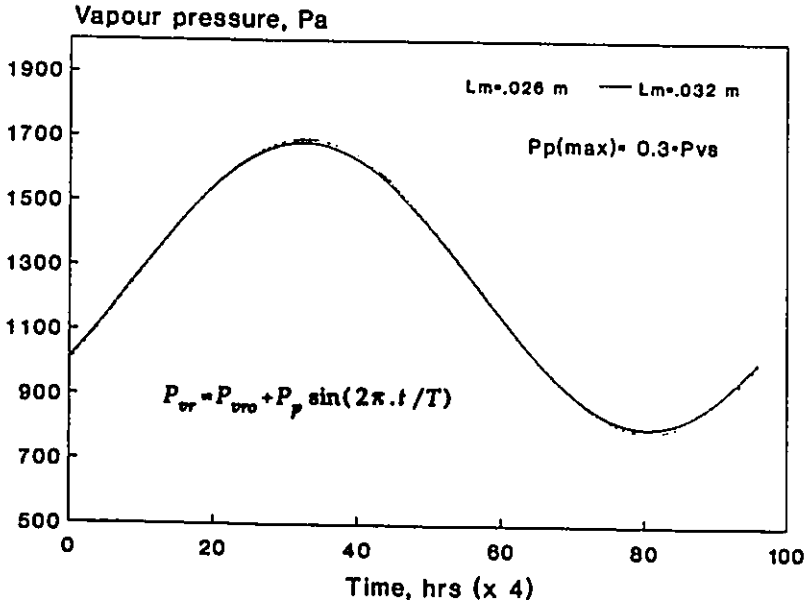

Fig. 3.16 Variation of vapour pressure at material surface under periodic boundary conditions when the peak value is increased by 50%.

in phase and with minor deviation experienced between them. This means that increasing the moisture interaction thickness beyond a certain value, which is evaluated from Fig. 3.14, will not increase the dynamic moisture capacity of the material and will not affect its moisture behaviour at the surface. For periodic boundary conditions, the moisture interaction thickness is not greatly influenced by the magnitude of the periodic fluctuation, but rather by the frequency of fluctuation. By increasing the maximum relative humidity periodic fluctuation to 30%, the moisture interaction thickness of 0.026 will still be able to characterize the material moisture behaviour as shown in Fig. 3.16, where it can be seen that increasing L_m by 0.006 *m* will have almost no effect on moisture behaviour at the material surface. However, it must be noted that higher frequency of fluctuation will result in smaller moisture interaction thickness, while lower frequency will result in a larger moisture interaction thickness.

3.5 Summary

Moisture absorption and desorption by interior materials is the most difficult time-dependent moisture transport process to model because of the moisture coupling which exists between the indoor air and the interior materials surfaces, in addition to the wide range of materials that could be available in the space. Interior materials with different moisture and physical characteristics interact differently with the indoor air, and will have different moisture responses when exposed to dynamic ambient conditions. Some materials attain instant moisture equilibrium with the surroundings, others will not respond at all. The Biot number, *Bi*, was used to classify materials according to their moisture and geometrical properties. Hence, the material moisture behaviour can be identified and appropriately modelled. As *Bi* approaches zero, a lumped- parameter analysis can be used to model material moisture behaviour, in this case a resistor-capacitor analogy can

be used. When Bi is very large, the material can be assumed passive since a negligible amount of moisture is transported to or from the material. In most cases, however, moisture interaction with the material occurs near the surface ($0<Bi<\infty$), resulting in a nonuniform moisture content distribution across the material moisture interaction thickness, L_m. In this case, determining the material surface moisture conditions is the main task in modelling moisture absorption and desorption processes. In this study, a practical and an efficient analytic-numeric technique for evaluating the material surface moisture conditions is proposed and validated against experimental results. The required parameters in the proposed model are mainly the material moisture properties which are normally available in literature for all common building materials, giving it an advantage over many existing models which require either extensive experimental work or unavailable material moisture properties. In addition, the proposed model has some advantages over numerical techniques by requiring less computations and being able to more accurately describe the moisture interaction between the ambient conditions and the material surface.

As part of a numerical formulation, this analytic-numeric method can be used to model moisture absorption and desorption by construction and furnishing materials in building. Both the dynamic and the alternating nature of these processes can be modelled. Although the proposed method cannot accurately model material response to sudden changes in ambient conditions for short times, it has been modified to tolerate such dynamic behaviour by relaxing the initial moisture conditions of the material. The solution resulting from such a procedure has been shown to be more accurate than the direct solution (i.e., no relaxation of initial conditions) for typical moisture interaction thicknesses of different materials. However, in order to model larger dynamic moisture capacity of the material, the non-relaxed solution was found to be more accurate when a relatively smaller

time step is used. Comparison with experimental results and numerical technique solutions shows good agreement with the proposed model. Using this model in conjunction with a numerical formulation, the dynamic effect of moisture absorption and desorption by interior materials on indoor air humidity can be modelled.

CHAPTER 4

MODELLING OF INDOOR AIR HUMIDITY: THE DYNAMIC BEHAVIOUR WITHIN AN ENCLOSURE

4.1 Introduction

Indoor air humidity is a major factor in determining the quality of the indoor environment as well as the building moisture and energy performance. Very high or very low humidity levels can lead to undesirable consequences ranging from occupants thermal discomfort to major health related problems [138]. In cold climates, high indoor humidity is normally associated with objectionable surface condensation on windows, and damaging interstitial condensation within the building envelope components. Furthermore, when indoor humidity is to be maintained at a constant level, either humidification or dehumidification is required resulting in additional energy consumption in both cases. In buildings where there is no humidity control, air humidity level depends on the natural balance between moisture gains and losses resulting from many time-dependent moisture transport processes. Indoor moisture generation and surface condensation are examples of these processes. Moisture generation in the space depends on many factors related to the type of activities performed in the space as well as the occupants life style and habits. In a residential building, an average of one gallon of water per occupant may be added daily to the indoor air by occupants and household related activities [22]. Surface condensation, on the other hand, is mainly dependent on the thermal characteristics of the condensation surface. In winter, the interior surface of a window could act as a dehumidifier removing a lot of water vapour from the space.

The relative impact of the different moisture transport processes is mainly determined by the outdoor climatic conditions as well as the building physical and functional characteristics. In cold climates, where infiltration rates are significantly reduced, the condensation and the absorption processes are expected to be the main natural moisture sinks within the building. In moderate climates, where air ventilation is put to maximum, indoor air humidity will follow the trend of the outdoor air conditions. Moisture absorption and desorption by interior materials as well as air infiltration are the main influencing processes in hot-humid climates although they may not be simultaneously active. At night when outdoor temperature is lower, more outdoor air is normally allowed indoors. During this process a lot of moisture is absorbed from the outdoor air and stored in the various materials within the space. At higher outdoor temperatures, when the air ventilation is reduced, the desorption process becomes active by releasing the stored moisture into the indoor air.

Models for indoor humidity calculations have been developed [64,68,80], however, a comprehensive theoretical model which accommodates all relevant moisture transport processes has not been available. The main objectives to be achieved in this chapter are to develop a mathematical model for predicting air humidity transient behaviour within single-zone enclosures, and to theoretically study air humidity response to the different moisture transport processes. Air humidity behaviour within an enclosure is described by a linear differential equation which includes; moisture absorption/desorption processes, air movement, surface condensation, indoor evaporation, moisture generation, and dehumidification processes. All the processes involved are nonlinear in behaviour, and hence the differential equation was solved as part of a numerical formulation by using a discrete time step during which linear behaviour can be assumed for all processes.

Numerical solution of the differential equation is performed by the Runge-Kutta method.

4.2 Model Logic and Development

4.2.1 Conceptual approach: Moisture content of the air inside occupied buildings is typically in a dynamic state. Many time-dependent processes such as, surface condensation, ventilation and absorption by interior materials, will determine the moisture content of indoor air and contribute to its dynamic behaviour as illustrated by the schematic shown in Fig. 4.1.

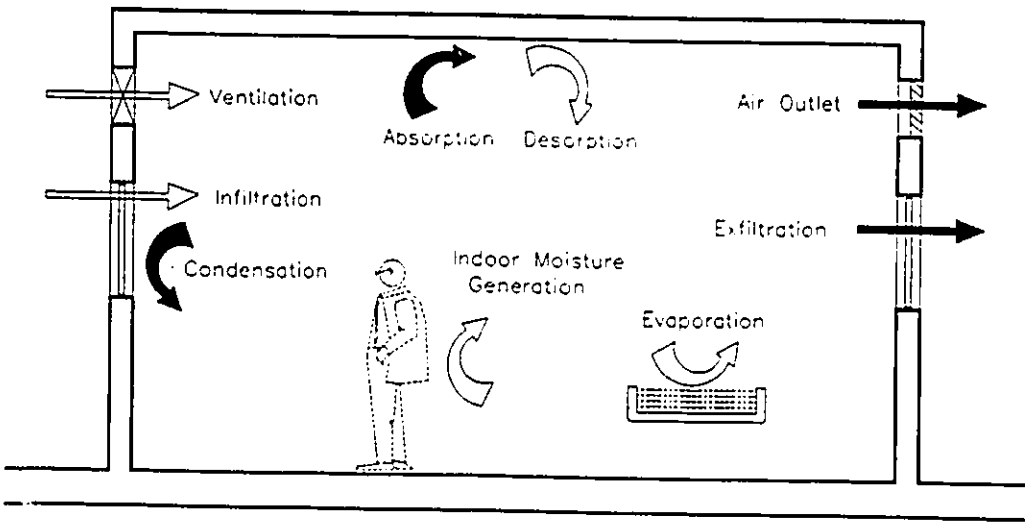

Fig. 4.1 A Schematic for Moisture Transport Processes within a Building Enclosure.

When indoor humidity is not mechanically controlled, its level is determined by the natural balance between moisture gains and losses within the space. Based on the moisture mass balance concept, the transient response of air moisture content inside a room can

be generally modelled via the following linear differential equation;

$$\frac{dW_r}{dt} = \frac{1}{\rho_a V}\left[\sum_{i=1}^{ns}\frac{dms_i}{dt} + \sum_{i=1}^{na}\frac{dma_i}{dt} + \sum_{i=1}^{nc}\frac{dmc_i}{dt} + \sum_{i=1}^{nv}\frac{dme_i}{dt} + \sum_{i=1}^{ng} mg_i + \frac{dmm}{dt}\right] \quad (4.1)$$

where,

dW_r/dt= rate of change in indoor air moisture content, *kg/kg·s*

dms/dt= rate of moisture absorption or desorption by interior materials, *kg/s*

dma/dt= rate of moisture added or removed due to air movement across room boundaries, *kg/s*

dmc/dt= rate of moisture removed by condensation, *kg/s*

dme/dt= rate of moisture added by evaporation, *kg/s*

mg= rate of moisture generation from indoor sources (i.e. people, indoor operations, etc.), *kg/s*

dmm/dt= rate of moisture removed by coil dehumidification, *kg/s*

For Equation 4.1 to be solved, several time-dependent parameters, which are needed to model the processes involved, must be expressed in terms of time. However, because of the transient nature of boundary conditions and the complexity of some processes, the variations of corresponding parameters cannot be expressed in terms of time in a continuous function. Moreover, Equation 4.1 involves many transient nonlinear moisture transport processes which are interrelated in a complicated manner. Therefore, Equation 4.1 can only be solved as an integral part of a comprehensive numerical technique through which the interrelation between the processes involved can be modelled. Depending on the room physical and functional characteristics, its air moisture content behaviour can be determined by one or more of the processes described by Equation 4.1.

In a real situation a combination of these processes will normally determine the state of the indoor air moisture content.

4.2.2 The time-dependent processes affecting indoor air humidity

I) Moisture absorption and desorption

When moisture absorption and desorption by interior materials are the only determining processes, the room air humidity response can be given by:

$$\frac{dw_r}{dt} = \frac{A_m h_{ms}}{\rho_a V}(W_m - W_r) \tag{4.2}$$

The material moisture conditions, W_m and room air conditions, W_r in Equation 4.2 are interdependent parameters. For materials where lumped-parameter analysis can be used (i.e. Bi≤ 0.1), to describe their dynamic moisture interaction, the surface air moisture content, W_m can be given by Equation 4.3:

$$\frac{dW_m}{dt} = (\frac{A_m h_{ms}}{R_v \rho_a V_m C_m T_m})(W_r - W_m) \tag{4.3}$$

Equations 4.2 and 4.3 represent a pair of coupled differential equations that describe the dynamic moisture interaction between room air humidity and a given material within the space. Utilizing Laplace transformation, this system of differential equations can be solved to give:

$$W_r = W_{ro}\exp[-(B+C)t] + (\frac{C W_{mo} + B W_{ro}}{C+B})[1-\exp(-(B+C)t)] \tag{4.4}$$

where,

$$B = \frac{A_m h_{ms}}{R_v \rho_a V_m C_m T_m}$$

$$C = \frac{A_m h_{ms}}{\rho_a V}$$

Equation 4.4 describes the air humidity response to moisture absorption/desorption by one single material which can be modelled by the lumped-parameter analysis. For each material within the space a separate differential equation must be written. To determine the air humidity response, the resulting differential equations must be solved simultaneously with Equation 4.2. As the number of differential equations increases, analytical solution becomes more complicated and more difficult to obtain. For most interior materials a lumped-parameter analysis is not possible, hence their moisture behaviour can not be directly modelled as in Equation 4.3. In addition, other moisture transport processes within the space, which can not be accounted for analytically, are indirectly affecting material's moisture conditions.

When Equation 4.2 is used as a part of a numerical formulations, it can be directly solved by assuming that W_m is constant during the time step used in the modelling. However, for most building materials, in order to assume a constant surface moisture conditions, the time step must be taken so small that the solution becomes impractical and the accumulative error becomes unacceptable for large modelling periods. When a practically large time step is used, the variability of W_m during the time step must be modelled. Assuming constant W_r during the time step, then for material where lumped-parameter analysis can be used, the material surface air moisture content can be given by:
Substituting Equation 4.5 into 4.2 and solving the resulting equation yields:

$$W_m(t) = W_r - (W_r - W_{mo})\exp(-Bt) \tag{4.5}$$

$$W_r(t) = W_{mo} + (W_{ro} - W_{mo})\exp[-\frac{C}{B}(1 - \exp(-Bt))] \tag{4.6}$$

Equation 4.6 describes the dynamic behaviour of indoor air humidity during the time step used in the numerical formulation. For a 600 m^3 enclosure, the exact air humidity response to moisture absorption by interior building materials given by equation 4.4 is compared with the solution of equation 4.6 when used as part of a numerical formulation. Fig. 4.2 shows very good agreement between the two equations when a time step of one hour is used. Full agreement is obtained when the time step is reduced to six minutes as shown in Fig. 4.3. For practical consideration, however, a time step of one hour is considered more appropriate. Both the material moisture condition, W_{mo} and the indoor air humidity condition, W_{ro} in equation 4.6 have to be updated at the end of each time interval. Equation 4.5 is used to evaluate material moisture conditions at the end of each time interval by using the time step average air moisture content, W_{ra}.

When moisture interaction occurs at the material surface (i.e. $Bi \neq 0$), a lumped-parameter analysis cannot be used because of the non-uniformity of moisture conditions across the material thickness. Instead, moisture interaction between the material and the ambient air can be expressed in terms of the air humidity ratio by Equations 4.7 through 4.7c. These equations describe the transient moisture transfer problem through the material and the corresponding boundary and initial conditions. Solution of the above mathematical problem in terms of vapour pressure has been discussed in Chapter 3.

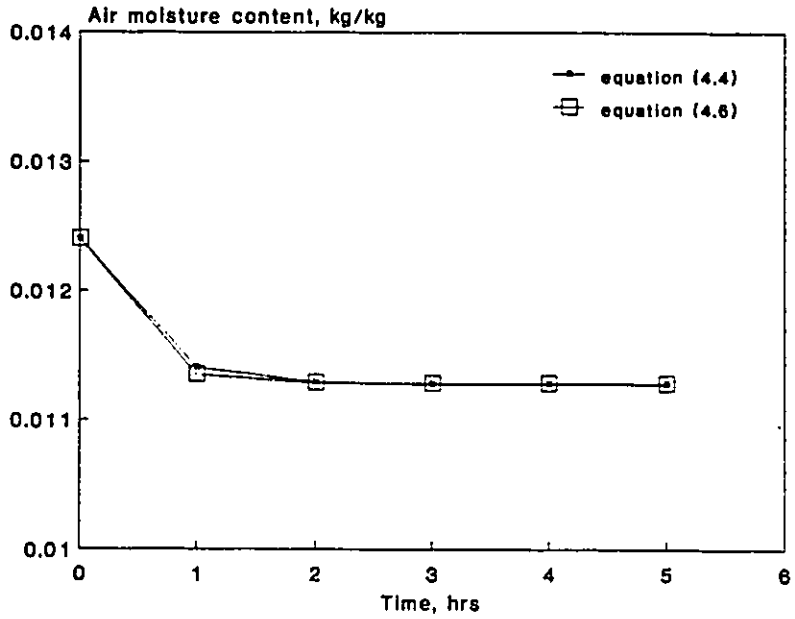

Fig. 4.2 Response of indoor air humidity to moisture absorption by interior materials using exact and proposed solutions for a time step of 1 hour.

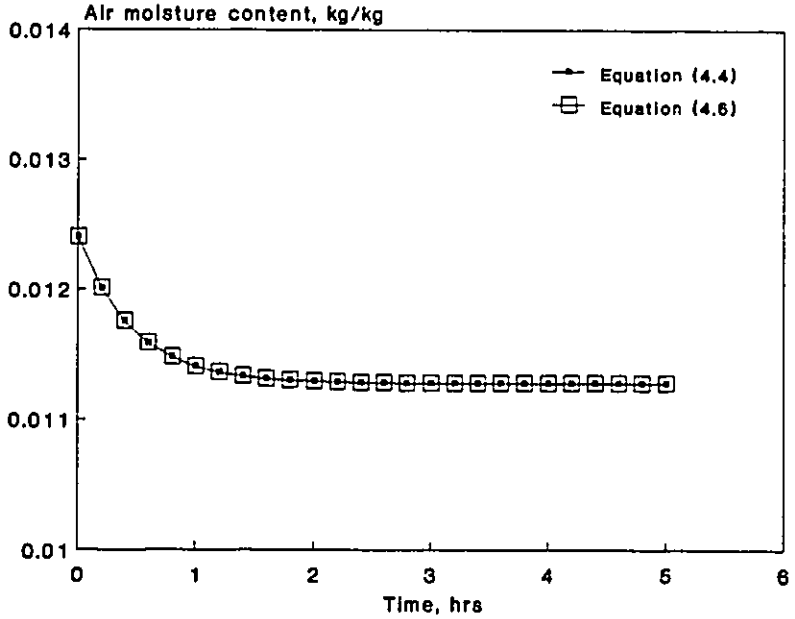

Fig. 4.3 Response of indoor air humidity to moisture absorption by interior materials using exact and proposed solutions for a time step of 1/10 hour.

$$\frac{\partial W_m}{\partial t} = \alpha_m \frac{\partial^2 W_m}{\partial x^2} \tag{4.7}$$

$$\frac{\partial W_m}{\partial x} = 0 \qquad at \quad x = L_m \tag{4.7a}$$

$$-D_v \frac{\partial W_m}{\partial x} = h_{ms}(W_r - W_m) \qquad at \quad x=0 \tag{4.7b}$$

$$W_m = F(x) \qquad at \quad t=0 \tag{4.7c}$$

The approximate analytic solution was obtained as part of a numerical solution using a discrete time step t. The surface air moisture content at the end of the time step can be determined by equation 4.8.

$$W_{ms}(t) = \left(\frac{1}{R_v T_m \rho_a}\right).P_m(o,\tau) \tag{4.8}$$

where, $P_m(0,\tau)$ is the vapour pressure at the material surface as defined by Equation 3.23 in Chapter 3.

Indoor air moisture content can be expressed by combining Equations 4.2 and 4.8 yielding:

$$\frac{dW_r(t)}{dt} = \frac{A_m h_{ms}}{\rho_a V}[W_{ms}(t) - W_r] \tag{4.9}$$

Equation 4.9 can be solved numerically to evaluate room air humidity response to moisture absorption and desorption. In reality, many materials with different moisture characteristics could exist inside a space within a building. The combined moisture interaction of these materials with indoor air humidity will determine its dynamic behaviour as given by:

$$\frac{dW_r}{dt} = \sum_{i=1}^{ns1} C_i (W_{moi} - W_r) \exp(-B_i t) + \sum_{j=1}^{ns2} C_j (W_{ms}(t) - W_r) \qquad (4.10)$$

II) Air movement across enclosure boundaries

Moisture transport associated with air movement is the fastest, and thus is the most important mode of moisture transport in buildings. Depending on the flow rate and the humidity conditions of the outdoor air, indoor air humidity could instantly and dramatically respond to air movement across enclosure boundaries. The response of indoor air humidity to air movement across enclosure boundaries (i.g. infiltration) can be expressed by equation 4.11.

$$\frac{dW_r(t)}{dt} = \frac{Q_a}{V \rho_a} [W_o - W_r(t)] \qquad (4.11)$$

For constant external conditions, Equation 4.11 can be solved to give:

$$W_r(t) = W_o + (W_{ro} - W_o) \exp(-\frac{Q_a}{V \rho_a} t) \qquad (4.12)$$

In practice, air flow across enclosure boundaries could occur through several different flow paths under different driving forces at the same time. For a given space within a building, air flow could occur through its exterior boundaries as well as through inter-space flow paths connecting it with other spaces (i.g. a door way). Air flow across exterior boundaries may occur due to a natural driving force through an arbitrary flow path (i.e. infiltration / exfiltration), or due to a controlled driving force (i.e. ventilation). Each air flow process across the enclosure boundaries will have a unique effect on the behaviour of air humidity inside the enclosure. For a combination of air flow processes, the dynamic behaviour of

indoor air moisture content can be given by:

$$W_r(t) = \sum_{i=1}^{na} \frac{Q_{ai} W_{oi}}{\sum_{i=1}^{na} Q_{ai}} + [W_{ro} - \sum_{i=1}^{na} \frac{Q_{ai} W_{oi}}{\sum_{i=1}^{na} Q_{ai}}] . \exp[-(\sum_{i=1}^{na} \frac{Q_{ai}}{V \rho_a})t] \qquad (4.13)$$

III) Surface condensation

Water vapour in an enclosure will condense on interior surfaces having a temperature less than the saturation temperature of the surrounding air. A cold surface, such as a window, could act as a major moisture sink removing a lot of moisture from the indoor air. The dynamic response of indoor air moisture content to surface condensation is given by:

$$\frac{dW_r(t)}{dt} = \frac{h_{mc} A_c}{\rho_a V} [W_{sc} - W_r(t)] \qquad (4.14)$$

As condensed water is deposited on the cold surfaces, the released latent heat will raise its temperature, and consequently, the saturation moisture content, W_{sc} which is a function of the surface temperature will increase. In order to solve Equation 4.14, variations of W_{sc} with time must be known. It is difficult to express the surface temperature as a function of time because of the thermal characteristics of windows (the most likely condensation surface in buildings) and the type of boundary conditions which are transient in nature. However, for short periods of time or when used as a part of a numerical formulation, Equation 4.14 can be solved by assuming constant saturation moisture content during the time interval to give:

$$W_r(t) = W_{sc} + (W_{ro} - W_{sc}) \exp(-\frac{h_{mc} A_c}{\rho_a V} t) \qquad (4.15)$$

In practice, it is likely to have several condensation surfaces in the building enclosure. The condensation behaviour of these surfaces could be different either due to different thermal

characteristics or different exterior environmental conditions. For a number of condensation surfaces in an enclosure, indoor air humidity response can be modelled by Equation 4.16.

$$W_r(t) = \sum_{i=1}^{nc} \frac{A_{ci} h_{mc}}{\sum_{i=1}^{nc} A_{ci} h_{mc}} W_{sci} + [W_{ro} - \sum_{i=1}^{nc} \frac{A_{ci} h_{mc}}{\sum_{i=1}^{nc} A_{ci} h_{mc}} W_{sci}] . \exp(-\sum_{i=1}^{nc} \frac{h_{mc} A_{ci}}{\rho_a V} t) \qquad (4.16)$$

iv) Indoor evaporation

Water vapour can be added to indoor air by the evaporation process. Evaporating surfaces could be a free water surface or the surface of a wet material or soil. The dynamic response of indoor air humidity to surface evaporation can be expressed as:

$$W_r(t) = W_{se} + (W_{ro} - W_{se}) \exp(-\frac{h_{me} A_e}{\rho_a V} t) \qquad (4.17)$$

For a number of evaporation surfaces, nv, the dynamic response is given by:

$$W_r(t) = \sum_{i=1}^{nv} \frac{A_{ei} h_{me}}{\sum_{i=1}^{nv} A_{ei} h_{me}} W_{sei} + [W_{ro} - \sum_{i=1}^{nv} \frac{A_{ei} h_{me}}{\sum_{i=1}^{nv} A_{ei} h_{me}} W_{sei}] . \qquad (4.18)$$

$$\exp(-\sum_{i=1}^{nv} \frac{h_{me} A_{ei}}{\rho_a V} t)$$

v) Indoor moisture generation

Indoor moisture generation processes differ from the indoor evaporation processes by being independent of indoor humidity conditions. Substantial amounts of moisture could be released indoor from occupants and moisture generating operations. The amount and the variational behaviour of indoor moisture generation are dependent on many factors

related to the type of indoor operations, the number of occupant, and their activities and habits. Practically, it is difficult to express the rate of indoor moisture generation in terms of time by a continuous function. Instead, a discrete variational profile can be used to describe its variations for each indoor operation and activity.

Assuming that perfect and instantaneous mixing occurs, then for a short period of time, where the moisture generation rate *Mg* can be assumed constant, the response of indoor humidity to moisture generation is given as:

$$W_r(t) = W_{ro} + \frac{Mg}{\rho_a V} t \qquad (4.19)$$

For a number of moisture generation operations, the response of indoor air humidity will follow Equation 4.20.

$$W_r(t) = W_{ro} + \sum_{i=1}^{ng} \frac{Mg_i}{\rho_a V} t \qquad (4.20)$$

vi) Cooling coil dehumidification process

In summer when the cooling process is needed, the cooling coil will act as a dehumidifier. Air dehumidification occurs when the inlet air moisture content (i.e. space air moisture content) is higher than the saturation moisture content corresponding to the coil temperature. The rate of moisture lost by coil dehumidification can be given by:

$$\frac{dmm}{dt} = Q_{sp}(W_{sp} - W_r) \qquad (4.21)$$

The response of indoor humidity to the dehumidification process can be expressed by:

$$\frac{dW_r(t)}{dt} = \frac{Q_{sp}}{\rho_a V}[W_{sp} - W_r(t)] \tag{4.22}$$

The supply air moisture content W_{sp}, depends on the coil characteristics and the space humidity response. The effect of coil characteristics can be modelled by relating the coil inlet and outlet conditions through the so-called coil bypass factor. For some HVAC systems, such as constant volume reheat system, the bypass factor and the coil temperature t_d can be assumed constant. Moreover, when no outdoor mixing is implemented, the coil outlet temperature can also be assumed constant. The supply air moisture content can be given by:

$$W_{sp} = [W_d t_r + t_{co}(W_r - W_d) - W_r t_d]/(t_r - t_d) \tag{4.23}$$

By substituting equation 4.23, equation 4.22 becomes:

$$\frac{dW_r(t)}{dt} = \frac{Q_{sp}}{\rho_a V}[(t_r - t_{co})/(t_r - t_d) W_d - \{1 - (t_{co} - t_d)/(t_r - t_d)\} W_r] \tag{4.24}$$

4.3 Air Humidity Dynamic Response Inside a Room

In practice, different combinations of moisture sources and sinks could contribute to air humidity behaviour inside a building enclosure as described by Equation 4.1. Two possible general cases will be discussed below.

I) No absorption or desorption by interior surfaces

When moisture absorption and desorption by interior materials can be neglected, Equation 4.1 can be written as:

$$\rho_a V\frac{dW_r}{dt}=\sum_{i=1}^{na}Q_{ai}(W_{oi}-W_r)+\sum_{i=1}^{nc}A_{ci}h_{mc}(W_{sci}-W_r)+\sum_{i=1}^{nv}A_{ei}h_{me}(W_{sei}-W_r)+\sum_{i=1}^{ng}Mg_i+Q_s(W_s-W_r) \tag{4.25}$$

The time dependent parameters describing the moisture transport process in Equation 4.21 (i.e. W_o, W_{sc}, W_{se}) experience negligible changes during a relatively small time interval. Therefore, these parameters can be assumed constant during the time interval used in the numerical solution. Equation 4.21 can be solved to give:

$$W_r(t)=\alpha+(W_{ro}-\alpha)\exp(-\frac{t}{t_R}) \tag{4.26}$$

where,

$$\alpha=\frac{1}{\beta}(\sum_{i=1}^{na}Q_{ai}W_{oi}+\sum_{i=1}^{nc}A_{ci}h_{mc}W_{sci}+\sum_{i=1}^{nv}A_{ei}h_{me}W_{sei}+\sum_{i=1}^{ng}Mg_i+Q_{sp}W_{sp})$$

and

$$\beta=\sum_{i=1}^{na}Q_{ai}+\sum_{i=1}^{nc}A_{ci}h_{mc}+\sum_{i=1}^{nv}A_{ei}h_{me}+Q_{sp}$$

Equation 4.26 describes the air humidity response to different moisture gain and loss processes within an enclosure. The parameter, t_R, is defined as the room air humidity response time. Physically, it describes the rate of response of air humidity to moisture transport by condensation, evaporation, and air flow processes. Each processes has a time constant associated with it that defines t_R according:

$$\frac{1}{t_R}=\frac{1}{t_a}+\frac{1}{t_c}+\frac{1}{t_e}+\frac{1}{t_m} \tag{4.27}$$

In terms of the influencing parameters of each process, t_R can be written as:

$$\frac{1}{t_R} = \frac{1}{\rho_a V}\left[\sum_{i=1}^{na} Q_{ai} + \sum_{i=1}^{nc} A_{ci} h_{mc} + \sum_{i=1}^{nv} A_{ei} h_{me} + Q_{sp}\right] \tag{4.28}$$

II) With absorption and desorption by interior surfaces

In most cases, moisture absorption and desorption processes within buildings substantially contribute to the behaviour of indoor air humidity. Considering the two types of material-moisture interaction (i.e. $Bi \leq 0.1$ and $Bi \gg 0.1$), Equation 4.1 can be rewritten as Equation 4.29.

$$\begin{aligned}\frac{dW_r}{dt} = &\sum_{i=1} \left[C_i(W_{moi} - W_r)\exp(-B_i t) + C_i(W_{ms}(t) - W_r)\right] \\ &+ \frac{1}{\rho_a V}\sum_{i=1}\left[Q_{ai}(W_{oi} - W_r) + A_{ci} h_{mc}(W_{sci} - W_r)\right. \\ &\left. + A_{ei} h_{me}(W_{sei} - W_r) + Mg_i + Q_{sp}(W_{sp} - W_r)\right]\end{aligned} \tag{4.29}$$

Solution of Equation 4.29 can be found through numerical techniques. One accurate and practical technique for solving first order differential equations is the Runge-Kutta method [139]. Since Equation 4.29 involves several time-dependent parameters, it can be solved only as a part of a numerical formulation through which the variability of these parameters can be modelled.

4.4 Evaluation of Moisture Transport Processes Parameters

Some moisture transport processes modelled by Equation 4.29 are determined by time-dependent parameters resulting either from variable outdoor boundary conditions (i.e., air flow rate) or variable indoor conditions (i.e., material surface moisture conditions). Therefore for equation 4.29 to be implemented for predicting indoor humidity behaviour due to the different moisture transport processes, the variations of the corresponding time-

dependent parameters have to be modelled. These parameters include; the air flow rate across the enclosure exterior boundary, saturation humidity ratio at the window's condensation surface, and the material surface moisture conditions.

4.4.1 Air leakage through exterior walls: The exterior wall is a complicated air flow element containing openings of different sizes which permit the movement of air through whenever there is pressure difference across it. Most air flow models are based on empirical relationship between the determining parameters which include the flow characteristics of the element, and the pressure difference across it. Airflow rate dQ across an incremental area dA of the exterior wall is generally expressed by [42]:

$$dQ = C_w \rho_a (\Delta P)^n dA \tag{4.30}$$

where,

C_w= flow coefficient, $m^3/m^2 \cdot s \cdot Pa^n$

n= flow exponent

ΔP= pressure difference, Pa

and for a uniform pressure difference over the surface, equation 4.30 can be written as:

$$Q = C_w A_w \rho_a (\Delta P)^n \tag{4.31}$$

The value of n in equation 4.31 can vary from 0.5 corresponding to orifice flow, to as much as 1 which corresponds to laminar or capillary flow. In real surfaces, a combination of capillary flow (i.e., n=1) and an orifice flow (i.e., n=0.5) was found to take place [42]. A value of n=0.65 is found to represent many cases of wall and window leakage.

Air leakage characteristics can be expressed in terms of an equivalent orifice area which will yield the same air flow at a particular pressure difference as the element in question.

The orifice flow equation can be expressed as:

$$Q = C A_{oe} \rho_a \sqrt{\frac{2\Delta P}{\rho_a}} \tag{4.32}$$

where,

C= discharge coefficient

A_{oe}= equivalent orifice area, m^2

From equations 4.31 and 4.32, the equivalent orifice area for a flow exponent different from 0.5 can be given by:

$$A_{oe} = \frac{C_w A_w}{C\sqrt{\frac{2}{\rho_a}}} \Delta P^{n-0.5} \tag{4.33}$$

From equation 4.33, it can be seen that for a flow exponent different from 0.5, the equivalent orifice area will be dependent on the pressure difference across the flow element. For n=0.5, equation 4.33 reduces to:

$$A_{oe} = \frac{C_w A_w}{C\sqrt{\frac{2}{\rho_a}}} \tag{4.34}$$

When modelling air flow across building elements, the orifice equation can only be used in cases where a flow exponent of 0.5 can reasonably represent the relationship between the air flow rate and the pressure difference across the element.

Pressure difference across the exterior building envelope arises from wind and thermal forces. Wind induced pressure on the building exterior walls are highly fluctuating and dependent on wind speed and direction as well as the building geometrical configuration.

In calculating air leakage rates due to wind, average pressure values are normally used. In this study, average wind pressures on the building exterior surfaces are evaluated based on the empirical formulation suggested by Swami and Chandra [45]. For low rise buildings, their formulation predicts the wind pressure in terms of wind angle of attack and the building side ratio. Evaluation of the air infiltration using the predicted pressure coefficients showed that using average pressure coefficients for predicting air is adequate for low rise buildings [45]. The wind pressure relative to the barometric pressure can be expressed by:

$$P_w = \overline{C_p} \cdot \frac{1}{2} \rho_a V^2 \qquad (4.35)$$

where,

V= average wind speed, m/s

ρ_a= air density, kg/m^3

Thermal induced pressures vary in magnitude and direction along the wall height depending on the location in terms of the neutral plane. By assuming uniform distribution of openings, the neutral plane can be taken at mid-height of the wall. At distance h from the neutral plane, the thermal induced pressure can be given by:

$$P_s = gh(\rho_{ao} - \rho_{ai}) \qquad (4.36)$$

where,

g= gravitational constant, m/s^2

In reality, more than one driving potential normally exist across the exterior walls at the same time. The total air flow can not be calculated by simply adding the air flows resulting from the different driving potentials since the air flow rate is non-linearly related to the

pressure. Instead, the total air flow is evaluated by integrating equation 4.30 over the wall height. Another alternative is to determine the effective uniform pressure over the wall surface that will result in the same airflow caused by the stack effect. By adding this pressure to the presumably uniform wind pressure, an effective total pressure over the exterior wall can be obtained:

$$P_{ws} = P_w + P_s^e \tag{4.37}$$

where,

P_w= wind pressure, Pa

P_s^e =effective stack pressure, Pa

The effective stack pressure can be expressed by:

$$P_s^e = [2(n+1)^{1/n}]^{-1} . g . H . (\rho_{\infty} - \rho_{a'}) \tag{4.38}$$

Depending on the wind direction and the location in terms of the neutral plane, different driving forces could act either in the same direction or try to cancel each other. To account for opposite flows, the exterior wall can be divided into two halves with an upper and a lower flow elements having the same leakage area. The effective combined pressure and the corresponding airflow rates can be calculated with sufficient accuracy for the upper and the lower halves of the wall without changing the level of the neutral plane. The pressure difference at any point in the upper half can be given by:

$$\Delta P_t = P_w - P_s^e - P_R \tag{4.39}$$

and for the lower half;

$$\Delta P_b = P_w + P_s^e - P_R \tag{4.40}$$

where,

P_R= room reference pressure, Pa

4.4.2 Interior condensation surface temperature: Condensation on an interior surface occurs whenever the saturation pressure evaluated at its temperature is lower than the ambient vapour pressure. In buildings, surface condensation mainly occurs on cold elements within the exterior envelope. Windows due to their thermal characteristics tend to be the coldest interior surfaces, and hence they determine the level of indoor humidity at which water vapour can be lost by surface condensation. Therefore, in order to determine the condensation potential of a particular surface and the amount of condensate, its temperature must be known. The surface temperature is determined by the windows thermal characteristics as well as the time-dependent boundary conditions. In the presence of surface condensation, associated latent heat will be released on the window's surface causing a rise in its temperature. Variations of window's internal surface temperature can be evaluated by solving the corresponding transient heat transfer problem with the appropriate boundary conditions. For formulating the present heat transfer problem, the following assumptions are made:

i) Heat transfer through windows is a uni-dimensional problem.

ii) In the presence of condensation, the water film on the window surface either in the form of liquid or solid has no effect on the heat transfer process.

iii) Absorbed solar radiation (only clear sky conditions are considered) and is uniformly distributed across the window thickness.

The transient heat conduction problem for a homogeneous slab can be described by:

$$\rho_g c_{vg} \frac{\partial T}{\partial t} = K \frac{\partial^2 T}{\partial x^2} + q_s / L_g \qquad (4.41)$$

the second term on the right hand side of equation 4.41 represent the absorbed solar radiation which is treated as an internal source of energy. The corresponding boundary conditions can be written as:

$$-K \frac{\partial T}{\partial x} = h_i (T_i - T_{si}) + h_{fg} \dot{m}_{sc}$$

for interior surface, and

$$K \frac{\partial T}{\partial x} = h_o (T_o - T_{so})$$

at the exterior surface.

For a single glazed window, equation 4.41 with the corresponding boundary conditions can be solved numerically to determine the window's internal surface temperature. For double glazed windows, however, an effective thermal resistance for the air space must be evaluated to be included in the numerical formulation. Heat transfer modes through the air space can be identified by checking the Rayleigh's number, Ra corresponding to the air space thickness. For an ordinary glazed window separating normal outdoor and indoor conditions, the Rayleigh's number Ra=Gr.Pr, can be found to be less than 1.10^3, indicating that no convective heat transfer is taking place. Therefore, conductive and radiative heat transfer will be assumed to take place within the air space. The air space overall heat transfer coefficient can be given by:

$$h_{as} = h_{rs} + \frac{K_a}{\delta_s} \qquad (4.42)$$

where,

K_a= air thermal conductivity, W/m·C

δ_s= air space thickness, m

the radiative heat transfer coefficient can be given by:

$$h_{rs}=(4\sigma\overline{T_k}^3/(\frac{1-\varepsilon_1}{\varepsilon_1}+\frac{1}{F_{12}}+\frac{1-\varepsilon_2}{\varepsilon_2}) \qquad (4.43)$$

where,

σ= Boltzmann constant, W/m^2·K^4

$\varepsilon_1,\varepsilon_2$= surface emittance

F_{12}= configuration factor

$\overline{T_k}$ = mean air space temperature, K

For glass, the surface emittance is equal to 0.82, and since F_{12}=1 for vertical parallel surfaces, equation 3.43 can be reduced to:

$$_{rs}=2.8\sigma\overline{T_k}^3 \qquad (4.44)$$

By assuming constant saturation air moisture content, W_{sc} at the window's surface temperature during the time step used in the numerical solution, then by utilizing the average indoor air humidity during the same time step, the mass condensation rate $\dot{m}_{sc}$ deposited on the window's interior surface can be evaluated by:

$$\dot{m}_{sc}=h_{mc}(W_{ra}-W_{sc}) \qquad (4.45)$$

The surface mass transfer coefficient h_{mc} can be evaluated from the surface heat transfer coefficient h_c based on lewis relationship:

$$h_{mc} = \frac{h_c}{c_p} \tag{4.46}$$

The rate of solar radiation absorbed by the window is determined by its physical characteristics, the amount and type of radiation incident on the surface as well as the angle of incidence. The rate of solar radiation absorbed by the window can be expressed by:

$$q_s = (1-\tau_a^b) I_{bv} + (1-\tau_a^d) I_{dv} + (1-\tau_a^r) I_{rv} \tag{4.47}$$

Where τ_a refers to the windows solar transmittance when only solar absorption losses are considered, and the superscripts *b*, *d*, *r* refer to the direct, diffused and reflected components of radiation. The solar transmittance τ_a is dependent on the glass characteristics and the angle of incidence θ_1, and can be given by [140]:

$$\tau_a = \exp(-K' L_g / \cos\theta_2)$$

and

$$\theta_2 = \sin^{-1}[\sin(\theta_1)/1.526]$$

where,

K'= extinction coefficient, m^{-1}

L_g= glass thickness, m

θ_2= refraction angle, deg.

For the direct radiation, the incident angle varies with time depending on the sun location relative to the surface. Its value can be determined by the relevant equations described by Duffie and Beckman [140]. On the other hand, for the diffusive and reflective components over a vertical surface, an effective incidence angle of 60° is used based on the assumption that isotropic conditions prevail. The different solar radiation components

in equation 4.47 are also evaluated based on the formulas provided by Duffie and Beckman [140].

In this study, equation 4.41 is solved numerically by using the implicit finite-difference formulations. For each pane three equally spaced nodes are used. By performing energy balance at each node, a set of algebraic equations are obtained. For an interior node *n*, the energy balance equation can be written as:

$$(1+2Fo+2C_i)T_n^{\tau+1}-2FoT_{n+1}^{\tau+1}=T_n^{\tau}+2C_iT_i+C_{mc}\dot{m}_{sc}+S_r \tag{4.48}$$

For an intermediate node *n*,

$$-FoT_{n-1}^{\tau+1}+(1+2Fo)T_n^{\tau+1}-FoT_{n+1}^{\tau+1}=T_n^{\tau}+2S_r \tag{4.49}$$

For an exterior node *n*,

$$-2FoT_{n-1}^{\tau+1}+(1+2Fo+2C_o)T_n^{\tau+1}=T_n^{\tau}+2C_oT_o+S_r \tag{4.50}$$

and for the air space boundary node *m* in the case of a double glazed window, the energy balance equation can be written as:

$$-2FoT_{m-1}^{\tau+1}+(1+2Fo+2C_{as})T_m^{\tau+1}-2C_{as}T_{m+1}^{\tau+1}=T_m^{\tau}+S_r \tag{4.51}$$

where,

$$C_i=\Delta t\, h_i/\rho_g c_{vg}\,\Delta x$$

$$C_o=\Delta t\, h_o/\rho_g c_{vg}\,\Delta x$$

$$C_{mc}=2\Delta t\, h_{fg}/\rho_g c_{vg}\,\Delta x$$

and

$$S_r = q_s \Delta t / \rho_g c_{vg} \Delta x$$

$$Fo = K_g \Delta t / \rho_g c_{vg} \Delta x^2$$

$$C_{as} = \Delta t \, h_{as} / \rho_g c_{vg} \Delta x$$

To determine the temperature distribution across the window at any given time, the nodal energy balance equations have to be solved simultaneously. In this study, the tri-diagonal matrix algorithm is used for solving this particular problem.

4.4.3 Moisture conditions at the interior materials surfaces: Surface moisture condition of a particular material at the end of each time step will be evaluated by using the time step average indoor air humidity W_{ra}, where,

$$W_{ra} = \frac{(W_r^{\tau} + W_r^{\tau+1})}{2}$$

Depending on the type of material moisture behaviour which is determined by the corresponding Biot number, the material surface moisture conditions can be determined by equation 4.5 in case of a lumped-parameter modelling, otherwise equation 4.8 will be used to evaluate the change of material surface moisture conditions. Once the surface moisture conditions are known, the moisture distribution across the material moisture interaction thickness L_m can be modified by updating the parameters *b1*, *b2* and *b3* using equation 3.22b, which in turn requires the evaluation of the time-dependent coefficients $a_i(\tau)$, i=0,1,...., 4. These coefficients can be evaluated by utilizing equations 3.17-3.21.

4.5 Applications and Discussion

Based on the mathematical formulation discussed previously in this chapter, a computer program called "SHVPM" has been developed to simulate air humidity behaviour within

a single zone space. Air humidity behaviour within an enclosure is determined by several interrelated time-dependent moisture transport processes. The degree of influence of a particular process, or even whether it is a participating factor or not, depends on the type and relative impact of the other moisture transport processes. In order to demonstrate the applicability and importance of the above mathematical development, a case study is presented through which the relative effects and the determining parameters of the different moisture transport processes on air humidity behaviour are investigated. In addition, the impact of some moisture transport processes on surface condensation potential as well as humidification and dehumidification requirement of the space are examined.

4.5.1 Influence of moisture transport processes on space air humidity response: In buildings, air humidity behaviour is normally determined by a combination of moisture transport processes. Some of these processes such as air leakage and surface condensation are dependent on the outdoor environmental conditions (e.g., air temperature, wind speed), while others are mainly determined by the building physical and functional characteristics (e.g., indoor moisture generation and moisture absorption by interior materials). In order to study the influence and interaction of these different processes, air humidity behaviour with a 600 m^3 building enclosure maintained at 21 deg. C. is studied under typical winter and summer outdoor conditions for different combinations of moisture transport processes. The modelled building geometrical configurations are shown in Fig. 4.4. Hourly outdoor air temperature and moisture content of the modelled winter and summer days are shown in Figs. 4.5-4.6, and hourly wind speed and direction are shown in Figs. 4.7-4.8. The daily indoor moisture generation profile used in the modelling is shown in Fig. 4.9. It is based on moisture prediction within

a typical residential building with four occupant.

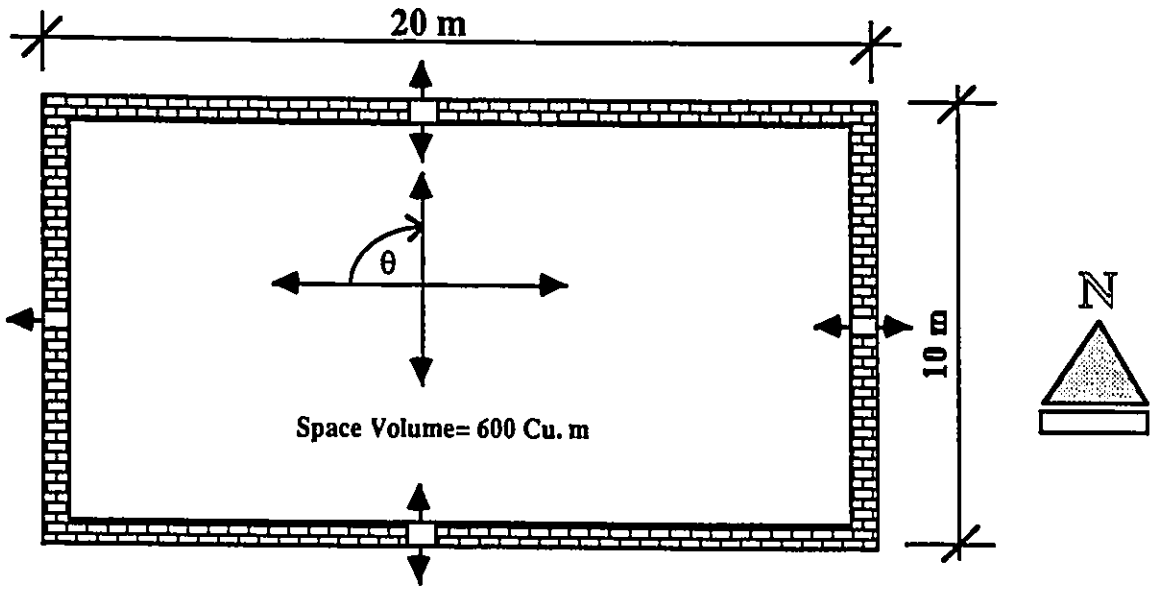

Fig. 4.4 Geometrical configuration for the modelled single zone enclosure.

Indoor air humidity behaviour is greatly influenced by air leakage through exterior walls. The rate of air leakage depends on the air leakage characteristics of the walls as well as the wind speed and direction. Space air humidity response in a winter day at different wall air leakage characteristics is shown in Fig. 4.10. By referring to Fig. 4.5, it can be seen that the space air humidity behaviour generally follows the same variational pattern of the outdoor air in all cases. However, space air humidity response to fluctuations in outdoor air moisture conditions are greatly influenced by the air leakage characteristics of the exterior walls. As the air leakage coefficient increases (i.e., air flow increases) space air humidity response follows more closely the variations of the outdoor air both in pattern and magnitude. In addition to the air flow rate across the exterior walls, the instantaneous response of space humidity to any change in outdoor conditions is dependent on the

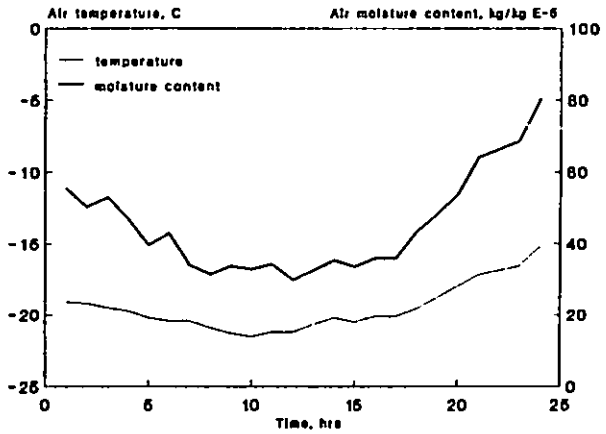

Fig. 4.5 Hourly air temperature and moisture content for a winter day in Montreal.

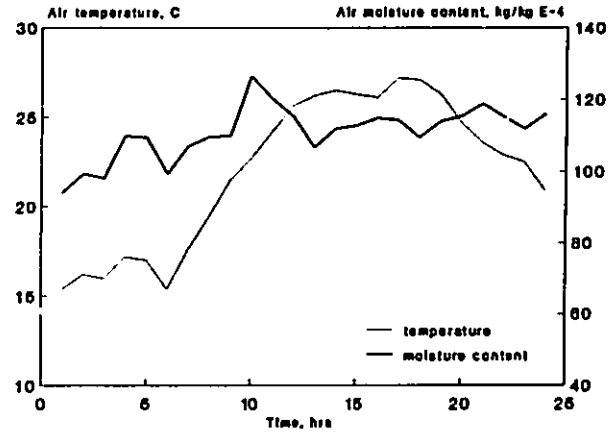

Fig. 4.6 Hourly air temperature and moisture content for a summer day in Montreal.

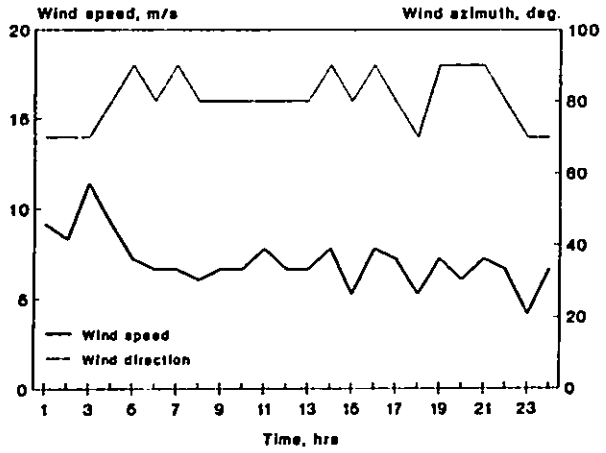

Fig. 4.7 Hourly wind speed and direction for a winter day in Montreal.

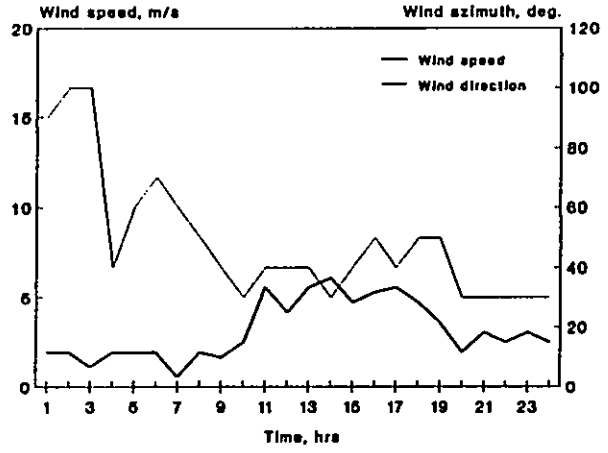

Fig. 4.8 Hourly wind speed and direction for a summer day in Montreal.

difference in absolute humidity between the outdoor air and the space air. For example, examination of Fig. 4.5 and Fig. 4.10 reveals that although outdoor humidity starts to rise at hour 12, space humidity continues to fall or remain unchanged for some hours until it begins to respond to rising outdoor humidity at different times. From Fig. 4.10 it can also be seen that increasing the air leakage coefficient by a certain magnitude does not mean an equal increase in the space humidity response since the air flow rate does not only depend on the air leakage coefficient, but also on the corresponding pressure difference which is non-linearly related to the air flow rate.

In many cases, no air flow occurs across certain walls in the building either due to special treatment or as a result of being physically attached to other adjacent buildings. Blocking air leakage through a certain wall will result in a unique space humidity response resulting from the alternation of the air flow pattern which is mainly determined by the wind speed and direction. Fig. 4.11 compares the humidity response of a space with all its exterior walls at equal air leakage coefficients to a similar space with no air flow across its west wall. It can be seen that space humidity response is significantly reduced. This can be explained by the reduced positive air flow rate (i.e., air infiltration) through the west wall which is subjected to positive wind pressure as can be found from Fig. 4.7 where the wind direction fluctuates between the west and south west directions. By eliminating the possibility of air flow through the north and south walls, air humidity response is further reduced as can be seen from Fig. 4.12. Such behaviour is caused by the considerable reduction in the total air leakage area through which both exfiltrating and infiltrating air can pass. Moreover, the south wall is critical to the determination of the positive air flow since it is subjected to positive wind pressure throughout most of the modelling period. On the other hand,when the air flow through the east wall is eliminated, it has almost no effect

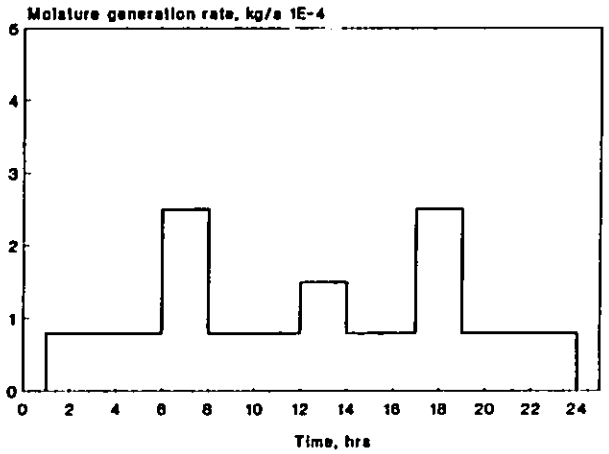

Fig. 4.9 Daily indoor moisture generation profile for the single space enclosure.

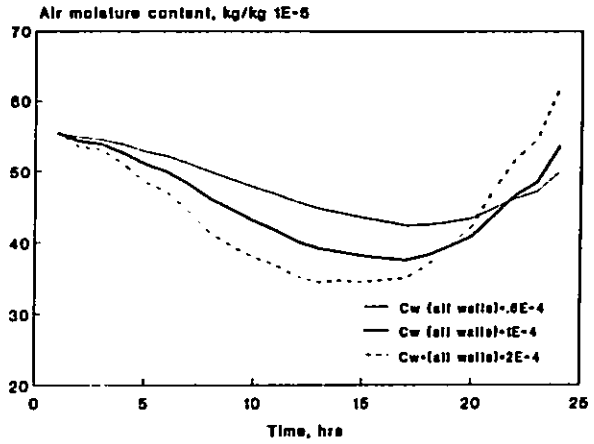

Fig. 4.10 Air humidity response due to air leakage in a winter day at different wall air leakage characteristics.

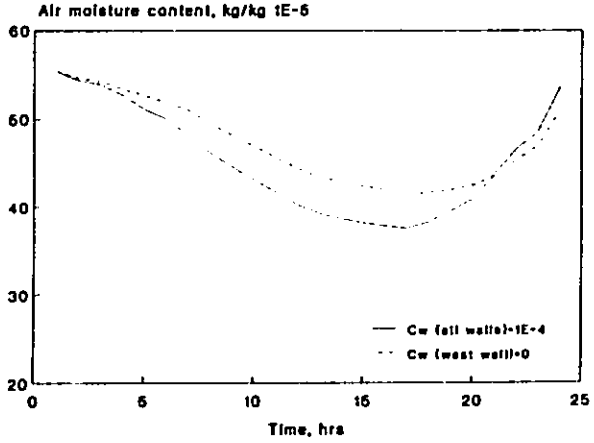

Fig. 4.11 Air humidity response due to air leakage when no airflow occurs through the west wall.

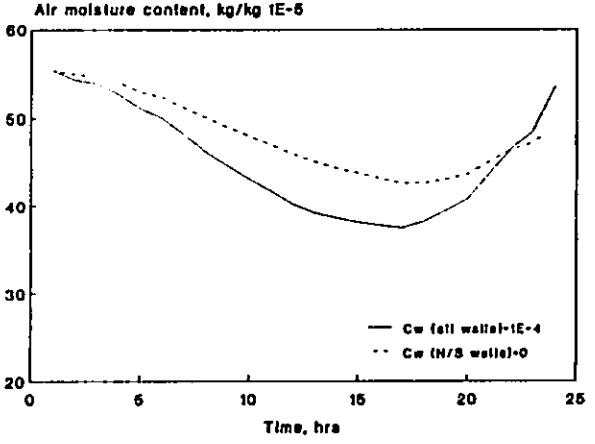

Fig. 4.12 Air humidity response due to air leakage when no airflow occurs through the north and south walls.

on the air humidity behaviour as can be seen from Fig. 4.13. This can be mainly attributed to the location of the east wall relative to the wind direction which makes it an exfiltrating wall, therefore, it has insignificant impact on the total air flow and hence on the space air humidity behaviour.

The effect of moisture absorption and desorption by interior materials on air humidity behaviour is illustrated by Fig. 4.14 through Fig. 4.16. Fig. 4.14 shows the effect of moisture absorption/desorption by a painted gypsum board (i.e., latex paint) at different material surface areas. It can be seen that in spite of the relatively high surface moisture transfer resistance, the presence of 100 m^2 of the gypsum surface has dampened the negative response of the space air humidity throughout the day. By increasing the material surface area to 400 m^2, the resulting modification in space air humidity behaviour is almost proportional to this increase. This modification of air humidity behaviour is due to the desorption of moisture previously stored within the material. At the beginning, the material was at equilibrium with its ambient air which was originally at an air moisture content of about $5 \cdot 10^{-4}$ kg/kg. As the space air humidity starts to be decreased by the air leakage process, an equilibrium status is created between the material surface and the ambient air resulting in moisture being drawn out of the material by the desorption process. The response of the material to changes in ambient conditions is greatly determined by the surface moisture transfer coefficient. Fig. 4.15 shows the change in air humidity response when the surface moisture transfer coefficient is changed from $5 \cdot 10^{-5}$ (representing two coats of latex paint) to $8.4 \cdot 10^{-4}$ kg/m^2·s (representing unpainted surface). By examining the two responses, it can be noticed that the moisture desorption process when space air humidity was decreasing due to air leakage, has moderated such behaviour by releasing moisture into the space. On the other hand, the moisture absorption process has

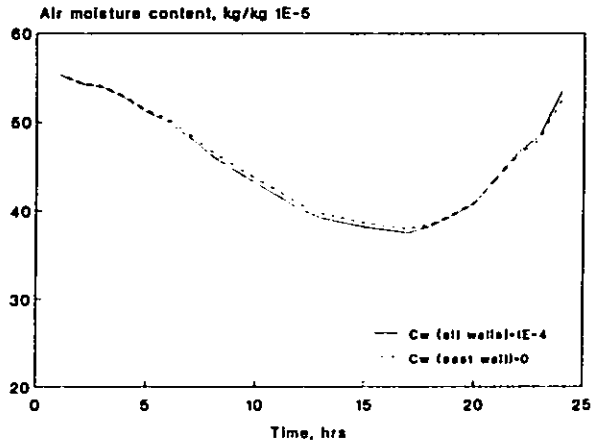

Fig. 4.13 Air humidity response due to air leakage when no airflow occurs through the east wall.

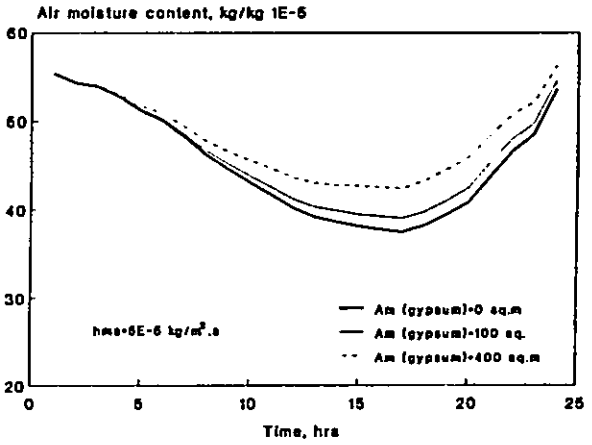

Fig. 4.14 Effect of moisture absorption/desorption by interior materials on air humidity behaviour in a winter day in the presence of air leakage.

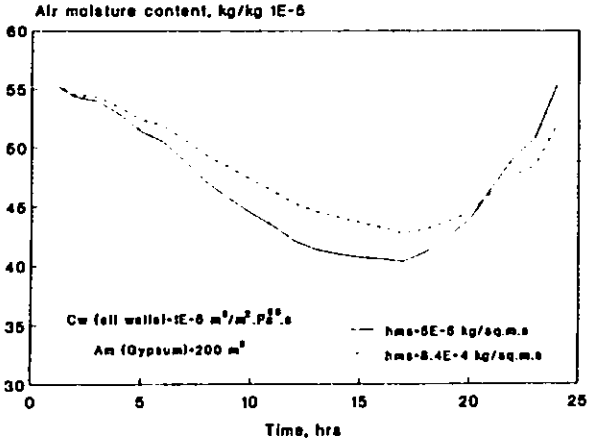

Fig. 4.15 Effect of moisture absorption/desorption on air humidity behaviour at different material surface conditions.

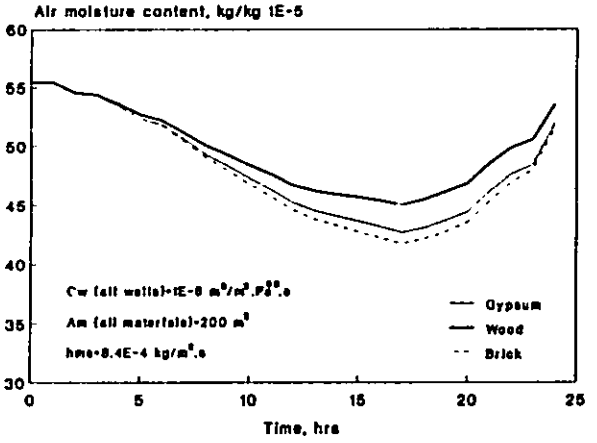

Fig. 4.16 Effect of moisture absorption/desorption on air humidity behaviour in a winter day for different interior materials.

constrained the rise in air humidity after the 21st hour in the simulation period. In addition to the surface coefficient, the impact of moisture absorption and desorption processes is determined by the moisture characteristics of the interior materials. Variations in air humidity behaviour due to moisture absorption/desorption by different interior building materials is shown in Fig. 4.16. Wood due to its high hygroscopic moisture capacity exercises the greatest influence on air humidity behaviour while brick offers the least influence.

Depending on the moisture generation scheme and the degree of participation of other moisture transport processes, indoor moisture generation can greatly influence the indoor air humidity behaviour. Fig. 4.17 shows the impact of indoor moisture generation in the presence of air leakage when the daily profile shown in Fig. 4.9 is used. It can be seen that the pattern of variations of air humidity follows the moisture generation profile with no sign of influence of the air leakage process, although it has contributed to the modification of the level of air humidity. In this case, the indoor moisture generation process is considered the controlling moisture transport process. The effect of moisture generation scheme is shown in Fig. 4.18 where moisture generation profile and constant moisture production rates have been compared. Clearly, air humidity behaviour within the space is determined by the pattern of indoor moisture generation. A constant moisture production rate within the space will result in a steady increase in its humidity with little fluctuations resulting from variations of the air leakage rates. When the moisture generation rate is higher than the rate of air humidity dilution by air leakage, saturation will be reached forcing moisture to be deposited on interior surfaces. In practice, however, other moisture transport processes, such as surface condensation, will be active, preventing indoor air humidity from reaching its saturation level.

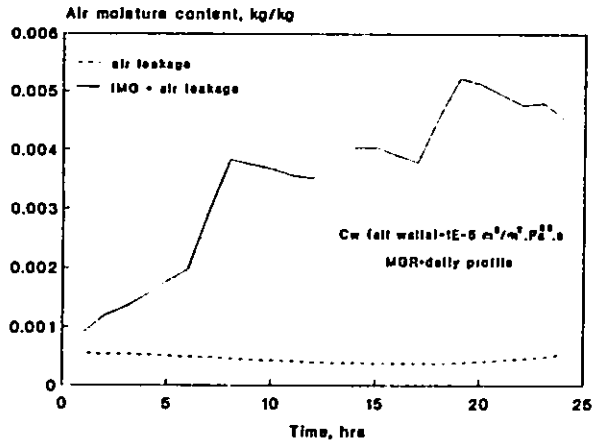

Fig. 4.17 Effect of indoor moisture generation on air humidity behaviour in the presence of air leakage at winter outdoor conditions.

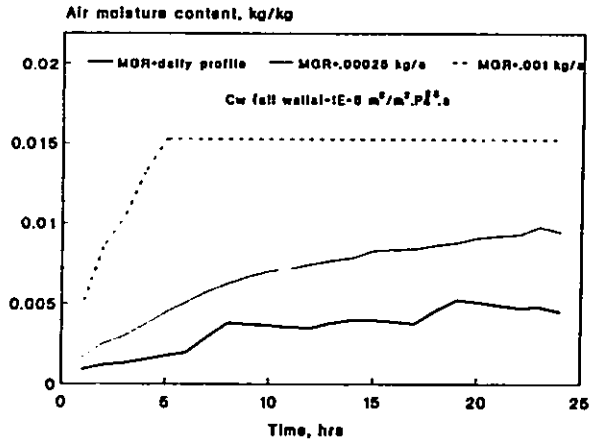

Fig. 4.18 Effect of indoor moisture generation on air humidity behaviour in the presence of air leakage.

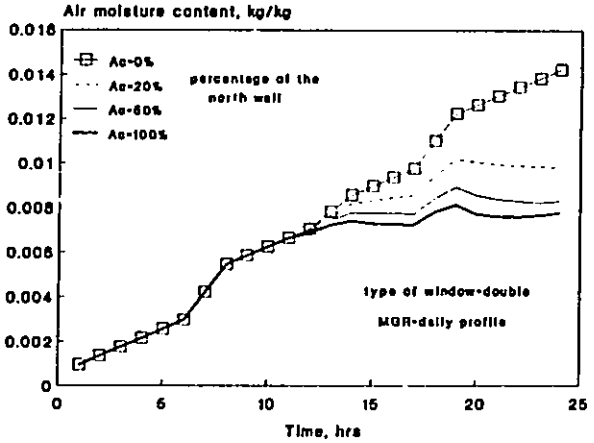

Fig. 4.19 Effect of surface condensation on air humidity behaviour in the presence of indoor moisture generation.

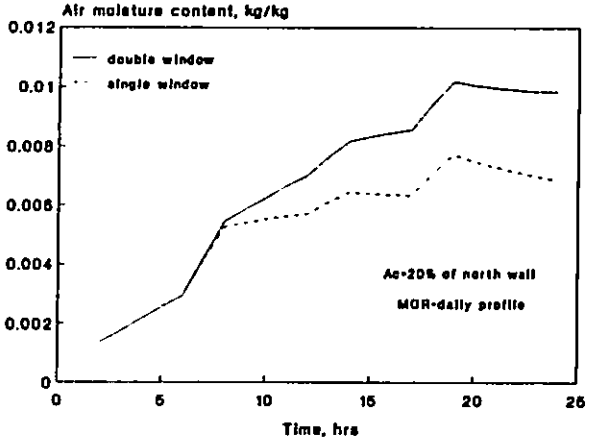

Fig. 4.20 Effect of surface condensation on air humidity behaviour for different condensation surface thermal characteristics.

The response of air humidity to moisture loss by surface condensation in the absence of air leakage is shown in Figs. 4.19-4.20. The impact of surface condensation on double glazed windows at different condensation surface areas is shown in Fig. 4.19, where it can be seen that condensation for all cases starts to occur at the same time when the space air humidity ratio is higher than the saturation air humidity ratio at the condensation surface. The instantaneous air humidity response in this case is determined by the net moisture gain which is the difference between the indoor moisture generation rate and the rate of surface condensation. Although the rate of surface condensation is directly proportional to the condensation surface area, the change in humidity response will not be proportional to the increase in surface area. This can be clearly recognized from Fig.4.19 where considerable reduction in air humidity is experienced by introducing a condensation surface area of 12 m^2 (i.e., 20% of the north wall), while a relatively less reduction is obtained when it is increased by four folds (i.e., 100% of the north wall). The pattern of air humidity variation in the presence of condensation depends on the moisture generation profile as well as the variational behaviour of the condensation surface temperature since it is an important factor in determining the driving potential of the condensation process. When moisture production within the space is a function of the space air humidity (e.g., evaporation process), then in the presence of condensation, the air humidity will reach to a certain level at which moisture loss by condensation will be equal to moisture gain by indoor moisture production. This equilibrium level will always be lower than the space saturation condition, but higher than the saturation condition at the condensation surface. The saturation air moisture content at the condensation surface is an important parameter not only in determining whether condensation occurs or not, but also in determining the rate of condensation. Therefore, for the same outdoor air temperature, air humidity response due to surface condensation on a single glazed

window is expected to be completely different from that due to condensation on a double glazed window. Fig. 4.20 compares space air humidity responses to surface condensation on single and double glazed windows. It can be seen that in the case of the single glazed window, condensation starts to occur much earlier with a considerable reduction in the air humidity level. In winter, the interior surface of a single glazed window is always at a lower temperature than that of a double glazed window, hence the associated space air humidity will always be less than or equal to that corresponding to a double glazed window.

Space air humidity behaviour due to different combinations of moisture transport processes is shown in Figs. 4.21-4.23. The impact of moisture absorption and desorption processes on air humidity behaviour in the presence of air leakage and indoor moisture generation is shown in Fig. 4.21. Although air leakage is the controlling moisture transport process, the effect of moisture absorption by the gypsum board on air humidity response is still appreciable even though the surface moisture transfer coefficient is relatively high. In this case, both the air leakage and the moisture absorption/desorption processes are acting as dampening processes reducing the level of air humidity at any particular point, while the indoor moisture generation process is acting as a shaping process determining the variational behaviour of the air humidity over time. The influence of some moisture transport processes can be limited or even eliminated in the presence of other controlling moisture transport processes. Fig. 4.22 shows that the process of surface condensation has no effect on space air humidity behaviour since the air leakage process has reduced it to a point below the saturation conditions at the condensation surface. However, at a certain reduced air leakage rate, the surface condensation process can be an influencing factor. The impact of air leakage of a moderately untight enclosure on air humidity behaviour in the presence of indoor moisture generation and surface condensation is

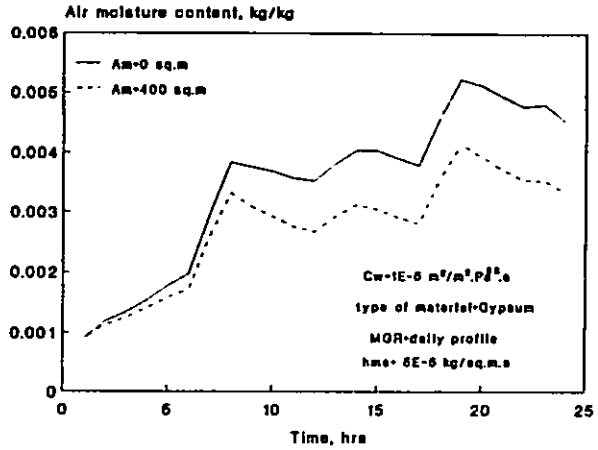

Fig. 4.21 Effect of moisture absorption/desorption on indoor air humidity behaviour in a winter day in the presence of indoor moisture generation and air leakage.

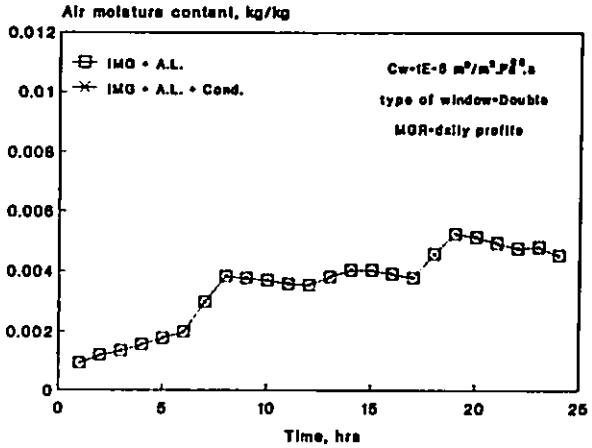

Fig. 4.22 Indoor air humidity response due to combined moisture transport processes at winter outdoor conditions.

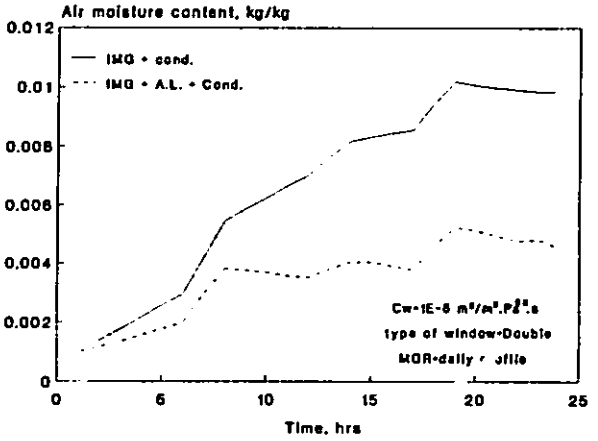

Fig. 4.23 Indoor air humidity response due to combined moisture transport processes at winter outdoor conditions.

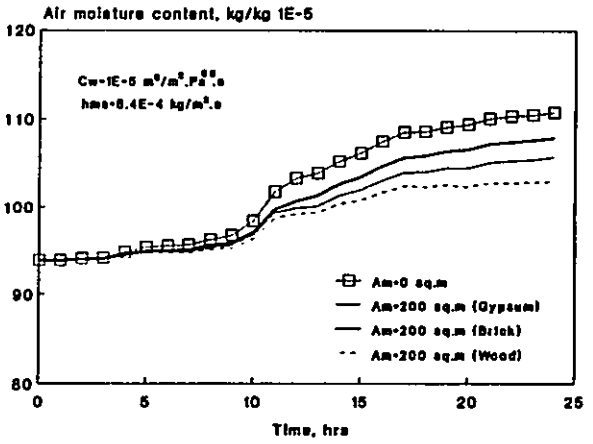

Fig. 4.24 Effect of moisture absorption/desorption by interior material on air humidity behaviour in a summer day in the presence of air leakage.

shown in Fig. 4.23. Clearly, the air leakage process has a significant and a controlling impact on modifying air humidity within the space while the influence of the other processes is either eliminated or minimized.

Depending on the outdoor environmental conditions, moisture transport processes can have a completely different impact on space air humidity behaviour since they may act and interact in a different manner. The influence of moisture absorption by different materials on air humidity behaviour under summer outdoor conditions is shown in Fig. 4.24. Because of its high moisture capacity, wood can absorb considerable amounts of moisture from ambient air causing a significant slow down in the rising trend of air humidity. On the other hand, the brick material exhibits the lowest impact causing a relatively minor modification. Comparison between Fig. 4.24 and Fig. 4.16 shows that the materials relative influence both in the desorbing and the absorbing processes is mainly the same. This means that whether in the absorption or the desorption processes, material impact on air humidity behaviour is determined by its hygroscopicity.

The impact of air leakage on air humidity behaviour in a summer day is shown in Fig. 4.25. In this case, the air leakage process has a limited impact on space air humidity since the outside humid air has very little moisture removing potential as can be found out from Fig. 4.6. The absence of moisture sink processes, such as dehumidification, has caused air to reach its saturation level in a relatively very short period of time. In reality, however, space air humidity is likely to be below the saturation level due to the presence of other moisture transport processes that will act as moisture sinks. These moisture transport processes (e.g., surface condensation), are normally activated at very high humidity level even though they are normally passive during the summer. Although it may

remain below the saturation level, indoor air humidity will normally be at an unacceptable high level, therefore, mechanical dehumidification may be required. The influence of the dehumidification process on indoor air humidity depends on the dehumidification capacity of the delivered air as well as the strategy of implementation. The air dehumidification capacity is determined by the delivery rate and its moisture conditions. The dehumidification system modelled in this study consists of a dehumidification coil which is kept at a constant temperature of 8 deg. C. The supplied air is a recirculated space air with no outdoor air introduced. In this case, the coil outlet temperature will be constant, but the air humidity conditions will vary depending on the space air moisture conditions. Fig. 4.26 shows the effect of continuous implementation of the dehumidification process at different air supply rates. It can be seen that by introducing the supply rate at 0.25 kg/s the space air humidity remains almost unchanged at a level around the coil dew-point conditions. By doubling the air supply rate, no significant change in air humidity behaviour is observed. The impact of the dehumidification process is dependent on the implementation strategy of the process. Figs.27-4.28 illustrate the two different behaviours of air humidity when dehumidification is implemented for certain periods during the day. Each strategy has resulted in a unique daily indoor air humidity variational pattern. In the presence of indoor moisture generation, the influence of the dehumidification process becomes more pronounced as shown in Fig. 4.29. Although its variational behaviour still follows the moisture generation profile, its fluctuations have been considerably constrained. The impact of the dehumidification process in the presence and absence of the air leakage process is shown in Fig. 4.30. The degree of influence of the air leakage process is dependent on the difference in moisture content between the indoor air and the outdoor air. When they are equal or close, the influence of the air leakage process is none or insignificant. When the dehumidification process is implemented, the influence of air

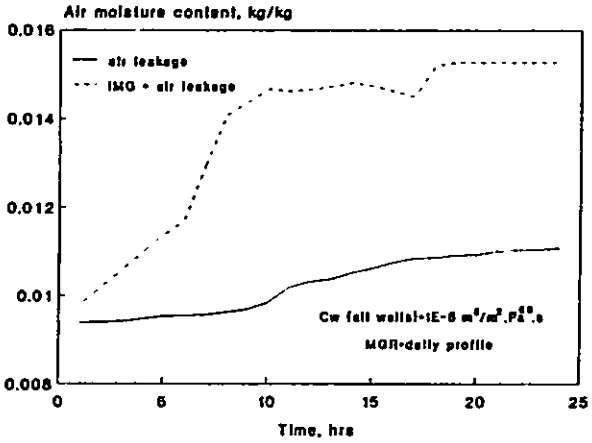

Fig. 4.25 Effect of indoor moisture generation on air humidity behaviour in the presence of air leakage at summer oudtoor conditions.

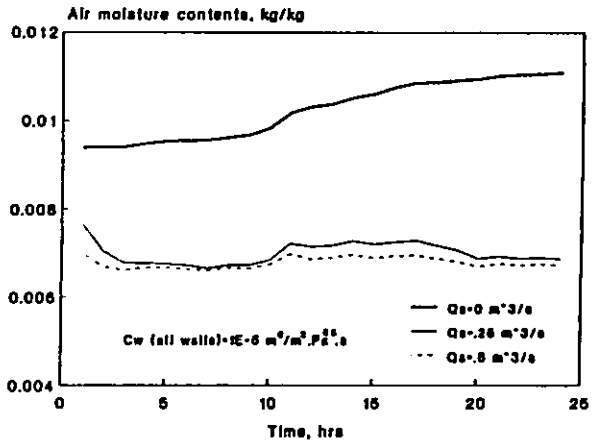

Fig. 4.26 Effect of the dehumidification process on air humidity behaviour in a summer day for different air supply rates in the presence of air leakage.

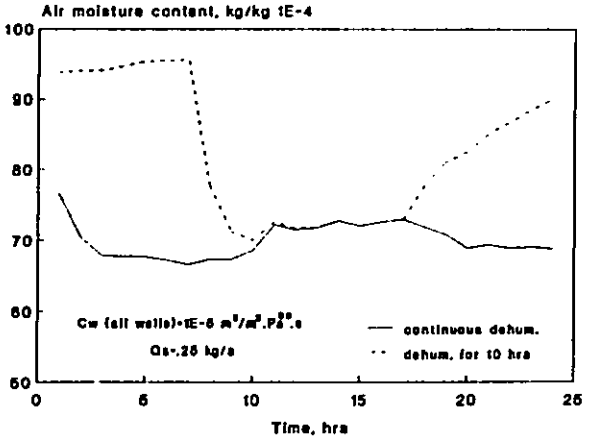

Fig. 4.27 Effect of the dehumidification process on air humidity behaviour in a summer day for different operating schedules in the presence of air leakage.

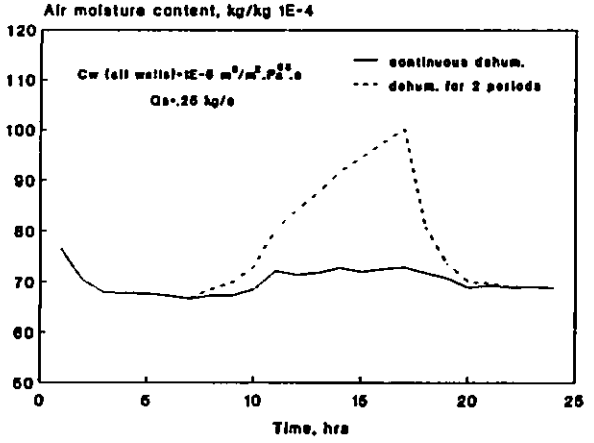

Fig. 4.28 Effect of the dehumidification process on air humidity behaviour in a summer day for different operating schedules in the presence of air leakage.

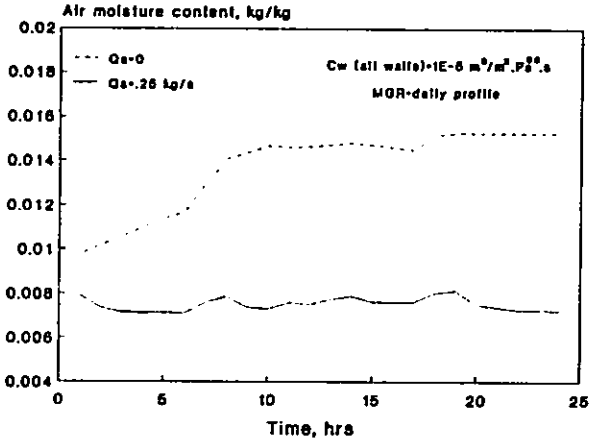

Fig. 4.29 Effect of dehumidification process on air humidity behaviour in the preaence of air leakage and indoor moisture generation.

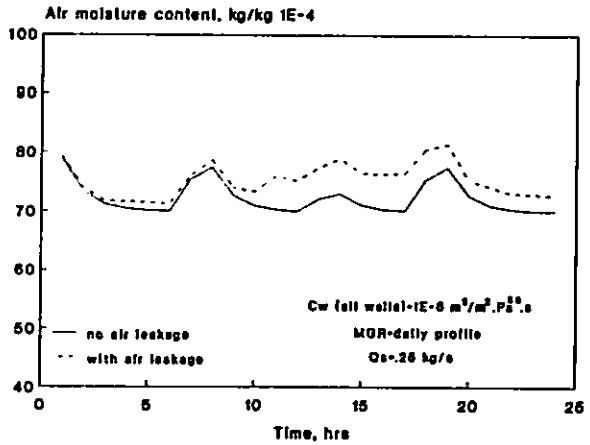

Fig. 4.30 Effect of dehumidification process on air humidity behaviour in the presence and absence of air leakage at summer outdoor conditions.

leakage as a moisture source is noticeable as can be seen from Fig. 4.30. In this case, the outdoor air humidity is always higher than the space humidity resulting in a positive impact of the air leakage process.

4.5.2 Assessment of surface condensation potential: In winter, surface condensation on interior surfaces of windows is a frequent phenomenon that could cause short term and long term problems. These problems could be as minor as obstructing the view through the window to as serious as damaging the windows framing system and creating pools of stagnant water which may result in mould and mildew growth. Therefore, it is important to assess the surface condensation potential corresponding to a particular environmental condition and space physical characteristics. Surface condensation occurs whenever the space air moisture content is higher that the saturation air moisture content corresponding to the interior window's surface. In order to assess surface condensation potential over a particular period of time, space air humidity behaviour as well as the behaviour of the interior surface temperature which is mainly a function of the outdoor air temperature. Surface condensation potential within a 600 m^3 space shown in Fig. 4.4 during a winter month in Montreal will be studied in order to assess the influence of the different parameters involved. The outdoor environmental parameters for the modelled month are shown in Figs. 4.31-4.33. These data are recorded at Dorval weather station in Montreal for 1985. Surface condensation potential over a double glazed window for a relatively light enclosure is shown in Fig. 4.34. It can be seen that for most of the simulation period, the air humidity is higher than the saturation humidity conditions at the window's interior surface. This means that for the modelled physical and functional characteristics of the space, there is high potential for surface condensation. The difference between the space air humidity and the saturation air humidity ratio at the surface temperature will determine

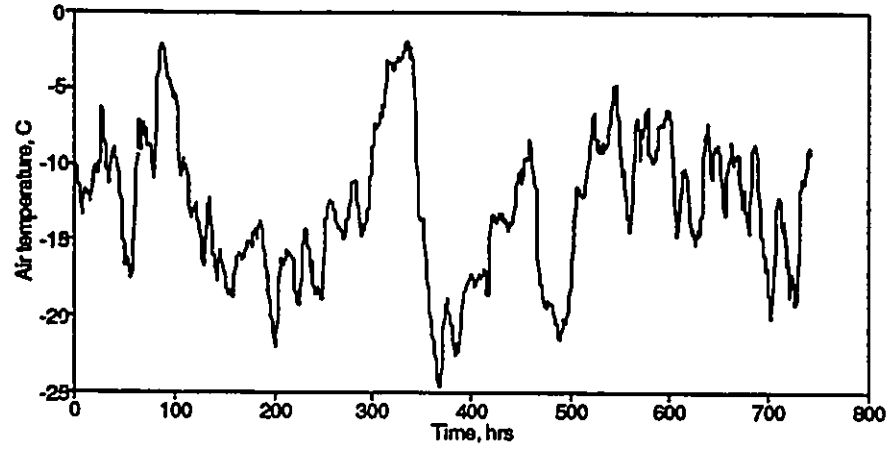

Fig. 4.31 Hourly outdoor air temperature during a winter month in Montreal.

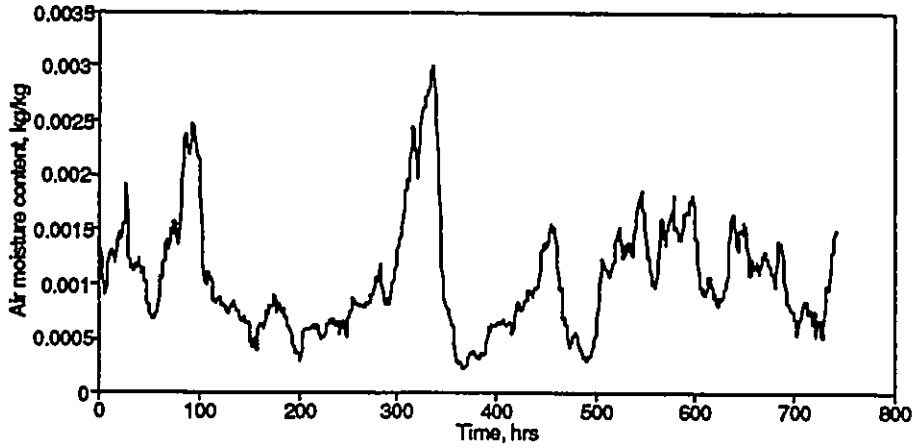

Fig. 4.32 Hourly air moisture content during a winter month in Montreal.

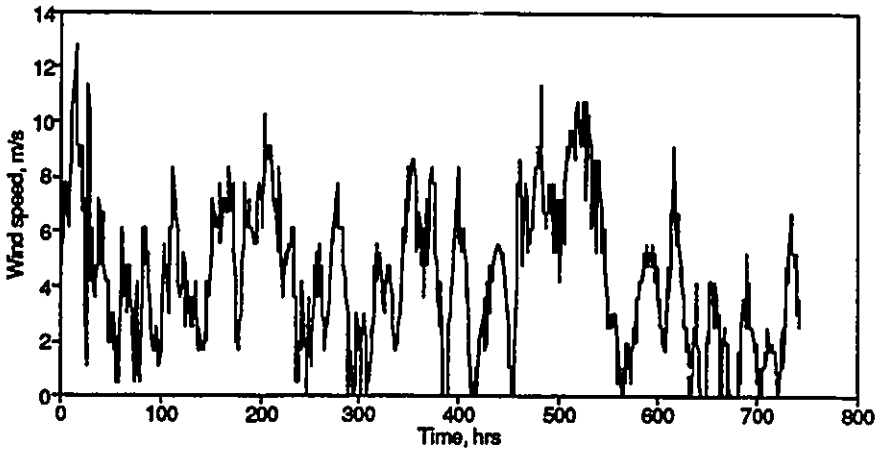

Fig. 4.33 Hourly wind speed during a winter month in Montreal.

the amount of condensed water at any particular time. However since air humidity behaviour in Fig. 4.34 is obtained without considering the condensation process, the difference between the curves will give an idea about the likely total moisture that will be deposited on the surface over a certain period rather than the actual instantaneous mass condensation rate. Examination of Fig. 4.34 shows that the pattern of variations of saturation humidity ratio at the condensation surface follow almost instantly the variation pattern of the outdoor air temperature shown in Fig. 4.31. Such response is an indication of the small thermal inertia exerted by the window system. Referring Fig. 4.34 to the variations in wind speed shown in Fig. 4.33 indicates the strong dependence between air humidity behaviour and the wind speed pattern of variation. From Fig. 4.34, it can be seen that towards the end of the simulation period, air humidity is kept at a relatively high level indicating reduced air leakage rate during this perioo. Examination of Fig. 4.33 indicated that during the same period, wind speed is maintained at a relatively lower level which confirms the previous explanation of the reduced air leakage rate as the main reason for the high humidity level.

Reducing the thermal resistance of the condensation element would undoubtedly result in higher surface condensation potential due to reduced interior surface temperature. Fig. 4.35 shows the condensation potential over a single glazed window for a relatively tight enclosure. Comparison with Fig. 4.34 shows the substantial increase in the surface condensation potential when a single glazed window is used instead of the double glazed system. The larger difference between the air humidity curve and the saturation curve indicates that greater amounts of water will be removed from the space by the condensation process.

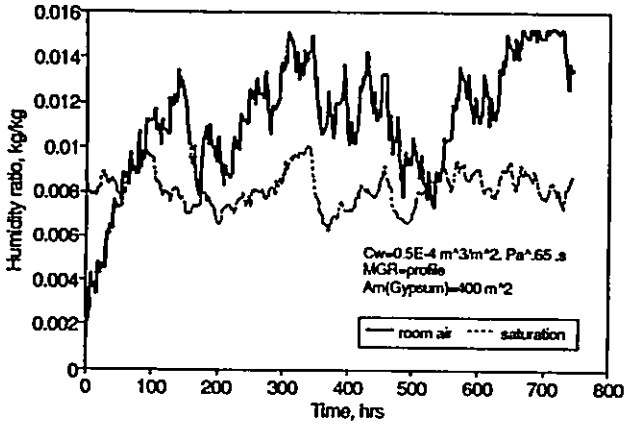

Fig. 4.34 Potential of surface condensation over double glazed windows for a relatively tight enclosure.

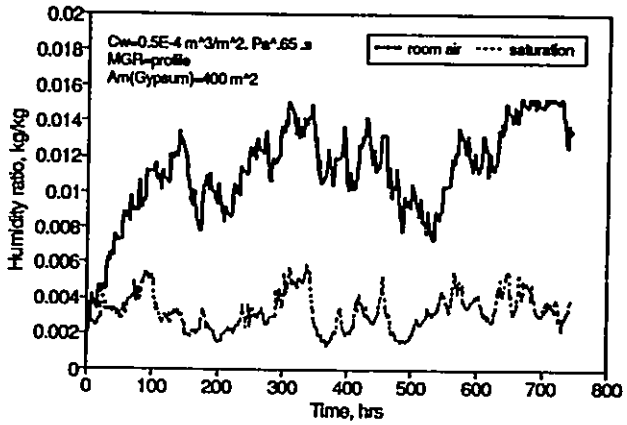

Fig. 4.35 Potential of surface condensation over single glazed windows for a relatively tight enclosure.

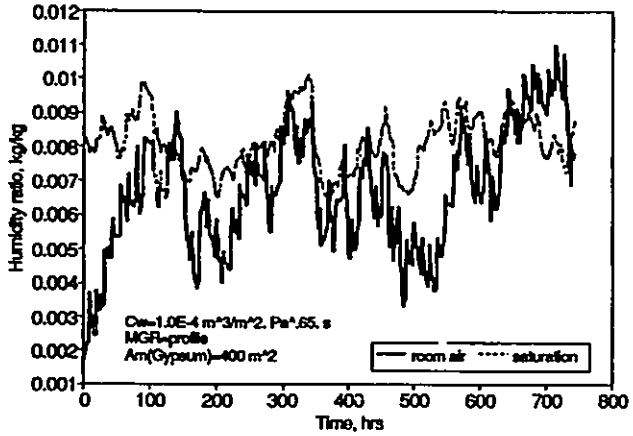

Fig. 4.36 Potential of surface condensation over double glazed windows at average enclosure airtightness.

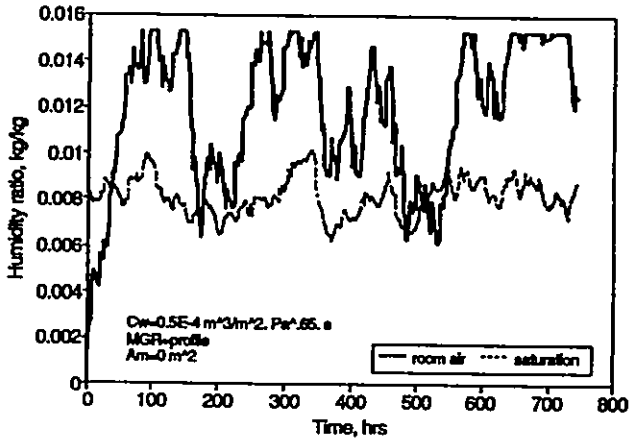

Fig. 4.37 Potential of surface condensation over double glazed windows for a relatively tight enclosure when no moisture absorption takes place. .

Surface condensation potential can be greatly minimized by increasing the rate of air infiltration. Increasing the air leakage coefficient of the exterior walls from $0.5 \cdot 10^{-4}$ to $1 \cdot 10^{-4}$ $m^3/m^2 \cdot Pa^{.65} \cdot s$ has considerably reduced the potential for surface condensation by pushing most of the air humidity curve below the saturation curve as shown in Fig. 4.36. By increasing the air leakage rate further, surface condensation can be completely eliminated. However, in most cases, other more important considerations will probably decide the air leakage level that can be tolerated. In this situation other moisture transport processes could have an important role in modifying air humidity behaviour to reduce surface condensation potential.

Moisture absorption and desorption by interior materials can play an important role in determining the air humidity behaviour within the space. Their influence depends on the material moisture and physical characteristics as well as the surface moisture transfer coefficient. Moisture absorption/desorption process has been a participating factor in determining the air humidity behaviour shown in Fig. 4.34. In that case, 400 m^2 of painted gypsum board surface have been available in the space. Although the gypsum material has a relatively low hygroscopicity level, it seems to have an appreciable impact on air humidity behaviour as can be observed by comparing Fig. 4.34 with Fig. 4.37 where no absorbing material is used. The absence of the absorbing material has caused broader fluctuations in the air humidity response since no moisture is absorbed to suppress its rise and no moisture is desorbed to moderate its fall. Examination of Fig. 4.34 and Fig. 4.37 reveals that in the absence of the hygroscopic material, air humidity has been below the saturation curve for a longer period of time. However, its presence can be generally judged as positive in terms of reducing surface condensation potential. This can be easily recognized by visually comparing the area bounded by the two curves for both cases. By

increasing the surface moisture transfer coefficient (i.e., no surface paint), the peaks in the space air humidity response have been reduced, but at the same time, the drops have been considerably raised as shown in Fig. 4.38. Hence in this particular case, the net effect of increasing the surface moisture transfer coefficient can be judged as negative in reducing the surface condensation potential. A more important parameter in determining the degree of influence of the moisture absorption/desorption process on air humidity behaviour is the moisture characteristics of the interior materials. When wood is used instead of the gypsum material, the potential of surface condensation is almost eliminated as can be seen from Fig. 4.39. At the beginning of the simulation period, space humidity is kept below the saturation curve, such behaviour is attributed to the high initial absorption capacity of rial which was initially almost dry. In practice, interior materials are almost in moisture equilibrium with the ambient air, therefore the influence of the absorption/desorption process on air humidity behaviour is unlikely to be as the initial impact shown in Fig. 4.39. Instead, it is likely to follow the pattern of influence shown at the end of the simulation period.

4.5.3 Assessment of humidification and dehumidification requirements: For many situations, indoor air needs either to be humidified or dehumidified in order to keep the indoor environment a suitable place to perform its intended functions. In cold climates, air humidification is normally needed to keep the indoor air at a certain desirable level, since the natural balance of moisture gains and losses is likely to produce very low indoor air humidity. Air humidification requirement for a 600 m^3 space during a winter month will be studied in the presence of different moisture transport processes. Fig. 4.40 shows the air humidification requirement for an enclosure with an average air tightness level when no indoor moisture generation occurs. It can be seen that there is a considerable difference

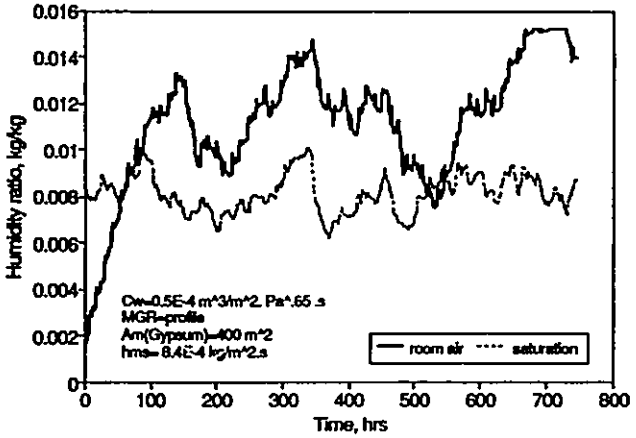

Fig. 4.38 Potential of surface condensation over double glazed windows with gypsum as the moisture absorbing interior material.

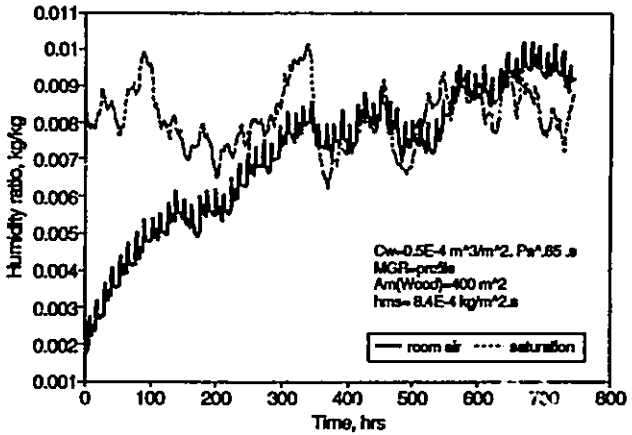

Fig. 4.39 Potential of surface condensation over double glazed windows with wood as the moisture absorbing interior material.

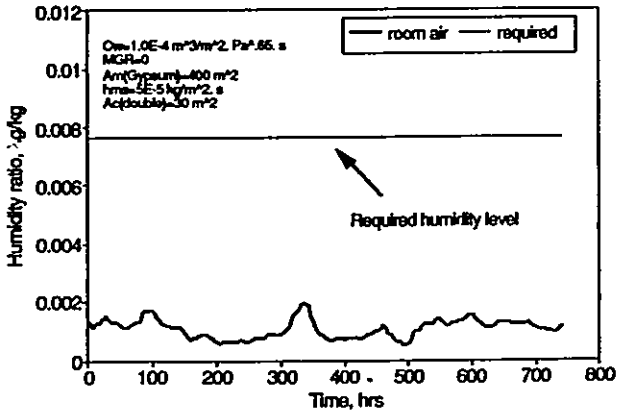

Fig. 4.40 Required and actual air humidty behaviour due to air leakage in the absence of indoor humidification.

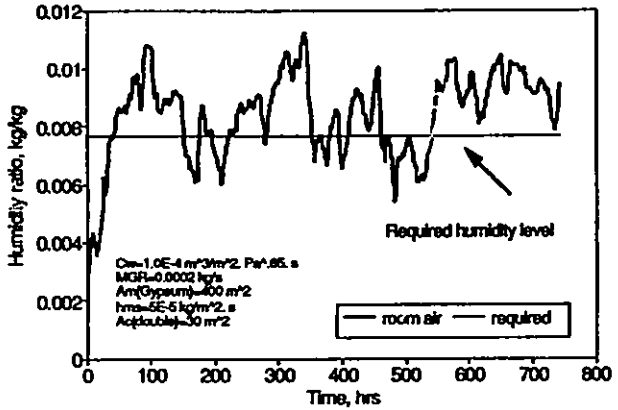

Fig. 4.41 Indoor air humidity behaviour during a winter month when moisture is directly added into the space at a rate of 2E-4 kg/s.

between the required humidity level and its actual behaviour. To achieve the required level, moisture has to be added into the space. The effect of any added amount of moisture towards achieving this goal, is dependent on other moisture transport processes that could be active during the humidification period. Fig. 4.41 shows that the space air humidity is fluctuating around the required level when the moisture is continuously added to the space with a rate of 2.10^{-4} kg/s. When the moisture generation rate is reduced by 50% for the same space physical characteristics, air humidity will be mainly fluctuating below the required humidity level as can be seen from Fig. 4.42. However, for this reduced moisture generation rate, air humidity behaviour relative to the required level remains almost unchanged when the air leakage coefficient of the enclosure exterior walls is reduced by 50% as can be observed by comparing Fig. 4.43 with Fig. 4.41.

When indoor air humidity is required to be maintained at a relatively high level during winter, surface condensation is probably an unavoidable consequence. Such process will put a limit on the level of air humidity that can be maintained within the space. Therefore, either the required humidity is reduced or other measures have to be taken to prevent surface condensation at the required humidity level. Surface condensation over a double glazed window has been a factor in determining air humidity behaviour shown in Fig. 4.41. In this case, its influence against achieving the required humidity level can be judged as minimal since air humidity has dropped below the required level for a relatively short period of time. On the other hand, when a single glazed window is used, air humidity is always maintained below the required level when all other moisture transport processes are kept the same as shown in Fig. 4.44. The required humidity could be achieved either by increasing the moisture generation rate or by decreasing the air leakage rate. Such measure will probably increase the level of indoor humidity, but at the same time will

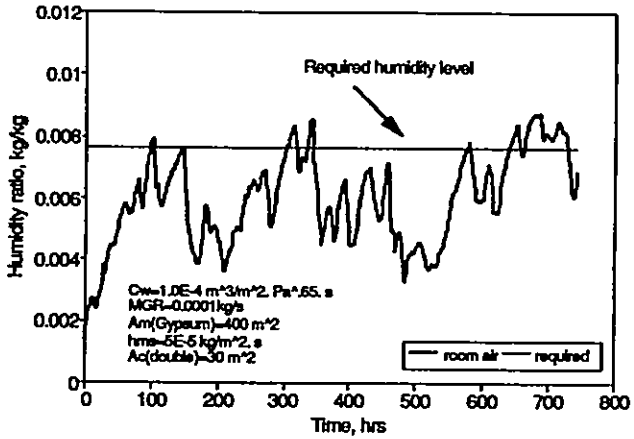

Fig. 4.42 Indoor air humidity behaviour during a winter month when moisture is directly added into the space at a rate of 1E-4 kg/s.

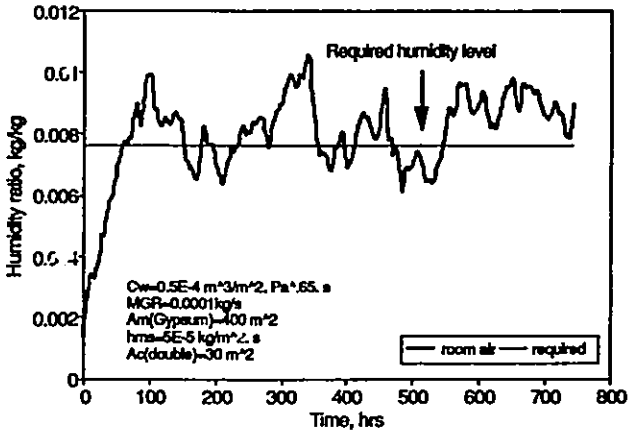

Fig. 4.43 Indoor air humidity behaviour during a winter month when moisture is directly added into a relatively tighter space at a rate of 1E-4 kg/s.

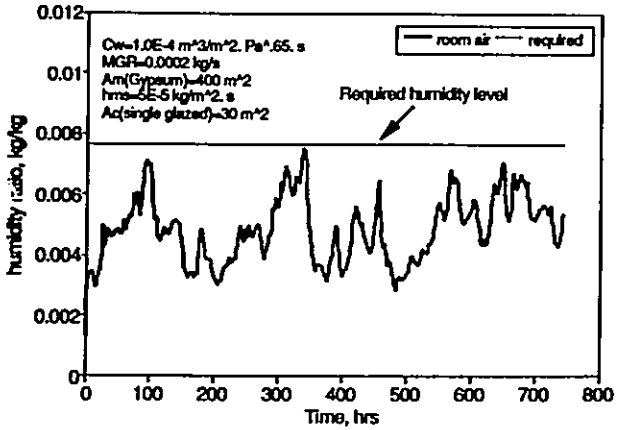

Fig. 4.44 Effect of winter humidification on indoor air humidity behaviour when single glazed window is used.

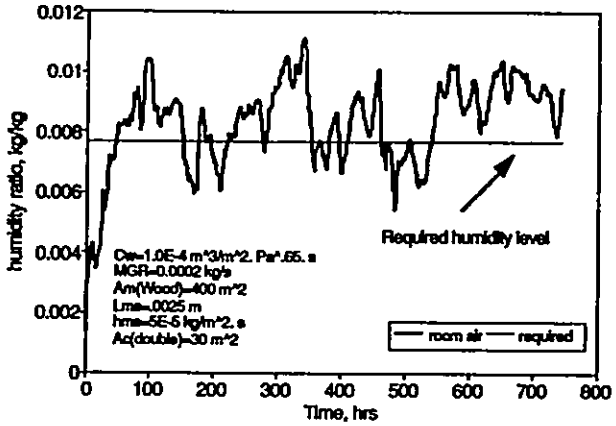

Fig. 4.45 Effect of winter humidification on indoor air humidity behaviour when painted wood is used as an interior material.

increase the amount of moisture removed by surface condensation. An appropriate measure towards achieving the required humidity level is either to use a double glazed window system or to substantially reduce the window's surface area if single glazed has to be used.

In contrast with the surface condensation process, where moisture is always lost from the space, moisture absorption/desorption by interior materials can be viewed as a regulatory process, absorbing moisture when ambient humidity is high, but releasing moisture when it is relatively low. Fig. 4.45 shows the impact of moisture absorption/desorption process when wood is used as an interior material. Comparison with Fig. 4.41 shows that wood as an absorbing material has almost the same impact on air humidity behaviour when the surface moisture transfer coefficient h_{ms} is relatively high. At high surface transfer coefficient, the wood material with a moisture interaction thickness of 2.5 mm seems to have considerable impact on moderating air humidity fluctuations around the required level as can be seen from Fig. 4.46. Increasing the moisture capacity of the interior material either by adding more hygroscopic materials or by increasing its moisture interaction thickness will undoubtedly result in less air humidity fluctuations around the required level. Such behaviour can be compared with the impact of the interior thermal mass on indoor air temperature fluctuations. However, moisture capacity of interior materials could greatly vary from one material to another while variations of their thermal capacity stays within a relatively narrow range. From the above discussion it can be said that air humidification requirements in buildings can be greatly affected by the type and the degree of influence of the prevailing moisture transport processes. Moreover, air humidity fluctuations around a desirable level can be significantly reduced by modifying the contribution of the right combinations of the moisture transport processes. However, when the resulting air

humidity fluctuations cannot be tolerated, a more sophisticated control strategy would have to be implemented. For example, instead of being constant, the rate of moisture generation within the space can be regulated so as to be reduced or increased at the appropriate time according to the space requirement.

In summer, air dehumidification is likely to be required to maintain indoor humidity at a desirable level. When the outdoor air is the main source of moisture it will not be possible to naturally reduce the level of space air humidity. For a relatively tight enclosure, Fig. 4.47 illustrates the indoor air humidity behaviour corresponding to the outdoor air summer conditions shown in Figs. 4.48-4.49 which were recorded during August 1985 at Dorval weather station in Montreal. It can be seen that even in the absence of indoor moisture generation, moisture needs to be removed from the space. The presence of the moisture absorbing materials will generally have negative impact even though it seems to have reduced the peaks of the air humidity response as can be observed from Figs. 4.50-4.51. Comparison between Fig. 4.47 and Figs. 4.50-4.51 shows that air humidity is maintained at a higher level at times when outdoor humidity is relatively very low. This means that the moisture absorbed earlier at higher air humidity level will be released later at lower ambient humidity. Therefore, by introducing a highly hygroscopic materials to the space, more moisture is needed to be removed to achieve the required level. The influence of decreased and increased air leakage rates on the dehumidification requirements is shown in Figs. 4.52-4.53. In this case, since the outdoor air is the source of moisture addition to the space, decreasing or increasing the air leakage rate will have a limited impact on the moisture removal potential. Comparison between Fig. 4.42 and Fig. 4.53 shows that by increasing the air leakage rate, the space was fast to respond to any drop in outdoor humidity, but it also responded quickly to rising outdoor air humidity. Such behaviour is

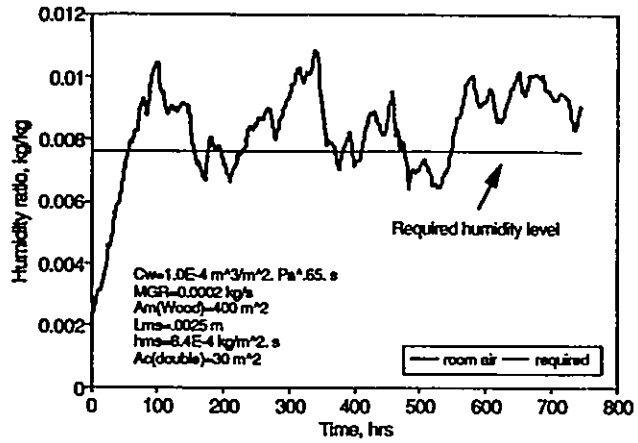

Fig. 4.46 Effect of winter humidification on indoor air humidity behaviour when unpainted wood is used as an interior material.

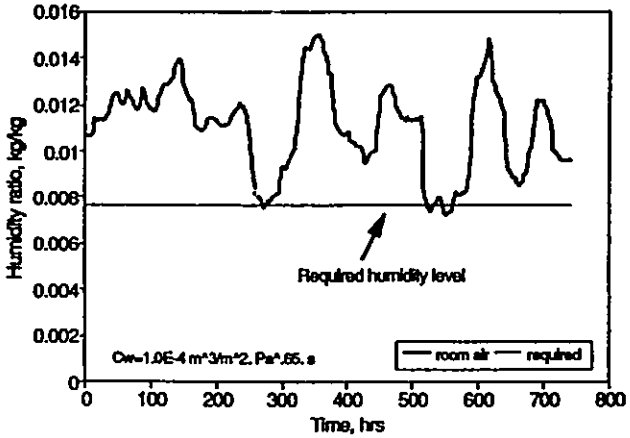

Fig. 4.47 Indoor air humidity behaviour during a summer month when no dehumidification is implemented.

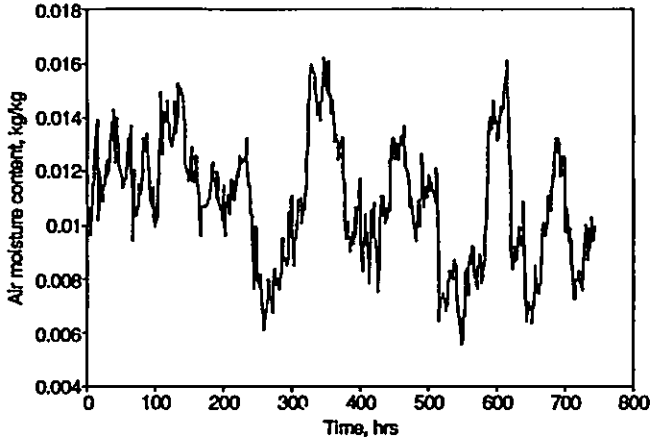

Fig. 4.48 Hourly outdoor air moisture content during a summer month in Montreal.

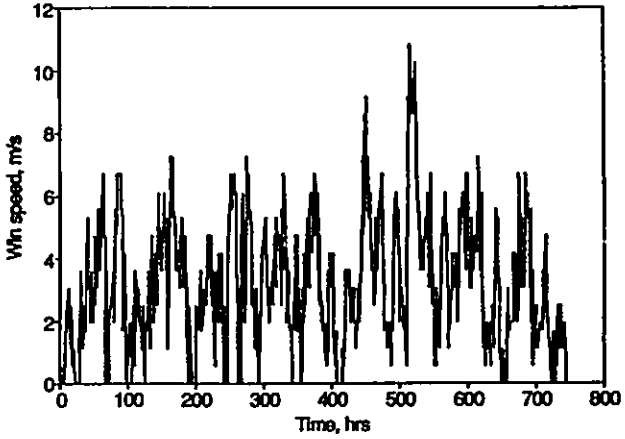

Fig. 4.49 Hourly wind speed during a summer month in Montreal.

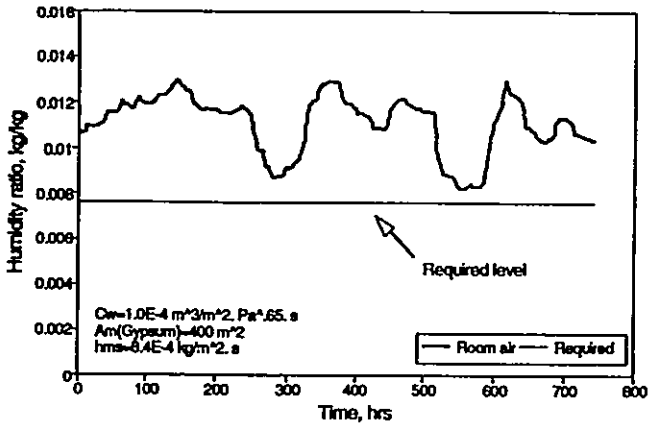

Fig. 4.50 Indoor air humidity behaviour during a summer month versus the required level in the presence of air leakage and moisture absorption/desorption by gypsum material.

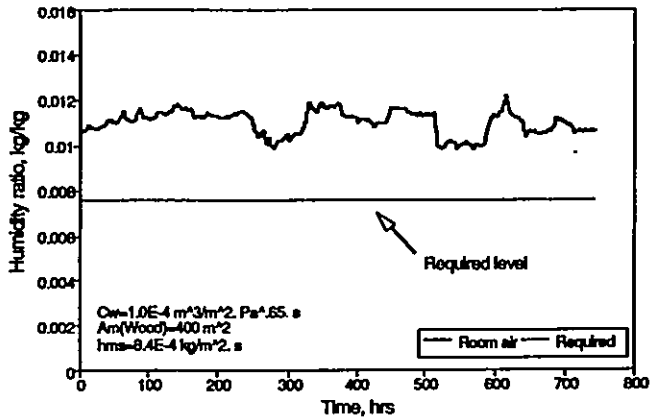

Fig. 4.51 Indoor air humidity behaviour during a summer month in the presence of air leakage and wood as moisture absorbing interior material.

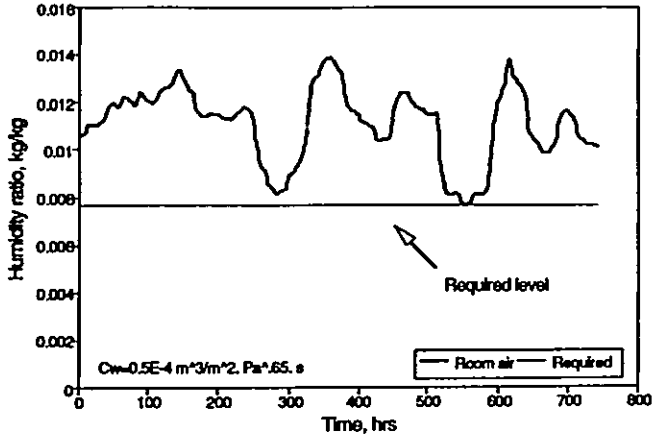

Fig. 4.52 !ndoor air humidity behaviour during a summer month for a relatively tight enclosure.

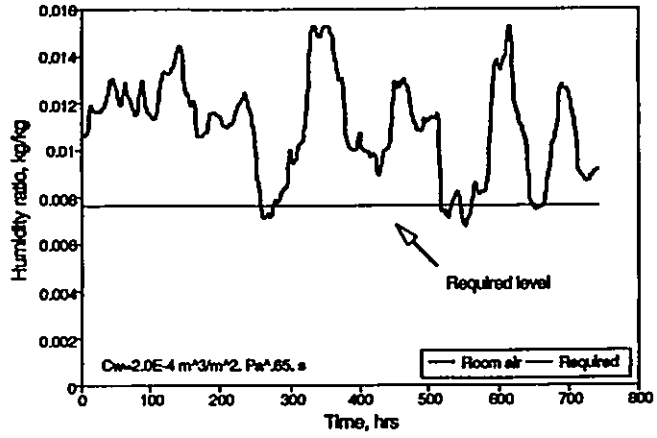

Fig. 4.53 Indoor air humidity behaviour during a summer month for a relatively untight enclosure.

not only determined by variations in outdoor air humidity, but also by variations in wind speed which is the main driving potential for air leakage during summer. The influence of the air leakage process on the dehumidification process will become more pronounced when substantial amount of moisture is generated with the space. This will likely result in a relatively higher indoor humidity giving the drier outdoor air a potential for removing moisture from the space.

4.6 Summary

Air humidity response within a single-zone enclosure has been theoretically modelled via a linear differential equation which takes into account all relevant moisture transport processes. The resulting equation was solved in conjunction with a comprehensive numerical formulation through which non-linear processes were linearized by using a discrete time step. A theoretical study of air humidity behaviour in a single-zone space has revealed that indoor air humidity behaviour, in response to the air leakage process, generally follows the same variational pattern as that of the outdoor air with different time lags determined by the air leakage rate. The relative influence of a particular moisture transport process depends on its time constant, continuity and its interaction with other processes. Some processes, such as surface condensation can have a considerable immediate impact on indoor air humidity, however when combined with air infiltration, it could become inactive in a short period of time. Moisture absorption and desorption by interior materials, on the other hand, offer continuous moisture sources and sinks which remain active as long as fluctuations in indoor humidity occurs. A more pronounced impact is experienced due to the indoor moisture generation process with resulting modifications determined by the rate and the pattern of moisture generation. At high moisture generation rates, surface condensation becomes a determining factor with or without air infiltration.

Indoor air humidity behaviour determines the surface condensation potential over interior cold surfaces. In addition, it determines the humidification (in winter) and the dehumidification (in summer) requirements of the space. Knowledge of the degree and type of influence of the different moisture transport process over indoor air humidity behaviour would be essential if certain measures ought to be taken to modify its behaviour in a certain way. Modifying indoor air humidity behaviour can be mainly achieved by changing one or more of the space functional or physical parameters. For example, reducing the risk of surface condensation can be achieved either by increasing the window's thermal resistance or by increasing the air leakage rate through the exterior walls or by implementing both measures. On the other hand, when indoor humidity is to be maintained at a relatively high level, air leakage rate may have to be reduced and moisture may be needed to be added to the space air. The impact of any or a combination of measures can only be appreciated when the moisture interaction between the various moisture transport processes is modelled and the resulting air humidity behaviour is predicted.

CHAPTER 5

MODE' 'ING OF AIR HUMIDITY TRANSIENT BEHAVIOUR IN A MULTI-ZONE SPACE

5.1 Introduction

Interior space in most buildings can be divided into several zones which are physically separated but connected through doorways or large openings. Each zone usually has its own interaction with the exterior environment, as well as, its own functional and physical characteristics, hence air humidity dynamics in each zone is expected to be different. However, inter-zonal air movement, which is associated with convective moisture transfer, could greatly enhance the interdependence of zonal air humidity behaviour, especially, when the zones are connected by large openings and there is enough driving force across them. Inter-zonal air movement occurs due to difference in barometric pressure or in air temperature between interconnected zones. In the absence of inter-zonal air movement, moisture transfer between zones could occur by vapour diffusion. However, in the presence of inter-zone air flow, this moisture transfer mechanism will have a negligible effect on inter-zonal moisture transfer.

Moisture transfer by convection either across exterior boundaries or across an inter-zonal flow path, could have a significant impact on the level and the variational behaviour of zonal air humidity. In order to evaluate the rate of air flow across a given flow path, its flow characteristics, as well as, the pressure differential across it must be known. The pressure difference across a particular flow path is dependent on the boundary conditions, such as wind pressure, and the flow characteristics of other flow paths. Therefore, a

multi-cell air flow model that describes the interactions between all flow paths must be used. In such a model, each zone and boundary condition is represented by a single node. By performing a mass balance at each zonal node, a set of nonlinear algebraic equations are obtained. These equations then have to be solved simultaneously in order to evaluate the pressure at each node. In this study, Newton's iterative technique is utilized to solve the resulting nonlinear equations.

In order to construct the mass balance equations, air flow across each flow path must be expressed in terms of the unknown nodal pressure. A review of related literature carried out in Chapter 2 has revealed that available theoretical models which relates the air flow rate to the pressure difference across the air flow element vary in terms of their sophistication and applicability. Basic models non-linearly relate the air flow rate to the pressure difference through a coefficient which represents the air leakage characteristics of the element. Air leakage values for various wall components are given by ASHRAE [20]. These values are based on laboratory tests. Evaluation of wind and stack pressures has been discussed in [20], and more detailed evaluation of wind pressure has been discussed in terms of pressure coefficients [45].

Inter-zonal flow paths are normally large openings (i.g. doorways) which tend to be more complex with the possibility of opposite flows across it in the presence of temperature difference between the connected zones. Most available models have described the natural convective process through large openings via a dimensionless correlation using Nusselt number, Prandtl number and Grashof number. However, by utilizing the orifice equation, it has been shown that when using the appropriate flow coefficient heat transfer and the corresponding mass flow predicted by a correlation equation for the two-way flow

through a doorway can also be expressed by the power law elements [49]. The orifice equation can also be used to evaluate air flow across large openings when pressure distribution is uniformly distributed over the height of the opening.

The main objective of this chapter is to mathematically model the transient behaviour of air humidity within multi-zone spaces. This has been achieved by incorporating a multi-cell air flow model with the room air humidity response model described earlier in Chapter 4. The model consists of a system of interrelated differential equations which describe the moisture mass balance in each zone as well as the moisture interaction between the different zones. Instantaneous zonal air humidity conditions have been evaluated by simultaneously solving the resulting differential equations using the Gill's modified Runge-Kutta method. In order to appreciate the relative influence of the different moisture transport processes involved on zonal air humidity behaviour and distribution, a study case is presented. The influence of the zonal physical and functional characteristics is investigated. Moreover, the impact of zonal arrangement and the combined effect of air leakage through the building envelope and the inter-space air movement on zonal air humidity behaviour is studied.

5.2 The Mathematical Model

Air humidity dynamics within a particular zone in a multi-zone space is dependent on its interaction with the exterior environment, its inter-zonal connections and its functional and physical characteristics. Zones which are physically separated or have small connections (i.e. flow paths) with other zones are likely to behave independently. In this case, local moisture transport process such as, surface condensation and moisture absorption will determine the dynamic behaviour of air humidity within the zone. Assuming that moisture

added or removed from the space through any moisture transport process will uniformly affect its air moisture condition, then by utilizing the moisture mass balance approach, air humidity dynamics within the space can be modelled. Air humidity behaviour in an independent zone with no inter-zonal connections can be given by Equation 5.1.

$$\rho_a V \frac{dW_r}{dt} = \sum_{i=1}^{ns} \frac{dms_i}{dt} + \sum_{i=1}^{na} \frac{dma_i}{dt} + \sum_{i=1}^{nc} \frac{dmc_i}{dt} + \sum_{i=1}^{nv} \frac{dme_i}{dt} + \sum_{i=1}^{ng} mg_i + \frac{dmm}{dt} \qquad (5.1)$$

where,

dW_r/dt = rate of change in indoor air moisture content, *kg/kg·s.*

dms/dt = rate of moisture absorption and desorption by interior materials, *kg/s.*

dma/dt = rate of moisture added or removed due to air flow across room boundaries, *kg/s.*

dmc/dt = rate of moisture removed by condensation, *kg/s.*

dme/dt = rate of moisture added by evaporation, *kg/s.*

mg = rate of moisture generation from indoor sources (i.e. people, indoor operations, etc.), *kg/s.*

dmm/dt= rate of moisture removed by the dehumidification process, *kg/s*

In reality, different zones in buildings are usually connected by flow paths through which moisture can be exchanged either by convective currents or by vapour diffusion. Consequently, air humidity behaviours in connected zones become interdependent. The degree of interaction between different zones depends on the effective area of the connecting opening as well as the pressure differential across it. Moisture transfer by convection occurs between exterior and interior zones since a pressure difference

normally exists across the connecting openings. A pressure difference could result either from the mass balance due to air leakage, or the stack effect caused by a temperature difference between the connected zones. Although inter-zonal diffusive moisture transfer is relatively small, however, considerable amount of moisture could be transported via this moisture transfer mechanism when large openings connect the zones.

Air humidity dynamic behaviour in a multi-zone space can be modelled by a system of linear differential equations. Each equations describes air humidity response in a particular zone. Based on the above assumption, the dynamic response of air humidity in a given zone can be generally given by Equation 5.2.

$$\frac{dW_r}{dt} = \frac{1}{\rho_a V}\left[\sum_{j=1}\frac{dms}{dt} + \sum_{j=1}\frac{dma}{dt} + \sum_{j=1}\frac{dmf}{dt} + \sum_{j=1}\frac{dmc}{dt} + \sum_{j=1}\frac{dme}{dt} + \sum_{j=1} mg + \frac{dmm}{dt}\right] \tag{5.2}$$

The second term on the right side of Equation 5.2 represents moisture transfer due to air leakage through exterior walls, as well as moisture transfer due to inter-zonal air movement. The third term represents moisture transfer by diffusion through large openings. Moisture transfer by diffusion is only considered when there is no air movement across the opening. This normally occurs between interior zones with the same air temperature. Substituting for the moisture transport processes, Equation 5.2 can be written for the k-th zone as given by Equation 5.3. In order to determine zonal air humidity behaviour in a multi-zone space of n zones, n differential equations, similar to Equation 5.3, have to be written and solved simultaneously through numerical techniques.

$$\frac{dW_r(k)}{dt} = \sum_{j=1}^{nsl} C_j[W_{mo_j} - W_r(k)]\exp(-B_j t) + \sum_{j=1}^{ns2} C_j[W_{ms_j}(t) - W_r(k)] +$$

$$M_a[\sum_{j=1}^{noi} Q_{oi_j} W_{o_j} - W_r(k)\sum_{j=1}^{nio} Q_{io_j}] + M_v \sum_{j=1}^{nop} A_{o_{ij}}[W_r(j) - W_r(k)] + \quad (5.3)$$

$$M_a[\sum_{j=1}^{nc} A_{c_j} h_{mc}\{W_{sc_j} - W_r(k)\} + \sum_{j=1}^{nv} A_{e_j} h_{me}\{W_{sej} - W_r(k)\} + \sum_{j=1}^{ng} mg_j +$$

$$Q_{sp}(W_{sp} - W_r(k)]$$

where

$$B = \frac{A_m\ h_{ms}}{R_v\ \rho_a\ V_m\ C_m\ T_m}$$

$$C = \frac{A_m\ h_{ms}}{\rho_a\ V}$$

$$M_a = \frac{1}{\rho_a V(k)}$$

$$M_v = \frac{D_{va}}{\Delta L V(k)}$$

However, for better understanding and appreciation of the influence of inter-zone moisture interaction on zonal air humidity behaviour, the analytical solution of a simple two-zone system will be discussed first. The two zones are assumed to be maintained at different air temperatures and are initially at different air humidity conditions. In order to simplify the problem, it is assumed that the only moisture transport process available is the inter-zone airflow through which moisture is exchanged between the two zones under the stack effect action. For this case, zonal air humidity response can be described by the following coupled differential equations:

$$\frac{dW_r(i)}{dt} = \frac{Q_{ji}}{\rho_{ai} V_i}[W_r(j) - W_r(i)] \quad (5.4a)$$

$$\frac{dW_r(j)}{dt} = \frac{Q_{ij}}{\rho_{aj} V_j}[W_r(i) - W_r(j)] \qquad (5.4b)$$

Where Q_{ji} represents the airflow from zone j to zone i, and Q_{ij} represents the opposite flow. By solving this system of differential equations, air humidity response for zone i can be given by:

$$W_r(i) = W_{ro}(i)\exp(-\alpha_r t) + \beta_r[1 - \exp(-\alpha_r t)] \qquad (5.5)$$

where

$$\alpha_r = \frac{Q_{ji}}{\rho_{ai} V_i} + \frac{Q_{ij}}{\rho_{aj} V_j}$$

$$\beta_r = [\frac{W_{ro}(j) Q_{ji}}{\rho_{ai} V_i} + \frac{W_{ro}(i) Q_{ij}}{\rho_{aj} V_j}] / \alpha_r$$

From Equation 5.5 it can be seen that air humidity behaviour in zone i is dependent on the air moisture conditions in zone j. Similarly, air humidity behaviour in zone j is dependent on zone i. This interdependence between the zones is a result of the two-way inter-zone airflow and is represented by a system characteristic time α_r, which incorporate the responses of the two zones. In this case, each zone acts as a moisture source and a moisture sink at the same time relative to the other. On the other hand, in a one-way inter-zone air flow, a given zone will either represent a moisture source or a moisture sink. Air humidity behaviour in the source zone will depend on air moisture conditions of an external source such as the outdoor environment in case of a two-zone system or possibly another connected zone in case of a multi-zone system. The airflow rates along the flow paths connecting the different zones are the main factors determining the system overall air humidity response and the degree of interaction between the different zones. Therefore

for solving the resulting system of differential equations which describes air humidity behaviour in a multi-zone space, the airflow rate along each flow path must be known.

5.3 Air Flow Through Building Enclosure Elements

In buildings, air flow occurs through different paths, ranging from a crack in the exterior envelope to a doorway connecting two zones. Knowledge of their leakage characteristics and the pressure difference across them is essential for evaluating the amount of air flow through each flow element.

5.3.1 Air flow through exterior building envelope: Air flow modelling through exterior building envelope due to different driving potentials have been discussed previously in Chapter 4. The same formulations can be used to evaluate the rate of air flow across the exterior walls of any particular zone. In this chapter discussion will be limited to the problem of air flow across inter-space openings which include large openings and closed doorways.

5.3.2 Inter-zonal Air Flow: An inter-zonal flow path could be a closed door or a large opening (i.e. doorway). Air flow through large openings tend to be more complex with the possibility of opposite flows due to temperature difference between the connected zones. In the absence of temperature difference (i.e. pressure distribution is uniform), air flow through both types of flow paths can be given by the orifice equation. For large openings air flow can be given by:

$$Q_{inz,o} = C\, A_o\, \rho_a \sqrt{\frac{2\Delta P}{\rho_a}} \tag{5.6}$$

where,

A_o= apparent area of opening

and for a closed door,

$$Q_{inz,d} = C\, A_{oe}\, \rho_a \sqrt{\frac{2\Delta P}{\rho_a}} \tag{5.7}$$

where,

A_{oe}= equivalent orifice area

The equivalent orifice area may be evaluated from the available leakage data of the door in question. Air flow through a closed door due to stack effect can also be modelled by the orifice area. However, to account for opposite flows, two flow elements are assigned. Assuming uniform distribution of leakage areas, the equivalent orifice area can be divided into an upper and a lower area, each representing the leakage paths in half of the door. The rate of air flow can be given by:

$$Q_{inz,d} = C\, (\frac{A_{oe}}{2})\, \overline{\rho}_a \sqrt{\frac{2\Delta P_s}{\overline{\rho}_a}} \tag{5.8}$$

the pressure due to stack effect can be evaluated by:

$$\Delta P_s = (2/9)\, g\, H_d(\rho_{a,i} - \rho_{a,j}) \tag{5.9}$$

where,

H_d= door height, m

and *i* and *j* refer to the connected zones.

In all of the above cases, a discharge coefficient of 0.6 can be used in the orifice equation, because in these cases either the opening is small or the pressure distribution does not vary with the opening height (*H*). However, for a large opening with the stack effect as the driving force, the problem cannot be modelled by the orifice equation using a discharge coefficient of 0.6. With the possibility of a positive pressure at the top and a negative pressure at the bottom or vice versa, the problem becomes more complicated. A review of previous research work on inter-zone convective heat transfer was carried out by Barakat [48]. Most researchers have attempted to describe the natural convective heat flow through large openings by developing a dimensionless correlation which takes the following general form [48]:

$$\frac{Nu_D}{Pr} = C_D \, Gr_D^b \qquad (5.10)$$

where,

$$Nu = h_c H/K \;, \quad Pr = c_p \mu/K \;, \quad Gr = g \beta \Delta T H^3/\nu^2$$

The value of b is approximately 0.5 and C_D lies between 0.22 and 0.33 depending on the temperature difference used for the correlation. For two full scale tests, some researchers tried to use their results to determine the coefficient C_D and the exponent b at different temperature differences, ΔT. Taking ΔT as the difference between the average temperature of the top and bottom halves of the doorway, C_D was found to be 0.26 and b equals to 0.5. For a temperature difference between a volume-weight average temperature calculated from vertically spaced thermocouples near the partition wall, C_D was found to have a value of 0.3 and b equals to 0.5. Based on the temperature measurement in the doorway, Equation 5.10 can then be written as:

$$\frac{Nu_D}{Pr} = 0.26\sqrt{Gr_D} \tag{5.11a}$$

and based on the average room temperature it can be written as:

$$\frac{Nu_D}{Pr} = 0.3\sqrt{Gr_D} \tag{5.11b}$$

Although the above equations can model air flow through large openings, a more suitable expression can be used by applying the orifice equation and appropriate flow coefficients. By dividing the opening into two equal halves, which is practically acceptable [141], and integrating over half of the opening, the flow rate is obtained by Equation 5.12 [141].

$$Q_{inz,o} = \int_{z=0}^{z=H/2} dQ = \frac{C}{3} W \sqrt{\frac{g \Delta \rho_a}{\overline{\rho}_a}} H^{3/2} \tag{5.12}$$

Substituting the expressions of Nusselt number, Prandtl number and Grashof number, it can be shown that Equation 5.12 is the same as Equation 5.10 with $C_D = C/3$ and b= 0.5 [49]. Comparison of equation 5.10 with Equations 5.11a and 5.11b requires the flow coefficient, C, to have a value of 0.78 or 0.9. According to Walton [49], a value of 0.9 seem unreasonably high when compared with other related studies. Therefore, a flow coefficient of 0.78 will be used in Equation 5.12.

5.4 Air Flow Network Modelling

In order to evaluate air flow through exterior building envelope or through inter-zone flow paths, air pressure in each zone must be known. Through an air flow network, or a multi-cell model as it is often called, a set of nodes are used to represent zones and ambient conditions. These nodes are connected by air flow elements which correspond to different air flow paths such as doorways and construction cracks. For evaluating the nodal

pressure, a mass balance is performed at each zonal node *i*,

$$\sum_{j=1}^{na} Q_{ij} = 0 \tag{5.13}$$

These mass balances will result in a set of nonlinear algebraic equations which have to be solved simultaneously by an iterative technique untill a certain convergence criterion is satisfied.

5.5 Diffusive Moisture Transfer

In the absence of air flow along inter-zone openings, vapour diffusion becomes the predominant moisture transfer mechanism. Although it is relatively a slow process, inter-zone vapour diffusion process could have a tangible effect on space air moisture distribution when large openings connect the zones. Vapour diffusion in air under isothermal conditions can be expressed by Fick's first law [20]:

$$g_v = D_{va} \left(\frac{d\rho_v}{dx}\right) \tag{5.14}$$

At non-isothermal conditions thermo-diffusion takes place when water vapour molecules diffuse towards higher temperatures. However, thermo-diffusion is often considered to be negligible [82]. The amount of vapour diffusion between two zones connected by a large opening and separated by a wall of thickness, ΔL can be expressed by Equation 5.15.

$$g_{v,inz} = D_{va} \frac{A_o}{\Delta L} \rho_a \Delta W_r \tag{5.15}$$

The vapour diffusion coefficient, D_{va} is dependent on the temperature and the pressure. An empirical equation for water vapour diffusivity in air is given by Equation 5.16 [20], where D_{va} is in mm^2/s, P in kPa and T_k in Kelvin.

$$D_{va}=(0.926/P)[\frac{T_k^{2.5}}{(T_k+245)}] \quad (5.16)$$

5.6 Solutions of Model Equations

5.6.1 A system of differential equations: The dynamic behaviour of air humidity in a multi-zone space can be determined by simultaneously solving a set of linear differential equations, generally given by Equation 5.3. Each equation includes several time-dependent parameters associated with different moisture transport processes. Because of the relationship between the boundary conditions and some of these parameters, their variations can not be expressed in terms of time via a continuous function. Instead, a discrete time interval, Δt, during which these parameters can be assumed constant, will be used. At each time interval a system of linear differential equations must be solved simultaneously. In addition, the values of all time-dependent parameters must be updated using appropriate mathematical models at the end of each time interval. The system of differential equations has been solved numerically using Gill's modified Runge-Kutta method [142]. This method handles the round-off errors in such a way that the highest attainable accuracy is obtained. In addition, it requires minimum storage capacity and a small number of computer instructions to implement [142].

5.6.2 A system of nonlinear algebraic equations: Evaluating the rates of air flow across exterior building envelope and inter-zone flow paths requires the solution of a set of *n* nonlinear algebraic equations which describe the mass balance at each zone. A widely utilized technique is the Newton's method. Although this method is not always convergent, it is the most commonly used method for the solution of a system of nonlinear

algebraic equations, because of its better convergence properties relative to other methods. The basis for the Newton's iteration method is a Taylor expansion of each of the nodal equations. For the i-th node,

$$f_i(P_1+\Delta P_1,...,P_n+\Delta P_n)=f_i(P_1,...,P_n)+\Delta P_1\frac{\partial f_i}{\partial P_1}+...,$$
$$\Delta P_n\frac{\partial f_i}{\partial P_n}+Higher\text{-}OrderTerms \qquad (5.17)$$

When the ΔP_i corrections in the nodal pressures values bring the function f_i to the root, the left hand side of Equation 5.17 can be put equal to zero. By dropping the higher-order terms, the problem is reduced to that of finding the corrections ΔP_i that achieve the goal by solving a linear system of equations given in the following matrix form:

$$\begin{bmatrix} \frac{\partial f_1}{\partial P_1} & \cdots & \frac{\partial f_1}{\partial P_n} \\ \vdots & & \vdots \\ \frac{\partial f_n}{\partial P_1} & \cdots & \frac{\partial f_n}{\partial P_n} \end{bmatrix} \begin{bmatrix} \Delta P_1 \\ \vdots \\ \Delta P_n \end{bmatrix} = \begin{bmatrix} -f_1 \\ \vdots \\ -f_n \end{bmatrix} \qquad (5.18)$$

For the i-th node, the value of the element in the right side column vector is given by:

$$f_i=\sum_{j=1}^{nq}Q_{ij} \qquad (5.19)$$

The derivative matrix and the vector on the right side can be easily evaluated at any nodal pressure values. Once ΔP_i values are known, a new estimate of the vector of all nodes pressures $[P]^{k+1}$, can be computed from the current estimate of pressures $[P]^k$ by:

$$[P]^{k+1} = [P]^k + [\Delta P] \tag{5.20}$$

The above process is repeated, till the absolute values of the functions f_j are less or equal a specified tolerance value ε.

$$|f_j| \leq \varepsilon \qquad j=1,2,...,n \tag{5.21}$$

The current pressure values are then taken as the solution on the nonlinear system of equations.

Utilizing Newton's method, a computer program has been developed to solve for the pressure distribution in a multi-zone space. The solutions obtained by the program for a single zone space and a two-zone space connected by a large opening (i.e. 2 m^2) are the same as the results obtained by the computer algorithm, AIRNET, developed by Walton [51] when a tolerance of 1E-5 is used. In both these cases, the wind pressure and the stack effect were considered.

5.7 Application and Discussions

The various mathematical formulations discussed previously in this chapter have been implemented for developing a multi-zone air humidity evaluation computer program called "MHVPM". The program can simulate zonal air humidity transient behaviour at different boundary conditions and zonal characteristics. In order to demonstrate the applicability of the proposed model, and to study the impact of zonal characteristics as well as the inter-zonal connectivity on zonal air humidity behaviour, a case study will be carried out and discussed by utilizing the developed computer program. Air humidity behaviour within a five-zone space with its zonal arrangement shown in Fig. 5.1 is investigated at different conditions. Each zone has a volume of 150 m^3, and is maintained at 21° C. The zones are

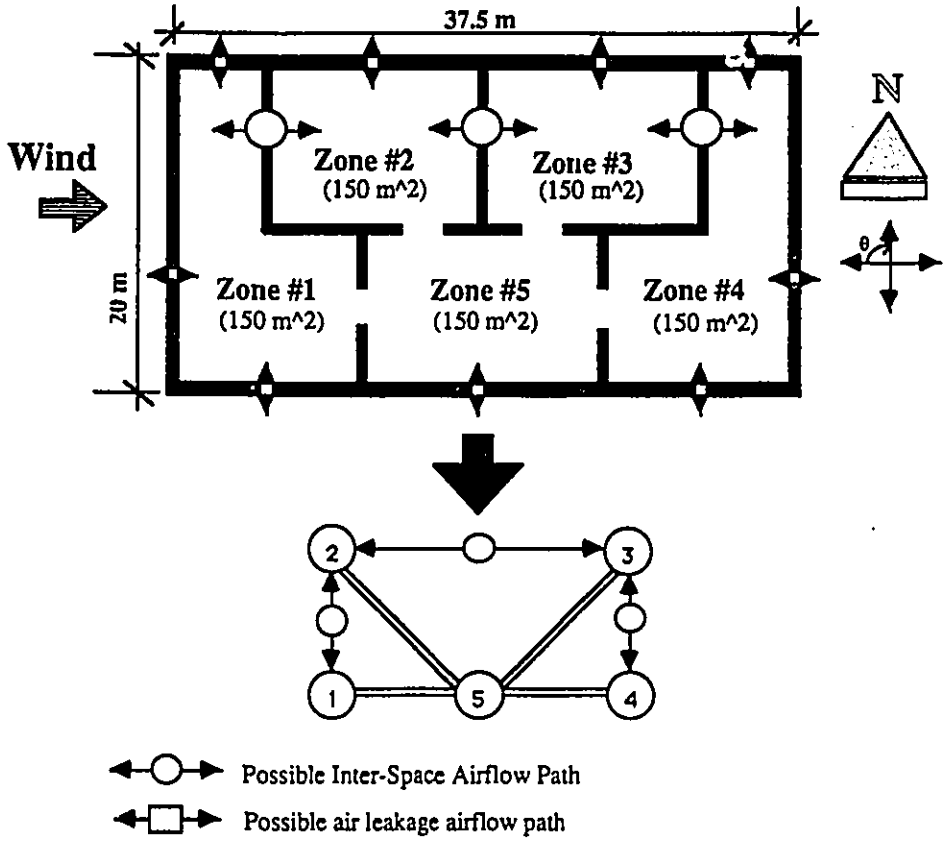

Fig. 5.1 A schematic for the first zonal arrangements for the modelled multi-zone building.

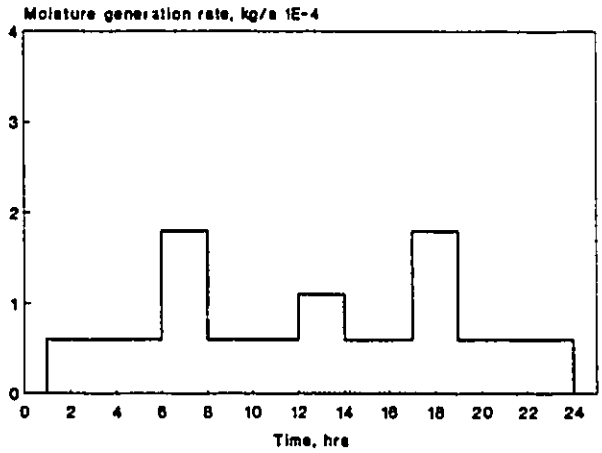

Fig. 5.2 Daily indoor moisture generation profile for the multi-zone space.

either connected by large openings (i.e., 2 m^2) or by closed door with an effective leakage area of 0.00385 m^2 depending on the modelled case. Tables 5.1-a and 5.1-b illustrate the zonal characteristics of the different cases considered.

The outdoor hourly environmental conditions used in the simulation are the same as those used in chapter 4 both for winter and summer conditions. The effect of wind speed and direction on wind pressure distribution is evaluated according to Swami and Chandra [45]. The moisture profile shown in Fig. 5.2 will be used to simulate the indoor moisture generation process.

5.7.1 Impact of exterior walls characteristics: Zonal air humidity behaviour due to air leakage during a winter day for different exterior wall air leakage characteristics is shown in Figs. 5.3-5.5. In all these cases, zone 5 is connected with all other zones by large openings. It can be seen that zonal response due to air leakage depends on the zone location in term of the flow path between the infiltrating and the exfiltrating air. In this particular case, positive wind pressure prevails over the west and south walls as can be predicted from the hourly wind azimuth shown in Fig. 4.7. This positive pressure causes outdoor air to directly infiltrate into zones 1, 4 and 5, and exfiltrate from zones 2, 3 and 4. From Fig. 5.3 it can be seen that zone 1 is the most responsive to the outdoor air humidity variations. This can be mainly attributed to its large exterior wall area and its location relative to the wind direction where most of its exterior walls is subjected to positive pressure. Furthermore, the presence of a large connecting area between zone 1 and zone 5 through which air can exfiltrate would result in a higher air change rate for zone 1. At the same time it would result in a greater degree of interdependence between zone 1 and zone 5.

Table 5.1-a: Air leakage characteristics and indoor moisture generation for the modelled multi-zone spaces.

Case #	Angle of Rotation	Zonal Arrangement	Space Air Leakage Characteristics											Indoor Moisture Generation	
			Leakage Coefficient $m^3/m^2.Pa^{.65}.s$ 1E-4				Inter-Zonal Connectivity								
								Connected Zones							
			W. Wall	N. Wall	E. Wall	S. Wall	Area, m^2	Zone 1	Zone 2	Zone 3	Zone 4	Zone 5		Location	Rate, kg/s
1	90	First	0.5	0.5	0.5	0.5	2.0	5	5	5	5	1,2,3,4		-	-
2	90	First	1.0	1.0	1.0	1.0	2.0	5	5	5	5	1,2,3,4		-	-
3	90	First	2.0	2.0	2.0	2.0	2.0	5	5	5	5	1,2,3,4		-	-
4	90	First	0.0	1.0	1.0	1.0	2.0	5	5	5	5	1,2,3,4		-	-
5	90	First	1.0	0.0	1.0	0.0	2.0	5	5	5	5	1,2,3,4		-	-
6	90	First	1.0	1.0	0.0	1.0	2.0	5	5	5	5	1,2,3,4		-	-
7	90	First	0.5	1.0	1.0	0.5	2.0	5	5	5	5	1,2,3,4		-	-
8	0	First	0.5	1.0	1.0	0.5	2.0	5	5	5	5	1,2,3,4		-	-
9	90	First	1.0	1.0	1.0	1.0	2.0	2,5	1,5	5	5	1,2,3,4		-	-
10	90	First	1.0	1.0	1.0	1.0	2.0	2,5	1,5	4,5	3,5	1,2,3,4		-	-
11	90	First	1.0	1.0	1.0	1.0	2.0	2	1,5	4,5	3	2,3		-	-
12	90	First	1.0	1.0	1.0	1.0	2.0	5	3,5	2,5	5	1,2,3,4		-	-
13	90	First	1.0	1.0	1.0	1.0	.0038	5	5	5	5	1,2,3,4		-	-

P= Moisture Generation Profile

Table 5.1-b: Air leakage characteristics and indoor moisture generation for the modelled multi-zone spaces.

Case #	Angle of Rotation	Zonal Arrangement	Space Air Leakage Characteristics										Indoor Moisture Generation	
			Leakage Coefficient $m^3/m^2.Pa^{.65}.s$ 1E-4				Inter-Zonal Connectivity							
								Connected Zones						
			W. Wall	N. Wall	E. Wall	S. Wall	Area, m^2	Zone 1	Zone 2	Zone 3	Zone 4	Zone 5	Location	Rate, Kg/s
14	90	First	1.0	1.0	1.0	1.0	2.0	5	5	5	5	1,2,3,4	Zone 1	P
15	90	First	1.0	1.0	1.0	1.0	2.0	5	5	5	5	1,2,3,4	Zone 5	P
16	90	First	1.0	1.0	1.0	1.0	2.0	5	5	5	5	1,2,3,4	Zone 3	P
17	90	First	1.0	1.0	1.0	1.0	0.0038	5	5	5	5	1,2,3,4	Zone 5	P
18	90	First	0.0	0.0	0.0	0.0	2.0	5	5	5	5	1,2,3,4	Zone 5	P
19	90	First	0.0	0.0	0.0	0.0	2.0	5	5	5	5	1,2,3,4	Zone 5	P
20	90	First	1.0	1.0	1.0	1.0	2.0	5	5	5	5	1,2,3,4	Zone 5	P
21	90	First	1.0	1.0	1.0	1.0	2.0	5	5	5	5	1,2,3,4	Zone 5	P
22	90	Second	1.0	1.0	1.0	1.0	2.0	5	5	5	5	1,2,3,4	-	-
23	90	Second	0.0	1.0	1.0	1.0	2.0	5	5	5	5	1,2,3,4	-	-
24	90	Second	1.0	0.0	1.0	0.0	2.0	5	5	5	5	1,2,3,4	-	-
25	90	Second	1.0	0.0	1.0	0.0	2.0	5	5	5	5	1,2,3,4	-	-

P= Moisture Generation Profile

Although the exterior wall of zone 5 is much smaller, it experiences relatively major air humidity changes similar to zone 1. This can be explained by the presence of the large connecting opening between the two zones through which most of the infiltrating air into zone 1 will flow into zone 5. Air humidity responses of zones 2 and 3 are identical since both of them are connected to the same zone with the same opening area. Both these zones are dependent zones where their air humidity behaviour is determined by the air moisture conditions in zone 5, hence they are expected to be less responsive than zone 5 as can be seen from Fig. 5.3. This behaviour is due to the fact that exfiltrating air from zone 5 will be split into these two zones in addition to zone 4. Air humidity response of zone 5 is almost the same as that in zone 2 and zone 3, however, because air can infiltrate through its south wall, its response is slightly different. By increasing the air leakage coefficient of the exterior walls, Zonal air humidity tends to be more responsive to variations in outdoor air humidity, but not proportional to changes in the air leakage coefficient. In addition, differences in zonal air humidity responses tend to diminish with increasing the air leakage rate although the relative zonal responses remain essentially unchanged.

Zonal air humidity behaviour can be considerably altered when the air leakage characteristics of the exterior walls are modified. Fig. 5.6 illustrates the impact of blocking air infiltration through the west wall. Comparison with Fig. 5.4 shows that air humidity responses in all zones have been considerably reduced except for zone 4 where it remains essentially unchanged. The reduced air infiltration into zone 1 has locally affected its air humidity behaviour as well as the air humidity behaviour of directly dependent zones such as zone 5, and the indirectly dependent zones such as zone 2. Zone 4 is less affected by the reduced response of zone 5 since its air humidity behaviour is mainly

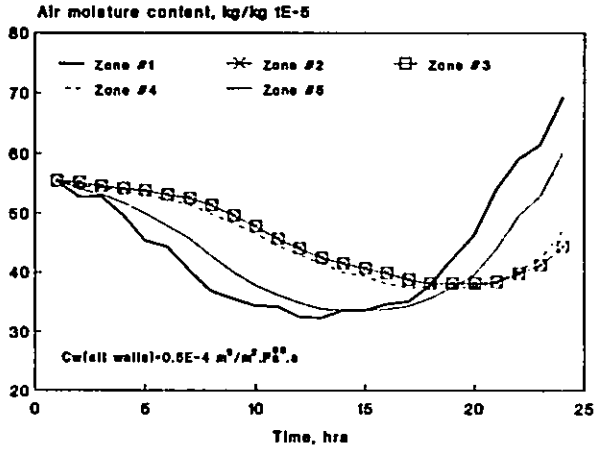

Fig. 5.3 Zonal air humidity response due to air leakage in a winter day for a relatively air tight enclosure (case #1).

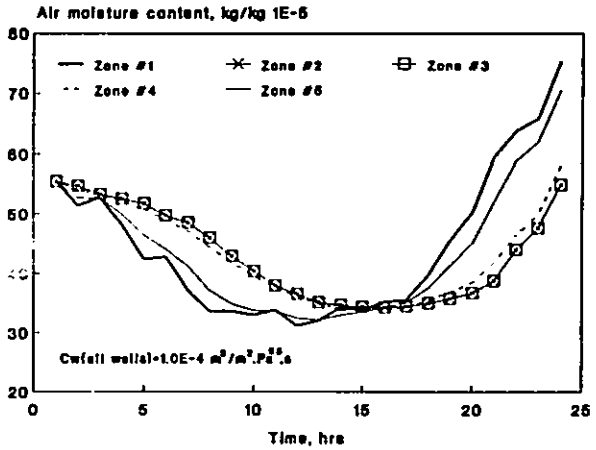

Fig. 5.4 Zonal air humidity response due to air leakage in a winter day for average enclosure air tightness (case #2).

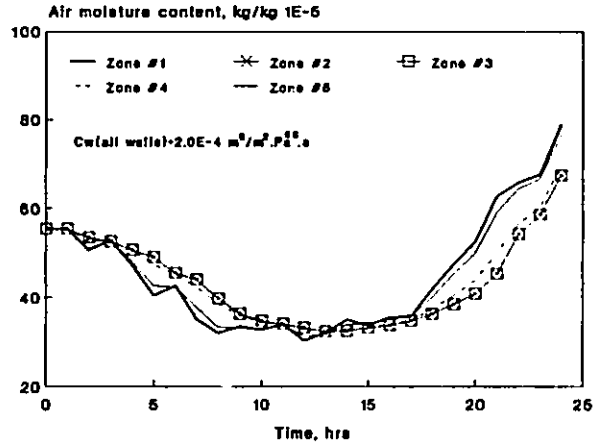

Fig. 5.5 Zonal air humidity response due to air leakage in a winter day for a relatively untight enclosure (case #3).

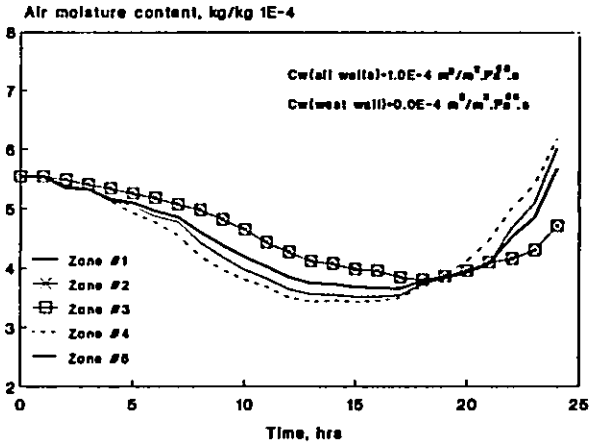

Fig. 5.6 Zonal air humidity response due to air leakage when no airflow occurs through the west walls (case #4).

determined by the air infiltration process across its exterior wall. When no air movement occurs through the south and the north walls, air will only flow through the short path connecting zones 1, 5 and 4. In this case, air humidity in zone 2 and zone 3 will experience a slight change, as shown in Fig. 5.7, resulting from the diffusion process across the large openings connecting them to zone 5. Comparison with Fig. 5.4, would indicate that the absence of air movement through the north and the south wall has limited impact on air humidity response of the other three zones. This would indicate that for the zonal arrangement shown in Fig. 5.1, air movement through the north wall is a determining process for zone 2 and zone 3, which means that the absence of air movement across that particular wall will eliminate the impact of the air flow process on air humidity behaviour on a particular zone. On the other hand, air humidity behaviour of the other zones is not determined by air movement through any particular wall because of their connectivity and exterior walls arrangement. Air movement across the exterior wall corresponding to a particular zone will undoubtedly affect air humidity behaviour in that zone and its dependent zones. By eliminating air movement across the east wall, zone 4 experiences a major decrease in its response as can be seen from Fig. 5.8. According to the mass balance concept, less air is able to flow into zone 4 either from zone 5 or through its south exterior wall. Since zone 4 is not a source zone (i.e., no air flow occurs from zone 4 to any other zones), the reduced air flow across it has no noticeable effect on the other zones.

The impact of reducing the air leakage coefficient of the west and south walls by 50% is shown in Fig. 5.9. Comparison with Fig. 5.4 indicates that air humidity response in all zones has been reduced since all zones either directly or indirectly are affected by the reduced air leakage through the these walls. On the other hand, the relative zonal

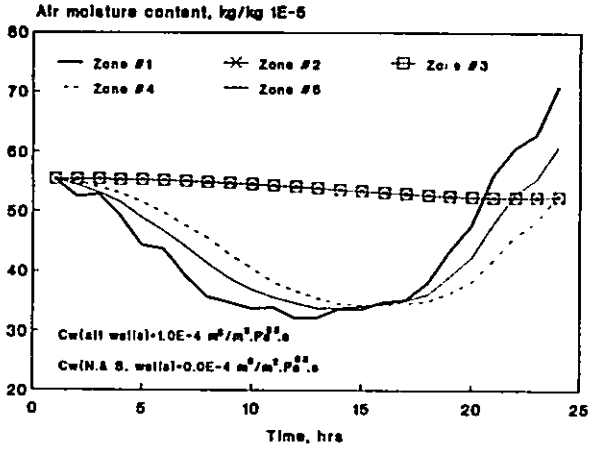

Fig. 5.7 Zonal air humidity response due to air leakage when no airflow occurs through the south & north walls (Case #5).

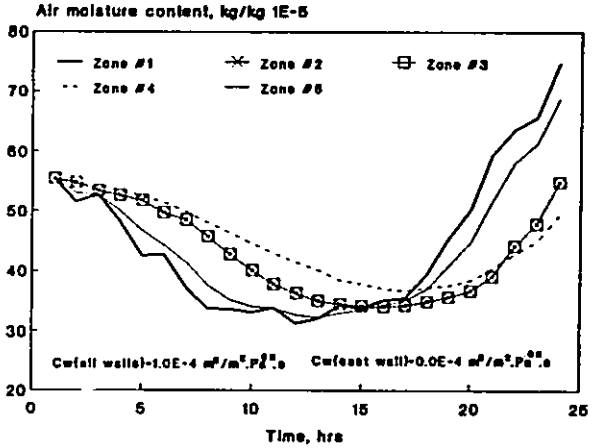

Fig. 5.8 Zonal air humidity response due to air leakage when no airflow occurs through the east walls (Case #6).

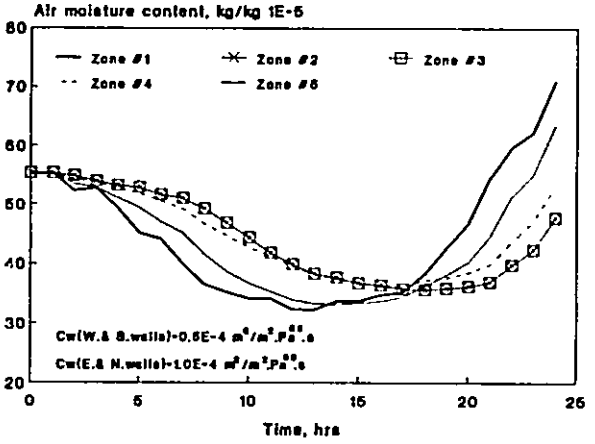

Fig. 5.9 Zonal air humidity response due to air leakage at different exterior walls air leakage coefficients (Case #7).

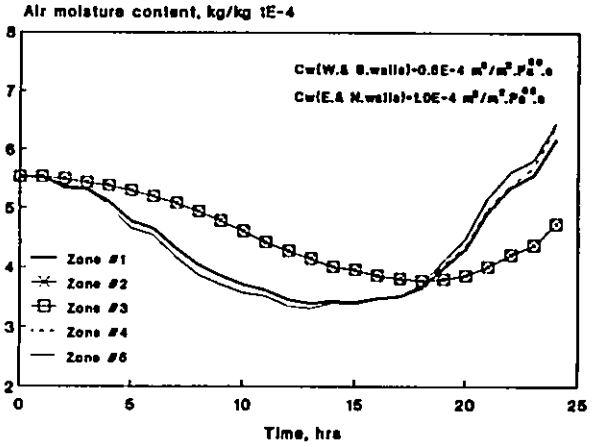

Fig. 5.10 Zonal air humidity response due to air leakage when the building is rotated 90 deg clockwise (Case #8).

response has remained unchanged since zone 1 is still the most responsive while zones 2 and 3 are the least responsive. When the modelled space, which is original oriented as shown in Fig. 5.9, is rotated 90° clockwise, air humidity behaviour in zones 1 and 4 experiences noticeable change while it remains unaltered in other zones as can be seen from Fig. 5.10. By rotating the building, air infiltration through the west wall corresponding to zone 1 has been eliminated. At the same time, air infiltration through the east wall of zone 4 has been introduced. For the other zones, the orientation of their exterior wall in terms of the wind direction remains unchanged resulting in minor modification in their air humidity behaviour. The nearly identical air humidity response in zone 1, 4 and 5 is an indication of the greater interdependence between these zones which has resulted from increased inter-zone air flow.

5.7.2 Impact of Inter-zone Connectivity: For given boundary conditions, the spatial pressure distribution and the rate of inter-zone air flow between any two zones will be determined by the way the different zones are connected. Consequently, zonal connectivity will be an important factor in determining air humidity behaviour in the different zones. In all previous cases, zone 5 was connected to the other zones by large openings. Connecting zone 2 with zone 3 by a large opening has no effect on zonal air humidity behaviour as can be seen by comparing Fig. 5.11 to Fig. 5.4. This means that essentially no air flow takes place across the connecting opening. However, by introducing a large opening between zone 1 and zone 2, the inter-zone air flow pattern is altered and hence different zonal air humidity responses are obtained as can be seen from Fig. 5.12. Introducing a large opening between zone 1 and zone 2 has caused air to directly flow from zone 1 into zone 2 causing air humidity in zone 2 to behave differently from zone 3. Comparison with Fig. 5.4 shows that while air humidity response in zone 2 is increased

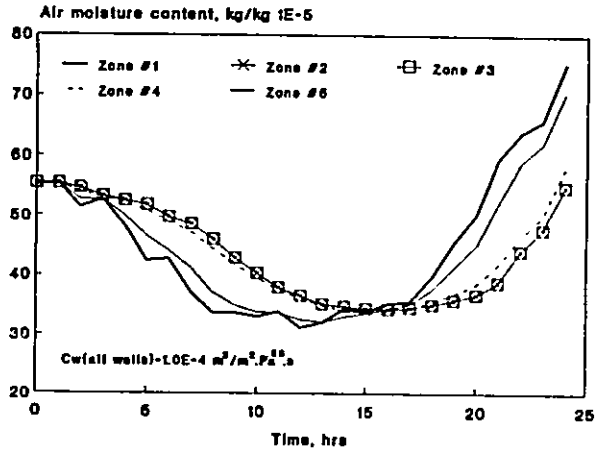

Fig. 5.11 Zonal air humidity response due to air leakage when a large opening connects zone #2 and zone #3 (Case #9).

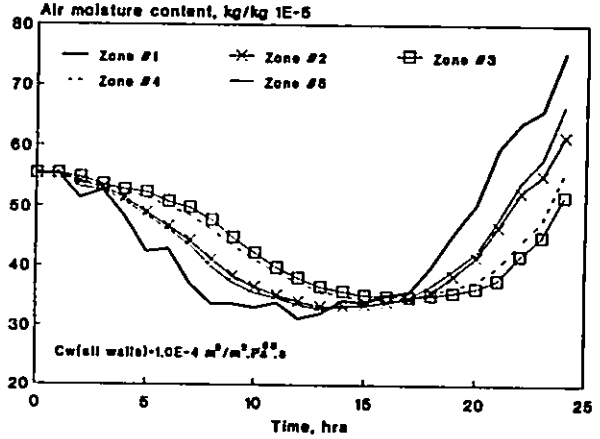

Fig. 5.12 Zonal air humidity response due to air leakage when zone #1 and zone #2 are connected by a large opening (Case #10).

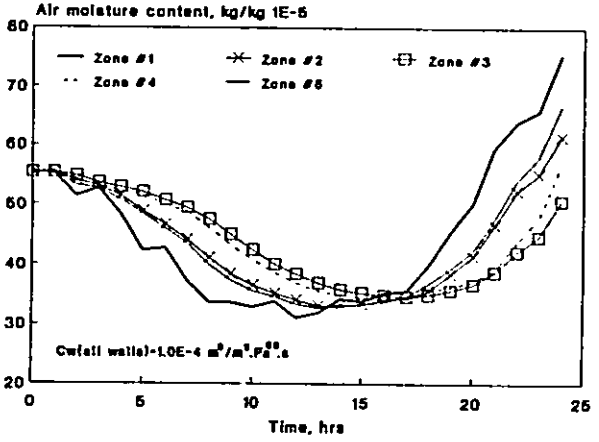

Fig. 5.13 Zonal air humidity response due to air leakage when large openings connects zone #1 with zone #2, and zone #3 with zone #4 (Case #11).

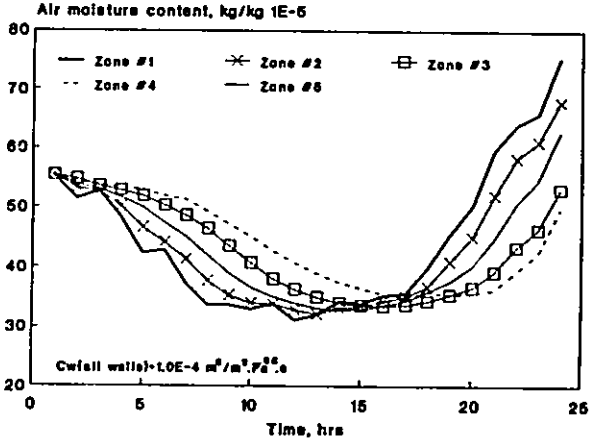

Fig. 5.14 Zonal air humidity response due to air leakage when zone #2 is connected with zone #1 and zone #5, and zone #3 is connected with zone #4 and zone #5 (Case #12).

due to increased air flow through the opening connecting it with zone 1, it is dampened in the other zones due to decreased air flow from zone 1 to zone 5. On the other hand, connecting zone 3 with zone 4 by a large opening has no noticeable effect on the overall zonal air humidity response as can be seen by comparing Fig. 5.13 with Fig. 5.12. When the openings connecting zone 5 with zone 1 and zone 4 are eliminated , the inter-zone air flow pattern and consequently the zonal air humidity responses are completely altered. Comparison with Fig. 5.13, shows that the response of zone 2 is considerably increased since it is the only one connected to zone 1 while zone 4 experiences the lowest response. By eliminating the opening connecting it with zone 5, zone 4 becomes dependent on zone 3 which means that zone 3 will be more responsive than zone 4 as can be seen from Fig. 5.14. In addition, it can be seen that zone 1 remains unaffected by the changes in the zonal connectivity since it does not depend on inter-space air flow from adjacent zones. When zone 5 is connected with the other zones by closed doors, all zones exhibit reduced air humidity response as can be seen from Fig. 5.15. Comparison with Fig. 5.4 shows that the most affected zones are zone 2 and zone 3 since their air humidity response is fully determined by the inter-zone air flow process

5.7.3 Zonal air humidity behaviour in ..ie presence of indoor moisture generation:

Moisture generation in a particular zone could have a considerable impact on local air humidity behaviour. Depending on the pattern of inter-space air flow and the location of the moisture generation source, air humidity behaviour in other zones can also be significantly modified. Consider the same arrangement shown in Fig. 5.1 when zone 5 is connected with all other zones by large openings. In the absence of indoor moisture generation, zonal air humidity behaviour is determined by the outdoor air humidity profile as illustrated in Fig. 5.4. However, in the presence of a moisture generation source in

zone 1, air humidity behaviour in all zones is positively modified as shown in Fig. 5.16. Zone 1 experiences the largest air humidity response, however, the variational pattern of the moisture generation profile is not reflected on the zone air humidity behaviour. Moreover, the response of the other zones to moisture generation in zone 1 is immediate and follows the same pattern of variations which is an indication of the important role of the air flow process in shaping zonal air humidity behaviour. The relative pattern of variation and the degree of response of air humidity in a particular zone indicate the degree of dependence between the different zones. From Fig. 5.16, it can be seen that zone 5 is the most responsive to air humidity variations in zone 1 since it is the only zone connected to zone 1, while all remaining zones are dependent on zone 5. Although zone 2 and zone 3 are fully dependent on zone 5, zone 4 shows the lowest response to humidity variations in zone 5 which is an indication that inter-zone air flow from zone 5 to zone 4 is less than that to either zone 2 or zone 3. The influence of the moisture generation process in a particular zone on air humidity behaviour in other zones depends on their locations in terms of the air flow stream. When the source zone (i.e., where the moisture is generated) is located down stream relative to a given zone , this zone will not be affected by the moisture generation process in the source zone. Fig. 5.17 shows zonal air humidity behaviour when the moisture source is located in zone 5. It can be seen that for this particular air flow pattern, moisture production in zone 5 has no effect on zone 1 since it is located up stream relative to the source zone. The relative impact of zone 5 on other zones is similar to that shown in Fig. 5.16, since the air flow pattern is unchanged. By locating the moisture source in zone 3, the moisture generation process has only a local effect as can be seen from Fig. 5.18, since all other zones are located down stream relative to the source zone. In addition to the location in terms of the source zone, the influence of moisture generation on zonal air humidity behaviour is dependent on the inter-

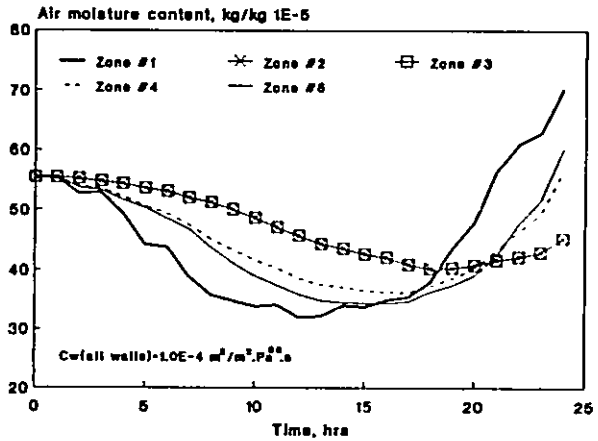

Fig. 5.15 Zonal air humidity response due to air leakage when all zones are connected with zone #5 by closed doors (Case #13).

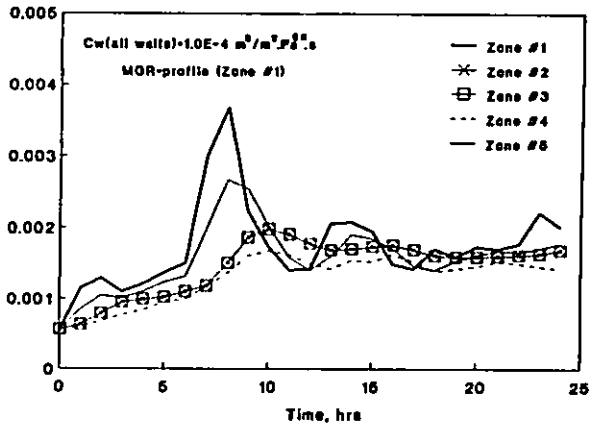

Fig. 5.16 Effect of moisture generation at zone #1 on zonal air humidity behaviour in the presence of air leakage (Case #14).

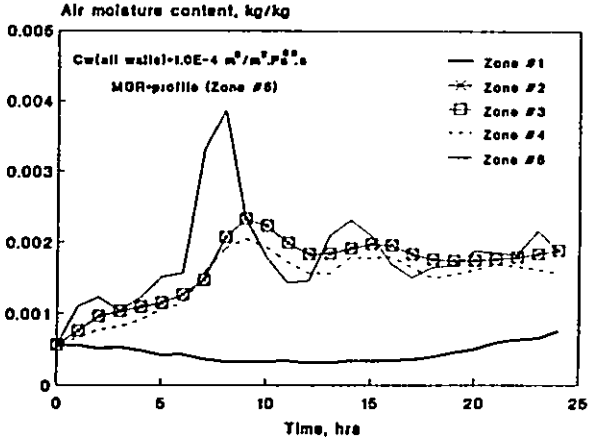

Fig. 5.17 Effect of the moisture generation process at zone #5 on zonal air humidity behaviour in the presence of air leakage (Case #15).

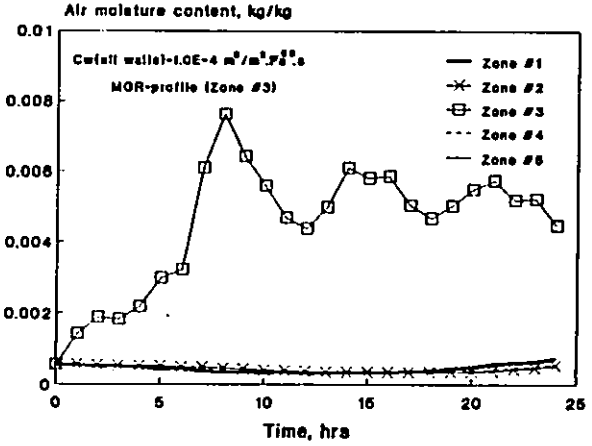

Fig. 5.18 Effect of moisture generation at zone #3 on zonal air humidity behaviour in the presence of air leakage (Case #16).

zonal connection between the source zone and the others. Fig. 5.19 shows the zonal air humidity behaviour when zone 5 is the source zone and is connected with other zones by closed doors. The reduced air flow from zone 5 has resulted in a considerable increase in its air humidity response as can be seen by comparing Fig. 5.19 with Fig. 5.17. Similarly, fully dependent zones like zone 2 show an increase in their air humidity response in spite of the reduced inter-zone air flow from the source zone. This behaviour can be attributed to the substantial decrease in moisture loss associated with the air exfiltrating from the space. On the other hand, reduced inter-space air flow has negatively affected partially dependent zones like zone 4 (i.e., air can flow in from other zones or by air leakage through exterior walls) which indicates that air movement through the exterior walls is still an influencing and important process. The absence of air leakage through exterior walls will eliminate any inter-zone air flow unless interconnected zones are maintained at different temperatures. In this case, moisture transfer by diffusion through the connecting openings will be the only active process. Fig. 5.20 shows zonal air humidity behaviour in the absence of inter-space air flow. It can be seen that all zones except the source zone, experience similar and slow increase in their air humidity, while the source zone reaches its saturation level within a short period of time. In practice, the saturation level is unlikely to be reached even in the absence of air leakage since other moisture transport processes will be activated at high air humidity levels. Surface condensation process is usually the process which determines how high the air humidity level can reach. Fig. 5.21 illustrates the impact of the surface condensation process on the source zone air humidity behaviour in the absence of air leakage. Such processes normally have an appreciable local impact, however, in the presence of inter-zone air flow, all dependent zones can be greatly influenced by local moisture processes within the source zone. This behaviour can probably be best demonstrated with the local dehumidification process

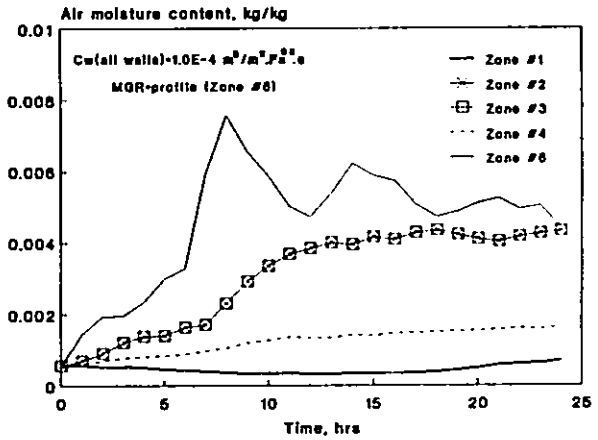

Fig. 5.19 Zonal air humidity response due to air leakage in the presence of indoor moisture generation at zone #5 when zone #5 is connected with others by closed doors (Case #17).

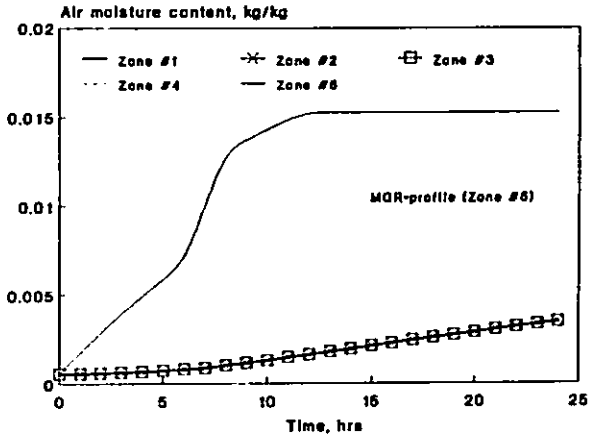

Fig. 5.20 Zonal air humidity behaviour in the absence of air leakage with moisture generation taking place at zone #5 (Case #18).

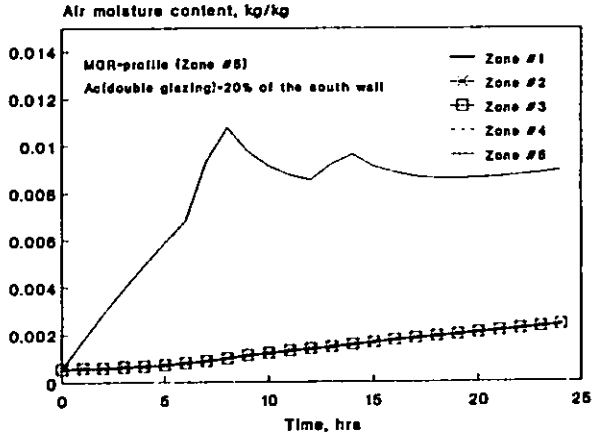

Fig. 5.21 Zonal air humidity behaviour in the absence of air leakage when moisture is generated at zone #5 with local surface condensation taking place (Case #19).

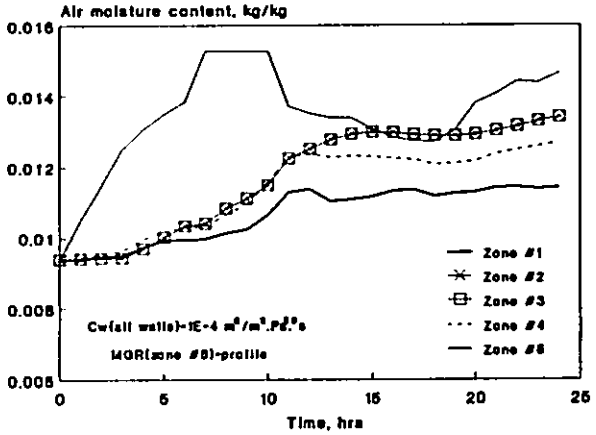

Fig. 5.22 Effect of moisture generation at zone #5 on zonal air humidity behaviour during a summer day in the presence of air leakage (Case #20).

during summer. Fig. 5.22 shows zonal air humidity behaviour during a summer day in the presence of moisture generation in zone 5. Comparison with Fig. 5.17 shows that the relative zonal response remains almost unchanged indicating that similar air flow pattern and zonal interdependence exist during the simulatod summer day. When a local dehumidification process is implemented in the source zone, its own air humidity behaviour as well as air humidity behaviour in all dependent zones are significantly modified as shown in Fig. 5.23. Because of their full dependence on zone 5, zone 2 and zone 3 respond very quickly to the reduced air humidity level in the source zone and reaching almost equal air humidity level at the end of the simulation period. The degree of influence of the local dehumidification process in zone 5 is less pronounced for zone 4 and is nil for zone 1. This demonstrates the importance of the inter-space air flow in determining the degree of interdependence between air humidity behaviours within the different zones.

5.7.4 Influence of zonal arrangement on air humidity behaviour: In order to demonstrate the effect of zonal arrangement, air humidity behaviour in a multi-zone space similar to that shown in Fig. 5.2 has to be studied. Fig. 5.24 shows the new zonal arrangement with the same space configuration as that shown in Fig. 5.2. Zonal air humidity behaviour due to air leakage, when zone 5 is connected with others by large openings, is shown in Fig. 5.25.

Comparison with Fig. 5.4 shows that with the new arrangement, zone 2 and zone 3 are no longer having the same air humidity behaviour. Furthermore, it can be seen that zone 2 and zone 4 experience a noticeable modification in their response while other zones experience little or no change. Zone 2 shows the greatest change in its behaviour since

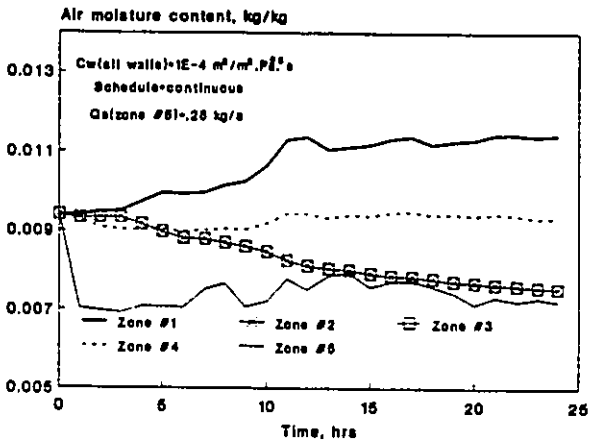

Fig. 5.23 Effect of moisture generation at zone #5 on zonal air humidity behaviour during a summer day when local dehumidification is implemented at zone #5 (Case #21).

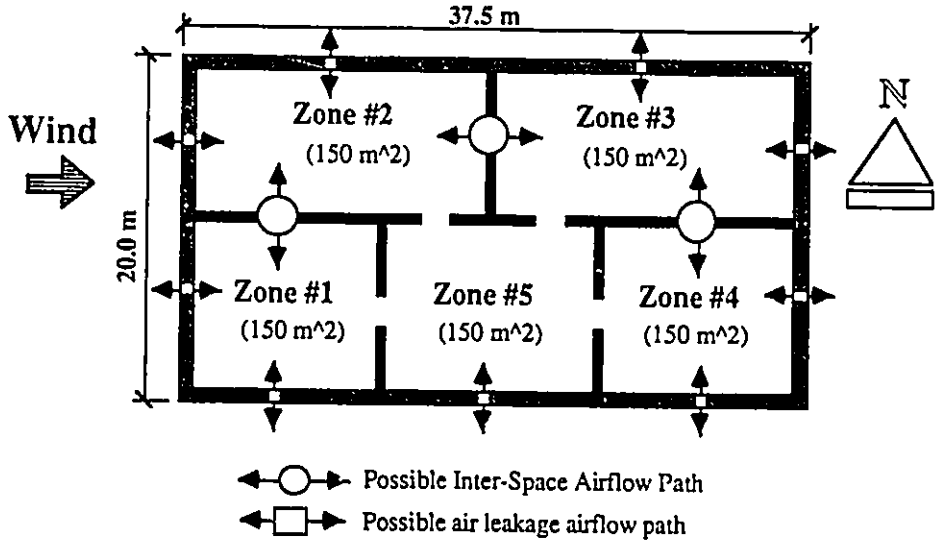

Fig. 5.24 A schematic for the second zonal arrangements for the modelled multi-zone building.

outdoor air can now directly infiltrate through its west exterior wall resulting in an increased air humidity response. The increased exterior wall area in zone 3 has not enhanced its response, since the zone is still dependent on zone 5 and no air infiltration occurs through any of its exterior walls. The reduced air infiltration through the exterior walls of zone 1 has minor impact on the response of the zone and its dependents. Zone 4, however, shows a considerable decrease in its response in spite of the increase in its south wall area. This can be explained by the significant reduction in its exterior walls from the exfiltrating side of the space which resulted in a reduced total air flow into the zone. The relative impact of eliminating air flow through the west wall on zonal air humidity behaviour is the same as the first zonal arrangement as can be seen by comparing Fig. 5.26 with Fig. 5.6. However, air humidity response of the zones 1, 4 and 5 show greater similarity in the second zonal arrangement. Zonal air humidity behaviour in the absence of air flow through the south and the north walls is shown in Fig. 5.27. Comparison with the zonal response of the first arrangement shown in Fig. 5.7, shows that eliminating air flow through these walls has a relatively marginal effect on zonal air humidity behaviour. In the first arrangement, air flow into zones 2 and 3 is dependent on the presence of air flow through the north wall, therefore its absence has completely eliminated the role of air flow as a moisture transport process. On the other hand, air flow can still occur through these zones in the second zonal arrangement even when no air flow takes place through the north wall. The impact of the zonal arrangement on zonal air humidity behaviour is dependent on the connectivity between the different zones as well as the type of the inter-zone air flow paths. Fig. 5.28 shows zonal air humidity behaviour when the large openings connecting zone 5 with other zones are replaced by closed doors. Comparison with Fig. 5.15 shows that in the first zonal arrangement connecting the zones by closed door has resulted in similar air humidity behaviour for the zones 4 and 5 while zone 1 behaves

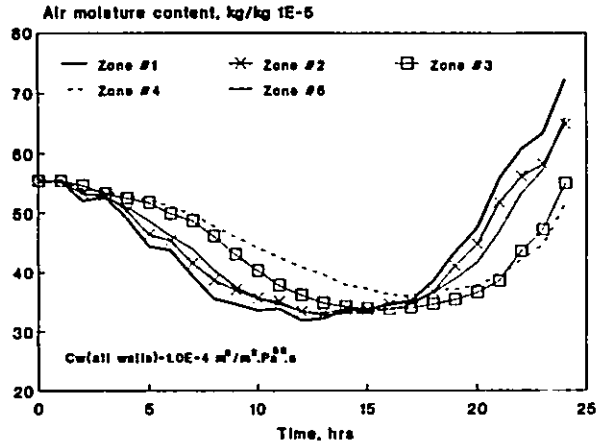

Fig. 5.25 Zonal air humidity response due to air leakage in a winter day for the second zonal arrangement (Case #22).

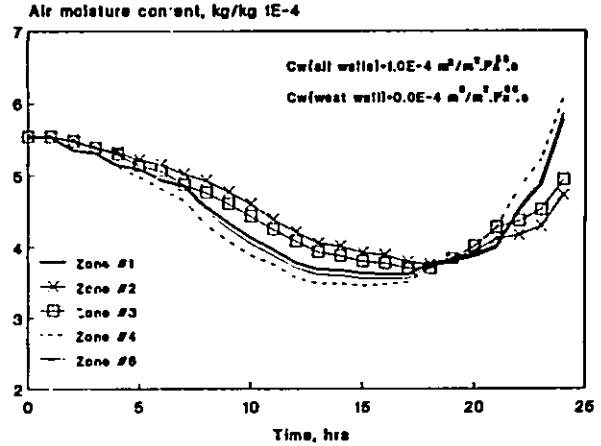

Fig. 5.26 Zonal air humidity response due to air leakage when no airflow occurs through the west walls (Case #23).

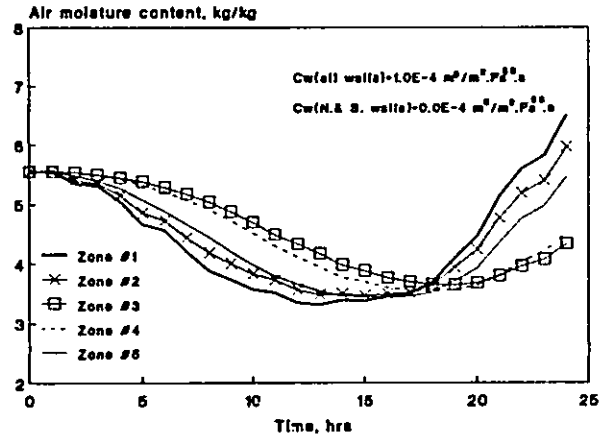

Fig. 5.27 Zonal air humidity response due to air leakage when no airflow occurs through the south and north walls (Case #24).

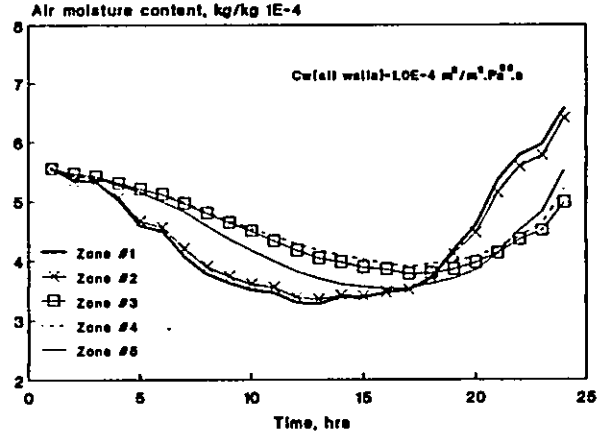

Fig. 5.28 Zonal air humidity response due to air leakage when all zones are connected with zone #5 by closed doors (Case #25).

independently. In the second arrangement, air humidity behaviour in zone 1 is similar to zone 2 and zone 3 behaves in the same manner as zone 4. This can be explained by the reduced inter-zone air flow from zone 5 to zone 3 which has resulted in a reduced response in zone 3. Similarly, the reduced air infiltration through the exterior walls of zone 1 has dampened its response bringing it closer to the behaviour of zone 2. Zone 2 and zone 4 show little response to changes in inter-zone air flow since they are less dependent on it. From the above discussion it can be clearly concluded that zonal air humidity behaviour in a multi-zone space is influenced by the arrangement of the different zones which determines the degree and the manner of interaction with the outdoor environment. Moreover, the impact of any particular zonal arrangement on zonal air humidity behaviour is determined by the inter-zone connectivity and the air leakage characteristics of the inter-zone airflow paths.

5.8 Summary

The dynamic behaviour of air humidity in a multi-zone space is modelled by a system of linear differential equations, each representing air moisture behaviour in a particular zone. By incorporating a multi-cell air flow model, this system of equations can be solved simultaneously to determine zonal air humidity response at different boundary conditions and zonal characteristics. Solution of the resulting system of equations can be carried out by a numerical technique through which constant boundary conditions can be assumed for the modelled processes during each time interval. Using this proposed model, zonal air humidity behaviour in a five-zone space with two different arrangements has been studied. In general, air leakage can greatly modify zonal air humidity conditions, especially in the zones which are directly exposed to outdoor air inflow. The degree of its impact depends to a great extend on the leakage characteristics of the exterior walls and the

inter-zone flow paths, and to a lesser extend on the wind speed. On the other hand, changing the orientation of the space in terms of the wind direction will completely alter the zonal air humidity response to the air leakage process. Air humidity behaviour in each zone is also influenced by the zonal arrangement of the space which determines the degree and type of interaction with the outdoor environment for each zone.

Moisture generation within a particular zone in a multi-zone space can greatly influence air humidity behaviour in other zones. Its influence depends on the location and the characteristics of the zone in which moisture is generated. For example, moisture generated in a zone from which no inter-zone air flow occurs will have no or little effect on air humidity behaviour of other zones. Similarly, other moisture transport processes such as surface condensation in winter, and air dehumidification in summer can greatly modify zonal air humidity conditions. Surface condensation has mainly a local effect, since it can directly affect air humidity conditions within exterior zones where surface condensation is likely to occur. However, in the presence of inter-zone air flow, the effect of surface condensation on zonal air humidity may not be limited to the zone where condensation occurs. In the absence of other moisture sinks (i.e. air leakage), surface condensation will be the determining factor of air humidity conditions, especially in the exterior zones. Air moisture conditions are maintained equal or less than the saturation conditions at the condensation surface temperature. In multi-zone space each zone will have a unique air humidity behaviour which depends on the boundary conditions, leakage characteristics, as well as the physical and functional characteristics of each zone. The degree of deviations in air humidity conditions among different zones depends on the level of their interdependence, which is determined by the type of inter-zone physical separation, as well as, the inter-zonal moisture transfer mechanism.

CHAPTER 6

EVALUATION OF EXTERIOR WALL TRANSIENT MOISTURE BEHAVIOUR

6.1 Introduction

The wall system is an important component of the building exterior envelope which could affect the building performance in many aspects. The composition of the wall system ranges from a single layer of homogeneous materials to a multi-layer of different materials with different thermal and moisture characteristics. The degree of complexity of the wall system is highly dependent on the climatic and the indoor conditions. Large temperature difference across the wall makes it necessary to utilize air as an insulating medium in the form of air gaps or add low thermal conductivity materials in order to decrease heat flow. In the presence of moisture flow potential across the wall system, the risk of interstitial condensation are substantially increased. This makes it necessary to control moisture flow through the wall system either by adding materials to reduce vapour and air flow or, if possible, by controlling the moisture source. The resulting wall system could be a composite of materials with widely different properties in close conjunction.

The exterior wall moisture performance is determined by the level of moisture accumulated and its duration within its various components. Moisture accumulation rate at any point within the wall is greatly influenced by the net moisture transfer potential at that particular point. The presence of condensation within the wall system will result in an increased net moisture transfer potential. This means that the total amount of moisture deposited at the point where condensation occurs is larger than the amount leaving it. In

the absence of condensation, however, the net moisture accumulation at any point at steady state conditions is nil, and the level of moisture content will be determined by the local value of relative humidity. Condensation within the wall system can occur whenever the vapour pressure at a particular location is greater than the local saturation pressure. Such conditions can normally exist in cold and hot-humid climates. However, in cold climates, the temperature and the vapour pressure difference across the wall is much higher than in hot-humid climates. Hence, the potential for moisture transfer and the risk of interstitial condensation is considerably increased. At low outdoor temperature, the outdoor air will be relatively dry and the indoor environment will be the only source of water vapour which may condense within the wall. Consequently, indoor humidity will be a major factor in determining the occurrence of interstitial condensation and the moisture performance of the exterior walls at low outdoor temperatures. Indoor humidity is subjected to considerable seasonal and even hourly variations, therefore, for accurate evaluation of wall moisture performance, its variational behaviour must be considered.

In order to evaluate the effect of indoor air humidity behaviour on exterior walls moisture performance, the wall moisture response to changing boundary conditions must be evaluated. In addition, modes of moisture interaction between the indoor environment and the wall system must be identified and modelled. The wall moisture response to changing ambient conditions is determined by its moisture as well as thermal behaviours. For example, a rise in indoor air humidity alone may not result in a significant change in wall moisture behaviour, however, when it is accompanied by a drop in outdoor temperature, condensation may occur resulting in a complete change in its moisture performance. Moreover, the occurrence of condensation could be associated with the release of substantial amount of heat that could cause local rise in the material temperature.

Therefore, for accurate assessment of wall moisture behaviour under changing boundary conditions, both heat and moisture transfer processes must be simultaneously considered. Furthermore, modes of interaction between the wall system and the surrounding environment, especially the indoor environment, must be identified and modelled. The short term and the long term effect of indoor humidity variations on wall moisture performance is dependent on the moisture interaction between the wall system and the indoor environment. For example, when moisture transfer through the wall occurs only by vapour diffusion, the short term effect of indoor humidity variations on wall moisture behaviour may not be recognized. However, the accumulative effect of these variations on the wall boundaries could be a determining factor for wall moisture performance. Indoor humidity variations can have an immediate effect on wall moisture behaviour provided that faster moisture transfer mechanism exists. In the presence of air flow paths between the indoor environment and the core of the wall system, moisture transfer by air convection may occur causing immediate modification of wall moisture conditions in response to any changes in indoor humidity. The response time depends on the leakage characteristics of the wall as well as, the driving potentials across it.

6.2 Modelling of Transient Heat and Moisture Transfer Through Porous Building Materials

6.2.1 Moisture transport potentials and coefficients: Moisture movement within a porous solid material is a complex phenomenon with vapour diffusion, capillary forces, and evaporation-condensation mechanisms operating. Proper modelling of moisture transport in walls requires that moisture transport by vapour and liquid phases be considered. Moisture transport can be expressed in terms of several driving potentials which include vapour pressure P_v, pore water pressure P_L, moisture content U and temperature T.

However, more than two driving potentials are not required to fully model the moisture transport process in porous building materials. Moisture transport in porous building materials is normally expressed in terms of two driving potentials which take into account vapour and liquid transports. The commonly used driving potentials are the material moisture content, *U*, and the material temperature, *T*. The total moisture transport can be given by [82]:

$$g_{tot} = -D_w \rho_m \nabla U - D_T \nabla T \tag{6.1}$$

The coefficients D_w and D_T are generally expressed as a combination of liquid and vapour coefficients which correspond to a particular potential. These coefficients are expressed as a function of D_v and D_L as follows [82]:

$$D_w = \frac{1}{\rho_m} [D_v P_{vs} \frac{1}{\xi} + D_L \frac{\partial P_L}{\partial U}] \tag{6.2}$$

$$D_T = D_v P_{vs} (\frac{\partial \phi}{\partial T} + \phi \frac{M h_{fg}}{R T_k^2}) + D_L \gamma P_L \tag{6.3}$$

where,

$$\gamma = \frac{1}{\sigma} \cdot \frac{d\sigma}{dT}$$

and σ= surface tension, *N/m*

Although the coefficients D_w and D_T can be evaluated experimentally, they are only available for a few materials. Moreover, values of liquid transfer coefficients are not available and are very difficult to evaluate. On the other hand, when one considers the large amount of data available on vapour diffusion coefficients of building materials, it becomes compelling to use the vapour pressure as the driving force. At low moisture

contents, moisture transport takes place mainly in vapour phase, and hence liquid transport can be assumed negligible. In this case Equations 6.2 and 6.3 are reduced to

$$D_w = D_v P_{va} \frac{1}{\rho_w \xi} \tag{6.4}$$

and

$$D_T = D_v P_{va} \left(\frac{\partial \phi}{\partial T} + \phi \frac{M h_{fg}}{R T_k^2}\right) \tag{6.5}$$

The above coefficients can be evaluated from the available data on vapour pressure diffusion coefficients provided by ASHRAE [20] and moisture sorption isotherm of the materials. Both coefficients represent moisture transfer by vapour diffusion with the moisture content and the temperature as the driving potentials. However, the use of the moisture content as a driving potential has some practical limitations since it is discontinuous at the boundaries with the ambient air as well as the boundaries with other materials. When modelling moisture transfer through multi-layered construction (i.e., walls), it becomes necessary to recalculate the moisture content into other driving potentials at the boundaries of each layer. To avoid such unnecessary computations, continuous driving potentials such as vapour pressure or air humidity ratio can be used to describe the moisture transfer process. In this study, the air humidity ratio expressed in terms of the material moisture content and temperature is used.

6.2.2 Simultaneous heat and moisture transfer: The combined heat and moisture transfer through porous building materials can be modelled by a system of differential equations. Using air humidity ratio and temperature as the driving potentials, the moisture

$$\frac{\partial W}{\partial t} = \frac{\partial W}{\partial U} \cdot \frac{\partial U}{\partial t} + \frac{\partial T}{\partial t} \cdot \frac{\partial W}{\partial T} \tag{6.6}$$

where,

$$\frac{\partial W}{\partial T} = \frac{\partial \phi}{\partial T} + \phi \cdot \frac{\partial W_s}{\partial T}$$

$$\frac{\partial W}{\partial U} = \frac{W_s}{\xi}$$

$$\frac{\partial U}{\partial t} = D_v R_v T_m \rho_a \frac{\partial^2 W}{\partial x^2}$$

Substituting into equation 6.6, it becomes:

$$\frac{\partial W}{\partial t} = \frac{W_s}{\xi} D_v R_v T_m \rho_a \frac{\partial^2 W}{\partial x^2} + \left(\frac{\partial \phi}{\partial T} + \phi \frac{dW_s}{dT} \right) \frac{\partial T}{\partial t} \tag{6.7}$$

The corresponding boundary conditions at both sides of the slab can be written as:

$$-D_v R_v T_m \rho_a \frac{\partial W}{\partial x} = h_m (W_\infty - W_{surf}) \tag{6.8}$$

Heat transport process through a porous slab can be generally described by [82]:

$$(\rho_m c_{vm})_{tot} \frac{\partial T}{\partial t} = K \frac{\partial^2 T}{\partial x^2} + c_v g_v \nabla T + c_l g_l \nabla T - h_{fg} I_v \tag{6.9}$$

Where, I_v represent the increase in vapour content by the evaporation process and can be given by:

$$I_v = \frac{\partial v}{\partial t} + \nabla g_v$$

The rate of change in local vapour concentration ∂v/∂t is relatively very small and can be neglected [82]. Furthermore, the second and third terms in the right side of equation 6.9, which represent heat transfer associated with vapour and liquid transport, are relatively

small and they can also be neglected. Hence, equation 6.9 becomes:

$$(\rho_m c_{vm})_{tot} \frac{\partial T}{\partial t} = K \frac{\partial^2 T}{\partial x^2} - h_{fg} \nabla g_v \tag{6.10}$$

Substituting for ∇g_v equation 6.10 becomes:

$$(\rho_m c_{vm})_{tot} \frac{\partial T}{\partial t} = K \frac{\partial^2 T}{\partial x^2} - h_{fg} (m_s'' + D_v R_v T_m \rho_a \frac{\partial W}{\partial x}) \tag{6.11}$$

The corresponding boundary conditions for both sides can be written as:

$$-K \frac{\partial T}{\partial x} = h_c (T_\infty - T_{surf}) + h_{fg} (m_s'' + D_v R_v T_m \rho_a \frac{\partial W}{\partial x}) \tag{6.12}$$

Equations 6.7 and 6.11 represent a pair of coupled differential equations describing simultaneous heat and moisture transfer through a continuous slab of material.

In order to account for the liquid transport, different moisture content levels which characterize the material have been identified. Fig. 6.1 shows a schematic for a typical water vapour equilibrium curves representing the material moisture content at different ambient relative humidity levels.

The moisture content which correspond to any relative humidity level is called the hygroscopic moisture content (HMC). At 100% relative humidity, the moisture content is called the maximum hygroscopic moisture content (MHMC). Beyond this level, the moisture content can increase independent from the ambient relative humidity until it reaches a maximum value called the saturation moisture content (SMC). In the present study. the vapour pressure is used to describe the moisture transport process within the material at any moisture content below the maximum hygroscopic level U_h. The maximum hygroscopic moisture content for the material, which can be determined either by the

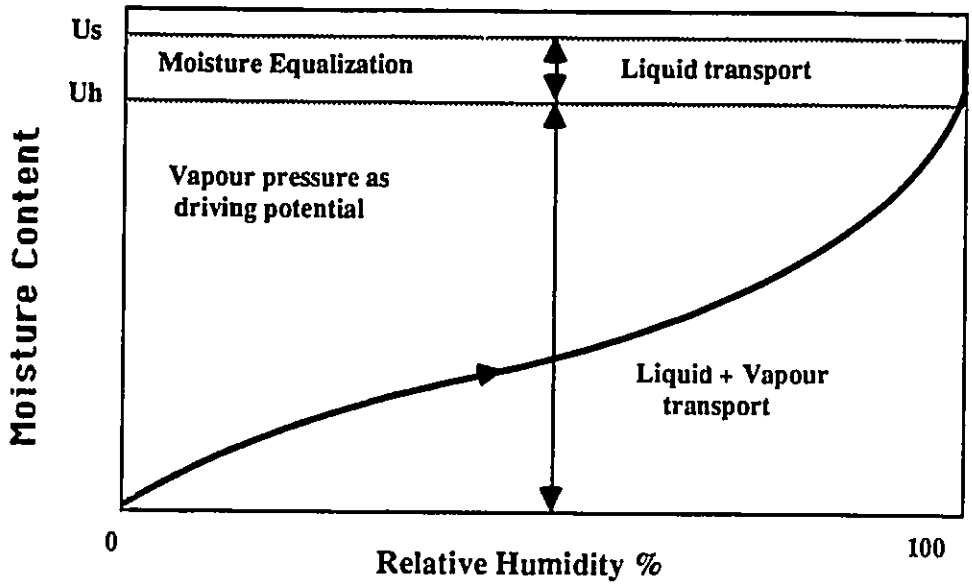

Fig. 6.1 Typical moisture equilibrium curve for building materials.

absorption or the desorption processes, is taken as the critical moisture content. at moisture content levels equal or higher than U_h, liquid transport becomes dominant and immediate moisture equalization occurs. Moisture equalization can be assumed to occur between any two points having an average moisture content greater than U_h. Such an assumption is practically justified because information about liquid transport in building materials is still sketchy. Furthermore, most materials in the wall system will not retain moisture content at these levels for long periods of time [92]. The validity of the moisture equalization concept has been examined in the literature [82] by comparing the theoretical prediction of an aerated concrete slab moisture behaviour, when both vapour and liquid transports are modelled, with the same slab moisture behaviour, when the moisture equalization concept is implemented. It has been found that the two predictions are almost

identical which indicates the applicability of the moisture equalization concept. By considering the hygroscopic range (i.e., $U \leq U_h$) and the wetting range (i.e., $U \geq U_h$), all possible moisture conditions of material would have been considered.

As the moisture content increases, menisci begin to form in the pores, leading to the formation of liquid-vapour series. As a result, the vapour diffusion coefficient D_v will be considerably increased. It is not possible to measure the amount of vapour and liquid transport separately, thus both have to be considered simultaneously. This is usually done by attributing the series transport to D_v and using the vapour pressure as the driving potential. Over a wide range of moisture content, different values of D_v, which correspond to smaller range of moisture content, must be used. At high moisture content, over the critical moisture content, a continuous liquid phase develops and capillary suction begins to dominate. In this case, the vapour pressure potential and its corresponding coefficients can no longer be used to describe the moisture transfer process within the material. Consequently, it becomes necessary to model moisture transfer in the liquid phase. However, for many materials, the liquid transfer coefficient D_L is so large at high moisture contents that almost immediate equalization of pore water pressure is obtained [82].

6.3 Material Properties Related to Moisture Transfer

The material properties required for modelling moisture transfer depend on the moisture driving potentials used. Regardless of the driving potentials, the total moisture transport must be the same in all cases. When the vapour pressure is used as the main driving potential, as is the case in the present study, the vapour diffusion coefficient D_v will be required for modelling moisture transfer. Fortunately, the vapour diffusion coefficients for many building materials can be found in literature. These coefficients are normally

evaluated at certain constant ambient humidity and temperature. In reality, however, the vapour diffusion coefficients are dependent on the material moisture content and temperature. Pure liquid moisture transport is highly dependent on temperature, while pure vapour transport can be relatively considered unaffected by the temperature. The vapour diffusion coefficient D_v normally describes both vapour as well as liquid transport at the same time, hence it is influenced by the temperature. The degree of influence is dependent on the material moisture content level, since liquid transport becomes more pronounced at higher levels. In addition to the temperature, the vapour diffusion coefficient is influenced by the moisture content. As the moisture content increases, islands of liquid will begin to form resulting in moisture transport in series of vapour and liquid. The dependence of the vapour diffusion coefficient on moisture content has been evaluated for some materials by expressing the variation in the vapour diffusion coefficient in terms of the relative humidity for a particular range as given by equation 6.13:

$$D_v(\phi) = C_0 + C_1\phi + C_2\phi^2 \qquad \phi_1 < \phi \leq \phi_2 \tag{6.13}$$

Values of the coefficients C_1, C_2,...C_n at different ranges of relative humidity are given in Table 6.1 for different building materials. These coefficients are either directly available in literature [82], such as that for brick and aerated concrete, or evaluated as part of this study based on the relevant data available in literature [29] (i.e., material moisture equilibrium curve and moisture diffusivity represented in terms of material moisture content. From Table 6.1 it can be seen that the vapour diffusion coefficient for materials with low hygroscopicity, such as fibre glass, does not depend on the relative humidity. On the other hand, materials with high hygroscopicity like wood show great variations with the relative humidity level.

The hygroscopic moisture capacity (ξ) is an important material moisture property which relates the vapour pressure within the material to its moisture content. Such property is necessary for modelling the transient moisture transfer through building materials. The material moisture capacity can be evaluated from its moisture equilibrium curve which is available for many building materials. Depending on the way the moisture equilibrium is achieved, different curves are usually obtained for the absorption and the desorption processes. Fig. 6.2 shows a typical material moisture behaviour during absorption and desorption processes where it can be seen that equilibrium moisture content obtained by desorption is always greater than that from absorption for the same relative humidity except at relative humidity ϕ=0% and 100% where the two curves meet. This difference in behaviour is known as hysteresis. Only for pure absorption or desorption it is clear what curve to be used. In a natural climate, building materials are exposed more or less to cyclic conditions, and hence their moisture conditions could lie anywhere between the two curves. It is not possible to trace material actual moisture behaviour in a real environment. To avoid this problem, a general theory on hysteresis and scanning curves is needed. Some theories have been proposed in this regard, however, they are yet to be verified. Furthermore, such theories are normally very complicated mathematical models which makes them impractical to be implemented in moisture transfer modelling in buildings. Some researchers have suggested the use of the moisture desorption curve since, according to their argument, it represents more accurately the changes in moisture content as a function of relative humidity and temperature [109]. The use of the desorption isotherm for building materials which are continuously exposed to absorption and desorption processes is a very rough assumption and could lead to significant inaccuracies. Other researchers [133] have suggested the use of an intermediate moisture equilibrium curve representing the average of the absorption and the desorption data.

Table 6.1 Variations of vapour diffusion coefficients with relative humidity for different building materials.

Material	Range of relative humidity	$C_0\ 10^{-12}$	$C_1\ 10^{-12}$	$C_2\ 10^{-12}$	reference
Brick	$\phi \leq 33\%$ $\phi > 33\%$	10.2 17.0	0 -37.3	0 50.9	82
Aerated Concrete	$\phi \leq 45\%$ $45\% < \phi \leq 98\%$ $98\% < \phi \leq 100\%$	21.7 32.5 62.0	0 -62.5 0	0 97.1 0	82
Gypsum	$0\% \leq \phi \leq 100\%$	42	0	0	29
Fibre Insulation	$0\% \leq \phi \leq 100\%$	78	0	0	133
Cellulose Insulation	$0\% \leq \phi \leq 100\%$	60	0	0	133
Wood	$0\% \leq \phi \leq 50\%$ $50\% < \phi \leq 70\%$ $70\% < \phi \leq 85\%$ $85\% < \phi \leq 95\%$ $95\% < \phi \leq 100\%$	1.82 -58.2 -480.0 -15.7 -727.0	9.69 201.6 1197.0 57.3 840.0	2.86 -140.0 -700.0 -9.45 0	29

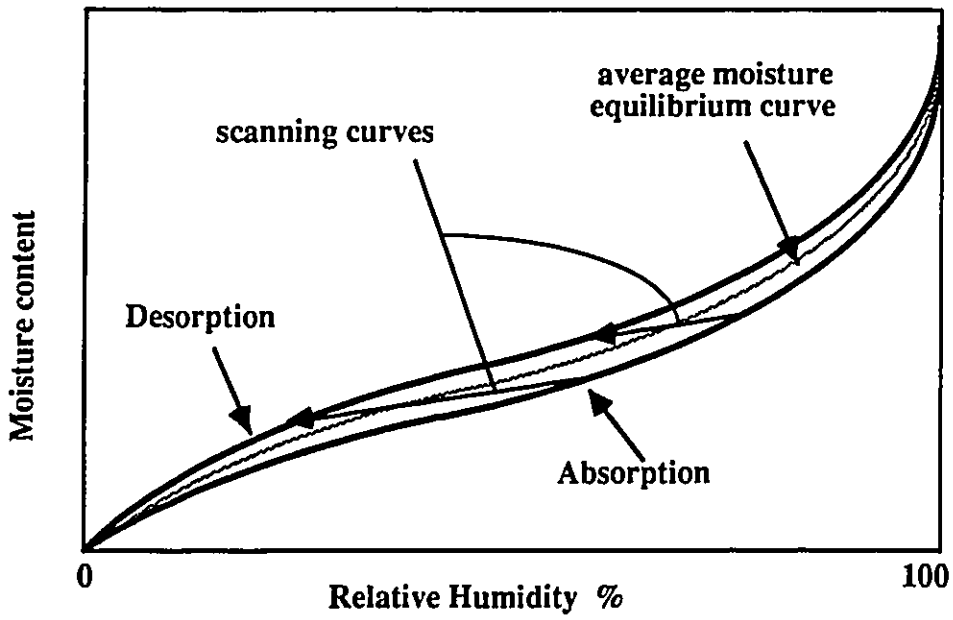

Fig. 6.2 Typical material moisture behaviour during the absorption and desorption processes.

Comparisons with experimental results have revealed the applicability of such an approach in accounting for the hysteresis phenomenon [133]. In the present study, the average equilibrium moisture content curve will be used to represent material moisture conditions when modelling moisture behaviour of exterior walls.

In addition to the moisture history of the material, the moisture equilibrium curve can be affected by the ambient temperature. However, by expressing the amount of absorbed water in terms of relative humidity, the influence of temperature is minimized. Equilibrium moisture capacity of hygroscopic materials is determined by the vapour pressure and the temperature of the ambient air. For a constant temperature, as the vapour pressure increases the equilibrium moisture content increases. However, for constant vapour pressure, increasing the temperature will result in a decrease in equilibrium moisture content. This means that the vapour pressure and the temperature are acting against each other. By expressing the equilibrium moisture content in terms of relative humidity, the net action of both these parameters would be considered. In other words, for the same relative humidity, increasing the temperature would mean decreasing the vapour pressure and increasing the vapour pressure would mean decreasing the temperature. Although the net action of the two parameters (i.e., vapour pressure and temperature) may not be zero, the equilibrium moisture content is not expected to show significant variation with temperature for the same relative humidity. As an evidence of this argument, it has been shown by ASHRAE [20] that, for at least solid sorbents, by expressing the equilibrium moisture capacity versus relative humidity, the resulting curve can normally be used for temperature ranging from about -18° C. to 82° C.

The material moisture capacity (ξ) is equal to the slope of the moisture equilibrium curve

and can be expressed by:

$$\xi = \frac{\partial U}{\partial \phi} \tag{6.14}$$

This moisture property of material can be thought of as equivalent to the material specific heat which relates the variations of material energy content to its temperature. However, while the specific heat experiences little dependence on temperature, the moisture capacity can relatively show significant variations with relative humidity. The equilibrium moisture content is normally expressed in terms of the relative humidity as following:

$$U_e = a\phi^b + c\phi^d \tag{6.15}$$

Hence, the moisture capacity ξ can be given by:

$$\xi = a\,b\,\phi^{b-1} + c\,d\,\phi^{d-1} \tag{6.16}$$

In many cases, equation 6.15 can not accurately describe the relationship between the equilibrium moisture content and the relative humidity over the whole range of relative humidity. Therefore, the moisture equilibrium curve is segmented into several ranges so as to get the best representation by equation 6.15. Table 6.2 shows the coefficients of equation 6.15 at different relative humidity ranges for some common building materials.

6.4 Moisture Interaction Between the Indoor Environment and the Exterior Wall System

In winter, moisture performance of exterior walls is mainly determined by the behaviour of indoor humidity. The degree of influence, however, is dependent on the modes of moisture interaction between the indoor environment and the wall system. Depending on the type and the air leakage characteristics of the wall system, moisture from the indoor can be transferred through by the diffusion and the convective processes. For a multi-layer

Table 6.2 Coefficients of Equation 6.15 for evaluating the equilibrium moisture content for different building materials at different ranges of relative humidity.

Material	Range of relative humidity	a	b	c	d	reference #
Brick	0% ≤ϕ≤ 20% 20% <ϕ≤ 70% 70% <ϕ≤ 98% 98% <ϕ≤ 100	.00264 .000117 .00359 -2.53	1 0 37.8 0	0 .00206 .00281 2.59	0 1 1.67 1	82
Aerated Concrete	0% ≤ϕ≤ 25% 25% <ϕ≤ 70% 70% <ϕ≤ 90% 90% <ϕ≤ 100%	21.7 32.5 62.0	0 -62.5 0		0 97.1 0	82
Gypsum	0% ≤ϕ≤ 100%	.02783	13.8	.00959	1.044	29
Fibre Insulation	0% ≤ϕ≤ 100%	.02039	12.02	.00611 3	.6902	133
Cellulose Insulation	0% ≤ϕ≤ 100%	.744	16.28	.3558	2.543	133
Wood	0% ≤ϕ≤ 100%	.1244	6.092	.1455	.9432	29

wall system, moisture transfer occurs mainly by diffusion through its fabric while convective moisture transfer occurs at the boundaries as illustrated by Fig. 6.3. However, walls with high air permeability through out its thickness, can be directly subjected to uniform convective moisture transport. In most cases, exterior walls are mainly composed of low air permeability materials, hence convective moisture transfer will not directly affect moisture conditions of the materials comprising the wall system. On the other hand, the presence of some holes or cracks in the outer layers of the system could result in a directed air flow that will transport moisture to the core of the wall system. The impact of the directed air flow on wall moisture behaviour depends on the air pressure across the flow path as well as its continuity. In reality, directed flow paths within walls are likely to

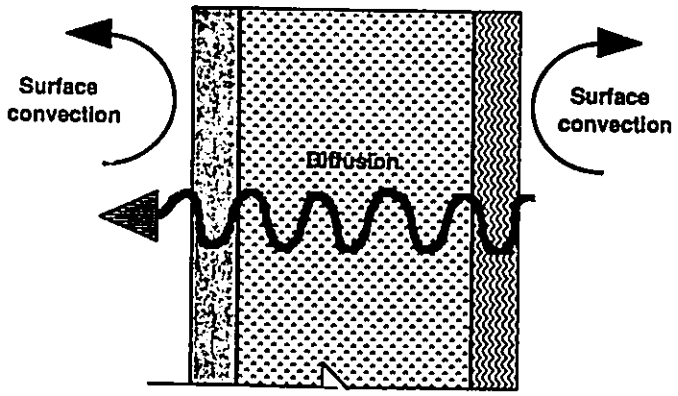

Fig. 6.3 Moisture transfer modes for a multi-layer wall in the absence of air flow.

be discontinuous with very high air flow resistance. Hence, the impact of the directed air flow on wall moisture behaviour is expected to be minimal even when a continuous air flow path does exist since its moisture impact will be mainly local.

In the absence of air flow through the exterior wall, moisture interaction between the indoor environment and the wall system can only occur at the interior boundary surfaces where moisture is continuously exchanged through the surface convective mechanism. Variations in indoor humidity will lead to fluctuations in the amount of moisture mass flux and probably in its direction at the boundary surface. Consequently, the interior surface moisture conditions will exhibit a variational behaviour in response to variation in indoor air humidity. The effect of a particular variational pattern of interior surface moisture conditions will be reflected on the moisture distribution across the wall system. The response of the wall moisture distribution, however, is dependent on the moisture characteristics of the different wall elements. The presence of a high moisture resistance

in the inner wall will reduce and delay the effect of variations in interior surface moisture conditions on moisture distribution within the wall system. On the other hand, when low moisture resistance materials comprise the inner wall, variations in interior surface moisture conditions will have an immediate effect on wall moisture distribution.

In addition to the diffusive moisture transfer, air-borne moisture convection is likely to be an important moisture transfer mechanism in the cavity wall system linking the indoor environment with the cavity space. In this wall system, air flow paths can normally connect the cavity space with the indoor and outdoor environments. Moisture interaction between the indoor environment and the cavity wall system occurs at two fronts as illustrated in Fig. 6.4.

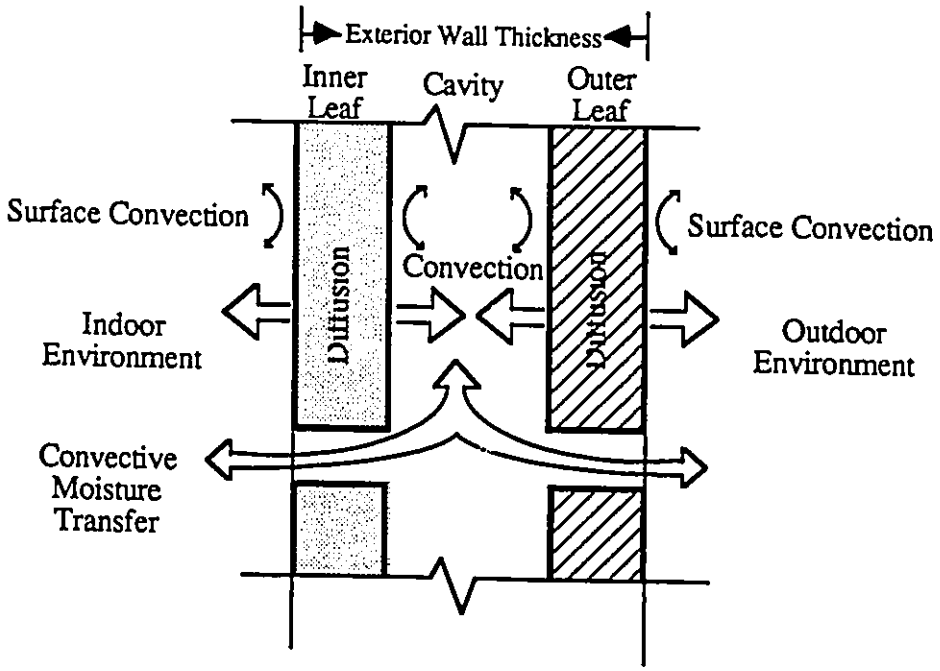

Fig. 6.4 Moisture transfer modes for a multi-layer cavity wall system.

Convective moisture transfer normally occurs through cracks and unsealed joints between mating surfaces. Although the actual flow paths of air within the wall may not be known, it can be safely assumed that these paths connect the indoor environment with the wall cavity. Consequently, cavity conditions can be directly affected by indoor air conditions. From the moisture analysis point of view, such an assumption can be shown to be valid for the following reasons:

i) Air cavity is a continuous layer dividing the wall system into an inner and an outer wall, therefore, for indirect flow through the wall, air has to pass through the wall cavity changing its air condition in the process.

ii) For air to flow from one point to another through the wall system, the shortest path with the minimum flow resistance is followed. Therefore, air will not normally pass between material layers comprising the wall, hence, convective moisture transfer will not affect inter-layer moisture conditions.

iii) Even when inter-layer convective moisture transfer occurs at any location in the warm side of the insulating material, no condensation is expected to occur at these locations, however local changes in moisture conditions are expected.

iv) The cavity is normally located on the cold side of the insulating material, and hence, its air moisture condition is an essential factor in determining wall moisture performance since it is a likely place for condensation.

In contrast with the diffusive moisture transfer, convective moisture transfer can

immediately alter the wall moisture conditions regardless of the moisture characteristics of the wall elements. When such moisture interaction exists between the indoor environment and the wall cavity, it will directly respond to any changes in indoor air humidity. Consequently, indoor air humidity behaviour will have a considerable impact on the wall short term and long term moisture performance. The degree of such influence is dependent on the wall air leakage characteristics as well as the pressure differential and distribution across it. Therefore, in order to evaluate the effect of indoor air humidity behaviour on wall moisture performance, moisture and thermal interaction between the indoor environment and the wall system through the various transfer mechanisms must be mathematically modelled.

Surface convection is the first and in many cases the only moisture interaction mode between the indoor environment and the exterior wall. The amount of heat and moisture transfer between the indoor air and the interior surface is determined by the surface transfer coefficient. The convective moisture transfer at the wall surface can be described by:

$$m = h_m (W_r - W_{si}) \tag{6.17}$$

where,

m= mass transfer rate, kg/m^2·s

h_m= surface mass transfer coefficient, kg/m^2·s

W_r= indoor air humidity ratio, kg/kg

W_{si}= air humidity ratio at the material surface, kg/kg

The surface mass transfer coefficient h_m, can be related to the surface heat transfer

coefficient by Lewis relationship given in Equation 6.18.

$$h_m = \frac{h_c}{c_p} \tag{6.18}$$

The effect of surface coatings such as paints can be included into the surface mass transfer coefficient by assuming that negligible amount of moisture is absorbed by the coating material. The effective surface moisture transfer coefficient can be expressed by:

$$h_{mf} = \left(\frac{1}{h_m} + \frac{1}{h_f}\right)^{-1} \tag{6.19}$$

Where $1/h_f$ represents the moisture transfer resistance of the coatings.

In order to model the convective moisture transfer through exterior cavity wall systems, the air flow rates and their directions through the various air flow paths must be determined. This requires the knowledge of the air pressure in all spaces including the cavity space. Depending on the indoor space arrangement and its connectivity with the cavity space, wind and thermal forces will contribute to the spatial pressure distribution in the whole system. By considering each wall cavity as a separate space connected to the indoor space through the inner wall a multi-cell air flow network can be constructed. As an illustrating example, the air flow network for a single rectangular space is shown in Fig. 6.5.

The system consists of four distinct cavity spaces and the indoor space each represented by a node. The four independent cavity spaces are connected to the main indoor space and the outdoor environment by air flow paths. In addition, the indoor space is directly connected to the outdoor environment. The air pressure at each space can be evaluated by performing a mass balance at each node and simultaneously solving the resulting

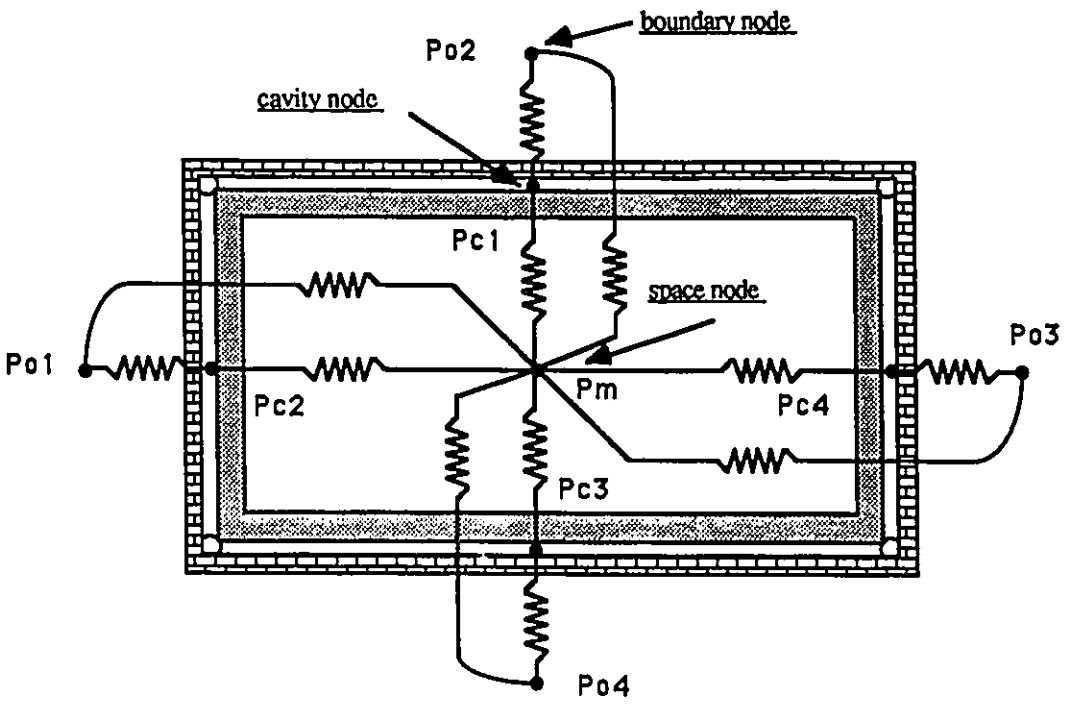

Fig. 6.5 Utilization of the air flow network modelling approach for describing moisture interaction between the exterior wall and the indoor environment.

nonlinear equation. The contribution of the different driving potentials and the method of solution of the resulting equations have been discussed earlier in chapter 4 and chapter 5.

6.5 Transient Heat and Moisture Transfer Through Exterior Walls

6.5.1 Modelling approach: Moisture performance of walls is highly dependent on their thermal behaviour since the state of moisture at any point within the wall is a function of the combined effect of its thermal and moisture characteristics. Heat flow in a porous

material induces moisture flow, which in turn affects heat flow through condensation and evaporation, as well as, the transport of heat with vapour and liquid water. Therefore, heat and moisture flows must be treated simultaneously in order to predict moisture performance of the wall system. The principles of heat and moisture transfer through porous building materials discussed in section 6.2 will be the basis for formulating combined heat and moisture transfer through exterior walls. For modelling moisture transport through the wall components, the following assumptions are made:

i) At moisture contents below the maximum hygroscopic moisture content of the material, moisture transfer is modelled by using the air moisture content as the driving potential, and at higher moisture contents instantaneous moisture equalization is assumed.

ii) The effects of temperature on vapour diffusion coefficients is neglected. This assumption can be justified since the average moisture content of a particular material on which the value of vapour diffusion will be based, will normally remain low.

iii) The effect of material history (i.e., hysteresis) and temperature on material moisture capacity is neglected. Instead, the average moisture equilibrium curve in terms of relative humidity will be used.

iv) Exterior walls are normally composed of several layers of different materials. Moisture transfer at the boundary between two layers is dependent on the boundary moisture transfer resistance. For materials in close contact, this

resistance will be very small and the two materials can be assumed at equilibrium at the boundary surfaces.

v) No liquid transport occurs between any two layers in the wall system since the moisture flow path is discontinuous at the boundary. Liquid moisture transfer could occur between adjacent layers at very high moisture content levels (i.e. saturation levels), however, such moisture content levels are unlikely to be attained at normal conditions. Furthermore, even at these moisture content levels, liquid moisture transfer can only occur when the two layers are closely attached to each other. In reality, however, perfect attachment of adjacent layers can not be achieved because of varying surface characteristics and construction methods.

vi) Moisture within the material comprising the wall system can only exist in the vapour and liquid forms, and local moisture equilibrium is always present within the material.

Walls are very complicated systems consisting of various building materials containing pores, voids and cracks of various shapes. Moisture and heat transfer in these walls take place in different mechanisms through a multi-dimensional process. For example, moisture can be transferred into the wall system from the indoor environment through the process of vapour diffusion and air leakage. In addition, moisture can also be transported to the different wall components through the rising damp from the ground and through the shedding of rain on its exterior surfaces. The presence of multi-dimensional driving potentials which include the gravitational forces makes the moisture transfer process through the exterior walls a multi-dimensional process. For comprehensive assessment

of exterior wall moisture behaviour, a three dimensional model may be required to accurately describe heat, moisture and air movement through exterior walls. However for the present study the main objective is to study the effect of indoor humidity behaviour on wall moisture performance, and hence, a comprehensive uni-dimensional model which accounts for all basic properties and transport processes of the wall system, is more feasible to use. In studying the process of heat and moisture flow through the wall, it has been found that a uni-dimensional model can describe heat and moisture transfer with sufficient accuracy, with variations in wall performance being accounted for by dividing the wall into vertical stacks [130]. Some processes such as, air flow, which cannot be fitted in the one dimensional model can be handled by considering the air cavity as an intermediate boundary layer which interacts with the interior and the exterior environments directly through air leakage and indirectly through the cavity surfaces. For a uni-dimensional model to be applicable, the following assumptions are made:

i) The wall is homogeneous in all directions except in the direction of flow.

ii) Over any plane across the flow path, which includes all boundaries, the wall is exposed to uniform conditions.

iii) No rising damp is taking place, since it is limited to untreated walls near the ground.

The use of a uni-dimensional model in the present study to describe heat and moisture flow through the wall can be justified as follows:

i) The main objective of this study is to investigate the effect of indoor humidity behaviour on wall moisture performance, hence neglecting other moisture sources

from the other directions (e.g. rising damp) will have no effect on achieving the objective of this study.

ii) Heat and moisture driving potentials across the wall will dominate the transfer process, while transfer potentials in the other two directions are negligible.

iii) A multi-dimensional model may not necessarily improve the accuracy of moisture transfer modelling, since moisture transfer characteristics, needed for such in-depth detailed analysis, are not available for many building materials. Moreover, a great deal of uncertainty and variability does always exist in the available data, which makes multi-dimensional analysis questionable.

iv) Theories for moisture interaction between adjacent materials, especially liquid transfer, have not been available for practical use.

Moisture transfer through composite wall systems, even in a uni-dimensional process is complex phenomenon that involve both liquid and vapour transports, and when combined with the wall thermal behaviour, phase change (i.e., condensation, evaporation, freezing) may be present. Therefore, an exact analytical description of the transfer process presents great difficulties [100]. In the present study, a numerical approach will be utilized for solving the simultaneous heat and moisture transfer problem through exterior walls.

6.5.2 Numerical formulation: Based on the above discussion and assumptions, the fully implicit finite-difference scheme will be used to model transient heat and moisture transfer through walls. In this method, each layer in the wall system is subdivided by equally

spaced nodes each representing the thermal and moisture conditions of a corresponding segment of the layer. Node distribution across the wall system is performed according to certain criteria which are determined by the required accuracy and efficiency of the solution technique.

6.5.2.1 Node distribution criteria: For finite-difference modelling of multi-layer walls it has been found that placing a node on each internal boundary provides satisfactory results [143]. In addition, the use of boundary nodes will result in more efficient formulation of the problem since material properties will be constant between any two nodes. accurate modelling of moisture interaction between the material surface and the ambient air requires a real representation of the material surface moisture conditions. Most building materials have very high moisture resistance relative to the surface mass transfer coefficient, consequently moisture distribution near the material surface is expected to be highly nonuniform. This makes it necessary to decrease the node spacing to the level where the average moisture condition of the surface segment (which is represented by the surface node) will reasonably represent the surface moisture conditions. The thickness of the surface segment can be related to the material moisture characteristics and the surface mass transfer coefficient by the Biot number as follows:

$$Bi = \frac{H_m \Delta x}{2 D_v} \tag{6.20}$$

In thermal analysis a reasonable value of Biot number that would indicate uniform conditions was found to be equal to 0.1. However, in moisture analysis, this value can be judged to be practically too small considering the relatively larger ratio between the surface mass transfer coefficient h_m, and the material vapour diffusion coefficient D_v. By evaluating the relative accuracy of the solution using a larger value of *Bi*, it has been

found that a Biot number value of 0.5 is practical and reasonably accurate for describing moisture uniformity near the surface. Hence, nodal distribution in the inner and outer layers of a multi-layer wall must satisfy the following criterion:

$$\frac{H_m \Delta x}{2D_v} \leq 0.5$$

The introduction of the boundary nodes as representative of equal driving potentials at the boundary surfaces of adjacent layers has initiated the need for another node spacing criterion. Analytical evaluation of the effect of nodal distribution in adjacent layers on solution accuracy has revealed the importance of the relative ratio between the material moisture diffusivity and the node spacing [143]. Based on these results, a node distribution criteria for moisture analysis in multi-layer wall can be formulated. For any two adjacent layers, the following criterion needs to be satisfied:

$$\frac{\alpha_{m1}}{\Delta x_1^2} \approx \frac{\alpha_{m2}}{\Delta x_2^2}$$

where

α_m= material moisture diffusivity, m^2/s

For certain building materials, satisfying the above criteria could require the use of unreasonably high number of nodes that makes the solution impractical to implement at certain conditions. Theretore, a sort of compromise may be required between the practicality and the accuracy of the solution. In certain situations, reducing the number of nodes recommended by the above criteria to a practical limit may not jeopardize the required accuracy of the solution. Such a decision must be made while being aware of the consequences on the solution accuracy.

The above criteria can be used to determine node distribution in multi-layer walls as well as cavity wall systems. The cavity space is represented by one single node which describes the average cavity thermal and moisture conditions. Fig. 6.6 illustrates typical but not specific nodal distribution for a cavity wall system.

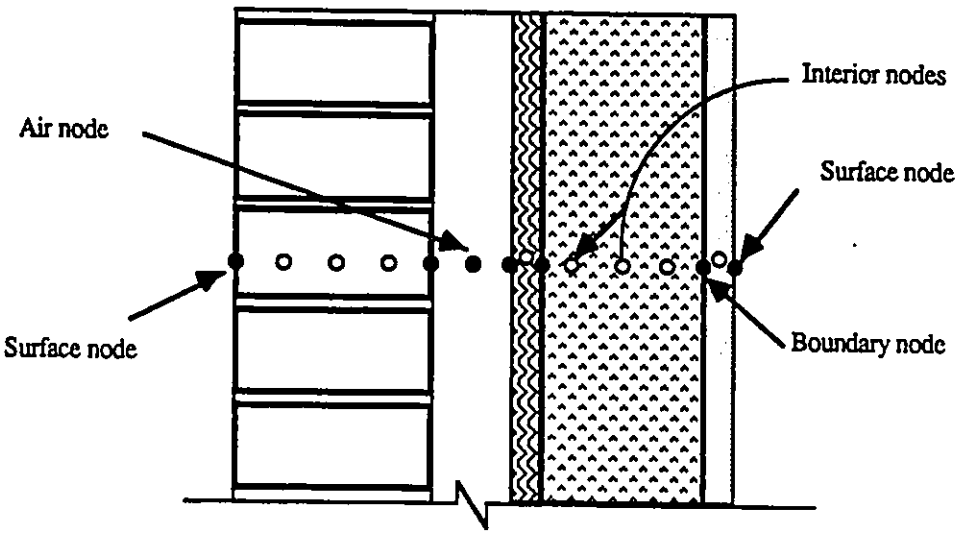

Fig. 6.6 Typical node distribution for a multi-layer cavity wall system.

6.5.2.2 Numerical formulation of simultaneous heat and moisture transfer: Establishing the node distribution is the first step in the finite-difference formulation. The numerical formulation of the present problem is completed by performing heat and moisture balance at each node. This will result in a number of algebraic equations twice the number of nodes that have to be solved simultaneously for evaluating the system thermal and moisture response to varying boundary conditions.

I) energy and moisture balance at the interior surface node

The energy balance equation for the interior surface node *n* can be written as:

$$(1+2Fo+2Fi)T_n^{\tau+1}-2FoT_{n+1}^{\tau+1}+(2Ae+2Fmi)W_n^{\tau+1}-$$
$$2AeW_{n+1}^{\tau+1}=T_n^{\tau}+2FiT_i+2FmiW_i \qquad (6.21)$$

and the moisture balance equation is given by:

$$(1+2Msi+2Mw)W_n^{\tau+1}-2MwW_{n+1}^{\tau+1}-MtT_n^{\tau+1}=$$
$$W_n^{\tau}+2MsiW_i-MtT_n^{\tau} \qquad (6.22)$$

ii) energy and moisture balance at intermediate nodes

The energy balance equation for the node *n* is:

$$FoT_{n-1}^{\tau+1}-(1+2Fo)T_n^{\tau+1}+FoT_{n+1}^{\tau+1}+AeW_{n-1}^{\tau+1}-$$
$$2AeW_n^{\tau+1}+AeW_{n+1}^{\tau+1}=-T_n^{\tau} \qquad (6.23)$$

and the moisture balance is;

$$MwW_{n-1}^{\tau+1}-(1+2Mw)W_n^{\tau+1}+MwW_{n+1}^{\tau+1}+MtT_n^{\tau+1}=$$
$$-W_n^{\tau}+MtT_n^{\tau} \qquad (6.24)$$

iii) energy and moisture balance at boundary nodes

The energy balance equation for a boundary node *b* between the layer *n* and the layer *m* when no vapour retarder is separating them can be written as:

$$\frac{K_n}{Eab\Delta X_n}T_n^{\tau+1}-(1+\frac{K_n}{Eab\Delta X_n}+\frac{K_m}{Eab\Delta X_m}T_b^{\tau+1}+\frac{K_m}{Eab\Delta X_m}T_m^{\tau+1}+$$
$$Ewb_nW_n^{\tau+1}-(Ewb_n+Ewb_m)W_b^{\tau+1}+Ewb_mW_m^{\tau+1}=-T_b^{\tau} \qquad (6.25)$$

and the moisture balance is given by:

$$Mwb_n W_n^{\tau+1} - (1 + Mwb_n + Mwb_m) W_b^{\tau+1} + Mwb_m W_m^{\tau+1} + Mt\, T_b^{\tau+1} = W_b^{\tau} + Mt\, T_b^{\tau} \tag{6.26}$$

When a vapour retarder is placed at the boundary between layer *n* and layer *m*, the energy balance equation for the boundary node *n* in layer *n* can be written as:

$$-2Fo\, T_{n-1}^{\tau+1} + (1 + 2Fo + 2Fb_n) T_n^{\tau+1} - 2Fb_n T_m^{\tau+1} - 2Ae\, W_{n-1}^{\tau+1} + (2Ae + 2Ar_n) W_n^{\tau+1} - 2Ar_n W_m^{\tau+1} = T_n^{\tau} \tag{6.27}$$

and the moisture balance equation is given by:

$$-2Mw\, W_{n-1}^{\tau+1} + (1 + 2Mw + Mr_n) W_n^{\tau+1} - 2Mr_n W_m^{\tau+1} - Mt\, T_n^{\tau+1} = W_n^{\tau} - Mt\, T_n^{\tau} \tag{6.28}$$

iv) energy and moisture balance at the exterior surface node

The energy balance equation for the exterior surface node *n* can be written as:

$$-2Fo\, T_{n-1}^{\tau+1} + (1 + 2Fo + 2Fe) T_n^{\tau+1} - 2Ae\, W_{n-1}^{\tau+1} + (2Ae + 2Fme) W_n^{\tau+1} = T_n^{\tau} + 2Fe\, T_o + 2Fme\, W_o \tag{6.29}$$

and the moisture balance is given by:

$$-2Mw\, W_{n-1}^{\tau+1} + (1 + 2Mso + 2Mw) W_n^{\tau+1} - Mt\, T_n^{\tau+1} = W_n^{\tau} + 2\, Mso\, W_o - Mt\, T_n^{\tau} \tag{6.30}$$

In the case of a cavity wall system, the cavity will be treated as a separate zone which interacts with the indoor environment as well as its bounding surfaces. Therefore, energy

and moisture balance must be performed both at the cavity space and the bounding surfaces.

v) energy and moisture balance at the cavity bounding surfaces

the energy balance equation for a cavity surface node *n* in a cavity bounded by layer *n* and *m* can be given by:

$$-2Fo\,T_{n-1}^{\tau+1}+(1+2Fo+2Fc+2Frc)\,T_n^{\tau+1}-2Fc\,T_{ca}^{\tau+1}-2Frc\,T_m^{\tau+1}-2Ae\,W_{n-1}^{\tau+1}+(2Ae+2Fmc)\,W_n^{\tau+1}-2Fmc\,W_{ca}^{\tau+1}=T_n^{\tau} \tag{6.31}$$

and the moisture balance is;

$$-2Mw\,W_{n-1}^{\tau+1}+(1+2Mw+2Msc)\,W_n^{\tau+1}-2Msc\,W_{ca}^{\tau+1}-Mt\,T_n^{\tau+1}=W_n^{\tau}-Mt\,T_n^{\tau} \tag{6.32}$$

vI) energy and moisture balance for the air cavity space

Energy balance at an air cavity bounded by layer *n* and layer *m* can be generally expressed by:

$$-Foc_n\,T_n^{\tau+1}+(1+Foc_n+Foc_m+Fai+Fao)\,T_{ca}^{\tau+1}-Foc_m\,T_m^{\tau+1}=T_{ca}^{\tau}+Fai\,T_i+Fao\,T_o \tag{6.33}$$

And the moisture balance is;

$$-Fod_n\,W_n^{\tau+1}+(1+Fod_n+Fod_m+Fai+Fao)\,W_{ca}^{\tau+1}-Fod_m\,W_m^{\tau+1}=W_{ca}^{\tau}+Fai\,W_i+Fao\,W_o \tag{6.34}$$

The coefficients of the heat and moisture balance equations are defined as following:

$$Fo = K\Delta t/(\rho_m c_{vm})_{tot}\Delta x^2$$

$$Fi = h_i \Delta t/(\rho_m c_{vm})_{tot}\Delta x$$

$$Fe = h_o \Delta t/(\rho_m c_{vm})_{tot}\Delta x$$

$$Fmi = h_{fg}\Delta t\, h_{Di}/(\rho_m c_{vm})_{tot}\Delta x$$

$$Fme = h_{fg}\Delta t\, h_{Do}/(\rho_m c_{vm})_{tot}\Delta x$$

$$Ae = h_{fg} D_v \alpha\, \Delta t/(\rho_m c_{vm})_{tot}\Delta x^2$$

where

$$\alpha = R_v \rho_a T_m$$

and

$$Msi = \Delta t\, h_{Di} W_s/C_m \Delta x$$

$$Mso = \Delta t\, h_{Do} W_s/C_m \Delta x$$

$$Mw = W_s D_v \alpha\, \Delta t/C_m \Delta x^2$$

$$Mt = \phi dW_s/dT$$

$$Eab = [\Delta x (\rho_m c_{vm})_{tot}|_n + \Delta x (\rho_m c_{vm})_{tot}|_m]/2\,\Delta t$$

where *n* and *m*, denote the two adjacent layers of material.

and

$$Ewb = h_{fg} D_v \alpha / Eab\, \Delta x$$

$$Mwb = 2 D_v \alpha\, \Delta t\, W_s/\Delta x\, M_a$$

where;

$$M_a = (\Delta x\, C_m)_n + (\Delta x\, C_m)_m$$

and

$$Fb = \Delta t\, C_{VR} / \Delta x\, (\rho_m c_{vm})_{tot}$$

$$Ar = h_{fg} P_{VR} \Delta t\, \alpha / \Delta x\, (\rho_m c_{vm})_{tot}$$

$$Mr = W_s P_{VR} \alpha\, \Delta t / C_m \Delta x$$

$$Fc = h_{ec} \Delta t / \Delta x\, (\rho_m c_{vm})_{tot}$$

$$Frc = h_{rc} \Delta t / \Delta x\, (\rho_m c_{vm})_{tot}$$

$$Fmc = h_{fg} \Delta t\, h_{Dc} / \Delta x\, (\rho_m c_{vm})_{tot}$$

$$Msc = \Delta t\, h_{Dc} W_s / C_m \Delta x$$

$$Foc = \Delta t\, h_{ec} / L_c\, \rho_a c_p$$

$$Fai = Q_{ic} \Delta t / V_c\, \rho_a$$

$$Fao = Q_{oc} \Delta t / V_c\, \rho_a$$

$$Fod = \Delta t\, h_{Dc} / L_c\, \rho_a$$

6.5.2.3 Evaluation of heat and moisture transport parameters: In porous materials, heat and moisture transport parameters vary with their moisture and thermal conditions. At transient conditions, these parameters are continuously varying. Therefore, for accurate modelling of the simultaneous heat and moisture transfer problem, variations in these parameters must be considered. In numerical modelling, these variations can be considered by updating their values at the end of each time step. The vapour diffusion

coefficient D_v is an important moisture transport parameter that can vary considerably with the moisture content of material. In exterior wall, moisture content normally varies across the thickness of the same layer of material. Considering the practicality of the numerical solution and the accuracy of the vapour diffusion coefficient, accounting for its variations within the same layer may not be necessary. Instead, an average moisture diffusion coefficient which is based on moisture content distribution within the layer is used to describe moisture transfer through the layer. For a layer with N number of nodes, the average diffusion coefficient is given by:

$$\overline{D_v} = \frac{\Sigma D_v(\phi)}{N} \tag{6.35}$$

The thermal and moisture capacities of material are also dependent on its moisture content. The slope of the moisture equilibrium curve for any porous material varies with relative humidity which is a reflection of the material moisture content. In this study, the variation of material moisture capacity C_m over the thickness of the material is taken into account by assigning a local moisture capacity for each node based on the corresponding moisture content. For node n, the material local moisture capacity can be expressed by:

$$C_m = \frac{\partial U}{\partial \phi} | \phi_n = f(U) \tag{6.36}$$

Similarly, the local thermal capacity is evaluated for each node based on its moisture content and can be given by:

$$(\rho_m c_{vm})_{tot} = (\rho_m c_{vm} + 4186\, U \rho_m) \tag{6.37}$$

Material air moisture content, which is the moisture driving potential used in this study, is dependent on the material moisture content as well as local temperature. For the same moisture content, the value of the of material air moisture content can decrease and

increase with temperature according to the corresponding saturation air moisture content. This relationship can be mathematically expressed by:

$$\frac{dW}{dT} = \phi \frac{dW_s}{dT} \tag{6.38}$$

The variation of the saturation air moisture content W_s relative to the temperature T at any given temperature can be evaluated from the slope of the saturation curve. In a numerical solution, this parameter can be evaluated at the end of each time step using the instantaneous predicted temperature. However, this calculated value can not accurately represent the actual change in saturation air moisture content during the subsequent time step if large temperature variations occur. By using the average temperature during the subsequent time interval for evaluating the slope of the saturation curve, it has been found that the calculated value can accurately represent the change in saturation conditions. The relationship between the air moisture content and the temperature can now be expressed as:

$$\frac{dW}{dT} = \phi \frac{dW_s}{dT} \Big| T = T_{avg} \tag{6.39}$$

The average temperature can be evaluated by predicting the instantaneous temperature at the end of the subsequent interval without considering the impact of moisture transport. The arithmetic average between the temperatures at the beginning and at the end of the interval will represent the interval average temperature T_{avg}.

6.5.2.4 Simultaneous solution of heat and mass balance equations: In order to simultaneously evaluate the temperature and air moisture content distribution across the exterior wall, a system of algebraic equations representing the heat and mass balance at each node must be solved simultaneously. In this study, the solution is carried out using

the Gauss-Jordan elimination method. Using this method, all off-diagonal matrix elements are reduced to zero through a process called diagonalization. Although other methods may require less computations, the Gauss-Jordan method provides a systematic means for the diagonalization of the system of linear simultaneous equations with an easy to extract solution. A potential problem in this method is that normalization of the pivot row may not be achieved in the presence of a zero element in the pivot row. This problem can be avoided by changing the order of equations in the system where the row with a zero or small pivot element is exchanged with the row below it that has the largest element in the same column. In addition, to circumvent the zero pivot problem, such procedure which is known as partial pivoting was found to achieve more computational accuracy especially when handling large numbers of simultaneous equations [142].

6.5.3 Evaluation of condensation and moisture content distribution within exterior walls: Condensation on a non-hygroscopic material surface, like glass, occurs when its temperature is below the dew point temperature of the ambient air. As soon as condensation starts to occur, the material surface is wetted and the air moisture content at the surface will be equal to the saturation level corresponding to its temperature. For hygroscopic materials, which are likely to form most of the exterior wall components, the material air moisture content is determined by the temperature and the moisture content of material. Since, moisture equilibrium is likely to be maintained within materials, the local relative humidity will be determined by the material moisture content. At moisture contents equal or greater than the maximum hygroscopic moisture content (MHMC), the material relative humidity will reach the saturation level (i.e., RH=100%) which is an indication of the occurrence of condensation. Therefore, for condensation to occur within the exterior wall components at a particular location, the following condition must be satisfied:

$$U \geq U_{hm}$$

At moisture contents equal or greater than the maximum hygroscopic level, the air moisture content within the material will only be dependent on the temperature.

$$W = f(T) \qquad For \qquad U > U_{hm} \tag{6.40}$$

In steady state analysis evaluation of interstitial condensation within exterior walls can be performed by merely using the moisture and heat transport coefficients of the layers comprising the wall. In transient analysis, however, material hygroscopicity will be an important factor in determining when condensation starts to occur. When evaluating interstitial condensation as part of the finite difference solution, the air moisture content at each node is compared with the saturation value corresponding to the nodal temperature at the end of each time interval. Whenever the value of the air moisture content at any particular node is greater than the saturation air moisture content or the material moisture content is greater than its maximum hygroscopic level, the air moisture content is set to the saturation value.

Moisture content distribution within the different materials of the wall system is evaluated using the corresponding moisture equilibrium curve when the relative humidity level is below 100%. For material i, the nodal moisture content is given by:

$$U = a_i \phi^{b_i} + c_i \phi^{d_i} \qquad \phi < 100\% \tag{6.41}$$

At 100% relative humidity, when interstitial condensation occurs, the moisture equilibrium curve cannot be used for evaluating nodal moisture content since the material moisture content is likely to be higher than its maximum hygroscopic level. Instead, the mass balance concept is used. Based on the average time interval moisture and temperature

conditions, the moisture content at each node can be calculated. For an intermediate node *n*, the moisture content can be given by:

$$U^{\tau+1} = U^{\tau} + \frac{D_v R_v \rho_a \Delta t}{\Delta x^2 \rho_m} (\overline{T}_{n-1} \overline{W}_{n-1} - 2\overline{T}_n \overline{W}_n + \overline{T}_{n+1} \overline{W}_{n+1}) \tag{6.42}$$

For an interior surface node *n*, the moisture content in the presence of condensation is calculated as following:

$$U^{\tau+1} = U^{\tau} + \frac{h_{Di} \Delta t}{\Delta x \rho_m} (W_i - \overline{W}_n) - \frac{D_v R_v \rho_a \Delta t}{\Delta x^2 \rho_m} (\overline{T}_n \overline{W}_n - \overline{T}_{n+1} \overline{W}_{n+1}) \tag{6.43}$$

Moisture content at other surface nodes are similarly evaluated using the appropriate ambient conditions. At the boundary between two layers, the moisture content is evaluated by performing the mass balance at each boundary surface. Since the boundary surfaces are likely to have different moisture contents, each is represented by a separate node that will have the same air moisture content but different material moisture content. Depending on its location relative to the moisture flow direction, the boundary node could be a source node or a sink node as illustrated in Fig. 6.7.

Since only vapour transport can take place between the two nodes, the sink node moisture content will be maintained at the maximum hygroscopic level as long as the source node is at that level or higher. The moisture content at the source node *b1* can be given by:

$$U_{b1}^{\tau+1} = U_{b1}^{\tau} + \frac{D_v R_v \rho_a \Delta t}{\Delta x^2 \rho_m} (\overline{T}_{n-1} \overline{W}_{n-1} - \overline{T}_n \overline{W}_n) - \Delta U_{b2} \tag{6.44}$$

where ΔU_{b2} is the moisture content that is required to maintain the sink node *b2* at the

maximum hygroscopic level.

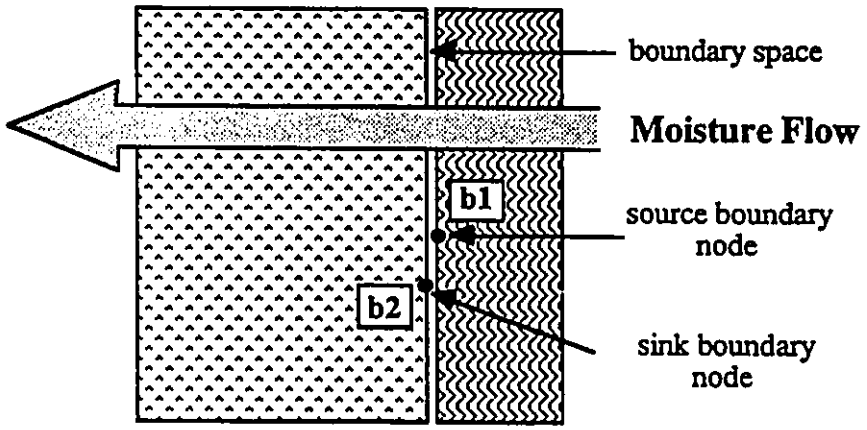

Fig. 6.7 Moisture flow between two adjacent layers of materials.

When the moisture content of the source node decreases below the maximum hygroscopic level or it is not high enough to keep the sink node at its maximum hygroscopic moisture content, moisture distribution between the nodes will be decided according to their relative moisture capacity so as to maintain equilibrium between them. At this point of transition in the material moisture content, the corresponding relative humidity within the material must be evaluated. For an intermediate or a surface node, the relative humidity can be evaluated from equation 6.41 using the material moisture content. However, since the relative humidity, ϕ, is non-linearly related to the moisture content U, the corresponding relative humidity can only be evaluated by iterative techniques such as Newton's method. At boundaries, the air moisture content at the point of transition is determined by the material moisture content of both layers. Since moisture equilibrium

must be maintained, the moisture content in both materials must correspond to the same relative humidity. For two adjacent layers *i* and *j*, the equilibrium moisture content for the boundary node in layer *i* can be expressed by:

$$Ue_i = U_i - \frac{1}{\rho_{mi}\Delta x_i}\left[1/(1/\Delta x_i\, C_{mi} + 1/\Delta x_j\, C_{mj})\right]\left(\frac{U_i \rho_{mi}}{C_{mi}} - \frac{U_j \rho_{mj}}{C_{mj}}\right) \qquad (6.45)$$

The equilibrium moisture content given in equation 6.45 can now be implemented in equation 6.41 for evaluating the air moisture content at the boundary. In the presence of a vapour retarder between the two layers, the boundary nodes will behave independently and the moisture interaction between them will be indirect through the defined moisture resistance of the vapour retarder.

The process of moisture equalization is performed between any two adjacent nodes having moisture content equal or greater than the critical value. In this process moisture movement can occur in a direction opposite to the vapour flow since the moisture content will be the determinant of such moisture movement. All adjacent nodes subjected to moisture equalization will be at the same moisture content and any loss or gain from any node will simultaneously and equally affect the rest.

6.6 Computer Models for Simulation and Applications

Theoretical modelling of simultaneous heat and moisture transfer through multi-layer exterior wall is a very complex process which gets more complicated with the presence of an air cavity within the wall. In order to solve for heat and moisture transfer through walls and to model their interaction with the indoor environment, numerical and iterative techniques are required for solving the resulting equations. Furthermore, evaluation of the

exterior wall moisture performance is a long term process that may require an extended period of time to simulate. To carry out all these numerous calculations, computer models have to be developed for simulating the moisture behaviour of different exterior walls subjected to varying boundary conditions. Based on the modelling approaches discussed earlier, a computer program called "Wall-MPM" has been developed for evaluating exterior wall moisture performance. The program is designed to evaluate moisture behaviour of multi-layer non-cavity and cavity wall systems. In the cavity wall system the cavity space is allowed to interact with the indoor and outdoor environments through air convection. A general flow chart illustrating the basic components of the program is shown in Fig. 6.8. As part of the program, two main modelling modules have been developed. One representing the heat and moisture transfer through the wall when no vapour retarder is used, and the other takes into account the presence of vapour retarder at the boundary between any two layers. In the cavity wall system, the vapour retarder can only be placed within the inner wythe at the boundary between any two layers.

Using the developed program, moisture and thermal behaviour of different exterior wall systems under different transient boundary conditions can be evaluated over any period of time. Evaluating the influence of indoor air humidity behaviour on wall moisture performance is one of the main objectives of the present research. Therefore, this wall moisture behaviour evaluation program can be used in conjunction with indoor air humidity evaluation programs to investigate the impact of indoor air humidity transient behaviour on the short term and long term wall moisture performance. In addition a parametric analysis can be performed to evaluate the relative influence of each of the parameters which indirectly affect wall moisture performance through their influence on indoor air humidity.

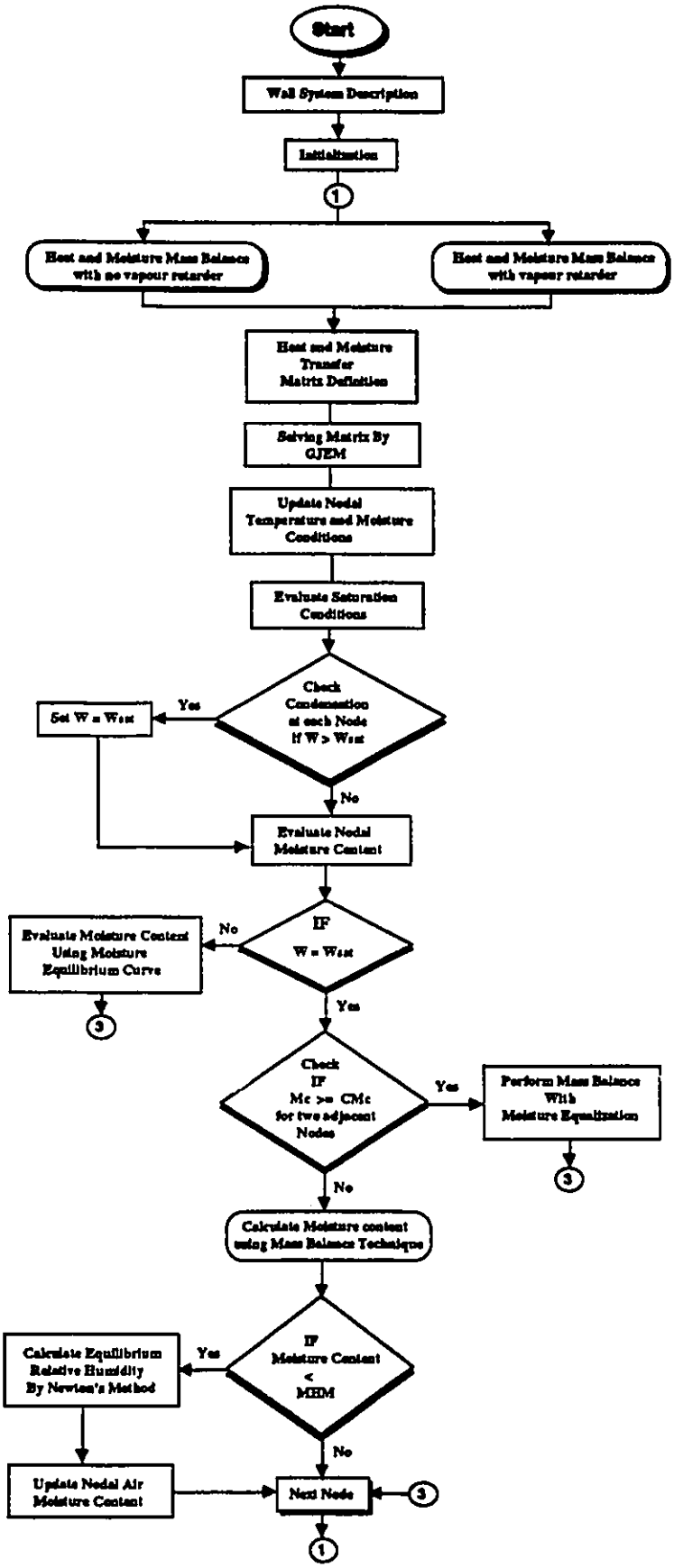

Fig. 6.8 A general flow chart illustrating the main components of the wall moisture behaviour evaluation programs.

6.7 Comparisons and Validation

6.7.1 Theoretical verification: The moisture behaviour evaluation program developed as part of this research is based on certain moisture transfer theories and assumptions. Furthermore, numerical techniques have been implemented to solve for heat and moisture distribution across the wall system. Therefore, the accuracy of this program results and the applicability of the theories behind them must be verified. This can be achieved by comparing the program predictions with the solutions of the basic theoretical cases as well as the results of representative experimental tests. As a first step towards validating this program, its steady state predictions of temperature and moisture distribution across the multi-layer cavity wall system shown in Fig. 6.9 will be examined. The thermal and moisture characteristics of the modelled wall are given in Table 6.3. The wall system was initially at uniform temperature and air moisture content when the boundary conditions were suddenly changed and maintained at constant levels.

The indoor air temperature is kept at 21° C. and the outdoor temperature is kept at 10° C. while the relative humidity at both sides is maintained at 50%. The hourly thermal and moisture responses of the wall system have been evaluated by the developed computer program. The solution process continued till steady state conditions were reached at the point when no further change occurred in the wall thermal and moisture conditions. Fig. 6.10 shows the steady state temperature distribution predicted by the program as compared with the calculated exact values at the same boundary conditions. It can be seen that there is almost perfect agreement between the two approaches. Similarly, good agreement is obtained for the air moisture content distribution as shown in Fig. 6.11. For the same boundary conditions, steady state temperature and air moisture content

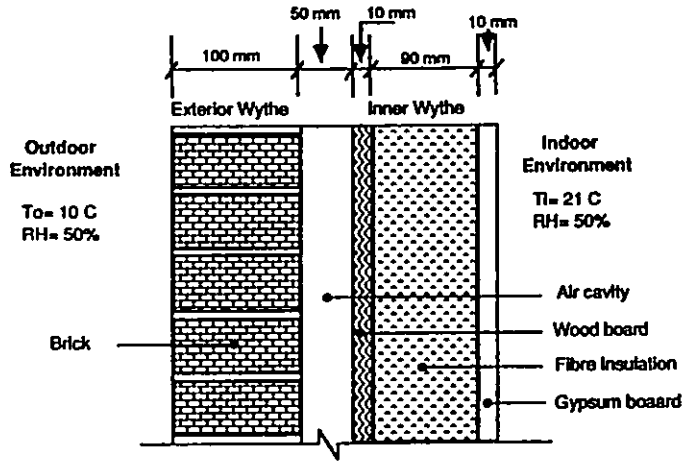

Fig. 6.9 Modelled multi-layer cavity wall system.

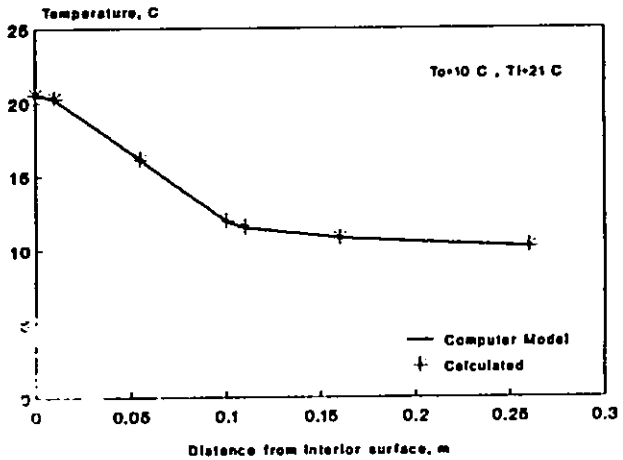

Fig. 6.10 Steady state temperature distribution across a multi-layer cavity wall system.

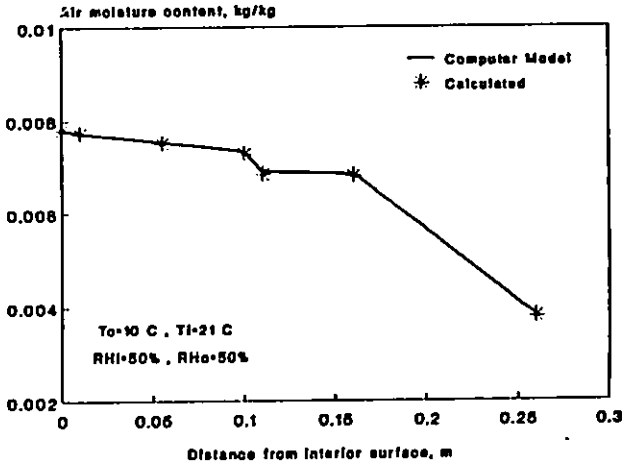

Fig. 6.11 Steady state air moisture content distribution across a multilayer cavity wall system.

distribution across

Table 6.3 Thermal and moisture characteristics of the modelled wall systems components.

Wall element	Thickness, mm	Thermal Conductivity, W/m·C	Thermal Conductance, W/m²·C	Diffusion Coefficient, kg/m·Pa·s 10^{-12}	Permeance, kg/m²·Pa·s 10^{-6}
Indoor Film	-	-	8.3	-	1.7
Gypsum Board	10	0.158	-	42	-
Insulation	90	0.0433	-	78	-
Wood	10	0.0966	-	7.6	-
Cavity Air Film (inner)	-	-	2.8	-	1.7
Cavity Air Film (outer)	-	-	2.8	-	1.7
Air Cavity	50	-	5.6	-	0.85
Brick	100	0.7	-	11	-
Outdoor Film	-	-	21.3	-	11

the multi-layer non-cavity wall system shown in Fig. 6.12 have been predicted by the program. Comparisons with calculated steady state temperature and air moisture content distributions have shown good agreement as can be seen from Figs. 6.13-6.14. Being able to accurately reach the steady state conditions from a transient state at the beginning of the solution, the computer model can be considered to be numerically validated. On the other hand, since both theoretical models, representing non-cavity and cavity wall systems, are based on the same moisture transfer theories and assumptions, validating any one in predicting moisture behaviour of multi-layer walls will automatically validate the other. For any theoretical model to accurately assess exterior wall moisture performance,

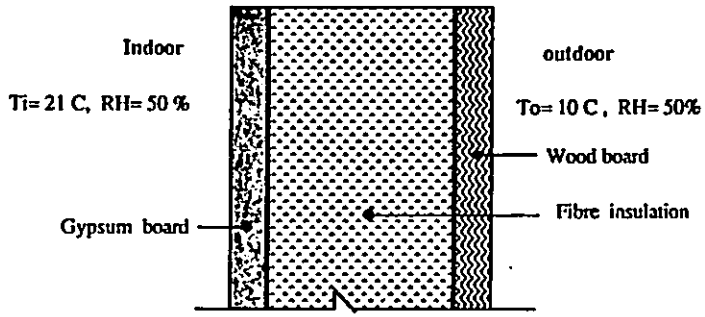

Fig. 6.12 Modelled multi-layer non-cavity wall system.

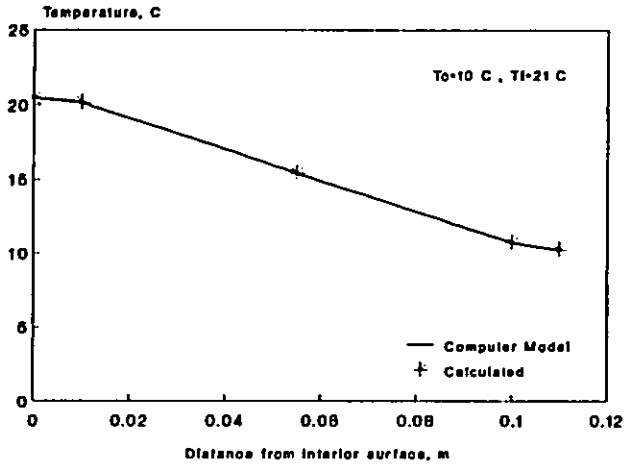

Fig. 6.13 Steady state temperature distribution across a multi-layer noncavity wall system.

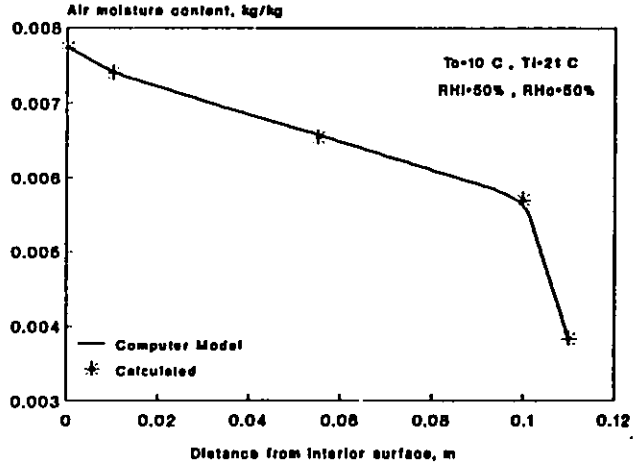

Fig. 6.14 Steady state air moisture content distribution a multilayer noncavity wall system.

it must be able to predict the occurrence of interstitial condensation at the right location. Furthermore, it must be able to predict the moisture content distribution and behaviour for the various wall system components with sufficient accuracy.

For the multi-layer wall system shown in Fig. 6.9, the steady state relative humidity distribution at an outdoor air temperature of 0° C is shown in Fig. 6.15. It can be seen that the relative humidity has a value of unity at two different locations within the wall. This means that interstitial condensation has occurred at the boundary between the insulation and the wood layers as well as the interior surface of the outer wythe (i.e., the brick layer). In order to verify these predictions, interstitial condensation within the same wall assembly can be checked using the vapour pressure profiles. Fig. 6.16 compares the saturation vapour pressure profile to the vapour pressure profile calculated based on the ambient vapour pressures. At any point when the saturation vapour pressure is less than the calculated vapour pressure, interstitial condensation can occur. From Fig. 6.16 it can be seen that interstitial condensation could occur over a wide region extending from the insulation layer to the brick layer. Although this condensation region includes the two condensation locations predicted by the computer model, yet the vapour pressure profile method can not specifically allocate these points. Determining the location of the first condensation point is very important since it will result in a completely different vapour pressure profile that may not result in further condensation at other locations. By setting the vapour pressure at the boundary between the insulation and the wood layers to the saturation level, the resulting new profile would still indicate that condensation occurs as shown in Fig. 6.17. The resulting new condensation region still includes the second condensation point at the inner face of the outer wythe. Setting the vapour pressure to saturation level at this point will completely push the vapour pressure profile below or at

the saturation curve which means that no more condensation will occur as can be seen from Fig. 6.18. From the above discussion, it can be concluded that the interstitial condensation predicted by the computer model at steady state conditions is in full accordance with the prediction of the multi-stage vapour pressure profile method. To further emphasize this conclusion, interstitial condensation is evaluated for the same wall system when the exterior surface of the wood layer is coated with a paint film having a permeance of $1.5 \cdot 10^{-10}$. At the same boundary conditions, the computer model predicts that the wood layer will be completely subjected to interstitial condensation as can be seen from Fig. 6.19. The corresponding steady state pressure profiles shown in Fig. 6.20 indicate that the wood layer is a potential location for condensation. By setting the vapour pressure at the boundary between the wood and the insulation layers to the saturation level, the vapour pressure profile is almost completely below or at the saturation profile as shown in Fig. 6.21. However, the vapour pressure curve will still be above the saturation curve within the wood layer region indicating the possibility of more condensation at this location. When the vapour pressure at the exterior surface of the wood layer is set to saturation level, the vapour pressure curve at all other locations will be maintained below the saturation curve as shown in Fig. 6.22. This behaviour confirms the validity of the computer model in predicting the occurrence and the location of interstitial condensation.

6.7.2 Experimental verification: In order to verify the modelling approach and the calculation methods implemented in the computer program for predicting moisture distribution and behaviour within multi-layer walls, predicted theoretical results need to be compared with the experimental results of representative test cases. In literature, many experimental studies have been carried out to investigate the moisture behaviour of multi-

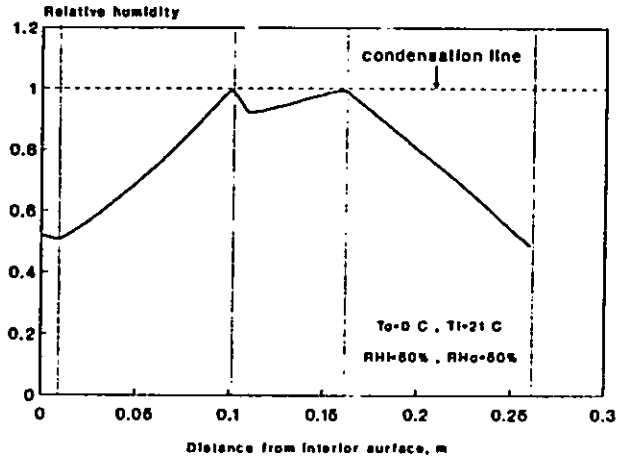

Fig. 6.15 Relative humidity distribution across a multilayer wall in the presence of interstitial condensation.

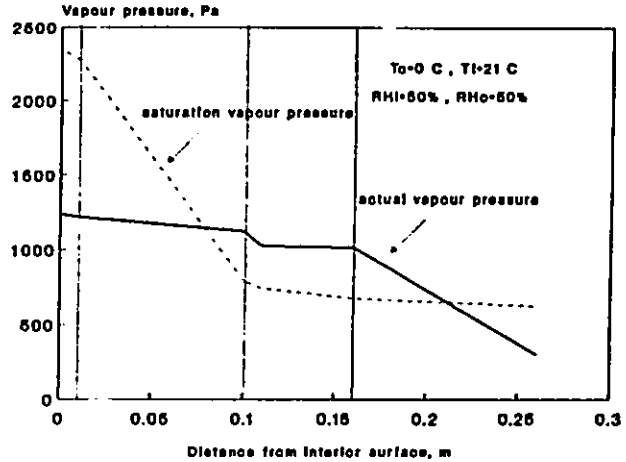

Fig. 6.16 Checking interstitial condensation using steady state pressure profiles (first stage).

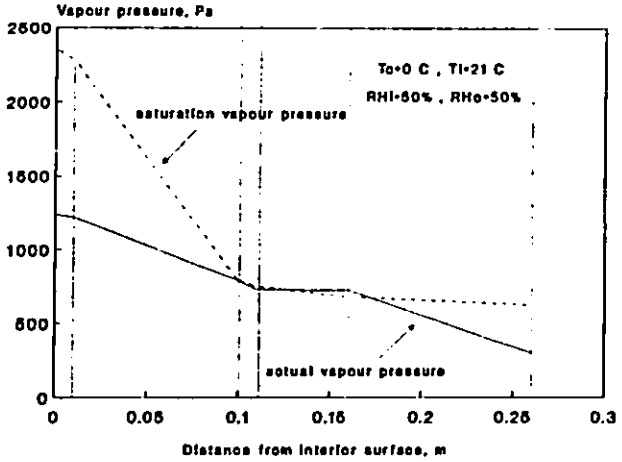

Fig. 6.17 Checking interstitial condensation using steady state pressure profiles (second stage).

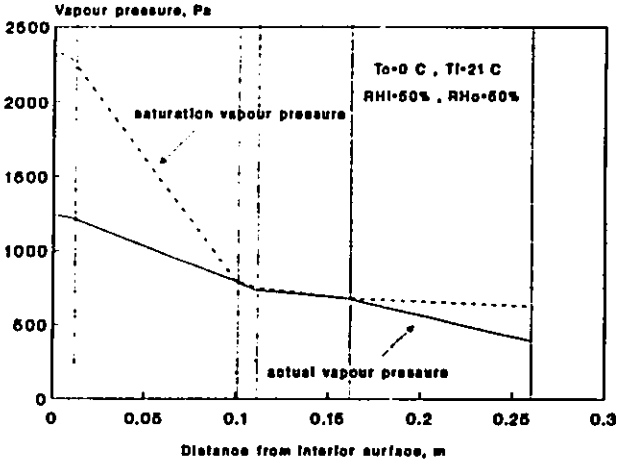

Fig. 6.18 Checking interstitial condensation using steady state pressure profiles (third stage).

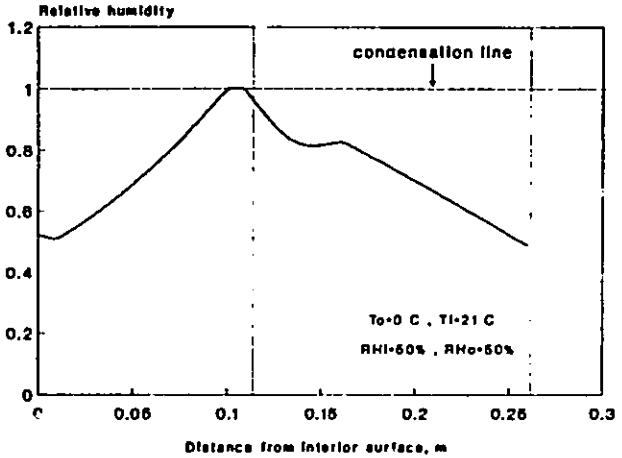

Fig. 6.19 Relative humidity distribution across a multilayer wall in the presence of interstitial condensation.

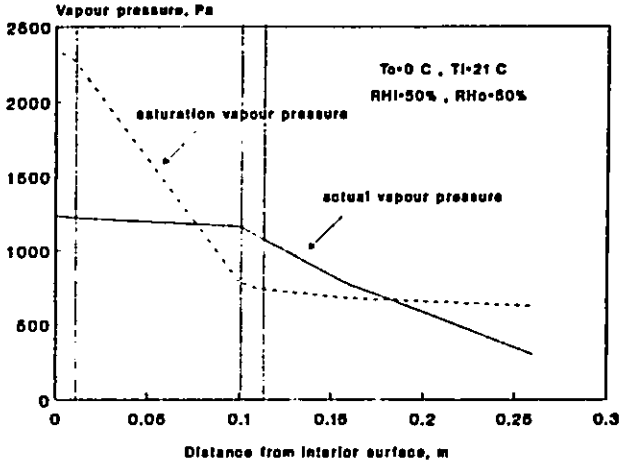

Fig. 6.20 Checking interstitial condensation using steady state pressure profiles (first stage).

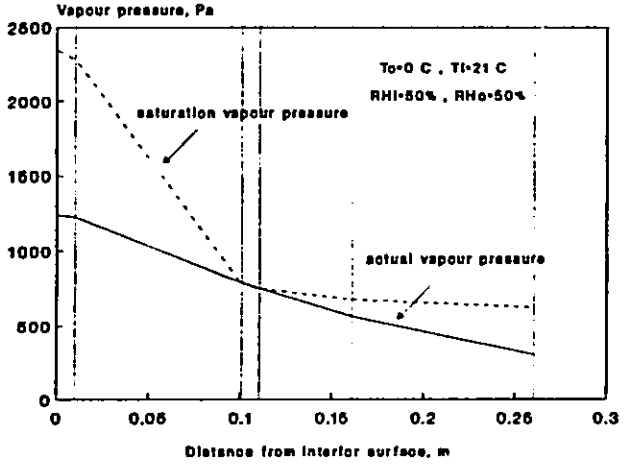

Fig. 6.21 Checking interstitial condensation using steady state pressure profiles (second stage).

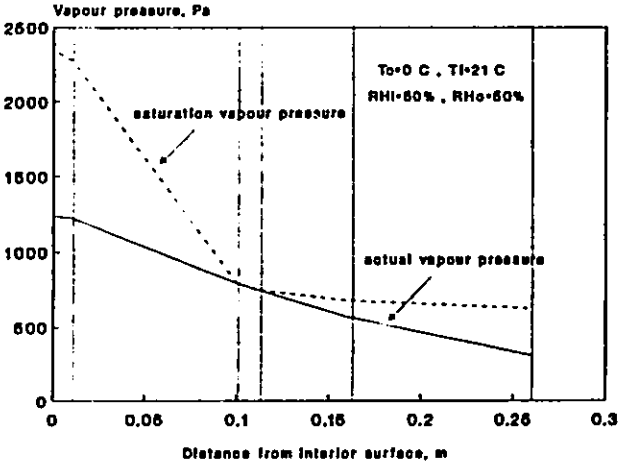

Fig. 6.22 Checking interstitial condensation using steady state pressure profiles (third stage).

layered components at specific boundary conditions. Therefore, the results of appropriate and well documented experimental studies can be utilized for comparisons with the predicted theoretical results without the need for further experimentation. One important experimental program is carried out by the Swedish Council for Building Research [82]. In this program the moisture behaviour of different specimens of one or more layers of common building materials is studied when the initially conditioned specimen is exposed to different boundary conditions. Each specimen has a face area of 0.00553 m^2 and a total thickness of 100 mm. For most of the experiments, the surface mass transfer coefficient ranging from 0.0027 to 0.0054 $kg/m^2.s$, has been found to be representative of the actual conditions. Therefore, theoretical calculations are carried out based on the lower and the upper limits of the surface mass transfer coefficient range. Furthermore, in order to account for all possible moisture transfer mechanisms, the selected tests include specimens at different initial moisture contents representing the hygroscopic and the near saturation level. Fig. 6.23 compares the experimental results and the theoretical predictions of moisture gain of a single aerated concrete layer initially at 50% relative humidity. As can be clearly seen, very good agreement is obtained for both values of the surface mass transfer coefficient. For the same boundary and initial conditions, good agreement is also obtained for a multi-layer specimen consisting of 50 mm thick insulation and 50 mm thick aerated concrete layers as can be seen from Fig. 6.24. In this case, better agreement is obtained when the lower value of the surface mass transfer coefficient is used. For the same specimen, very good agreement is also obtained in the absence of temperature gradient as can be seen from Fig. 6.25. In this case, variations in the surface mass transfer coefficient has no noticeable impact on the moisture gain by the specimen. Theoretical predictions of moisture desorption from a single aerated concrete layer initially at a moisture content of 225 kg/m^3 was found to be in very good agreement

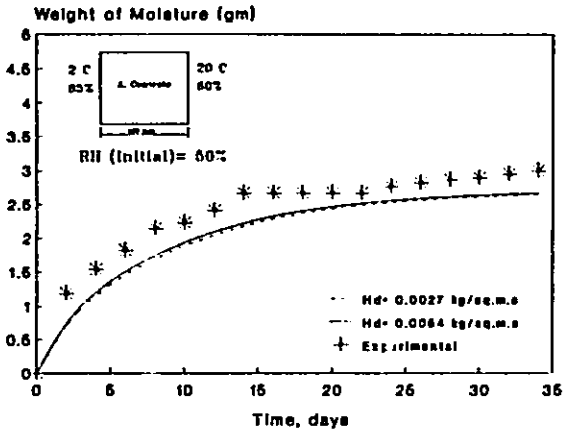

Fig. 6.23 Theoretical and experimental evaluation of weight change of aerated concrete due to moisture absorption in the hygroscopic range.

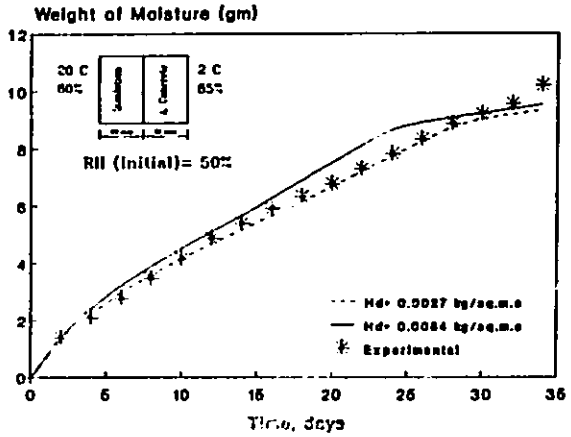

Fig. 6.24 Theoretical and experimental evaluation of weight change of a multi-layered building material system due to moisture absorption in the hygroscopic range.

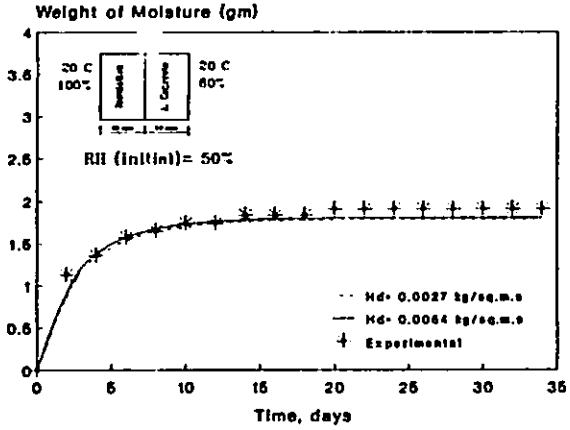

Fig. 6.25 Theoretical and experimental evaluation of weight change of a multi-layered building material system due to moisture absorption in the hygroscopic range.

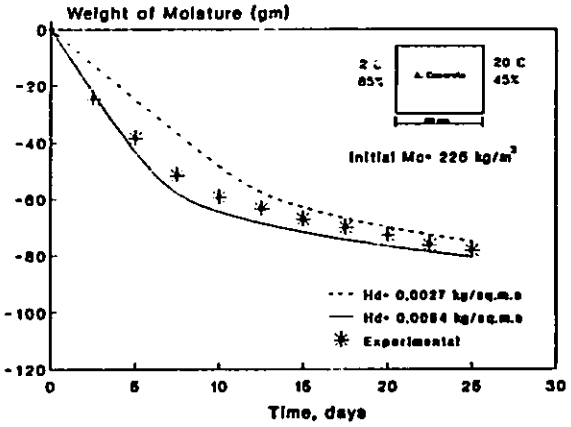

Fig. 6.26 Theoretical and experimental evaluation of weight change of aerated concrete due to moisture desorption.

with experimental results both in the presence of a thermal gradient as shown in Fig. 6.26, and in the absence of thermal and moisture gradients as shown in Fig. 6.27. In both cases, the higher limit of the surface mass transfer coefficient seem to give better agreement with the experimental results. The initial moisture content of the aerated concrete specimen in both cases was much higher than its critical moisture content (i.e., 120 kg/m^3), however, by the end of the simulation period, the specimen moisture content has dropped to a lower level below its critical value. This means that the concept of moisture equalization has been implemented at the beginning of the simulation period until a transition occurs from the wetting level to the hygroscopic level when moisture distribution across the specimen is likely to be nonuniform. Theoretical predictions and experimental results of moisture desorption of a composite specimen consisting of a 50 mm aerated concrete layer initially at a moisture content of 225 kg/m^3, and a 50 mm insulation layer initially at 50% relative humidity are shown in Fig. 6.28. For this particular case, the agreement is not as good as the previous cases, however, the theoretical prediction corresponding to the lower surface moisture transfer coefficient can still be judged to be in good agreement with the experimental results. Much better agreement is obtained at the same boundary conditions for the composite specimen consisting of brick layer at an initial moisture content of 214 kg/m^3, and an insulation layer initially conditioned at 50% relative humidity as illustrated in Fig. 6.29. Good agreement is still obtained when the insulation layer is replaced by an aerated concrete layer having the same thickness and initially conditioned at 50% relative humidity as can be seen from Fig. 6.30. In both cases, the lower surface mass transfer coefficient gives a much better agreement with the experimental results. For the same brick and aerated concrete specimen, theoretical and experimental results are in good accordance when no temperature gradient exist across the specimen as shown in Fig. 6.31. However, in this case, the theoretical predictions

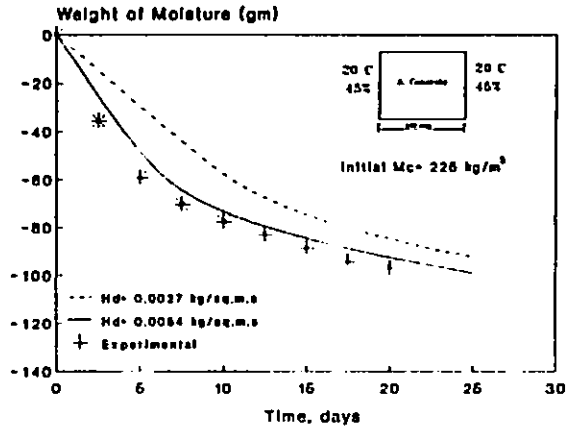

Fig. 6.27 Theoretical and experimental evaluation of weight change of aerated concrete due to moisture desorption.

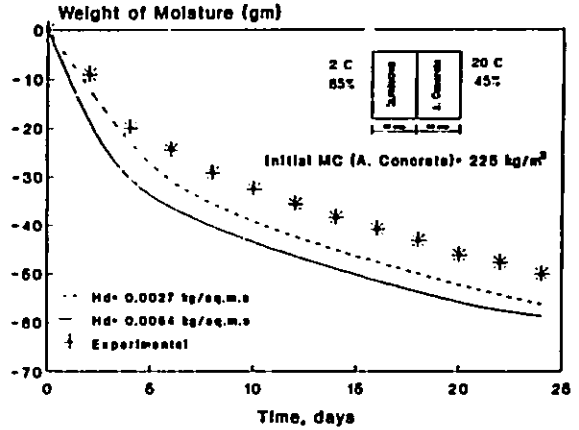

Fig. 6.28 Theoretical and experimental evaluation of weight change of a multi-layered building material system due to moisture desorption.

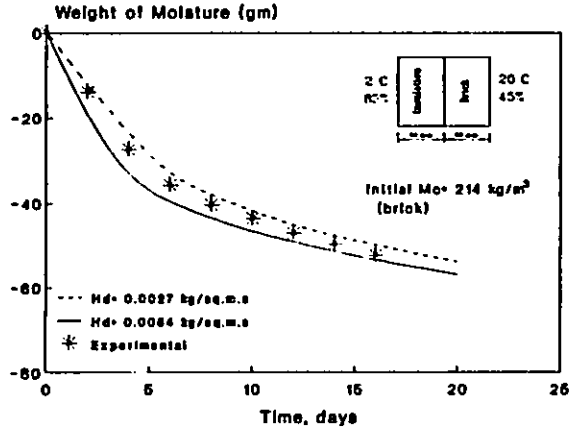

Fig. 6.29 Theoretical and experimental evaluation of weight change of a multi-layered building material due to moisture desorption.

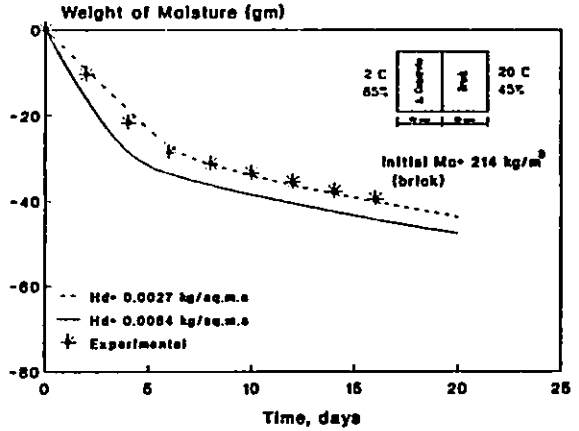

Fig. 6.30 Theoretical and experimental evaluation of weight change of a multi-layered building material due to moisture desorption.

corresponding to the higher value of surface mass transfer coefficient is in a better agreement with experimental results. In spite of the influence of the surface mass transfer coefficient, the theoretical prediction can be generally judged to be in good accordance with the experimental results considering the variability that may be experienced by it in real test conditions.

In a more practical experimental program conducted by Burch, D.M., et al [133], two different initially conditioned wall specimens each with a face area of 0.372 m^2 were placed between two chambers representing the indoor and the outdoor environments. The first wall specimen consists of a 13 mm gypsum board, 89 mm fibre insulation and 13 mm wood board. In the second specimen, the fibre insulation was replaced by cellulose insulation having the same thickness. In both cases, the interior surface of the gypsum board was painted with a latex paint system with a moisture permeance value of $3 \cdot 10^{-10}$ $kg/m^2 \cdot Pa \cdot s$, and the exterior surface of the wood board was painted with an oil-based paint system with a moisture permeance value of $1.5 \cdot 10^{-10}$ $kg/m^2 \cdot Pa \cdot s$. Both specimens were initially conditioned at about 24° C. and 51% relative humidity. The interior side of the specimen was exposed to the same initial ambient conditions while the exterior side of the specimen (i.e., wood board exterior surface) was exposed to a conditioned environment with an air temperature of about 1° C. and a relative humidity level of about 28%. At the beginning of simulation, the relative humidity level has dropped to about 7% and reached the 28% level at about the tenth day of the simulation period. After a 34-day test period, the mean moisture content of the inner and outer halves of the wood layer were measured. In order to compare these experimental results with the theoretical prediction of the computer model developed in this study, the same experimental case was theoretically modelled. Theoretical prediction of the wood board moisture content was

carried out for a convective surface heat transfer coefficient of 2.8 W/m^2·C at the wood board surface. This surface heat transfer coefficient value corresponds to natural convection. However, for the test conditions, air movement is forced over the surface resulting in a higher convective surface transfer coefficient. For the purpose of illustrating its impact on the theoretical prediction, a convective surface heat transfer coefficient of 11.2 W/m^2·C is also used. Fig. 6.32 and Fig. 6.33 compare the predicted average moisture content for the inner and outer halves of the wood board to the corresponding measured values at the end of the 34th day of the experiment. In both cases, the model predicts with good agreement the material moisture content for a convective surface transfer coefficient of 2.8 W/m^2·C. A slightly better agreement is obtained for the higher value of the surface transfer coefficient. The vapour diffusion coefficient of the fibre insulation (D_v=78·10^{-12} kg/m·Pa·s) used in the modelling so far seems to underestimate the moisture permeability of the material. For the fibre insulation used in the experiment (density=11.5 kg/m^3), the vapour diffusion coefficient must be higher. According to ASHRAE [20], the vapour diffusion coefficient of such fibre insulation material is around 170·10^{-12} kg/m·Pa·s which is more than double its original value. Figs. 6.34 and 6.35 show the predicted material moisture content for the inner and outer halves of the wood board when a convective surface transfer coefficient of 2.8 W/m^2·C is used. In both cases, the experimental results are in good agreement with the theoretical predictions. Comparisons with Figs. 6.32 and 6.33 would indicate that by increasing the vapour diffusion coefficient of the insulation layer, the predicted moisture content, especially for the inner half, will be in better agreement with measured data. Predicted and measured moisture accumulation for the inner and outer halves of the wood board when cellulose insulation is used, instead of the fibre glass insulation, are shown in Figs. 6.36-6.37. It can be seen that the theoretical predictions in both cases are generally in accordance with the

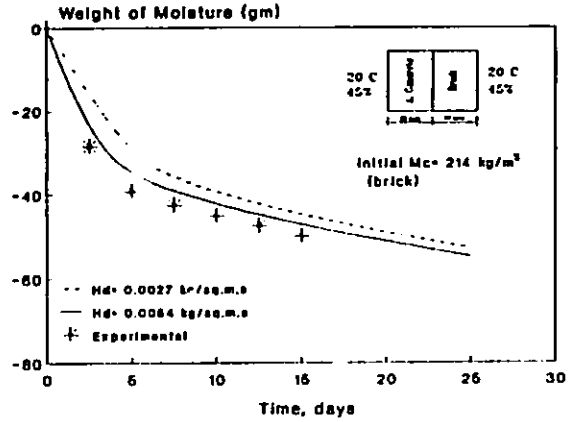

Fig. 6.31 Theoretical and experimental evaluation of weight change of a multi-layered building material due to moisture desorption.

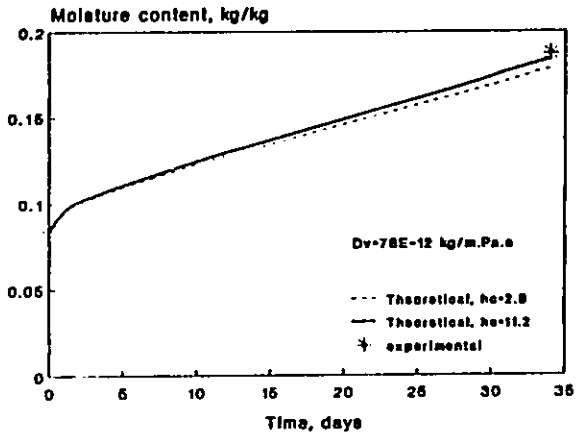

Fig. 6.32 Comparison between measured and predicted moisture accumulation at the inner surface of wood (fibre glass insulation wall).

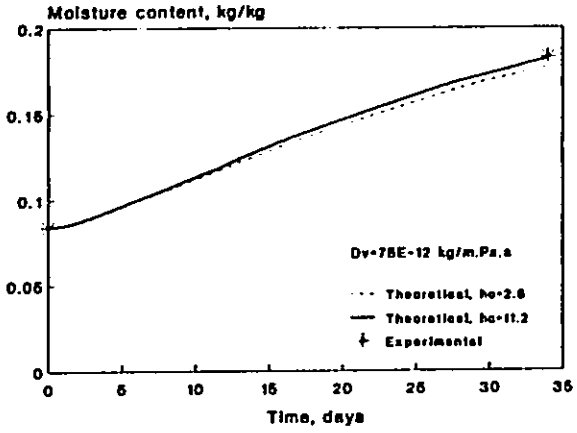

Fig. 6.33 Comparison between measured and predicted moisture accumulation at the outer surface of wood (fibre glass insulation wall).

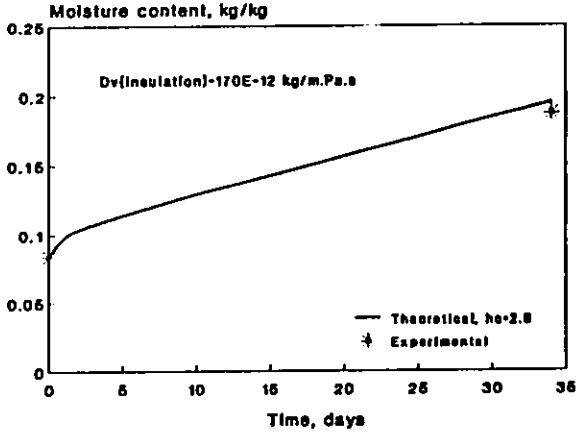

Fig. 6.34 Comparison between measured and predicted moisture accumulation at the inner surface of wood (fibre glass insulation wall).

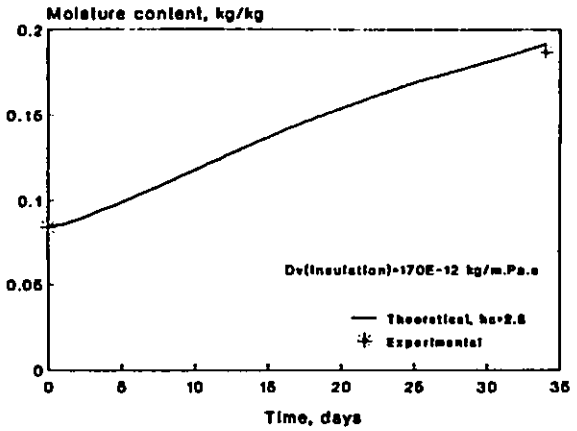

Fig. 6.35 Comparison between measured and predicted moisture accumulation at the outer surface of wood (fibre glass insulation wall).

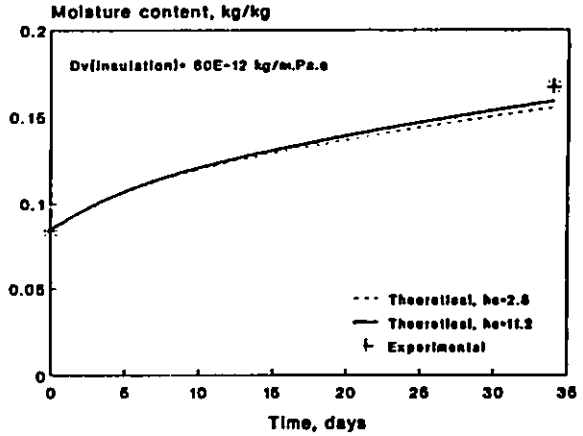

Fig. 6.36 Comparison between measured and predicted moisture accumulation at the inner surface of wood cellulose insulation wall).

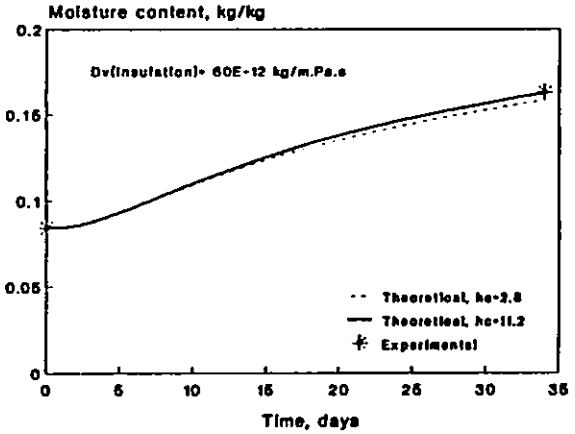

Fig. 6.37 Comparison between measured and predicted moisture accumulation at the outer surface of wood cellulose insulation wall).

experimental results for both convective surface transfer coefficients. However, much better agreement is obtained for the outer half especially at a convective transfer coefficient of 11.2 $W/m^2 \cdot C$. Based on the above discussion, the model can be judged to be successful in predicting the moisture accumulation in the wood layer. In addition, the model can accurately predict the occurrence and the location of interstitial condensation.

6.8 Summary

In this chapter, the transient moisture behaviour of non-cavity and cavity exterior wall systems has been theoretically modelled by simultaneously solving for the heat and moisture transport through their various components. In the cavity wall system, the cavity space is linked with the indoor and outdoor environments by air flow paths that allow moisture to pass through under thermal and wind driving potentials. In order to evaluate the air flow rate across these paths under certain boundary conditions, the multi-cell air flow modelling approach is implemented for evaluating the pressure differential across the different air flow paths.

For practical considerations, the air moisture content is used as the main driving potential when the material moisture content is below its maximum hygroscopic level. At higher moisture contents, the moisture equalization approach is implemented. The combined heat and moisture transport through porous materials is modelled by a system of coupled differential equations which represent the base for modelling simultaneous heat and moisture transfer in multi-layer walls. The instantaneous temperature and air moisture content distribution across a multi-layer wall are evaluated by simultaneously solving the corresponding heat and moisture transfer equations. Solution for these equations are

obtained numerically by implementing the finite-difference implicit scheme. For this numerical approach, two node distribution criteria have been suggested. At each node, both heat and moisture balance is performed. Therefore, for *N* number of nodes, *2N* number of equations are simultaneously solved. Solution of these equations is obtained by the Gauss-Jordan elimination technique. In the hygroscopic moisture range, the instantaneous material moisture content is evaluated from the material moisture equilibrium curve. As condensation occurs, variations in the local material moisture content is determined by applying the mass balance approach at the condensation points. Condensation within the wall various components is considered to occur whenever the local material moisture content is equal to or greater than the maximum hygroscopic level which corresponds to 100% relative humidity at moisture equilibrium.

Evaluation of exterior walls moisture performance involves a considerable amount of calculations which are almost impossible to perform without the computer. As part of this research, a wall moisture behaviour evaluation program has been developed for evaluating the moisture behaviour of multi-layer non-cavity and cavity wall systems. Results from this program have been used to validate the implemented calculation techniques as well as the moisture transfer theories on which the program was based. Comparisons with experimental as well as standard theoretical results (steady state analysis) have indicated very good agreement with the theoretical predictions. Within the frame work of its applicability, the developed computer model can be judged to be a good tool for predicting moisture behaviour of exterior multi-layer wall systems.

CHAPTER 7

EFFECT OF INDOOR AIR HUMIDITY VARIATIONAL BEHAVIOUR ON EXTERIOR WALL MOISTURE PERFORMANCE

7.1 Introduction

Moisture accumulation in exterior walls is a by-product of many factors related to the indoor and the outdoor conditions as well as the thermal and moisture characteristics of the wall. Among all these factors, indoor humidity remains the most interesting parameter to be looked at for three reasons. First, it is a prime factor in determining the wall moisture performance; second, in many buildings, very little, if any, attention is normally given to the problem of indoor humidity control allowing it to naturally fluctuate according to the natural balance of the different available moisture transport processes; and third, indoor humidity is the only controllable environmental parameter which in most cases offers sufficient flexibility to be modified for better exterior wall moisture performance without endangering the functional requirements of the space.

In winter, indoor humidity is the main source of moisture that can be transferred to the core of the wall system. Furthermore, the drying potential of the wall components during summer can be determined by the level of indoor humidity, especially for humid outdoor conditions. For more realistic and accurate assessment of exterior walls moisture performance, the transient behaviour of indoor air humidity must be considered. Depending on the modes of moisture interaction between the indoor environment and the wall system, variations in indoor air humidity can have immediate as well as long term impacts on the wall moisture conditions. For non-cavity multi-layer wall systems, moisture

transfer occurs mainly by diffusion which is a relatively slow process. In this case, the impact of a particular pattern of variations of indoor humidity on the short term wall moisture performance may not be appreciable. On the other hand, the accumulative effect of a certain variational pattern will likely result in a unique long term moisture performance. In a cavity wall system, the cavity space is normally connected with the indoor environment by air flow paths through which air can flow under wind and thermal driving potentials. The presence of these paths will result in a fast moisture transfer mechanism linking the indoor space with the core of the wall system. In this case, any short term fluctuations in the indoor air humidity can be quickly reflected on the cavity space moisture conditions. However, this will depend on the pattern and the rate of air flow across the connecting paths which are determined by the boundary conditions (e.g., wind speed and direction), as well as the air leakage characteristics of the exterior walls.

Although the importance of indoor humidity in determining moisture performance of exterior walls has been emphasized in related literature, the impact of its transient behaviour has not been considered either in the theoretical or the experimental investigations. In this chapter, the effect of indoor air humidity behaviour, within a single space enclosure, on the moisture performance of its bounding exterior walls is theoretically investigated. Two different wall systems with different modes of moisture interaction with the indoor space have been considered. The first system is a non-cavity multi-layer wall, and the second wall is a cavity wall consisting of a multi-layer interior wythe and a single layer exterior wythe.

Moisture performance of exterior walls is an important issue in almost all types of climates. However, in cold climates, it is of a particular importance because of the complexity of the

wall system and the higher interstitial condensation potential involved. In studying the effect of indoor air humidity behaviour on wall moisture performance, it is more appropriate to use the environmental conditions corresponding to a typical cold climate as the outdoor boundary conditions for the simulation of the problem. In addition, the simulation period must be long enough so as to be able to assess the long term impact of indoor air humidity behaviour over an extended period of time. In this study, a simulation period of one year is used through which the hourly thermal and moisture responses of the wall system are evaluated. The employed hourly weather data are representative of Montreal's weather conditions over a full year. The relative influence of indoor air humidity behaviour on exterior wall moisture performance is demonstrated by mainly comparing the variations of the average moisture content of the wall components over the simulation period at different patterns of indoor humidity variations. Some physical and functional characteristics of the space can have significant impact on the indoor air humidity pattern of variation which will ultimately be reflected on the moisture performance of the exterior walls. This indirect relationship between the space characteristics and the moisture performance of exterior walls will be discussed towards the end of this chapter.

7.2 Evaluation Approach

Indoor air humidity behaviour and exterior wall moisture behaviour are interdependent processes since considerable amounts of moisture can be absorbed or desorbed at the walls interior surfaces. Furthermore, moisture from the indoor air can be transferred to the wall system by the diffusion and the convective transport mechanisms. For assessing the moisture interaction between the exterior wall and the indoor environment, an indoor air humidity prediction model needs to be used in conjunction with a wall moisture behaviour evaluation model. Fig. 7.1 illustrates the integrated modelling approach which includes

both moisture transport models.

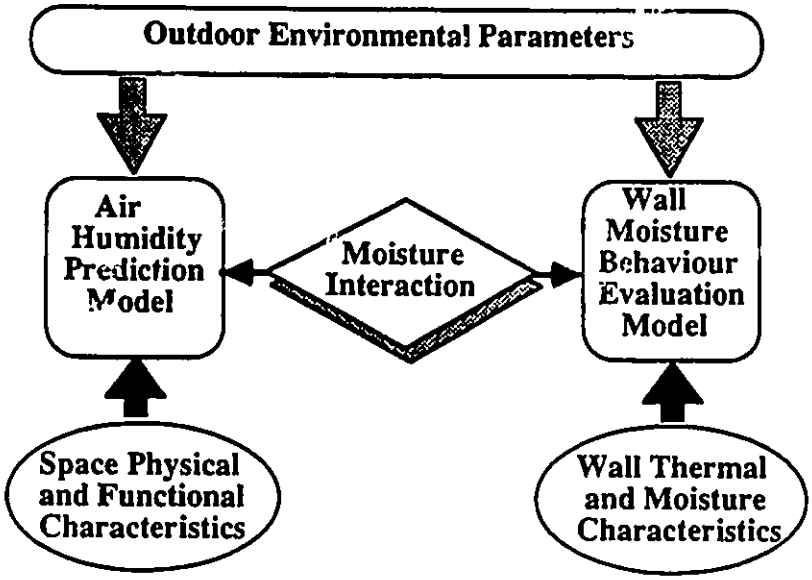

Fig. 7.1 An integrated modelling approach of the transient moisture transport problem in buildings.

In order to be able to compare between the wall moisture behaviours at different indoor air humidity variational patterns, all environmental parameters used in the modelling are kept the same with the exception of indoor air humidity. The different indoor air humidity variational patterns are obtained by mainly changing the space physical characteristics since they have no direct influence on the wall moisture behaviour. Using a time step of one hour, simultaneous heat and moisture transfer through the wall system is numerically evaluated for a period of one year. Transient heat and moisture transfer calculations are based on the formulations and assumptions described in chapter 6, but with an additional assumption that the effect of solar radiation on exterior walls is negligible. The hourly outdoor air conditions used for the simulation are shown in Figs. 7.2-7.3, and the wind

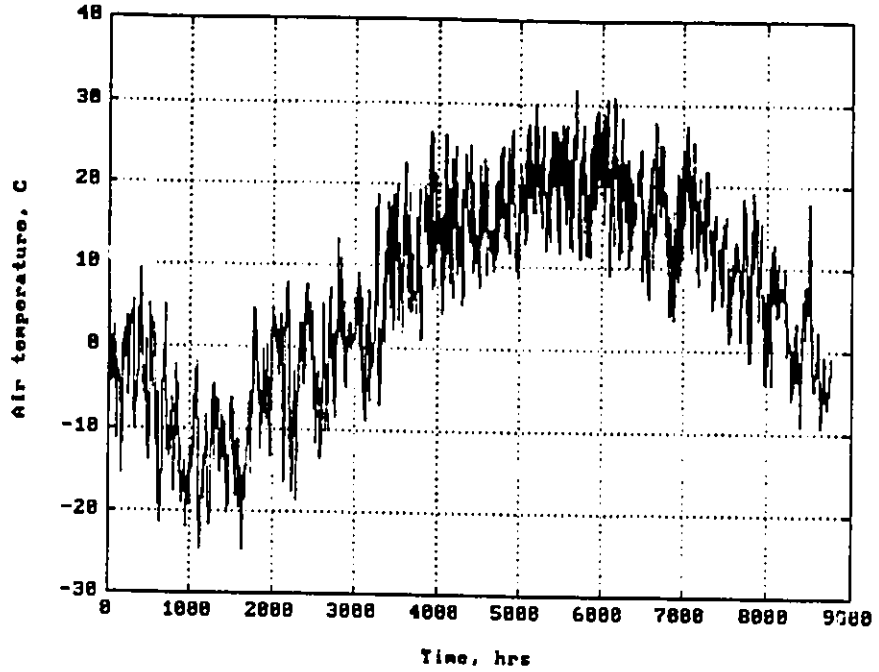

Fig. 7.2 Hourly air temperature variation over a period of one year.

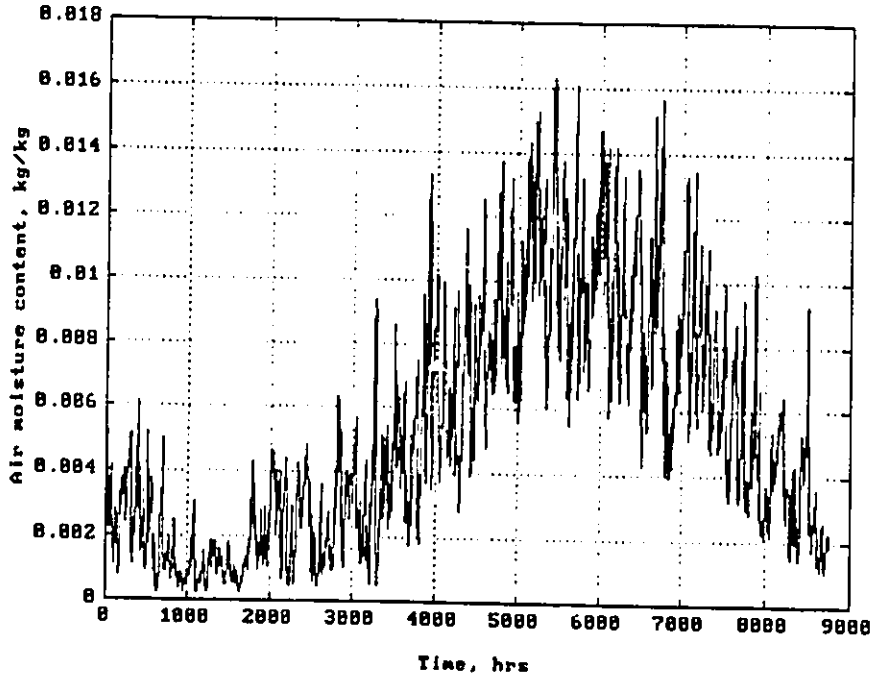

Fig. 7.3 Hourly air moisture content variation over a period of one year.

speed and direction are represented by Figs.7.4a-7.5b. These conditions, which were recorded at Dorval weather station in Montreal from December 1984 to November 1985 can be considered as representative of cold climate conditions. Based on the same outdoor conditions, the hourly air humidity variations within the space are calculated using the mathematical formulations described in Chapter 4.

Moisture interaction between the indoor air and the wall interior surface is modelled by the lumped-parameter approach where a very thin layer (equivalent to have the nodal spacing used in the numerical formulation) can be assumed at uniform moisture conditions. The response of indoor air humidity during a time step, Δt, due to moisture absorption or desorption at the interior wall surface can be expressed by:

$$\frac{dW_r}{dt} = -\frac{A_w h_{Di}}{\rho_a V}(W_r - W_m^t)\exp(-\frac{2h_{Di}}{\alpha \Delta x}t) \qquad (7.1)$$

where,

$$\alpha = \rho_a T_m R_v C_m$$

The parameter, Δx, in equation 7.1 represents the nodal spacing used in the numerical formulation for the interior layer, while the parameter, W_m^t, represents the material surface moisture conditions at the beginning of the time step. As the solution progresses, the material surface moisture conditions need to be updated at the end of each time step and submitted to the air humidity perdition model. Similarly, the time step average indoor air humidity, W_m, is calculated and used in evaluating the wall moisture behaviour.

7.3 Moisture Accumulation and Distribution within a Multi-layer Non-Cavity Wall System

Moisture behaviour of exterior walls in response to a particular pattern of variations of

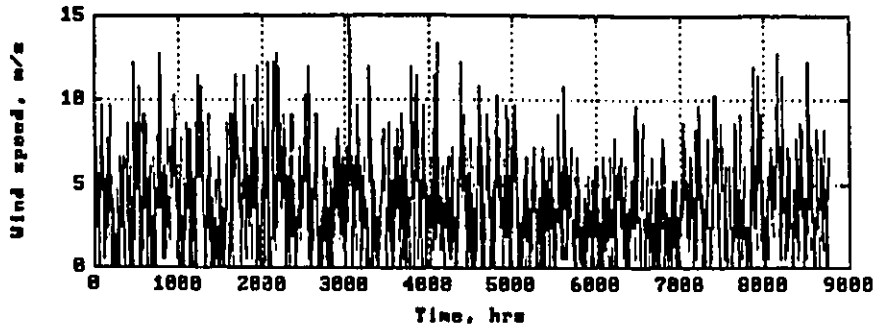

Fig. 7.4-a Hourly wind speed variation over a period of one year.

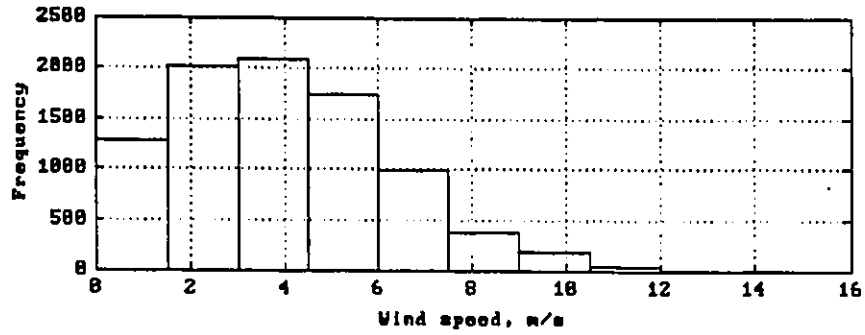

Fig. 7.4-b Frequency of wind speed occurrence.

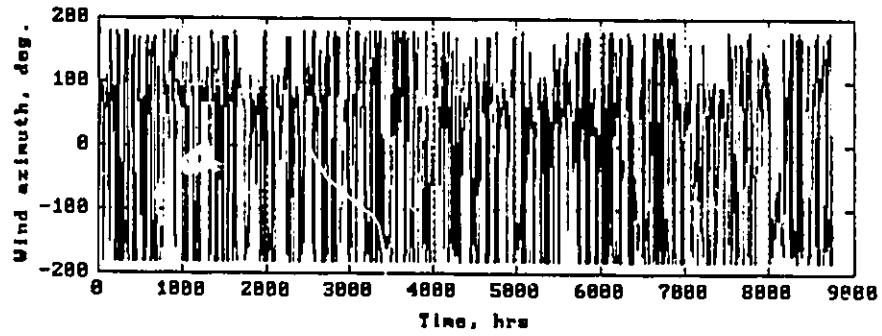

Fig. 7.5-a Hourly wind azimuth variation over a period of one year.

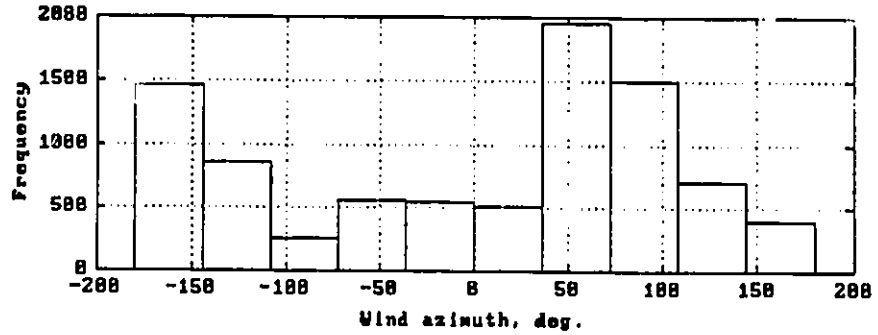

Fig. 7.5-b Frequency of wind azimuth occurrence.

Indoor humidity is greatly influenced by the modes of moisture interaction with the indoor environment. In a non-cavity wall system, moisture interaction occurs at the wall's interior surface with moisture diffusion as the only moisture transfer mechanism. Moisture accumulation and distribution in the multi-layer non-cavity wall system shown in Fig. 7.6 are evaluated at different indoor air humidity variational patterns. Although such system is unlikely to be used in cold climates to be tested under representative climatic conditions, studying its moisture behaviour will form the base for comparisons with the cavity wall system which interacts differently with the indoor environment. The modelled wall system consists basically of a 10 mm gypsum board with its interior surface painted with a latex paint system, 90 mm fibre glass insulation and 10 mm wood board with an oil -based paint system. For the purpose of investigating the impact of certain wall characteristics on its moisture performance under a given indoor humidity variational pattern, basic physical characteristics of the wall system may occasionally be changed.

Moisture and thermal properties of the wall components are the same as those given in Tables 6.1 through 6.3 in Chapter 6. This wall forms the exterior vertical boundaries of the 600 m^3 space with its geometrical configurations shown in Fig. 7.7, and the basic physical characteristics are given in Table 7.1. The modelled space is maintained at constant temperature of 21° C through out the simulation period and continuous summer dehumidification is carried out for a period of three months. The dehumidification process is performed by cooling the indoor humid air to below its saturation temperature. A schematic of the dehumidification system is shown in Fig. 7.8. In this system, the condensed water is assumed to have no effect on the moisture conditions of the inlet air. In reality, this can be achieved either by continuous drainage of the collected water or by physically separating the inlet air stream from the free water surface. The daily indoor

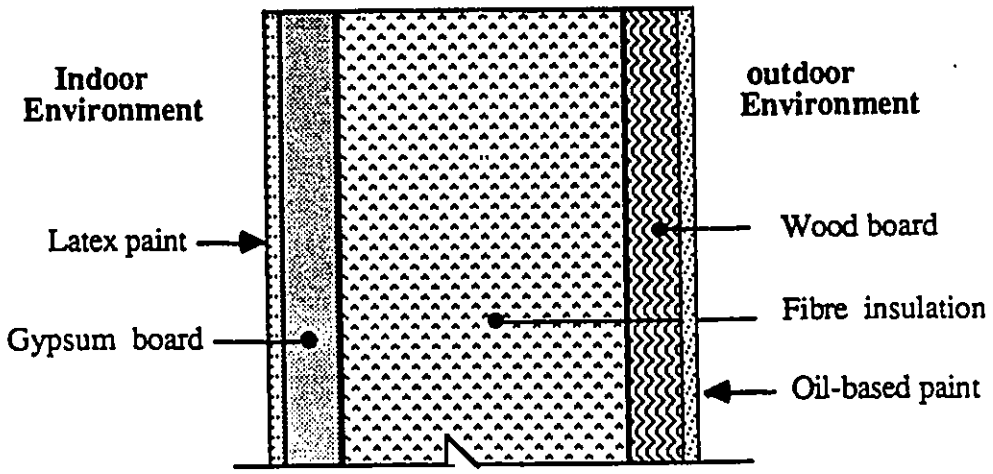

Fig. 7.6 Modelled multi-layer non-cavity wall system for assessing exterior wall moisture performance.

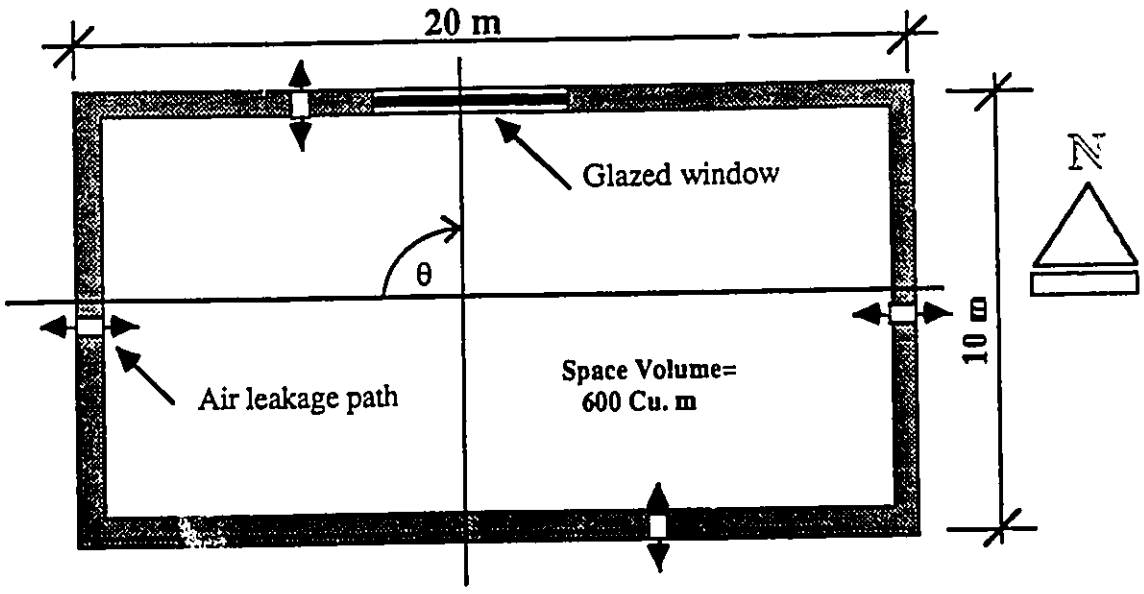

Fig. 7.7 Geometrical configuration of the modelled building enclosure.

moisture generation profile given in Fig. 4.9 is used through out the simulation period.

Table 7.1 Modelled space basic physical characteristics.

Air Leakage Coefficient $m^3/m^2 \cdot Pa^{45} \cdot s\ 10^{-4}$				Orient-ation, θ	Moisture Abs./Des.		Surface condensation		IMG kg/s
W. Wall	N. Wall	E. Wall	S. Wall		Material Type	Area (m^2)	Window Type	Area (m^2)	
1.0	1.0	1.0	1.0	90	Exterior Wall	168	Double	12	P

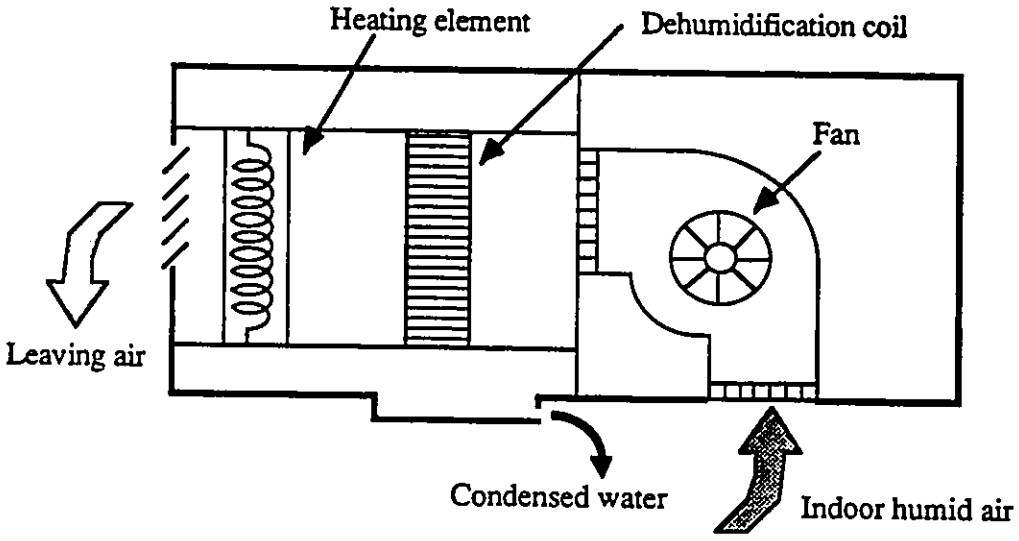

Fig. 7.8 A schematic of the dehumidification system.

Moisture performance of the modelled multi-layer wall system is evaluated by determining the moisture accumulation and distribution within the insulation and the wood layers. These layers, because of their thermal and moisture characteristics, will determine the

moisture performance of the whole wall system. The gypsum board, on the other hand, is not as important as the other two layers in determining the wall thermal and moisture performance. In addition, its moisture content is not expected to reach high levels under normal conditions. Variations of the average moisture content in the insulation and wood layers at different indoor air humidity behaviours are shown in Figs. 7.9-7.10. At constant air humidity levels, both layers show the same pattern of variations of material moisture content which is a reflection of the variations of the outdoor air conditions shown in Figs. 7.2-7.3. The insulation layer, however, is less responsive to changes in outdoor air conditions. While the wood layer started to lose moisture at the end of the winter months, the moisture content of the insulation layer continued to rise until the end of the fifth or sixth month when it started to decrease. Such behaviour can be attributed to the fact that at higher temperature gradient across the insulation layer, which has a relatively high vapour diffusion coefficient, the bulk of the moisture from the indoor space is transferred to the interface with the wood layer leaving the insulation layer relatively dry. During the fifth month, when the temperature gradient is relatively low, the average moisture content of the insulation layer has experienced a considerable increase at all indoor air humidity levels as can be seen from Fig. 7.9. As the outdoor temperature starts to moderate, both the insulation and the wood layers experience a sharp decrease in their moisture content indicating the prevalence of drying conditions. These conditions continue to prevail for the insulation layer during the rest of the simulation period (summer and fall months), especially at a relative humidity level of 30%. As soon as the outdoor temperature starts to fall, moisture accumulation in the wood layer is increased. From the above discussion, it can be said that at constant indoor humidity, moisture behaviour of exterior walls is mainly determined by the hygro-thermal variations in the outdoor air. At variable indoor humidity, on the other hand, variations in moisture accumulation are determined by the

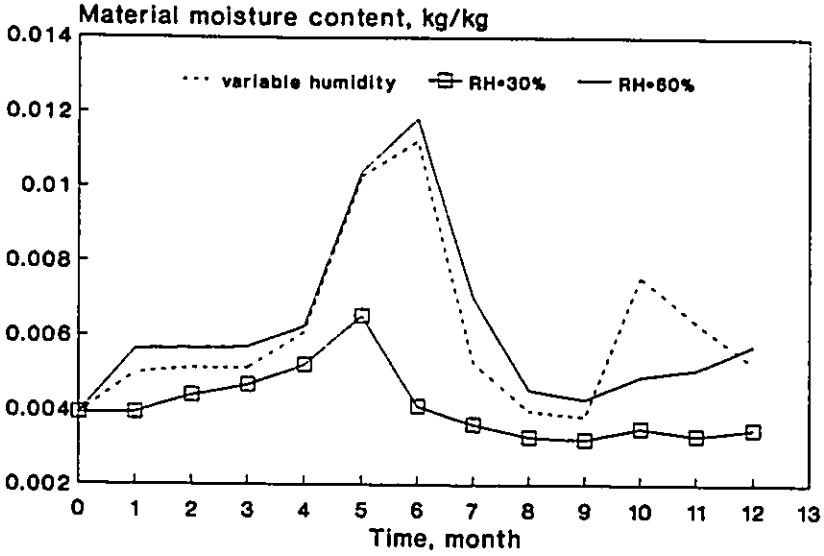

Fig. 7.9 Variations of the insulation layer average moisture content at variable and constant levels of indoor humidity.

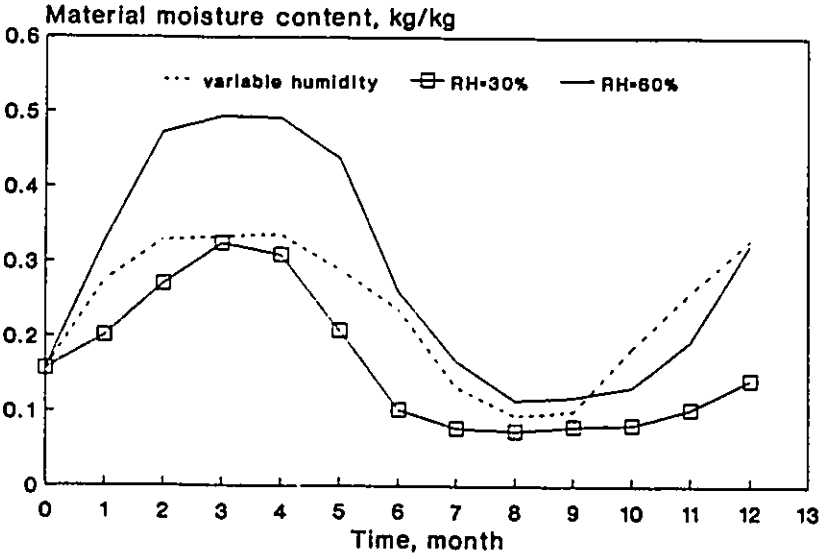

Fig. 7.10 Variations of the wood layer average moisture content at variable and constant indoor humidity levels.

outdoor air conditions as well as the indoor air humidity behaviour.

Variations in air humidity behaviour in the modelled space during the simulated period are shown in Fig. 7.11 through Fig. 7.14. This behaviour can be described as having a fluctuating trend during the first three months (winter), an increasing trend during the second three months (spring), and a decreasing trend during the last three months (fall). During summer, indoor air humidity fluctuates within a narrow range due to the implementation of the dehumidification process. By relating the variations in indoor air humidity to the pattern of moisture accumulation in Figs. 7.9-7.10, it can be recognized that moisture accumulation in the insulation layer is a strong function of indoor humidity since it continues to rise with indoor humidity until the end of the sixth month when dehumidification starts to be implemented. During the dehumidification period, when indoor relative humidity is maintained at nearly 50% as shown in Fig. 7.13, moisture accumulation has been reduced to its lowest level. In the early fall months, the higher indoor humidity shown in Fig. 7.14 has resulted in higher moisture accumulation in the insulation layer which quickly responded to the lower indoor humidity level towards the end of the fall months. The wood layer response is less dependent on the variation of indoor humidity, however, the corresponding rate of wetting and drying is clearly dependent on the level of indoor humidity. Generally, it can be said that the pattern of variations of the average moisture content of the different layers is dependent on indoor air humidity behaviour. The level of dependence is determined by the thermal and moisture characteristics of the material, as well as its location within the wall system.

The amount of moisture accumulated within the wall components is directly related to the level of indoor humidity. At 30% relative humidity, the average moisture accumulation in

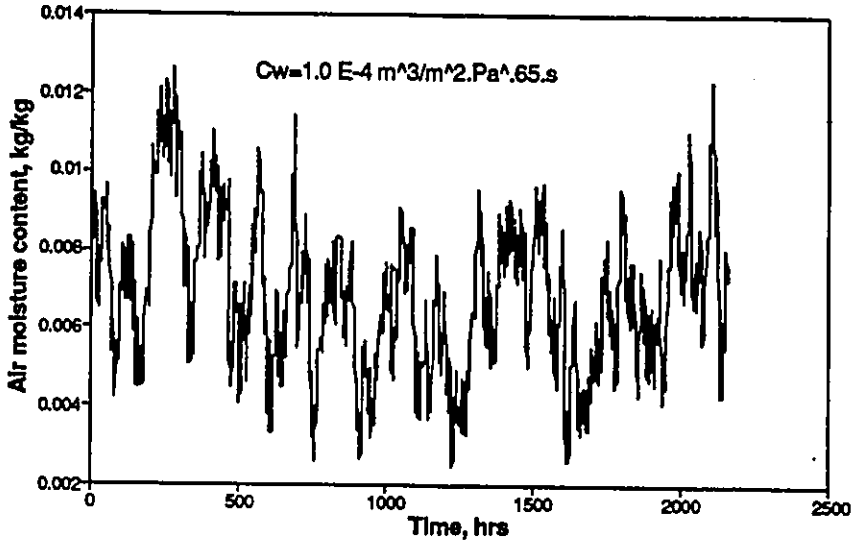

Fig. 7.11 Indoor air humidity variational behaviour during the winter months (Dec.-Feb.).

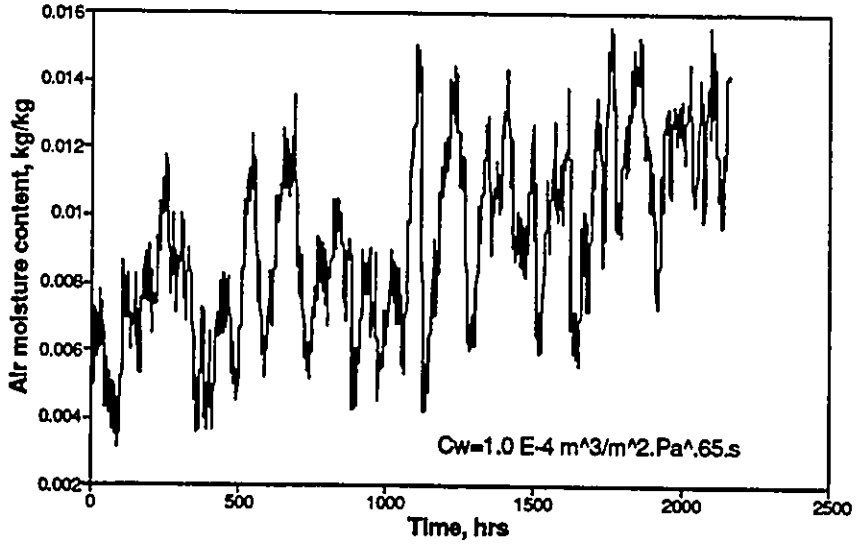

Fig. 7.12 Indoor air humidity variational behaviour during the spring months (Mar.-May).

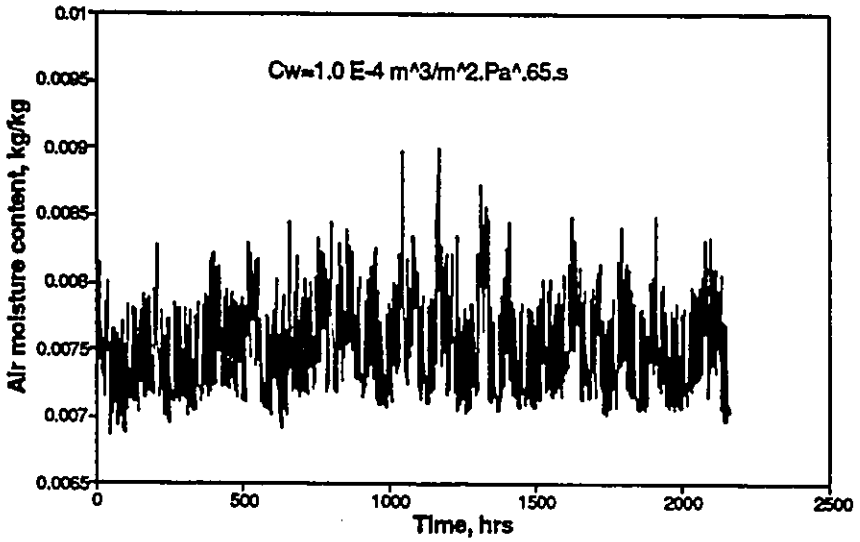

Fig. 7.13 Indoor air humidity variational behaviour during the summer months (Jun.-Aug.) when dehumidification is used.

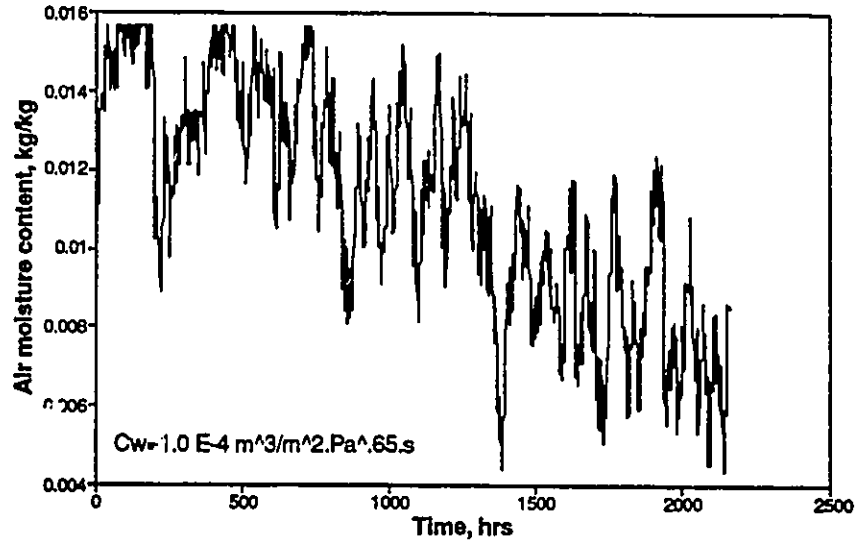

Fig. 7.14 Indoor air humidity variational behaviour during the fall months (Sep.-Nov.).

the wood layer is about 10% by weight at the end of the simulation period. By increasing the indoor relative humidity to 60%, the moisture accumulation has risen to about 30%. Moisture accumulation in the wood layer during winter has increased by more than 40% when the indoor relative humidity is increased from 30% to 60%. A more proportional increase is experienced by the insulation layer where as much as 80% more moisture has accumulated by the end of the spring months.In addition to its impact on the average moisture accumulation, indoor humidity can greatly influence the moisture distribution and the condensation potential within each layer. Figs. 7.15-7.18 show the variations in the seasonal moisture content distribution across the insulation and the wood layers at 30% and 60% indoor relative humidity levels. At 30% relative humidity, major local moisture accumulation occurs during winter, while major local moisture accumulation occurs during the winter and the fall months at a relative humidity level of 60%. In both cases, the highest moisture concentration level within the insulation layer occurs at the interface with the wood layer. Similarly, the maximum moisture concentration within the wood layer is obtained at its coldest point near the exterior surface. The presence of high moisture resistance paint at the exterior wall surface has resulted in the occurrence of condensation and hence the accumulation of substantial amounts of moisture at that particular point. For the insulation layer, higher indoor humidity has generally resulted in an increase in its moisture content through out its thickness at the end of all seasons, but more noticeably at the interface with the wood layer at the end of the spring and the fall periods when moisture accumulation is more than tripled. Increasing the indoor relative humidity by 30% has significantly altered the moisture distribution in the wood layer as can be seen by comparing Fig. 7.16 and Fig.7.18. At 60% relative humidity, the condensation region within the wood layer has been pushed inward with a significant increase in the local material moisture content. Moreover, at the higher indoor humidity level, interstitial condensation

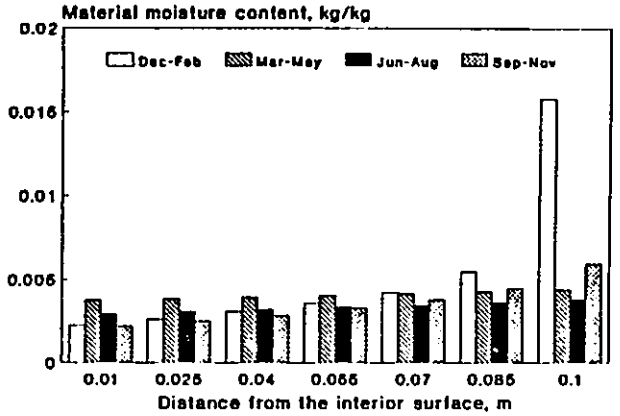

Fig. 7.15 Seasonal moisture content distribution across the insulation layer at a constant indoor humidity level of 30%.

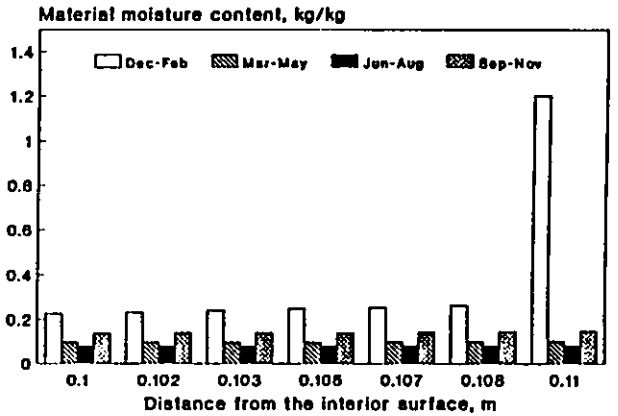

Fig. 7.16 Seasonal moisture content distribution across the wood layer when indoor humidity level is maintained at 30%.

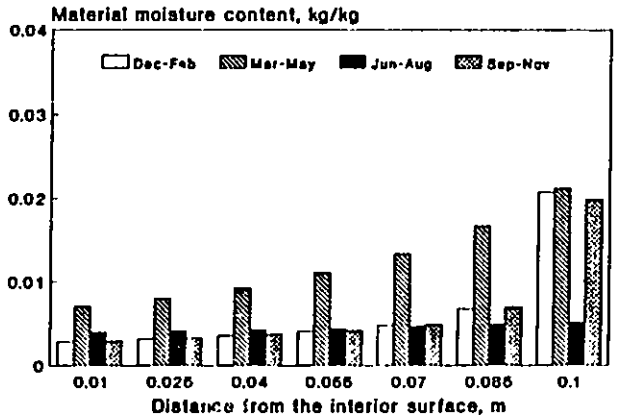

Fig. 7.17 Seasonal moisture content distribution across the insulation layer when indoor humidity level is kept at 60%.

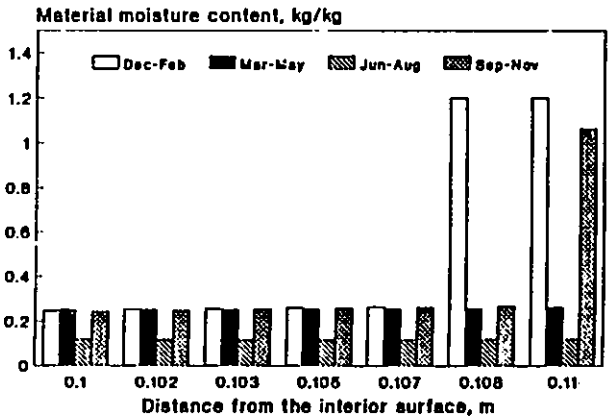

Fig. 7.18 Seasonal moisture content distribution across the wood layer when indoor humidity level is maintained at 60%.

at the wood layer exterior surface has been initiated during the fall months, while it was absent at the lower indoor humidity level. During spring, the wood layer moisture content has uniformly increased by more than 100%. A similar but less pronounced increase in material moisture content occurs during summer. From the above discussion, the impact of indoor air humidity on the moisture behaviour of the exterior wall's components can be clearly appreciated.

7.3.1 Air leakage process: A particular pattern of indoor air humidity variations over a period of time will undoubtedly result in a unique wall moisture performance. Such patterns of variations are determined by the degree of participation of the different moisture transport processes, such as the air leakage process, which contribute to the moisture balance within the indoor air domain. Figs. 7.19-7.20 show the moisture behaviour of the insulation and the wood layers at different exterior wall air leakage characteristics representing the tight, the average and the untight enclosures. It can be seen that by increasing the exterior walls air leakage coefficient, moisture accumulation in both layers is reduced due to reduced indoor air humidity level. However, increasing the air leakage coefficient by a certain magnitude does not necessarily mean a constant proportional reduction in material moisture accumulation since for the same boundary conditions, the air leakage rate can substantially vary with the exterior walls air leakage characteristics. In addition, the moisture transport process within the exterior wall components will uniquely react to any particular variation in the boundary conditions especially the indoor air humidity. For example, reducing the air leakage coefficient has resulted in more reduction in the insulation layer moisture content by the end of the sixth month relative to the reduction obtained during the previous period. Furthermore, reducing the air leakage coefficient from $2 \cdot 10^{-4}$ to $1 \cdot 10^{-4}$ $m^3/m^2 \cdot Pa^{.65} \cdot s$ has almost no effect on the

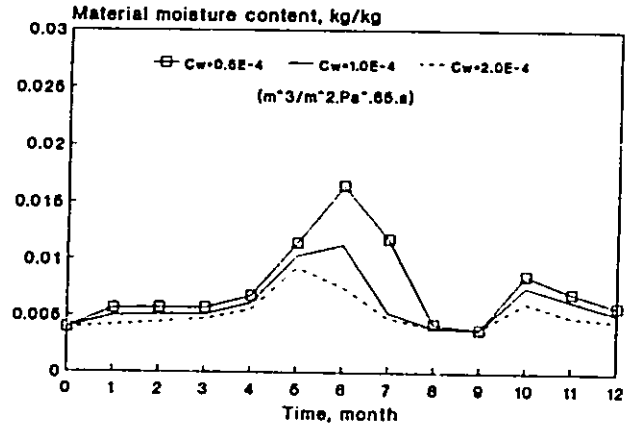

Fig. 7.19 Variations of insulation layer average moisture content at different wall air leakage characteristics.

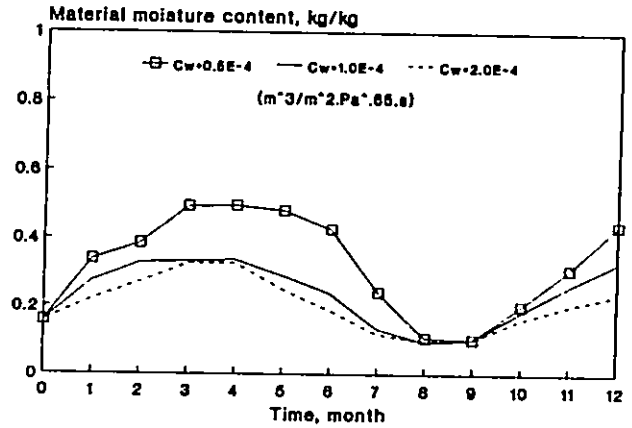

Fig. 7.20 Variations of wood layer average moisture content at different wall air leakage characteristics.

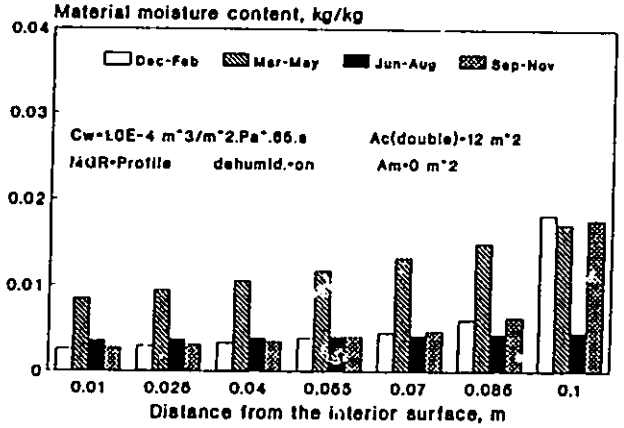

Fig. 7.21 Seasonal moisture content distribution across the insulation layer at average enclosure air tightness.

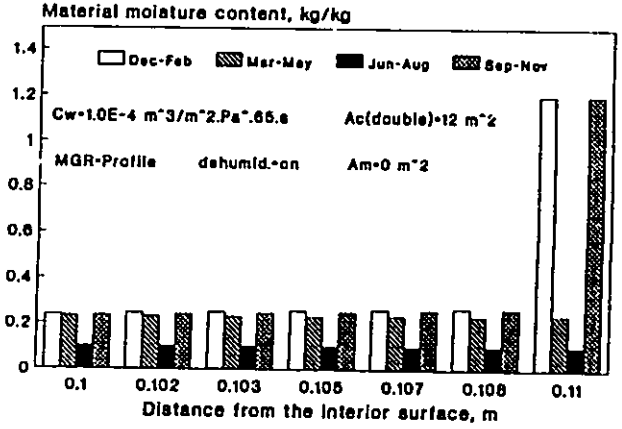

Fig. 7.22 Seasonal moisture content distribution across the wood layer at average enclosure air tightness.

moisture accumulation within the wood layer during the fourth month. This means that the resulting variations in indoor humidity are not enough to force a change in the wood average moisture content at that time. Besides the differences in the magnitude of reduction, the pattern of moisture accumulation in both materials considerably vary with the exterior wall air leakage characteristics. At an air leakage coefficient of $2 \cdot 10^{-4}$ $m^3/m^2 \cdot Pa^{.65} \cdot s$, the insulation layer starts to dry out at the end of the fifth month, but continues to accumulate more moisture in the other two cases as illustrated by Fig. 7.19. Similarly, while moisture content in the wood layer experiences no change during the third month at an air leakage coefficient of $1 \cdot 10^{-4}$ $m^3/m^2 \cdot Pa^{.65} \cdot s$, it continues to rise in both other cases. During the dehumidification period (June-August), indoor air humidity will have almost the same behaviour for all cases since the air leakage process is not likely to reduce the indoor air humidity below the resulting levels in the absence of the dehumidification process. The dehumidification process has significantly reduced the indoor relative humidity during the summer months to a level slightly fluctuating around 50% in all cases. Since this level is considerably lower than the outdoor air humidity conditions, introducing dehumidification has prompted a quick drying regime during the early summer months. At the end of the dehumidification process, the material moisture content has been reduced to the same level for all air leakage coefficients, but start to behave independently soon. Seasonal moisture distribution within the insulation and the wood layers for the different air leakage characteristics are shown in Figs. 7.21-7.26. Comparison between Figs. 7.21-7.22 and Figs. 7.23-7.24 shows that decreasing the air leakage coefficient by 50% has resulted in a major modification in the insulation layer moisture content distribution with the occurrence of condensation at the interface between the insulation and the wood layers by the end of the spring period. More pronounced modification occurred in the wood layer as can be seen by comparing Fig. 7.22 to Fig.

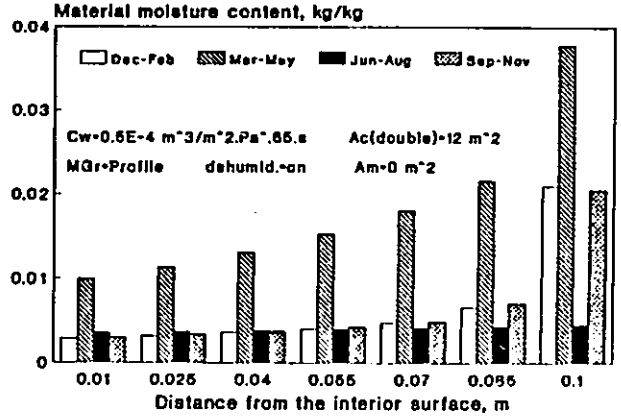

Fig. 7.23 Seasonal variations of moisture content across the insulation layer for an air tight building enclosure.

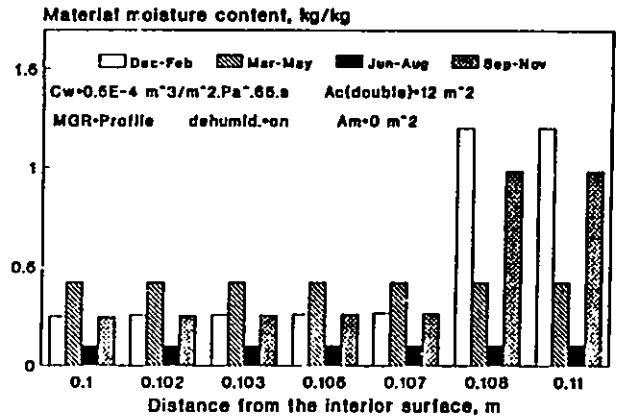

Fig. 7.24 Seasonal variations of moisture content across the wood layer for a relatively air tight building enclosure.

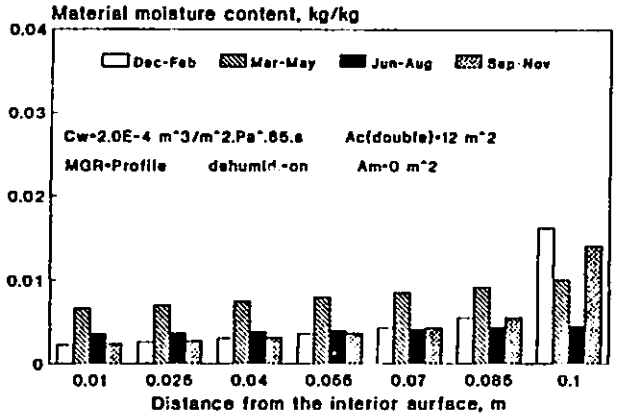

Fig. 7.25 Seasonal moisture content distribution across the insulation layer for a relatively untight building enclosure.

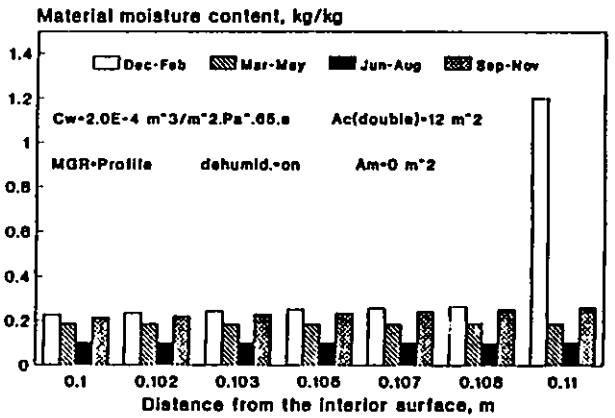

Fig. 7.26 Seasonal moisture content distribution across the wood layer for a relatively untight building enclosure.

7.24. At reduced air leakage coefficient, condensation within the wood layer had advanced further inward at the end of the winter and fall periods allowing more moisture to accumulate near the outer surface of the wood layer. Furthermore, at an air leakage coefficient of $0.5 \cdot 10^{-4}$ $m^3/m^2 \cdot Pa^{.65} \cdot s$, the whole wood layer has been subjected to interstitial condensation by the end of the spring resulting in twice as much moisture to be accumulated within the material. Increasing the air leakage coefficient to $2 \cdot 10^{-4}$ $m^3/m^2 \cdot Pa^{.65} \cdot s$ has more noticeable impact in the moisture distribution in the wood layer where condensation near the outer surface is eliminated by the end of the fall months, but it remained unchanged for the winter period. Changes in the moisture distribution within the insulation layer are generally less pronounced and is limited to the reduction in the material hygroscopic moisture as can be detected by comparing Fig. 7.21 to Fig. 7.25.

In many buildings, air flow through some exterior walls could be blocked for different reasons, such as, the presence of adjacent physical boundaries. Depending on their relative orientation to the prevailing wind direction, the absence of air flow through a certain wall can significantly affect the behaviour of the indoor air humidity and consequently the moisture behaviour of exterior walls. The effect of blocking air flow, through the north and south walls of the modelled space, on moisture accumulation in the insulation and the wood layers is shown in Figs. 7.27-7.28. It can be seen that blocking the air flow through the two major walls has resulted in a substantially increased moisture accumulation in both layers. By the end of the winter and the fall months, moisture accumulation in the wood layer has increased by about 50%. The corresponding seasonal moisture distributions are shown in Figs. 7.29-7.30. Comparison with Figs. 7.23-7.24 indicates that eliminating the air flow through the north and south walls of the modelled space have almost the same effect as reducing the air leakage coefficient of the exterior

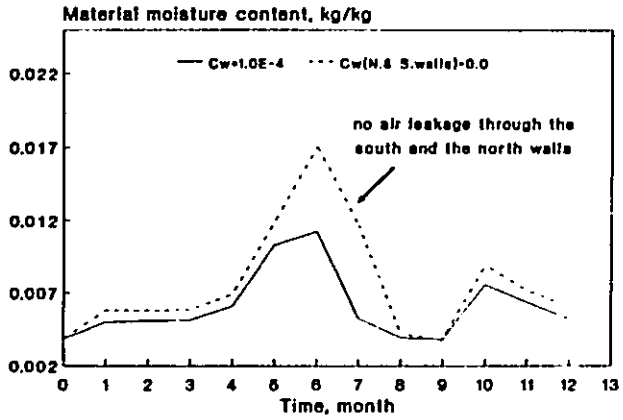

Fig. 7.27 Average moisture content of the insulation layer in the absence of air leakage through some exterior walls.

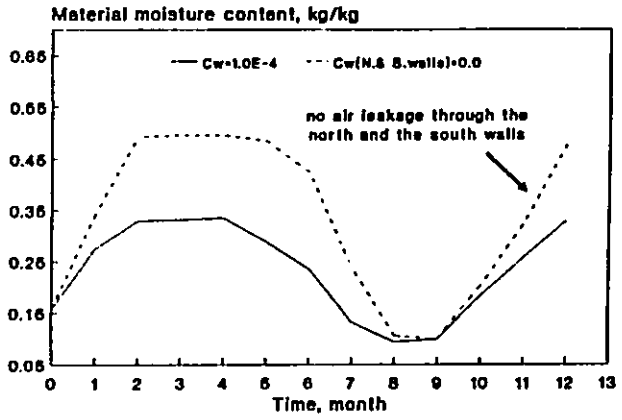

Fig. 7.28 Average moisture content of the wood layer in the absence of air leakage through the some exterior walls.

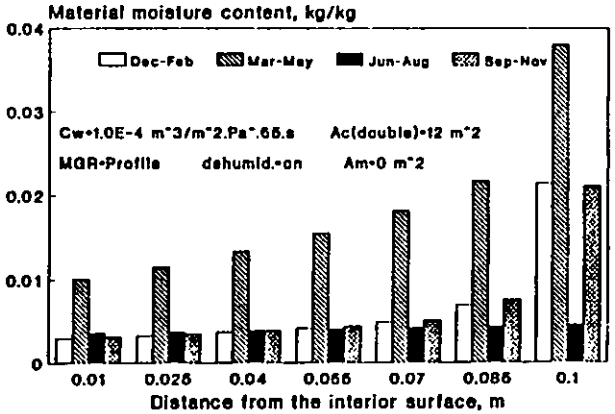

Fig. 7.29 Seasonal variations of moisture content across the insulation layer when no air flow occurs through the north and south walls.

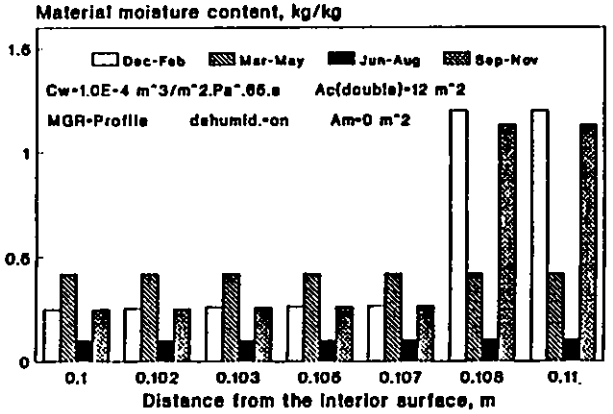

Fig. 7.30 Seasonal variations of moisture content across the wood layer when no air flow occurs through the south and north walls.

walls by 50%.

7.3.2 Moisture absorption/desorption process: The effect of moisture absorption and desorption by interior materials on the moisture accumulation in the insulation and the wood layers is shown in Fig. 7.31-7.32. It can be seen that the impact of the moisture absorption/desorption process is highly dependent on the type of interior materials used. Gypsum being of very low hygroscopicity relative to the wood material, has a relatively marginal impact on indoor air humidity and consequently on the exterior wall moisture behaviour. The influence of the moisture absorption/desorption process becomes more pronounced when indoor air humidity experiences a significant change in behaviour (i.e., a decreasing or increasing trend). A noticeable impact on the moisture accumulation within the insulation layer can be seen at the end of the sixth month during which a significant increase in indoor air humidity occurs as can be observed from Fig. 7.12. A similar impact can also be noticed following the end of the dehumidification period when indoor humidity starts to substantially increase. Moisture accumulation within the wood layer follows almost the same kind of behaviour. In spite of its reactionary impact (i.e., its effect is dependent on major variations in indoor air humidity behaviour), the moisture absorption/desorption process did not have any noticeable impact on the final moisture accumulation in any layer. Seasonal variations of the moisture content distribution across the insulation and the wood layers in the presence of moisture absorption/desorption are shown in Figs. 7.33-7.34. Comparison with Figs. 7.21-7.22 indicates that beside some minor modification in the insulation layer moisture content at the end of the spring months, the overall moisture content distribution remained almost unchanged. Because of the moisture inter-dependence that exist between the indoor air and the surrounding materials, the impact of the absorption/desorption process on indoor air humidity is limited to dampening its

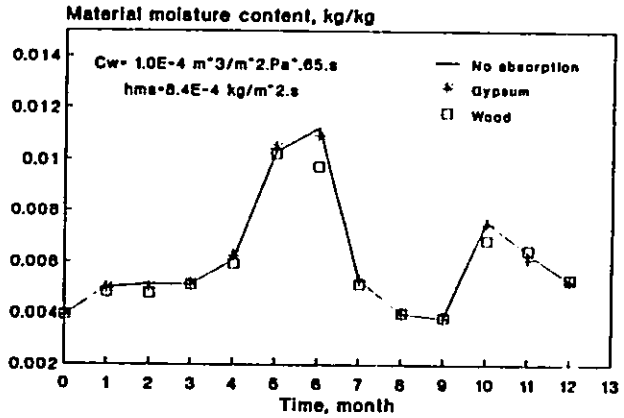

Fig. 7.31 effect of moisture absorption/desorption process on the variations of the insulation average moisture content.

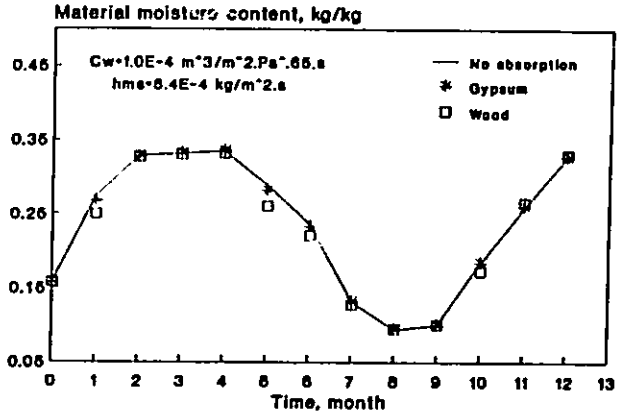

Fig. 7. 32 Effect of moisture absorption/desorption process on the variations of the wood layer average moisture content.

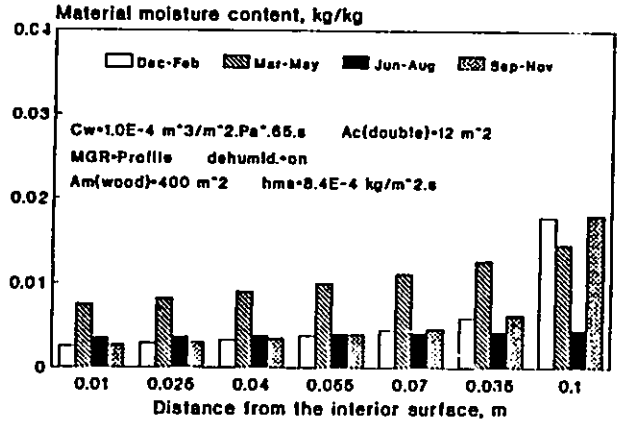

Fig. 7.33 Seasonal moisture content distribution across the insulation layer in the presence of moisture absorbing interior materials.

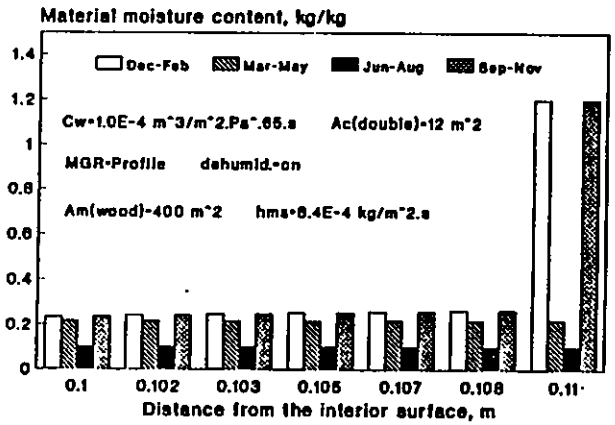

Fig. 7.34 Seasonal moisture content distribution across the wood layer in the presence of moisture absorbing interior materials.

level of fluctuations rather than changing its variational pattern. This means that the role of the moisture absorption/desorption process in determining the behaviour of indoor humidity will be more pronounced as the degree of fluctuation increases, while it will be completely pacified in the absence of fluctuations. Since higher air leakage rate is likely to result in more fluctuations, the influence of the moisture absorption/desorption process on indoor air humidity and hence on the moisture performance of exterior walls will be more appreciable at higher air leakage rates. At very low air leakage rates, on the other hand, indoor humidity experiences mild fluctuations and it will remain either at low level in the absence of indoor moisture generation or at high level when moisture is generated within the space. Figs. 7.35-7.36 show the effect of the moisture absorption/desorption process at a relatively high air leakage rates. In this case, the impact of the absorption/desorption process on moisture accumulation is more appreciable especially for the wood layer. In addition, the gypsum material, which showed almost no impact at lower air leakage rates, has a noticeable influence on the moisture behaviour of both layers. The effect of moisture absorption/desorption process on moisture content distribution at high air leakage rates when wood is used as an interior material is illustrated in Figs. 7.37-7.38. Comparison with Figs. 7.25-7.26 show that while moisture distribution in the insulation layer is subjected to limited modification by the end of the spring months, the moisture content at the wood layer exterior surface has been reduced by about 25% by the end of the winter months.

7.3.3 Surface condensation process: Condensation on internal cold surfaces, such as windows, can have a significant impact on indoor air humidity and consequently on the moisture performance of the exterior walls. However, surface condensation is not a continuous process since its occurrence is dependent on the level of indoor humidity and

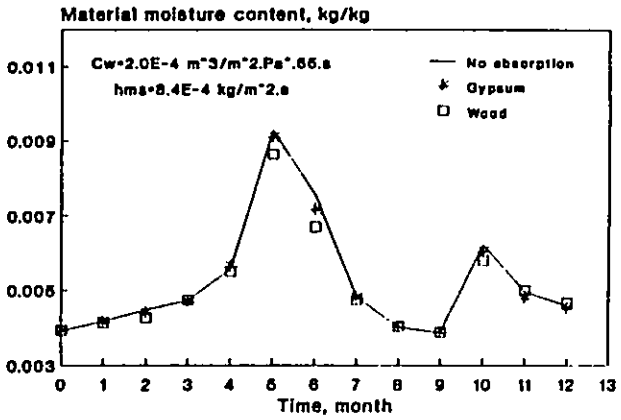

Fig. 7.35 Effect of moisture absorption/desorption process on the insulation moisture content for untight enclosure.

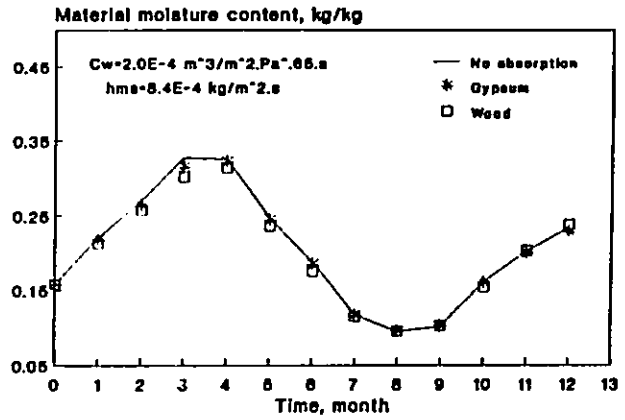

Fig. 7.36 Effect of moisture absorption/desorption process on variations of wood moisture content for untight enclosure.

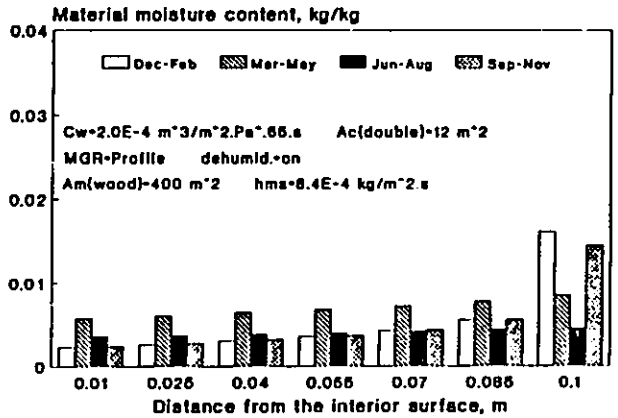

Fig. 7.37 Seasonal moisture content distribution across the insulation layer for a relatively untight building enclosure when moisture absorption/desorption is taking place.

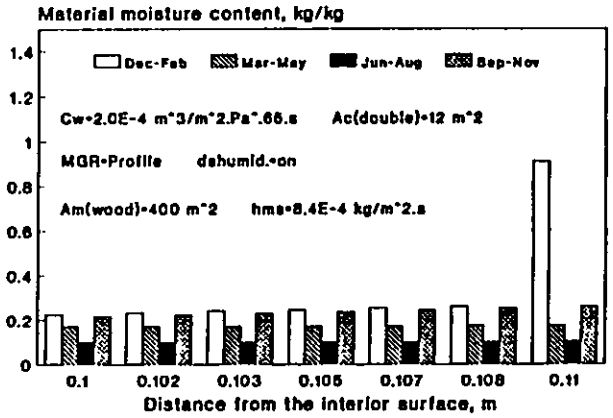

Fig. 7.38 Seasonal moisture content distribution across the wood layer for a relatively untight building enclosure when moisture absorption/desorption is taking place.

the temperature of the condensation surface which are both variable with time. The absence or the presence of surface condensation and the degree of its impact on the wall moisture behaviour can be determined by examining the relative influence of other moisture transport processes, primarily the air leakage process. Furthermore, the physical characteristics of the condensation surface can have a significant effect on the role of the condensation process in determining the moisture performance of the exterior walls. Figs. 7.39-7.40 show the effect of surface condensation on moisture accumulation within the insulation and the wood layers at average space air tightness. It can be seen that under this air tightness level, the surface condensation process is generally nonactive which indicates that the air leakage process is the determining factor of indoor humidity during the cold periods. Infiltrating dry outdoor air keeps the indoor humidity at low level and reduces the potential for surface condensation. However, the condensation process can be seen to have some impact, although limited, on the moisture accumulation within both the insulation and the wood layers during the late spring and early fall periods. The occurrence of surface condensation during these periods can be mainly attributed to the conditions of the outdoor air which is at a sufficiently low temperature and high moisture content to initiate surface condensation at interior surfaces even when the air leakage process is the determining process of indoor humidity. At reduced air leakage rates, surface condensation becomes an important factor in determining the exterior wall moisture performance. Figs. 7.41-7.42 illustrates the effect of surface condensation when the air leakage coefficient is reduced by 50%. By reducing the air leakage rate, the surface condensation precess has a more appreciable impact on the moisture accumulation within both layers particularly the wood layer. By the end of the winter months, as much as 30% less moisture is accumulated in the wood layer when the condensation surface area is increased from 12 m^2 to 60 m^2. On the other hand,

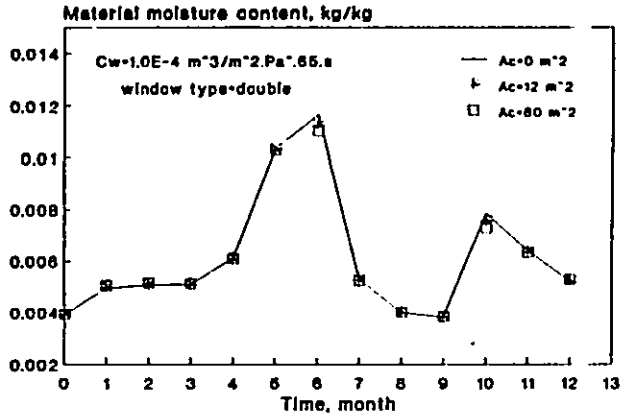

Fig. 7.39 Effect of surface condensation on the variations of the insulation layer moisture content.

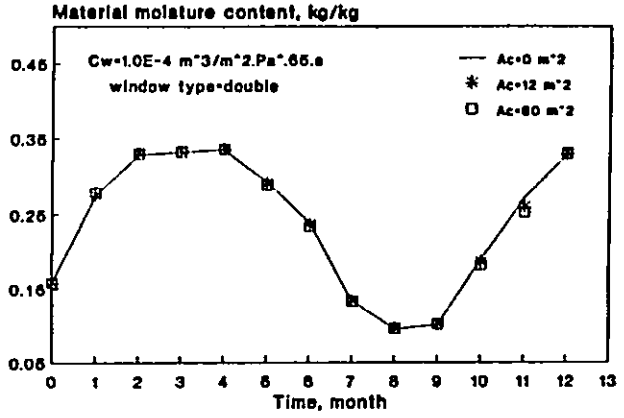

Fig. 7.40 Effect of surface condensation on the variations of the wood layer average moisture content.

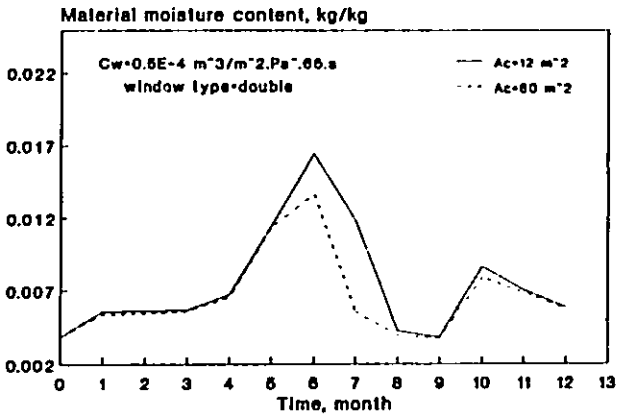

Fig. 7.41 Influence of surface condensation on insulation layer moisture content for air tight building enclosure.

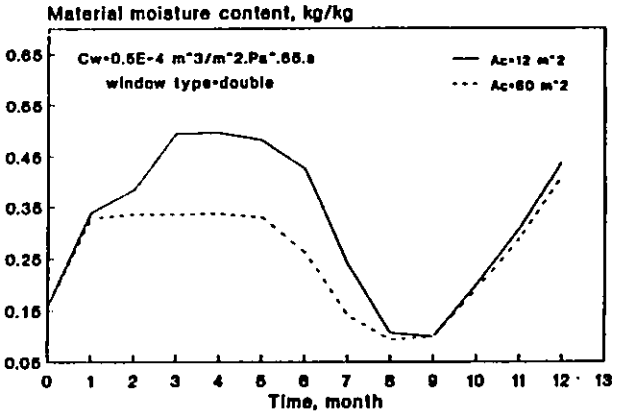

Fig. 7.42 Influence of surface condensation on wood layer average moisture content for air tight building enclosure.

Increasing the area of surface condensation by five times had no noticeable impact on the moisture accumulation in the insulation layer until the end of the sixth month when the moisture accumulation is reduced by about 17%. The reduction in moisture accumulation within the insulation layer occurs when the temperature gradient across the layer is significantly reduced by late spring. The resulting seasonal moisture content distribution when the north wall is fully glazed (i.e., A_c=60 m^2) is shown in Figs. 7.43-7.44. Comparison with Figs. 7.23-7.24 shows that increasing the condensation area by five times has eliminated condensation in the insulation and the wood layers at the end of the spring months. Furthermore, it has reduced the condensation zone in the wood layer at the end of the winter months and has limited it to its exterior surface. Besides the window's surface area, its thermal characteristics can have an appreciable impact on the condensation process and hence on the moisture performance of exterior walls. The use of a single glazed window will substantially increase the surface condensation potential since the interior surface temperature will be considerably lower than that corresponding to a double glazed window. Consequently, Moisture accumulation within the wall components which is associated with a single glazed window will always be equal (when no condensation occurs) or less than that for a double glazed window. Figs. 7.45-7.46 illustrate the reduction in moisture accumulation in the insulation and the wood layers when a single glazed window is used at average enclosure air tightness level. Although the reduction in moisture accumulation is noticeable and is sustained for most of the time, it is clear that at this air tightness level, reduction in indoor humidity level due to surface condensation over a single glazed window is not substantial enough to introduce a major reduction in moisture accumulation within the non-cavity wall components.

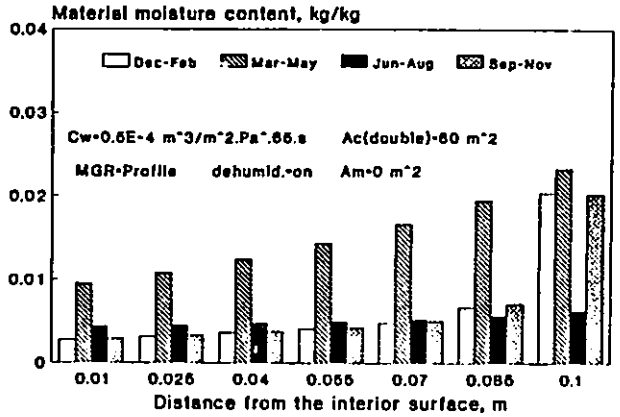

Fig. 7.43 Seasonal moisture content distribution across the insulation layer for a relatively tight building enclosure when the north wall is fully glazed.

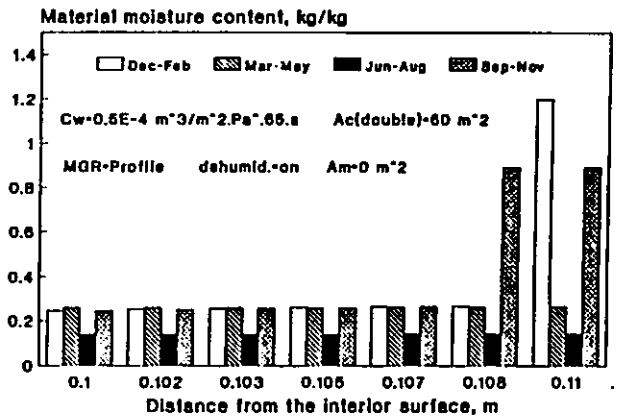

Fig. 7.44 Seasonal moisture content distribution across the wood layer for a relatively tight building enclosure when the north wall is fully glazed.

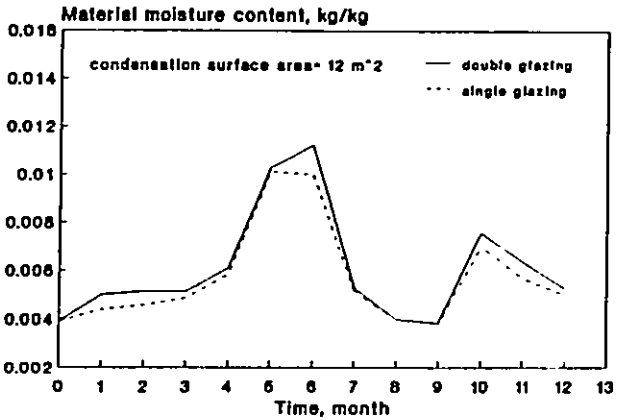

Fig. 7.45 Variations of insulation layer moisture content at different thermal characteristics of condensation surface.

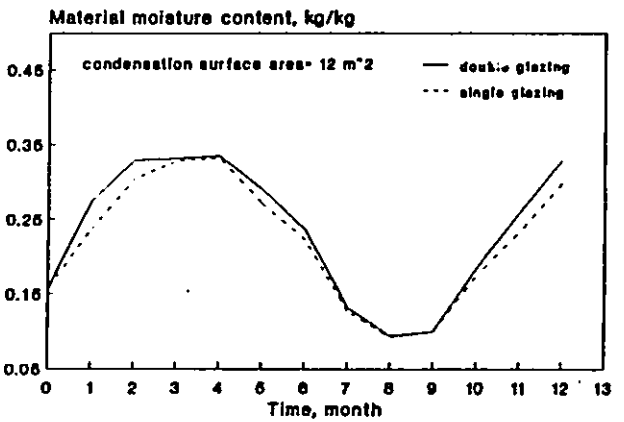

Fig. 7.46 Variations of wood layer average moisture content at different thermal characteristics of condensation surface.

7.3.4 Indoor moisture generation and summer dehumidification: Moisture accumulation with the exterior wall components is greatly influenced by the indoor moisture generation process. Fig. 7.47-7.48 illustrates the variations of moisture accumulation in the insulation and the wood layers at different moisture generation patterns. In the absence of indoor moisture generation, the average moisture contents in both layers remain relatively unchanged during the whole simulation period. By introducing moisture into the space, material moisture content in both layers experiences a considerable increase determined by the rate of moisture generation. However, increasing the moisture generation rate by a certain amount does not necessarily mean a proportional constant increase in material moisture content. The response of the wall system moisture conditions to a particular increase in indoor moisture generation is dependent on the impact of this increase on indoor air humidity and how the wall system responds to the increased air humidity. This is generally determined by the degree of involvement of the moisture transport processes within the space as well as the moisture transfer potentials across the wall system. By doubling the moisture generation rate relative to the daily average value, the material moisture content experiences more than a proportional increase in some instances (e.g., the end of the sixth month in the wood layer) but some what less increase in others (e.g. the end of the fourth month in the insulation layer). This means that any particular level of indoor moisture generation will result in a unique wall moisture behaviour. The pattern of variations of indoor moisture generation, however, may not be a factor in determining the moisture behaviour of exterior walls. Examinations of Figs. 7.47-7.48 indicates that the use of a constant moisture generation rate representing the daily average will result in exactly the same wall moisture behaviour. This can probably be explained by the relatively short period of fluctuations (i.e., one day) as compared to the wall moisture simulation period. In addition, the wall

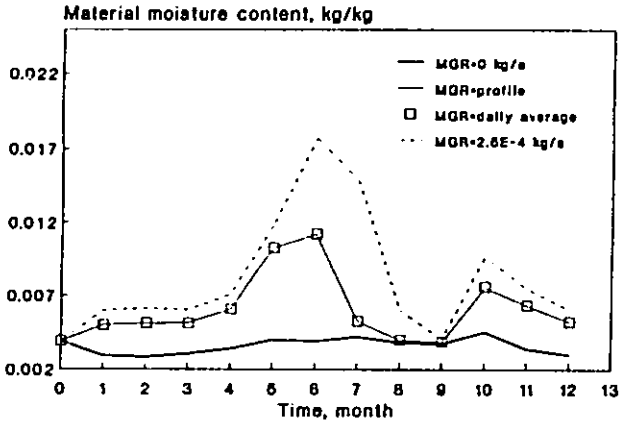

Fig. 7.47 Effect of indoor moisture generation on insulation layer average moisture content variations.

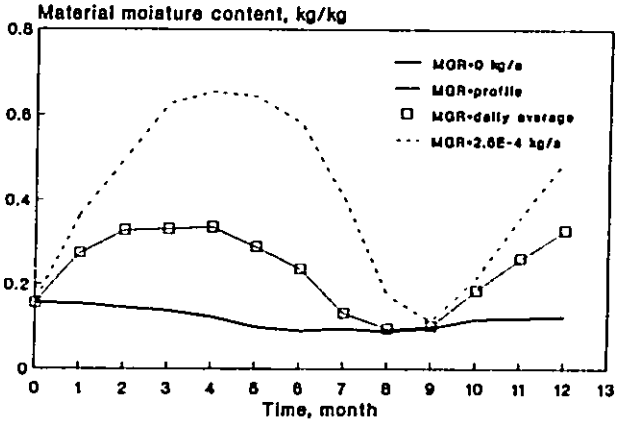

Fig. 7.48 Effect of indoor moisture generation on wood layer average moisture content variations.

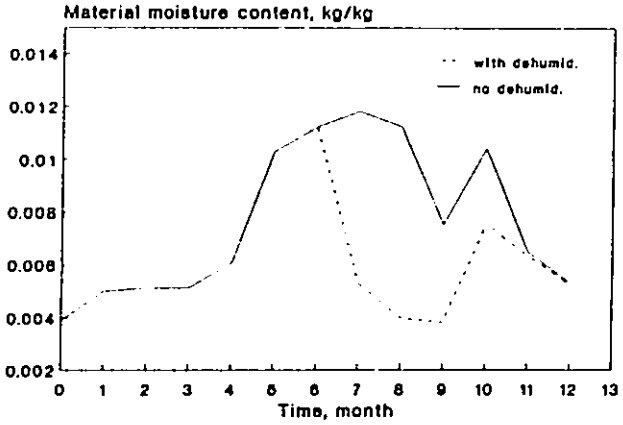

Fig. 7.49 Variations of insulation layer average moisture content with and without summer dehumidification.

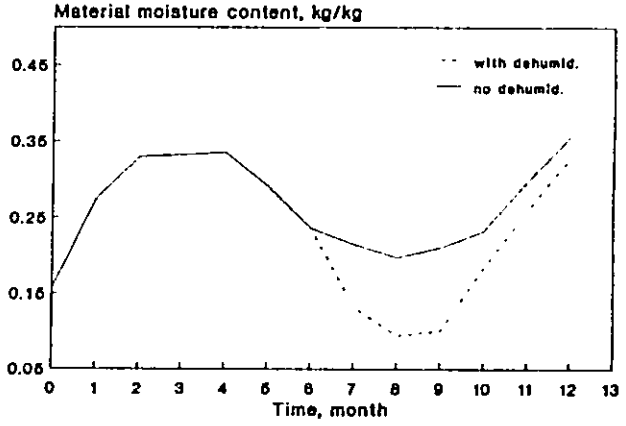

Fig. 7.50 Variations of the wood layer average moisture content with and without summer dehumidification.

system is less responsive to sudden and short term fluctuations in indoor moisture generation when moisture diffusion is the only moisture transfer mechanism, as it is the case for the non-cavity wall system. Generally, it can be said that the use of the daily average moisture generation rate is good enough when modelling the long term impact of indoor air humidity on moisture performance of non-cavity multi-layer wall systems.

Summer dehumidification process and its implementation strategy can result in a significant modification of exterior walls moisture behaviour. The drying potential of the exterior wall components is greatly determined by the level of indoor air humidity especially for humid outdoor conditions. Figs. 7.49-7.50 compare moisture behaviour of the insulation and the wood layers with and without dehumidification. In this particular case, the continuous dehumidification strategy is implemented from the month of June until the end of August. The impact on both layers during these months can be clearly recognized. For the insulation layer, its moisture content continues to rise during the seventh month when no dehumidification is implemented, while it significantly dropped during the same period with the implementation of dehumidification. The average moisture content of both layers in the absence of dehumidification remained relatively very high during the summer months. This behaviour had no effect on the moisture content level of the insulation layer at the end of fall period, but has resulted in a noticeable increase in the wood layer moisture content by the end of the same period. When a scheduled dehumidification strategy is implemented by which dehumidification is performed for a period of 10 hours every day during the summer months, both layers still experience an increase in their moisture content during this period but none by the end of the fall as can be seen in Figs. 7.51-7.52.

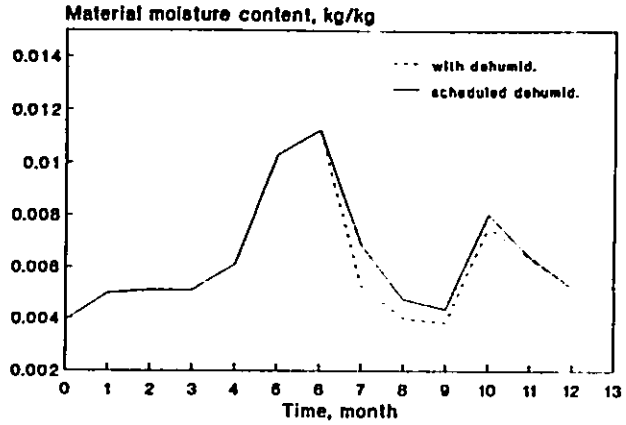

Fig. 7.51 Impact of summer dehumidification strategy on the variations of the insulation layer average moisture content.

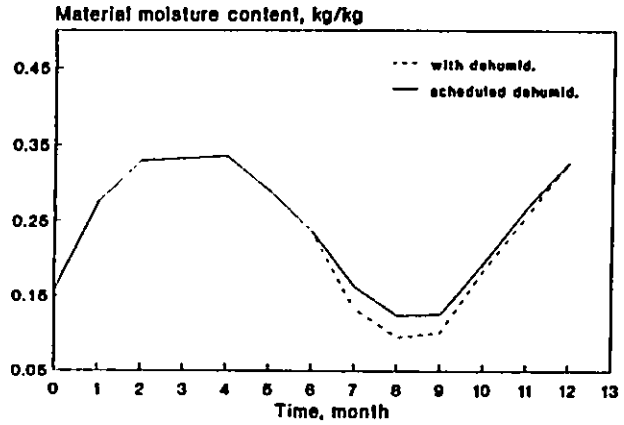

Fig. 7.52 Effect of summer dehumidification strategy on the variations of the wood layer average moisture content.

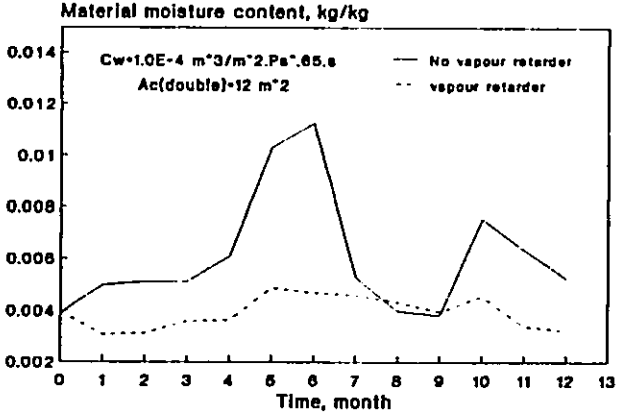

Fig. 7.53 Variations of insulation moisture content when a vapour retarder is used between wood and insulation layers.

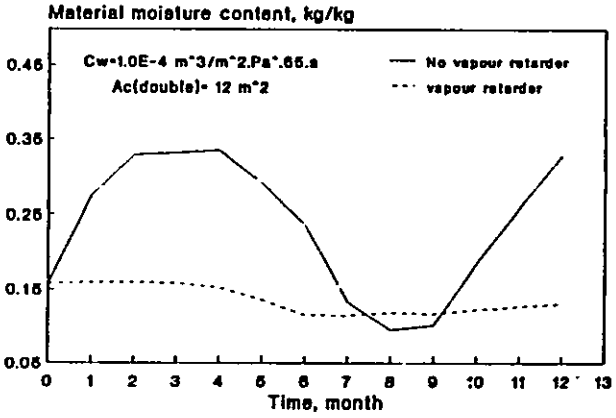

Fig. 7.54 Variations of wood layer moisture content when a vapour retarder is used between wood and insulation layers.

7.3.5 Influence of wall physical characteristics on its moisture performance under transient indoor humidity conditions: The impact of indoor air humidity behaviour on the exterior wall moisture performance can be greatly altered by changing the physical characteristics of the wall system. For example, by adding a commonly used vapour retarder having a permeance value of $9 \cdot 10^{-12}$ kg/m^2·Pa·s between the gypsum board and the insulation layer, the impact of indoor air humidity behaviour is much less noticeable for both layers especially the wood layer as illustrated in Figs. 5.53-5.54. However, the insulation layer being closer to the indoor environment shows a better association with the behaviour of indoor humidity than the wood layer. Similar kind of moisture response is obtained when the exterior surface of the wood layer is not painted as can be seen from Figs. 7.55-7.56. In this case, however, the moisture behaviour of the wood layer is more responsive to variations in outdoor air conditions. In spite of its reduced influence on the exterior wall moisture behaviour at certain conditions, indoor air humidity behaviour can still affect the pattern of moisture accumulation within exterior walls. Figs. 5.57-5.58 show the effect of indoor air humidity behaviour, obtained at different enclosure air tightness levels, on the moisture accumulation within the insulation and the wood layers when no exterior paint is used. It can be seen that except during the dehumidification period, when indoor humidity is kept mainly constant, both layers exhibit different moisture accumulation patterns at different indoor air humidity conditions. In fact, as much as 25% more moisture is accumulated in the wood layer by the end of the second month when the air leakage coefficient of the exterior walls is reduced from $2 \cdot 10^{-4}$ to $0.5 \cdot 10^{-4}$ m^3/m^2·Pa$^{.65}$·s. Furthermore, more than 40% additional moisture is accumulated within the insulation layer by the end of the second month when the air leakage characteristics of the exterior walls are similarly changed.

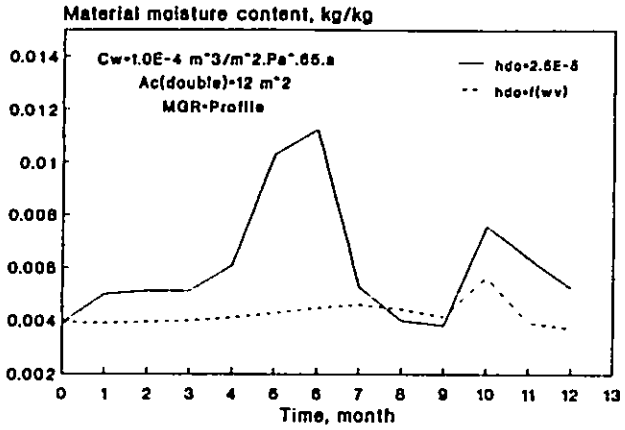

Fig. 7.55 Effect of wood layer exterior surface conditions on the variations of insulation layer moisture content.

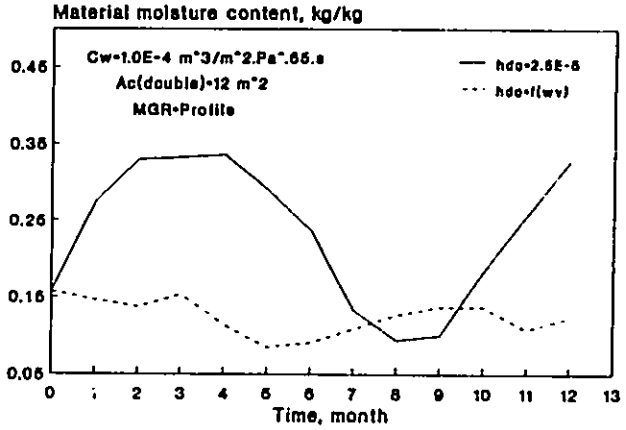

Fig. 7.56 effect of wood layer exterior surface conditions on the variations of its average moisture content.

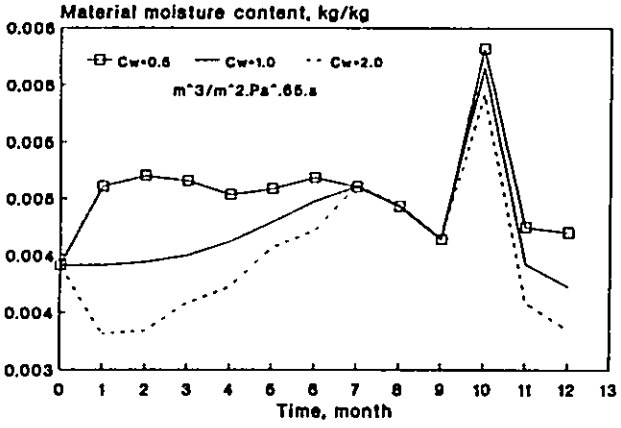

Fig. 7.57 Variations of insulation layer moisture content at different air leakage characteristics when no paint is used for the exterior surface.

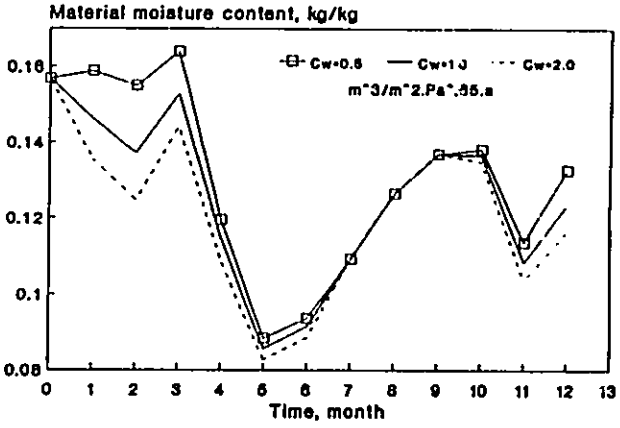

Fig. 7.58 Variations of the wood layer moisture content at different air leakage characteristics when no paint is used for the exterior wall surface.

7.4 Moisture Accumulation and Distribution within a Multi-Layer Cavity Wall System

Moisture interaction between the indoor environment and a multi-layer cavity wall system is likely to occur at two fronts. Through the surface convection process, moisture from the indoor space is transferred to the wall interior surface and then slowly transferred to the core of the wall system by the diffusion process. A faster mode of moisture interaction exists when air flow occurs between the indoor environment and the cavity space of the wall. In this case, the wall moisture behaviour will be more responsive to any changes in indoor humidity. In order to investigate the impact of indoor air humidity behaviour on wall moisture performance in the presence of convective moisture transfer, moisture accumulation and distribution in the multi-layer cavity wall system shown in Fig. 6.9 are evaluated. The modelled wall system consists of an inner and an outer wythes separated by a 50 mm air gap. The inner wythe consists of a 10 mm gypsum board painted at the interior with latex paint, a 90 mm fibre glass insulation and a 10 mm wood board. The outer wythe consists only of a 100 mm brick layer. Thermal and moisture characteristics of the wall various components are given in Table 6.1-6.3 in Chapter 6. The modelled wall forms the exterior vertical boundaries of a 600 m^3 space similar to that shown in Fig. 7.7. The space is maintained at a constant temperature of 21° C and the same dehumidification strategy and indoor moisture generation profile are used. The basic physical characteristics of the space are the same as those given in Table 7.1 except that the air leakage characteristics of the exterior wall are described by three coefficients representing air flow through the inner wythe, the outer wythe and the direct air flow path connecting the indoor and outdoor environments. The basic air leakage coefficients of the exterior wall which represent average air tightness, are given in Table 7.2. The degree of moisture interaction between the indoor environment and the wall system is dependent

on the air leakage characteristics of the inner wythe as well as the direction of air flow which is determined by the spacial pressure distribution.

Table 7.2 Air leakage coefficients of the modelled cavity wall system.

Air Leakage Coefficients, $(m^3/m^2 \cdot Pa^{45} \cdot s) \cdot 10^{-4}$		
Inner Wythe	**Outer Wythe**	**Direct air flow Path**
0.2	1.0	0.8

At a certain wind direction, a positive air pressure may be created between the indoor space and the cavity space of a particular wall while a negative pressure is created for another. In reality, wind speed and direction are continuously changing resulting in variable degrees of moisture interaction between the indoor environment and the exterior walls. Variations in moisture interaction are determined by evaluating the hourly spacial pressure fluctuations within the indoor and the cavity spaces using the multi-cell air flow modelling approach described in section 6.3 of Chapter 6.

Moisture performance of the modelled wall is assessed by determining the variations in moisture accumulation and distribution within the insulation, the wood and the brick layer. The influence of indoor air humidity is generally more pronounced near its interior surface while the greater part of the brick layer remains relatively unaffected. In order to clearly appreciate the moisture response of the brick layer to variable indoor air humidity, a thin sub-layer of 10 mm at the brick interior surface is taken as a representative of the outer wythe moisture conditions. Such representation is fairly accurate under the assumption that only diffusive moisture transfer occurs through the brick layer. However, the presence

of continuous cracks in the outer wythe will result in a faster moisture transfer mode that could carry moisture from the cavity space to the core of the brick layer. In this case, the effect of indoor air humidity behaviour will probably not be limited to a thin layer near the brick interior surface. However, the impact of moisture transfer through these paths on moisture accumulation within the brick layer is extremely difficult to model since the physical characteristics of these paths are difficult to mathematically describe. Depending on the path characteristics, its presence can have an appreciable impact on moisture distribution within the material, however, this impact is likely to be local and will not reflect the behaviour of the system as a whole. Therefore, evaluating the moisture conditions of the thin layer at the brick interior surface can be seen as a practical and a reasonably accurate approach for representing the brick layer overall moisture performance.

Moisture performance of the exterior cavity wall system is greatly dependent on its moisture interaction with the indoor environment. The degree of interaction between the indoor environment and a particular wall is determined by its position relative to the prevailing wind direction. Therefore, different exterior walls (i.e., east, west, etc.) are expected to respond differently under the same indoor air humidity pattern of variations. In this study, moisture response of the west and the east walls and occasionally the south wall of the modelled space are investigated under different indoor air humidity conditions. Comparisons between moisture behaviour of the east and west wall at constant indoor humidity are shown in Fig. 7.59. It can be seen that the east wall accumulates more moisture within all its layers during the first five months, but it is faster to loose moisture during the summer months. Such behaviour is due to the difference in degree and form of moisture interaction between the wall and its surroundings. This difference in behaviour is more pronounced in the brick layer since it is the most affected by the cavity moisture

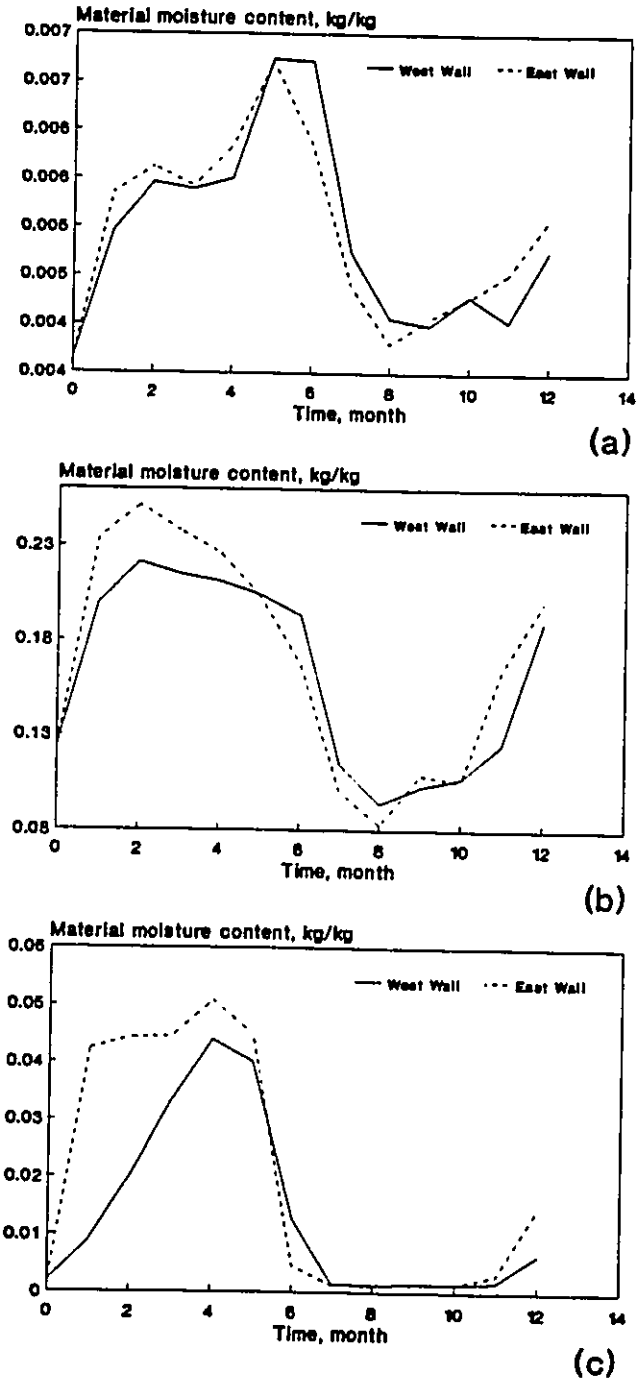

Fig. 7.59 Variations of monthly average moisture content of different exterior walls components; (a) insulation, (b) wood, (c) brick.

conditions which is highly dependent on the convective moisture transport process. By the end of the first month, moisture accumulation near the interior surface of the east wall brick layer is more than four time larger than that of the west wall. Similar behaviour can be seen during the sixth month when the brick layer of the east wall experiences a larger drying rate. In both cases, the difference in behaviour can be attributed to the fact that more air flow occurs from the indoor space to the cavity space, but for two different reasons. In winter, air flow to the cavity of the east wall will increase its air moisture content which in turn will result in more moisture deposition on the brick layer interior surface. On the other hand, air flow from the indoor space during late spring will increase the air temperature of the cavity space resulting in more drying potential for the interior brick surface which has been accumulating moisture during winter. Convective moisture transfer seems to have a relatively littie or no impact on wall moisture behaviour during the period when there is no significant difference between the indoor and outdoor conditions. This is evident during the summer and the early fall periods in all wall layers especially the brick layer which behaves almost the same in both the east and the west walls.

Indoor air humidity behaviour has been shown to have a considerable influence on the moisture performance of the multi-layer non-cavity wall system. For the cavity wall system, however, this influence will be more appreciable due to the presence of convective moisture transfer. Fig. 7.60 compares the moisture behaviour of the west wall at constant and variable indoor air humidity conditions. The difference in behaviour can be clearly noticed for all layer but in particular for the brick layer where the moisture accumulation at the end of the fourth month at constant humidity level is 50% more than that corresponding to variable humidity. When such level of variation is compared with that

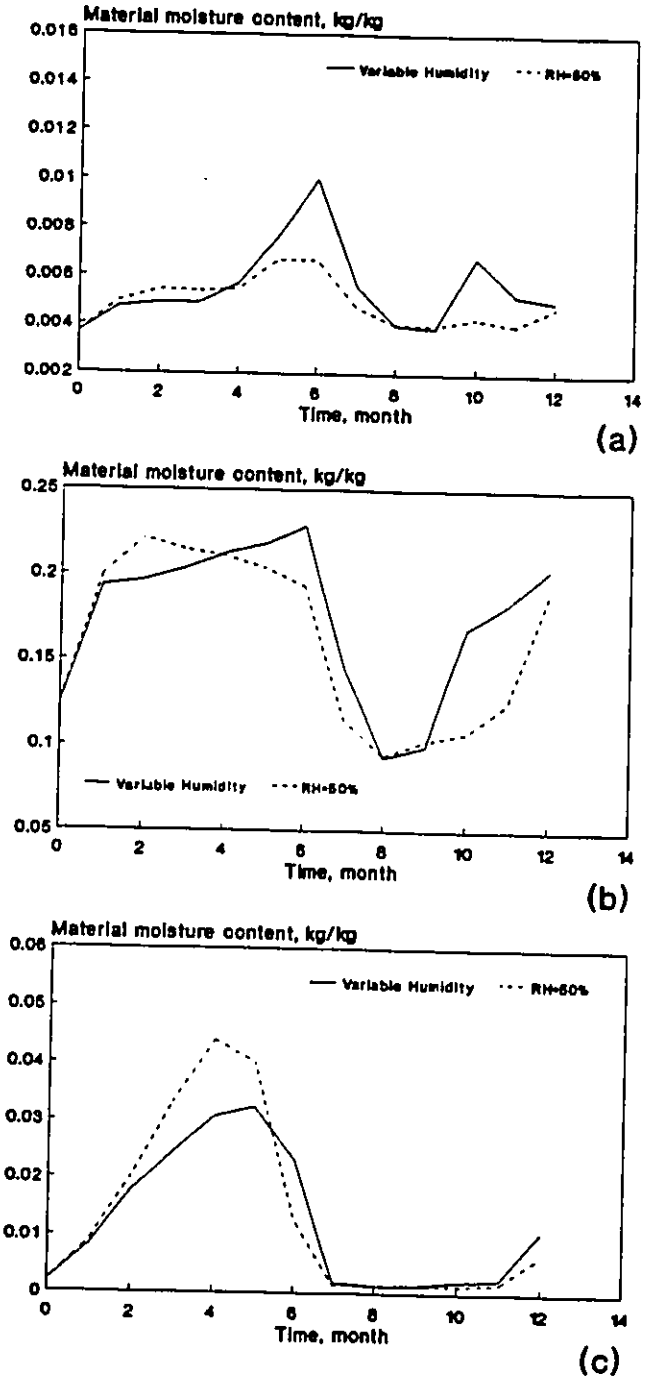

Fig. 7.60 Effect of indoor humidity behaviour on variations of average moisture content of the west wall componenets; (a) insulation, (b) wood, (c) brick.

corresponding to the non-cavity wall system shown in Figs. 7.9-7.10, the increasing influence of indocr air humidity behaviour in determining the exterior wall moisture performance can be appreciated.

7.4.1 Air leakage process: Variations of moisture accumulation within the insulation, the wood and the brick layers of the west wall at different air leakage characteristics are shown in Fig. 7.61. It can be seen that moisture accumulation in the insulation and the wood layers follows a pattern of variations similar to that of the non-cavity wall. Although this general behaviour is mainly related to the variations in outdoor air temperature, the moisture accumulation pattern in both layers can be specifically related to indoor air humidity behaviour. A typical variational pattern of indoor air humidity for an average air tightness enclosure bounded by a cavity wall is similar to that shown in Figs. 7.11-7.14. By relating the indoor air humidity behaviour to the moisture accumulation patterns in the insulation and the wood layers, its impact can be recognized with higher moisture accumulation during the tenth month in response to higher air humidity level for the same period. Lower indoor humidity has resulted either in a decrease in the moisture accumulation rate or a decrease in the material moisture content. The brick layer, on the other hand, is less dependent on indoor air humidity since nearly no change occur in its moisture content in response to air humidity fluctuations during the first two months of the fall period. In winter and fall months, when the outdoor air is relatively dry, higher air leakage coefficient of the exterior wall will generally result in lower indoor humidity and hence, lower moisture accumulation rate in all layers. As an example, increasing the air leakage coefficient of the direct air flow path from $0.3 \cdot 10^{-4}$ to $1.8 \cdot 10^{-4}$ $m^3/m^2 \cdot Pa^{.65} \cdot s$ has resulted in up to 30% reduction in moisture accumulation for the insulation and the wood layers, and up to 90% reduction in the brick layer. Moisture distribution across the different

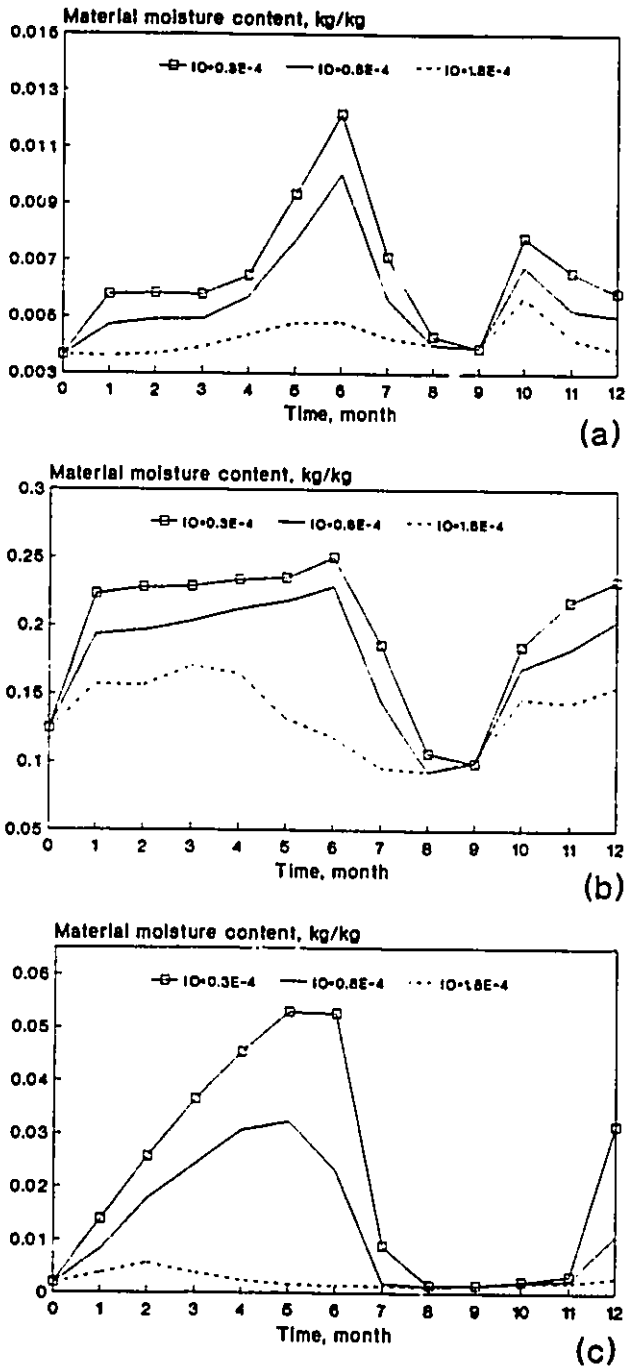

Fig. 7.61 Variations of monthly average moisture content of the west wall components at different air leakage characteristics. (a) insulation (b) wood, (c) brick.

layers of the west wall are illustrated in Fig. 7.62 through Fig. 7.64 for different exterior wall air leakage characteristics. At an average exterior wall air tightness, more than twice as much moisture accumulates during the winter and the fall months in the insulation layer at the boundary with the wood layer as compared with the rest of the material. On the other hand, more evenly moisture distribution is obtained during the summer and the spring months for the insulation layer and all year round for the wood layer. The largest moisture accumulation level within the brick layer occurs during winter at the interior surface of the layer. This level of moisture content is much higher than the material maximum hygroscopic level indicating the occurrence of interstitial condensation. No significant moisture accumulation occurs during the summer and spring months, and the resulting moisture accumulation is uniformly distributed across the material. Decreasing the air leakage rate through the exterior walls has substantially increased the local moisture accumulation in all layers, but in particular at the brick interior surface where interstitial condensation occurs during the winter, the spring as well as the fall months. The occurrence of condensation has completely altered the pattern of moisture distribution within the brick layer especially during the spring period when as much as five times more moisture has accumulated at its interior surface. The seasonal moisture distribution patterns in the insulation and the wood layers remain unaffected by changes in indoor air humidity behaviour. In summer, increasing the exterior walls air leakage coefficient has no effect on the moisture behaviour of any of the wall's components mainly because indoor humidity is less influenced by fluctuations in air leakage rates in the presence of the dehumidification process. Seasonal moisture content distributions within the wall components for a relatively untight enclosure are shown in Fig. 7.64. It can be seen that by increasing the air leakage coefficient of the exterior walls, the moisture content gradient across the insulation and the brick layers is almost eliminated. In addition, at this level of

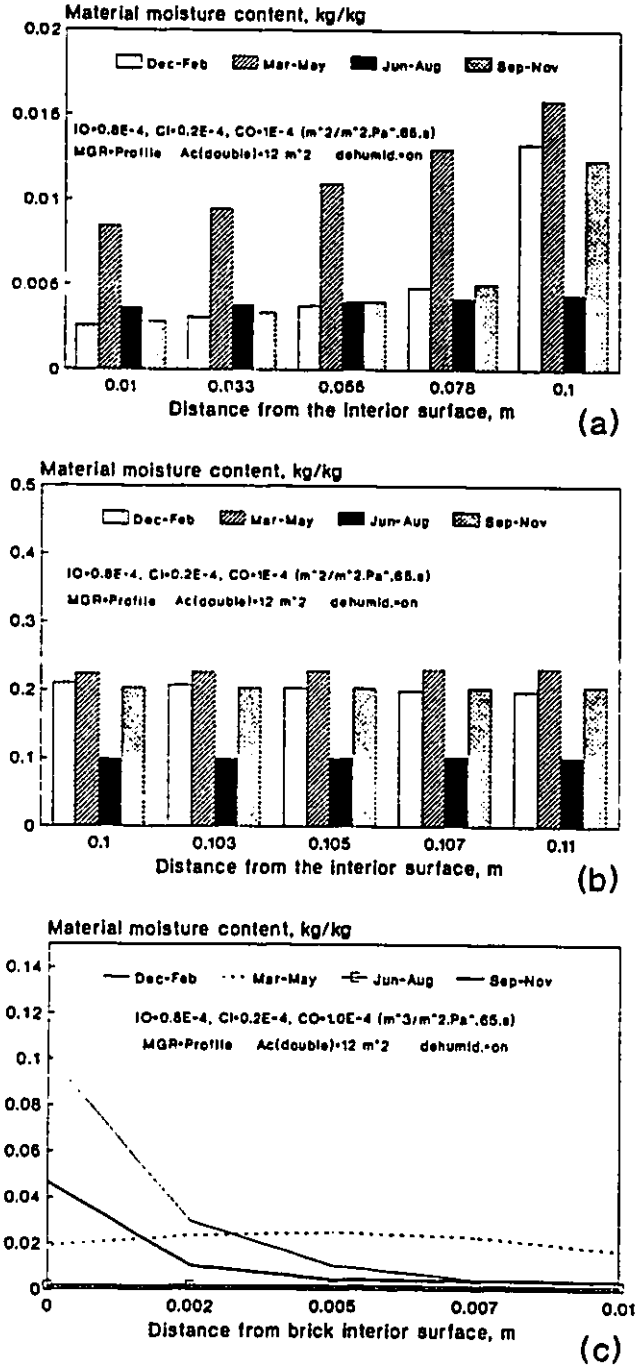

Fig. 7.62 Seasonal moisture content distribution across the west wall components for average enclosure air tightness (a) insulation, (b) wood, (c) brick.

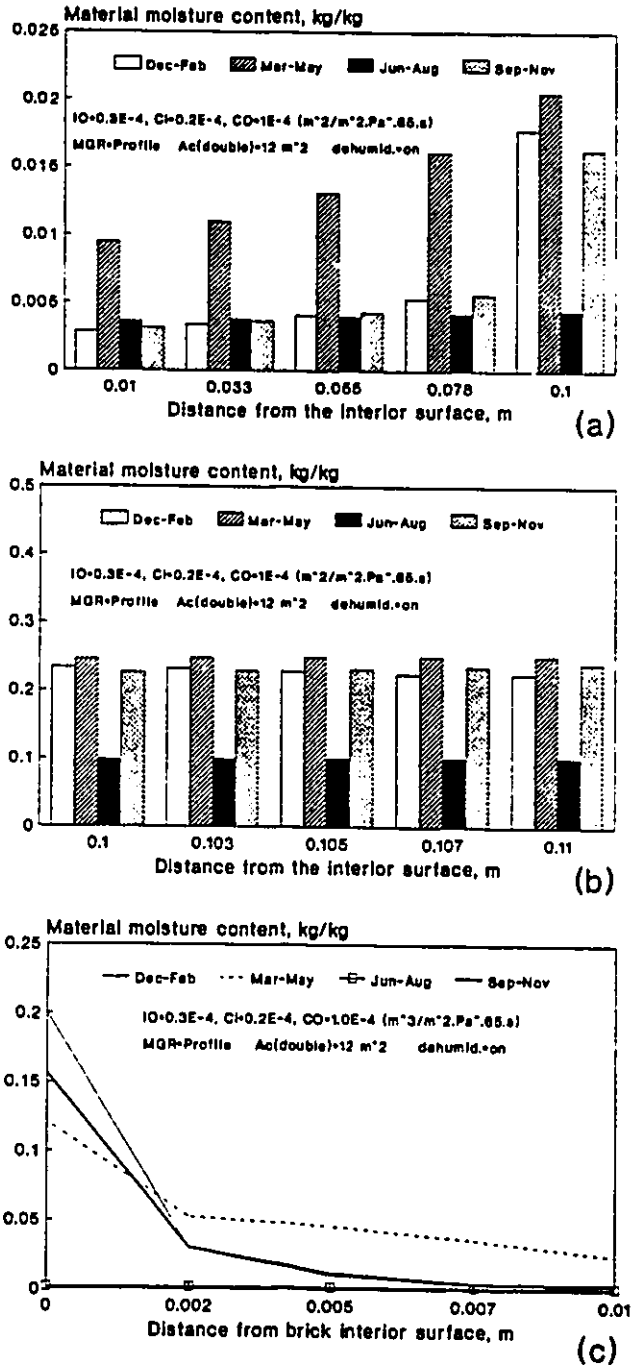

Fig. 7.63 Seasonal moisture content distribution across the west wall components for a ralatively air tight building enclosure. (a) insulation, (b) wood, (c) brick.

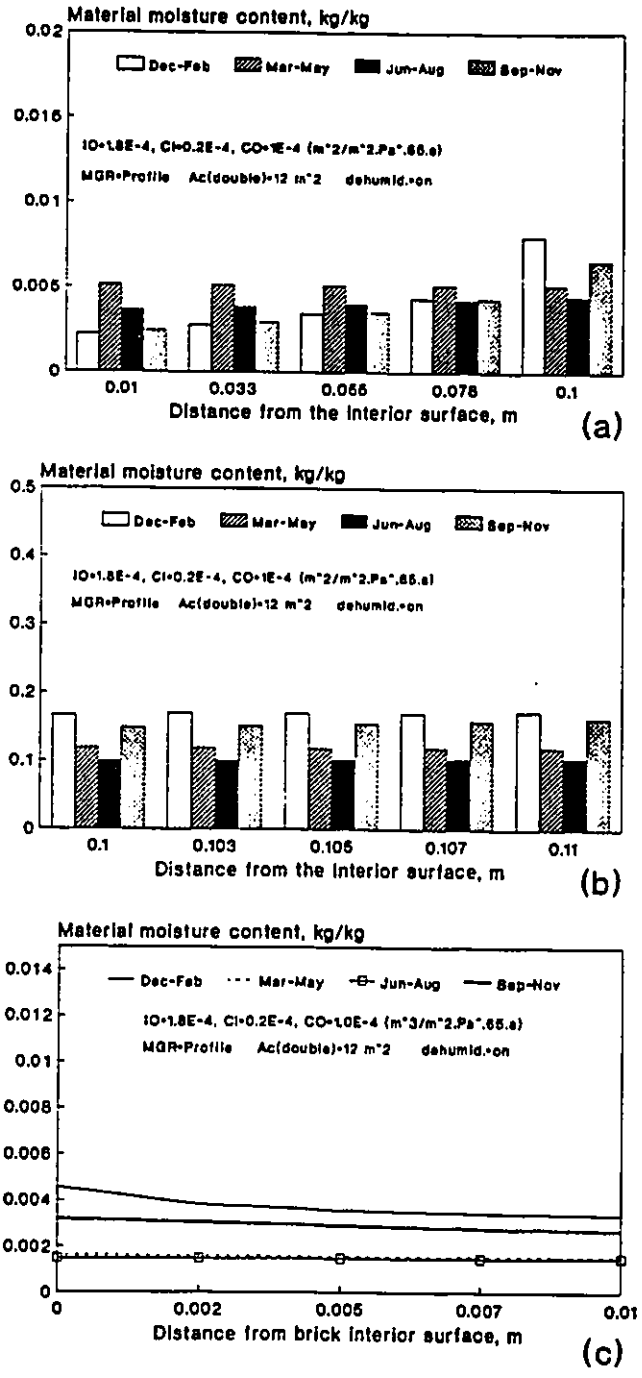

Fig. 7.64 Seasonal moisture content distribution across the west wall components for a ralatively air untight building enclosure. (a) insulation, (b) wood, (c) brick.

enclosure air tightness, the moisture content of all layers is maintained well below the corresponding maximum hygroscopic level making it unlikely for interstitial condensation to occur. As a result of reduced indoor air humidity level, local moisture content in the insulation and the brick layers has been reduced by as much as 50%. A similar but a uniform reduction in the moisture content level is experienced by the wood layer during the spring period.

Moisture behaviour of the east wall layers at different enclosure air tightness levels is shown in Fig. 7.65. Comparison with the moisture behaviour of the west wall components shown in Fig. 7.61 confirms that the east wall is generally more responsive to indoor air humidity behaviour which is an indication of the presence of a faster mode of moisture transfer between the indoor environment and the east wall. At low exterior wall air tightness level, moisture accumulation in the wood and the insulation layers of the east wall during spring months is much higher than that of the west wall. This difference in moisture behaviour is more pronounced for the brick layer since more moisture accumulates in the east wall during winter, spring and fall months at all level of air tightness. At low air tightness level, the moisture behaviour of the brick layer is not affected by the indoor air humidity behaviour most of the time. The influence of indoor humidity on the brick layer moisture performance can be appreciated more at the end of the fall months when the material moisture content is increased by as much as 20 times by changing enclosure air tightness level (i.e., from untight to tight). Seasonal moisture distribution across the three layers in the east wall for an average air tightness enclosure is shown in Fig. 7.66. Comparison with moisture distribution in the west wall under the same conditions shows that the major difference between the two walls in terms of moisture accumulation occurs during the winter months at the brick layer interior surface

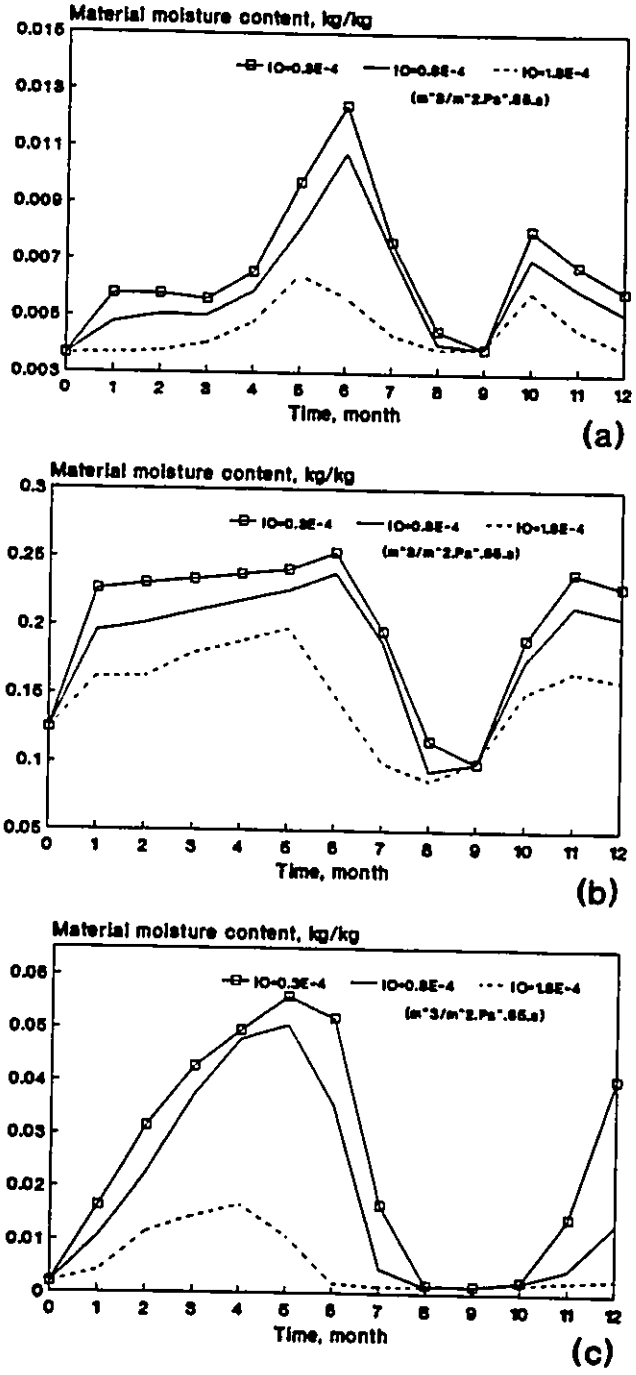

Fig. 7.65 Variations of monthly average moisture content of the east wall components at different air leakage characteristics. (a) insulation (b) wood, (c) brick.

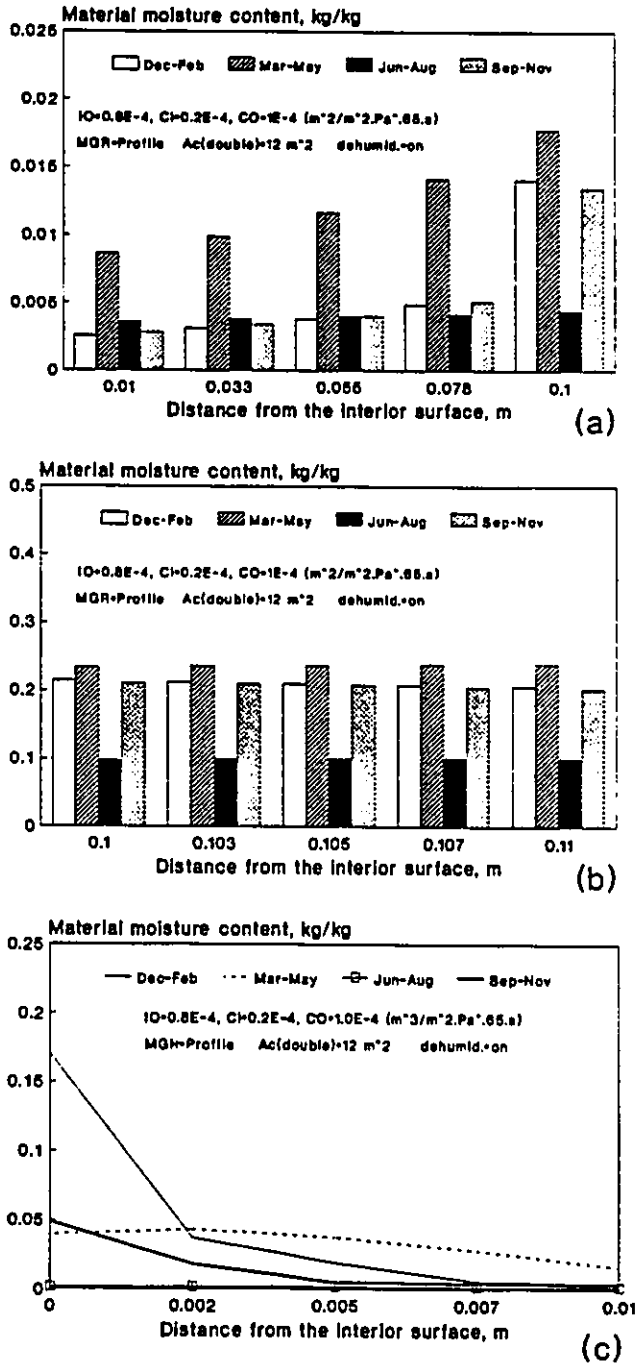

Fig. 7.66 Seasonal moisture content distribution across the east wall components for average enclosure air tightness. (a) insulation, (b) wood, (c) brick.

where as much as 70% more moisture has accumulated in the east wall. The other layers show almost the same behaviour both in the magnitude and the moisture distribution patterns within the material. From the above discussion, the importance of the air leakage process in determining the level and distribution of moisture content within all layers of the cavity wall, particularly, the layer of the outer wythe can be clearly recognized.

7.4.2 Moisture absorption/desorption process: The impact of the absorption/desorption by the interior materials within an average air tightness enclosure on the moisture behaviour of the west wall components is shown in Fig. 7.67. Moisture absorption process has resulted in a reduced material moisture content for all layers during the winter and spring periods, while the desorption process has increased the material moisture content at the end of the fall period. The most appreciable impact of the absorption/desorption process is experienced at the brick layer where the moisture accumulation has been reduced by about 16% by the end of the fifth month during the spring period, and more than 30% during the fall at the end of the twelfth month. Because of its low hygroscopicity, the gypsum material is having a less noticeable influence on the overall moisture behaviour of the wall. A similar moisture behaviour modification is experienced by the east wall as a result of the moisture absorption/desorption process as illustrated in Fig. 7.68. However, the impact of moisture absorption/desorption by the gypsum material is more pronounced for the brick layer of the east wall than the west wall. Fig. 7.69 illustrates the impact of the moisture absorption/desorption process within a relatively untight enclosure on the moisture behaviour of the west wall. Comparison with Fig. 7.67 shows that at higher air leakage rates, the wood and the insulation layers are generally more responsive to the moisture absorption/desorption process, while less change is experienced by the brick layer. The reduced moisture response of the brick layer is an indication of the

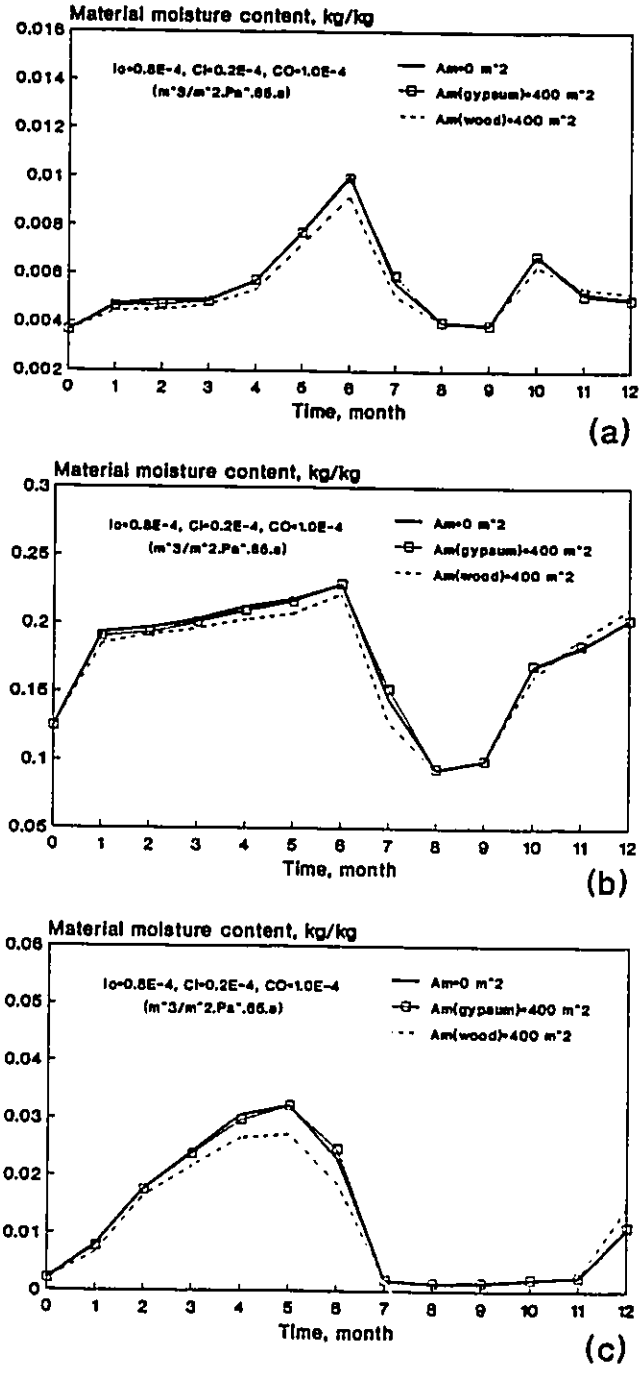

Fig. 7.67 Effect of moisture absorption/desorption on the variations of average monthly moisture content of the west wall components; (a) insulation, (b) wood, (c) brick.

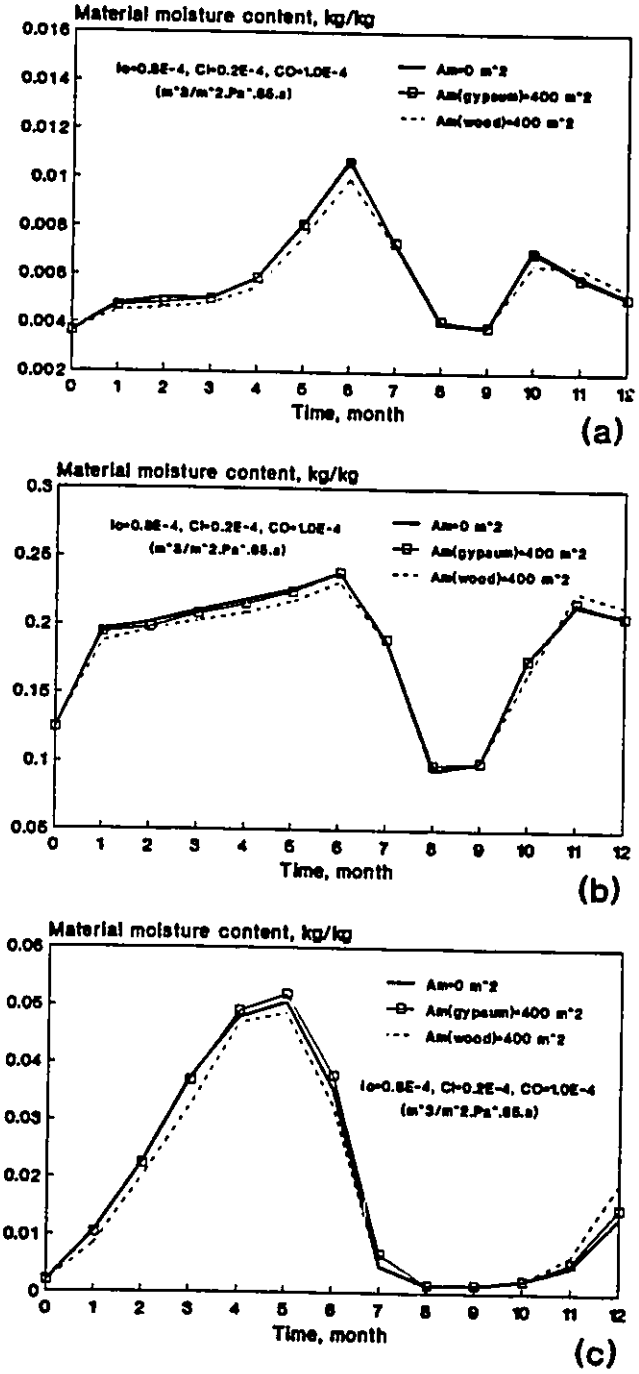

Fig. 7.68 Effect of moisture absorption/desorption on the variations of average monthly moisture content of the east wall components; (a) insulation, (b) wood, (c) brick.

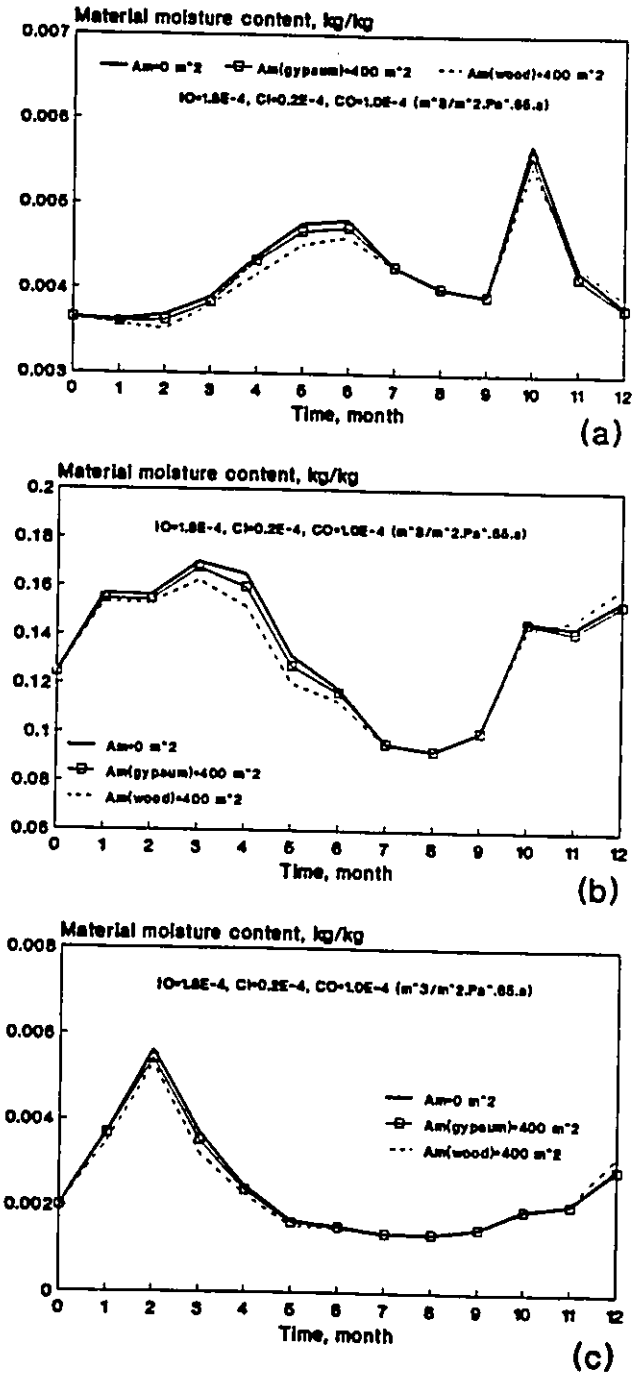

Fig. 7.69 Effect of moisture absorption/desorption on the average moisture content of the west wall for a relatively untight enclosure. (a) insulation, (b) wood, (c) brick.

prevalence of the slow moisture transfer mechanism (i.e., the diffusion mode). For the same air tightness level, the east wall shows considerable change in behaviour due to the moisture absorption/desorption process particularly in the brick layer as shown in Fig. 7.70. The presence of wood as a moisture absorbing interior material has reduced the moisture content of the brick layer by 60% at the end of the fifth month, while the presence of gypsum material has no significant impact on the moisture behaviour of any layer. A more pronounced modification is experienced by the south wall as can be seen from Fig. 7.71. In this case, moisture absorption/desorption by the gypsum material has a greater impact on the wall moisture behaviour. During the sixth month, the presence of gypsum material has resulted in as much as 25% more moisture accumulation in the insulation and the wood layers, while significantly slowing the drying process in the brick layer. From the above discussion, it can be recognized that the impact of the moisture absorption and desorption by interior materials is influenced by the characteristics of material, the fluctuation patterns of indoor air humidity, the wall characteristics and its interaction with the indoor environment. Any particular combination of these factor will result in a unique modification of wall moisture behaviour in response to the absorption/desorption process.

7.4.3 Surface condensation process: The degree of its influence is dependent on the frequency of occurrence and the degree of reduction in indoor air humidity level as well as the type of moisture interaction between the wall and the indoor environment. In a cavity wall system, the presence of the convective moisture transport process can greatly enhance the influence of the surface condensation process. However, for a particular wall, the type and degree of interaction varies with time according to wind speed and direction. In addition, the surface condensation process is a non-continuous process determined by

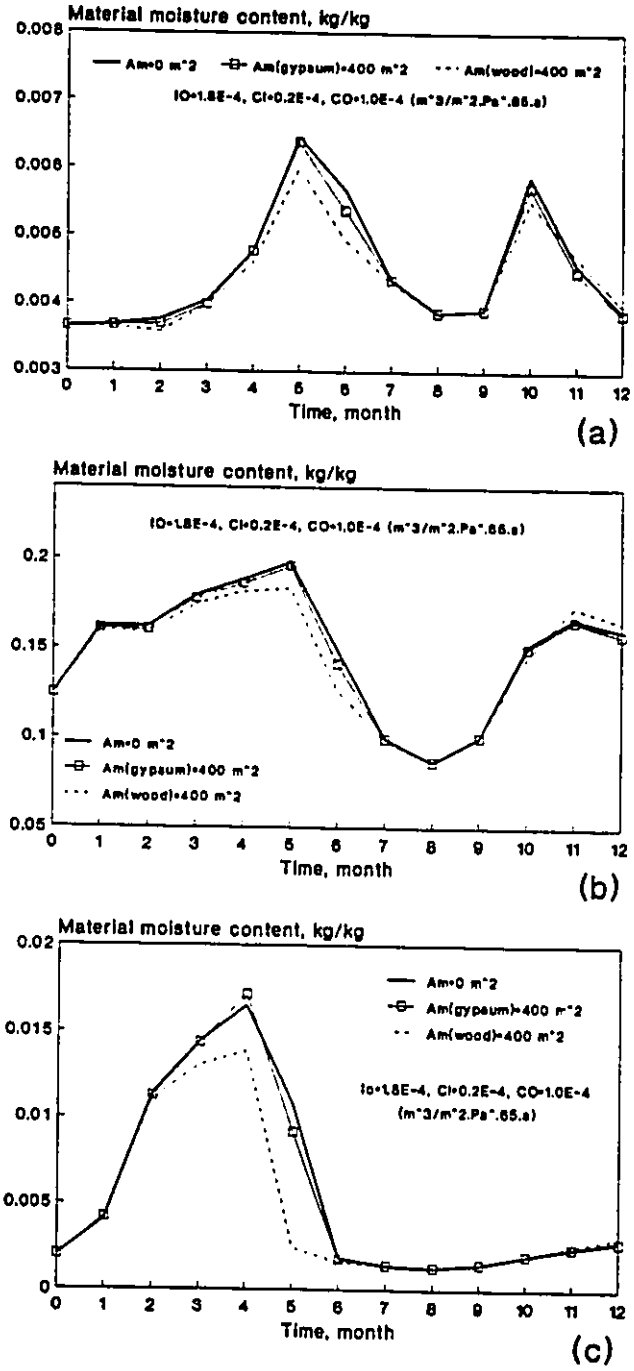

Fig. 7.70 Effect of moisture absorption/desorption on the average moisture content of the east wall for a relatively untight enclosure. (a) insulation, (b) wood, (c) brick.

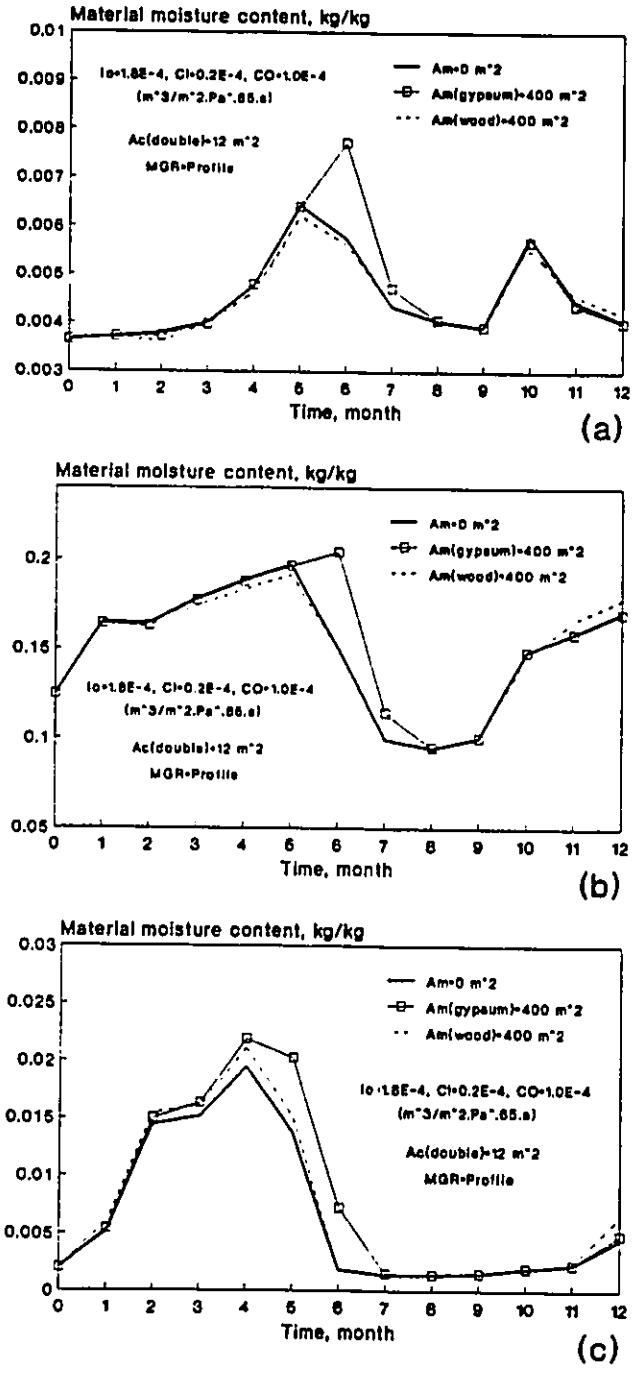

Fig. 7.71 Effect of moisture absorption/desorption on the average moisture content of the south wall for a relatively untight enclosure. (a) insulation, (b) wood, (c) brick.

several time-dependent parameters such as the level of indoor air humidity and the outdoor air temperature. This means that for the surface condensation process to be an influencing factor in determining the moisture behaviour of a particular wall, convective moisture transfer must be taking place during the occurrence of condensation. Different walls are therefore expected to react differently to the surface condensation process. Fig. 7.72 shows the impact of the condensation process on the moisture accumulation with in the west wall components at different condensation surface areas. For this particular wall, the surface condensation process has no negative effect on the moisture accumulation in the insulation and the wood layers except some minor effect during the spring period. In the contrary, increasing the condensation surface area has resulted in more moisture accumulation in the brick layer during the early spring period. Such behaviour can be explained by the minor role of the condensation process in influencing indoor air humidity at the present average enclosure air tightness level. In addition, it is clear that little or no air outflow occurs through the west wall during the duration of condensation. At these conditions, the moisture absorption/desorption process by interior wall surfaces can play a more noticeable and an adverse role. By fully glazing the north wall (i.e., A_c=60 m^2), a good percentage of the exterior wall which acts as an absorbing/desorbing material is eliminated. When indoor air humidity is higher than the outdoor air humidity, which is the case during winter, the interior surface of the exterior wall (i.e., hygroscopic material) will act as a moisture absorbing surface. Therefore, by replacing the exterior wall by a glazed window, a moisture sink will be eliminated resulting in higher or similar air humidity level when no condensation occurs. The impact of the continuous moisture absorption process by the exterior wall surface on indoor air humidity behaviour has over shadowed the impact of the condensation process in shaping the moisture behaviour of the west wall. The role of the surface condensation process can be more visible at low air leakage rates.

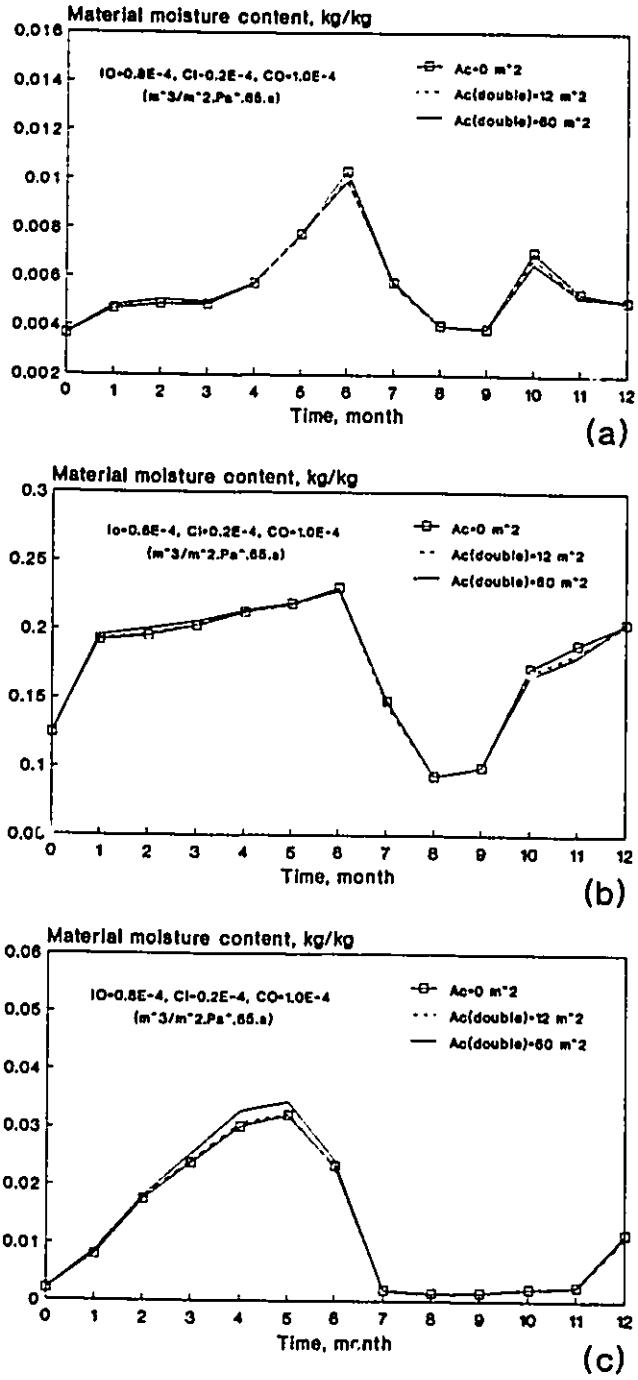

Fig. 7.72 Effect of surface condensation on the average moisture content variations of the west wall for average enclosure air tightness. (a) insulation, (b) wood, (c) brick.

By reducing the exterior air leakage coefficient by 50% (i.e., C_w=0.5·10^{-4} m^3/m^2·Pa$^{.65}$·s), the impact of the reduced air humidity level due to the condensation process becomes more apparent as shown in Fig. 7.73. For the same air tightness level, the surface condensation process has resulted in a significant modification for the south wall moisture behaviour as illustrated in Fig. 7.74. The presence of 60 m^2 condensation surface area has reduced moisture accumulation in the brick layer by more than 20% at the end of the sixth month and by more than 60% in the wood layer at the end of the ninth month. This significant impact of the condensation process is an indication of the dominance of the convective moisture transfer mode through the south wall. Even for the average enclosure air tightness (i.e., C_w=1.0·10^{-4} m^3/m^2·Pa$^{.65}$·s), the impact of the condensation process can be significant when the thermal resistance of the condensation surface is reduced. Fig. 7.75 illustrates the impact of the condensation process on the moisture accumulation within the west wall components when a single glazed window is used. It can be seen that the use of a single glazed window has considerably reduced the moisture accumulation in all layers particularly in the brick layer where the maximum moisture accumulation level has been reduced by more than 60%. In the insulation layer, the maximum moisture accumulation has been reduced by about 30% and by about 15% for the wood layer. In addition to the reduction in the maximum moisture accumulation level, the presence of surface condensation has pushed back the peak moisture accumulation in all layers which caused the drying process to start one month earlier. The east wall is less responsive than the west wall to the surface condensation process since the reduction in the moisture accumulation level within its components is proportionally less than that of the west wall as can be seen from Fig. 7.76. In the east wall, the largest reduction in moisture accumulation is experienced by the brick layer where as much as 30% less moisture has accumulated in the presence of surface condensation. Nevertheless, none of the moisture

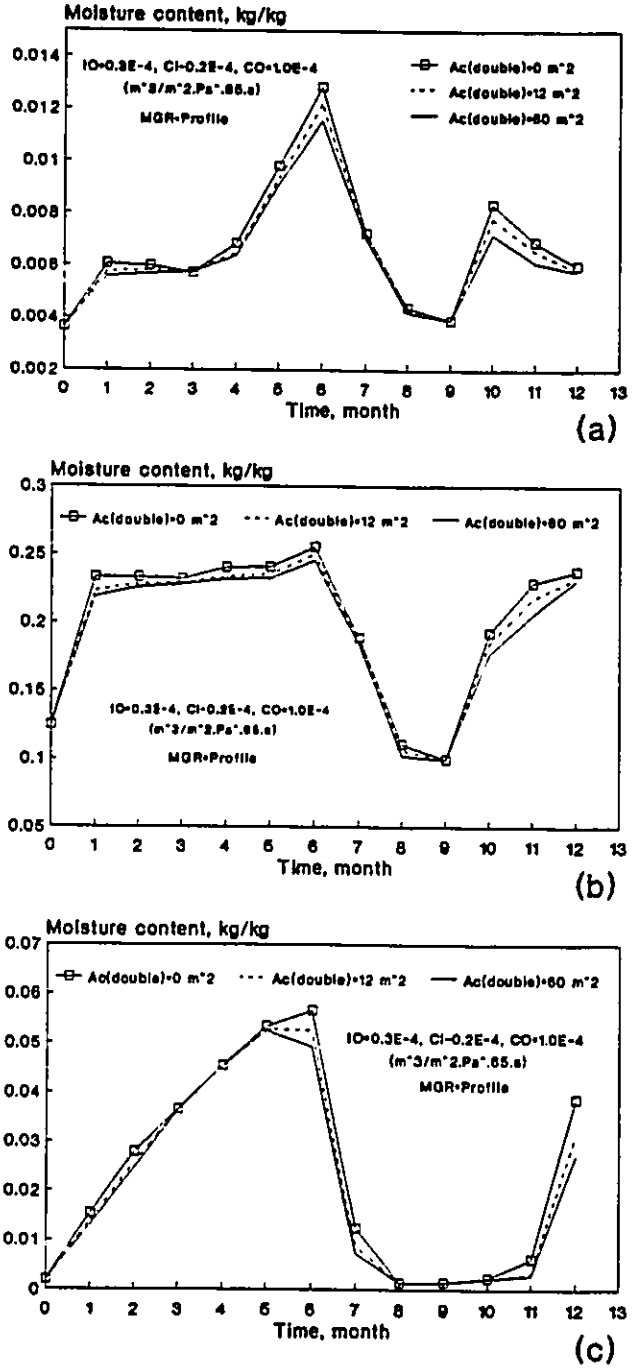

Fig. 7.73 Effect of surface condensation on the average moisture content variations of the west wall for an air tight enclosure. (a) insulation, (b) wood, (c) brick.

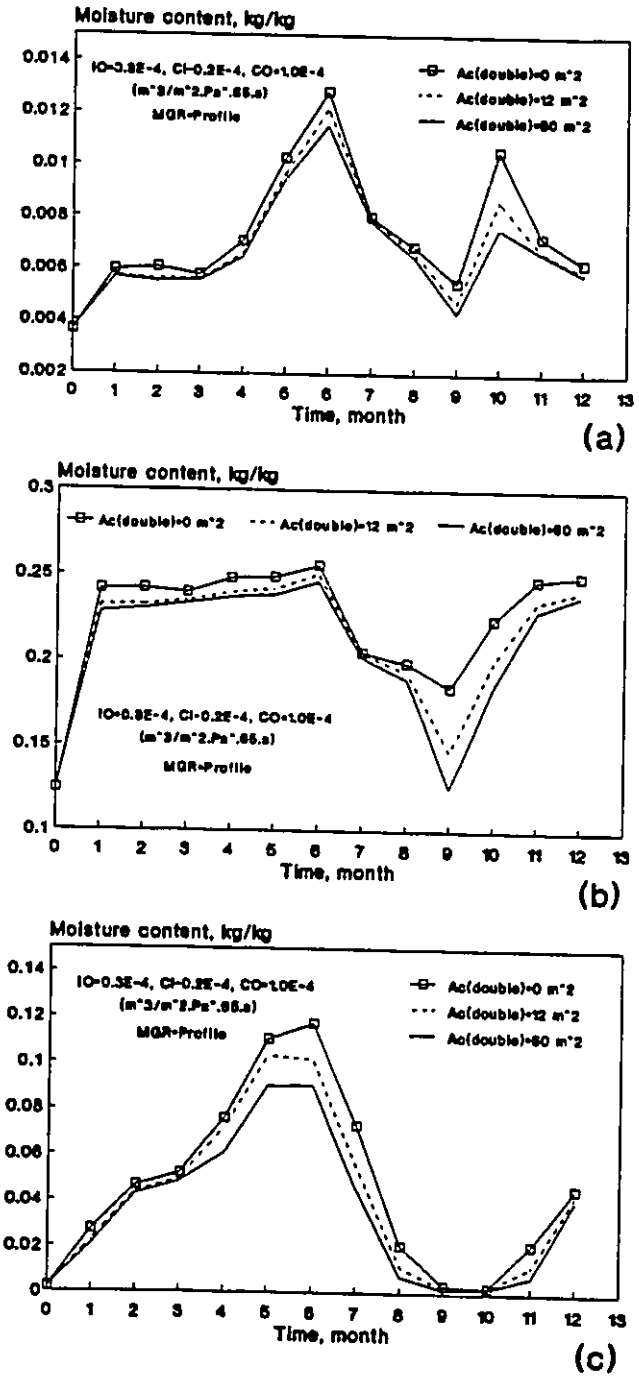

Fig. 7.74 Effect of surface condensation on the average moisture content variations of the south wall for an air tight enclosure. (a) insulation, (b) wood, (c) brick.

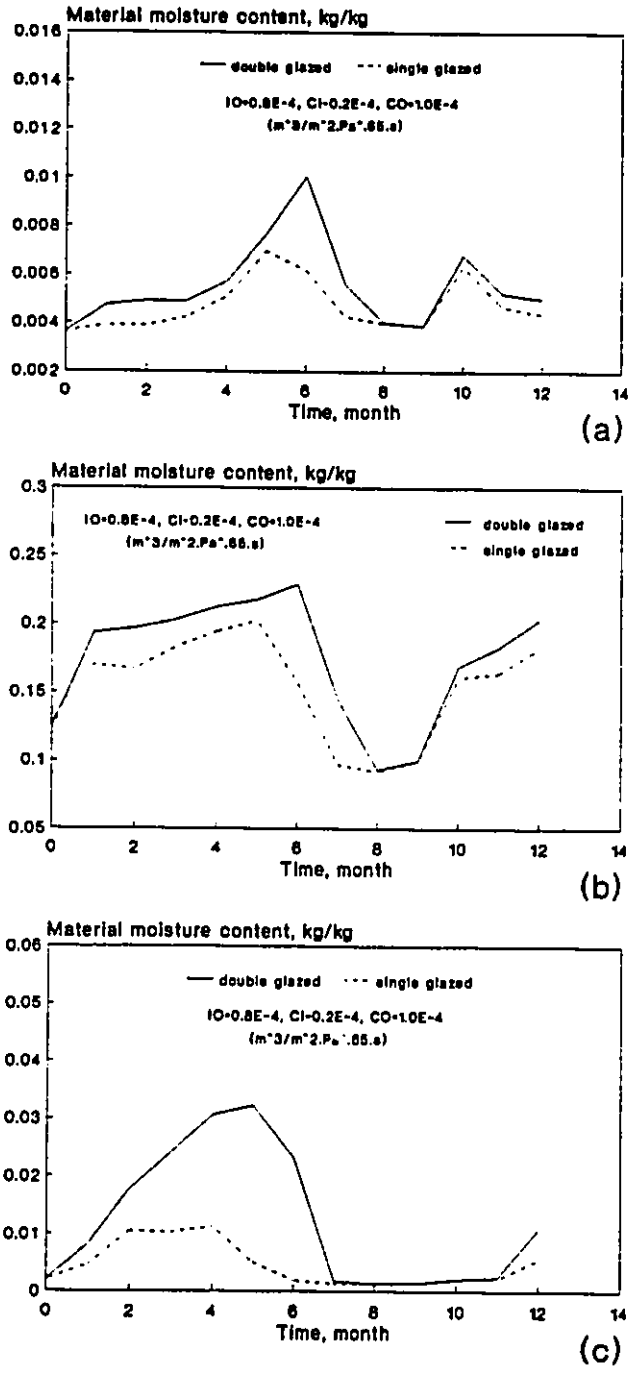

Fig. 7.75 Effect of condensation surface characteristics on the moisture content variations of the west wall components. (a) insulation, (b) wood, (c) brick.

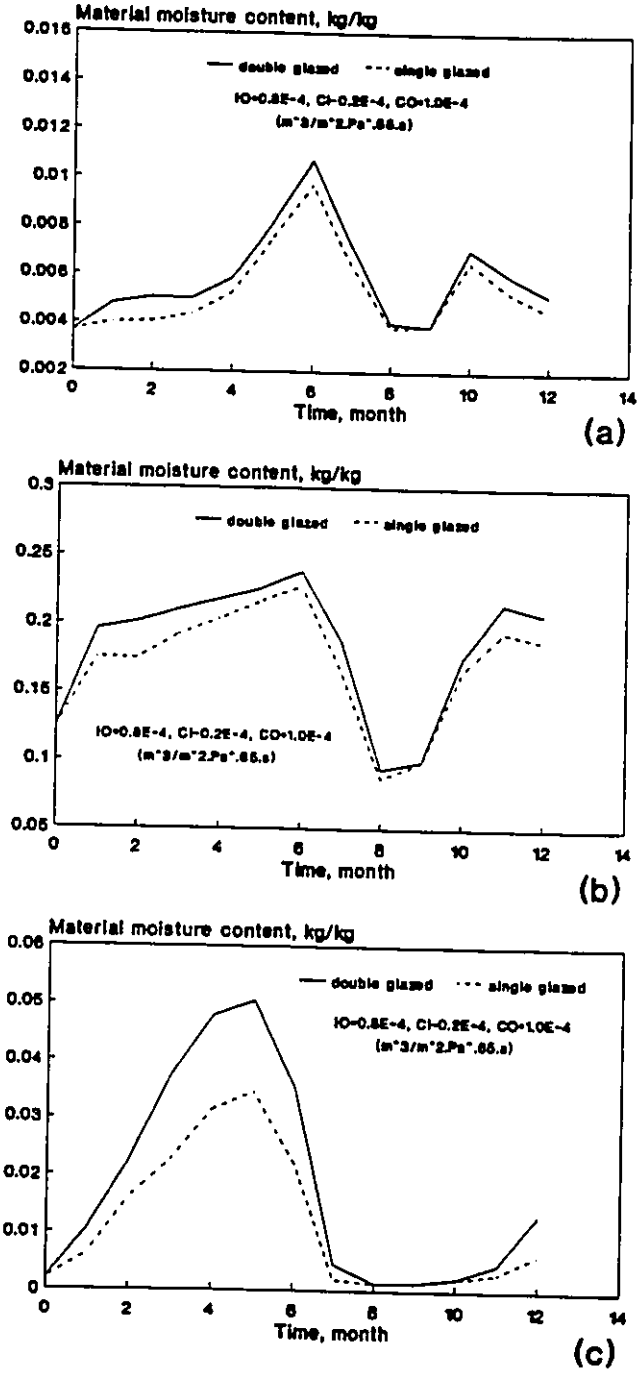

Fig. 7.76 Effect of condensation surface characteristics on the moisture content variations of the east wall components. (a) insulation, (b) wood, (c) brick.

accumulation curves experience any shift in behaviour in terms of time which means that the wetting and the drying behaviour of the material remains unchanged with time. Seasonal moisture distribution within the west wall components in the absence and presence of surface condensation are shown in Figs. 7.77-7.78. Comparison between Fig. 7.77-a and Fig. 7.78-a shows that the presence of surface condensation over a single glazed window has considerably reduced the moisture content gradient across the insulation layer during the winter and fall months, but almost eliminated it during the spring period. The most noticeable local reduction in the insulation layer moisture content occurs at the interface with the wood layer where it is reduced by more than 50% during the spring period. Similarly, the major change in the wood layer moisture content occurs during the spring with a uniform reduction of about 35%, however, the moisture content gradient across the layer remains unchanged. The most important change in the material moisture behaviour due to surface condensation occurs in the brick layer where the interstitial condensation at its interior surface has been eliminated and the local moisture content has been reduced by about 70%. During the spring period, the presence of surface condensation has resulted in a uniform reduction in the material moisture content in the brick layer.

7.4.4 Indoor moisture generation and summer dehumidification processes: The influence of the indoor moisture generation and its production pattern on the moisture accumulation within the west wall components is shown in Fig. 7.79. The absence of indoor moisture generation in winter has eliminated the only source of moisture which is to be accumulated within the various wall components. Variations in the material moisture content occur only in response to changes in ambient humidity conditions. When moisture is generated into the space with a daily average value of about 115 10^{-6} kg/s, moisture

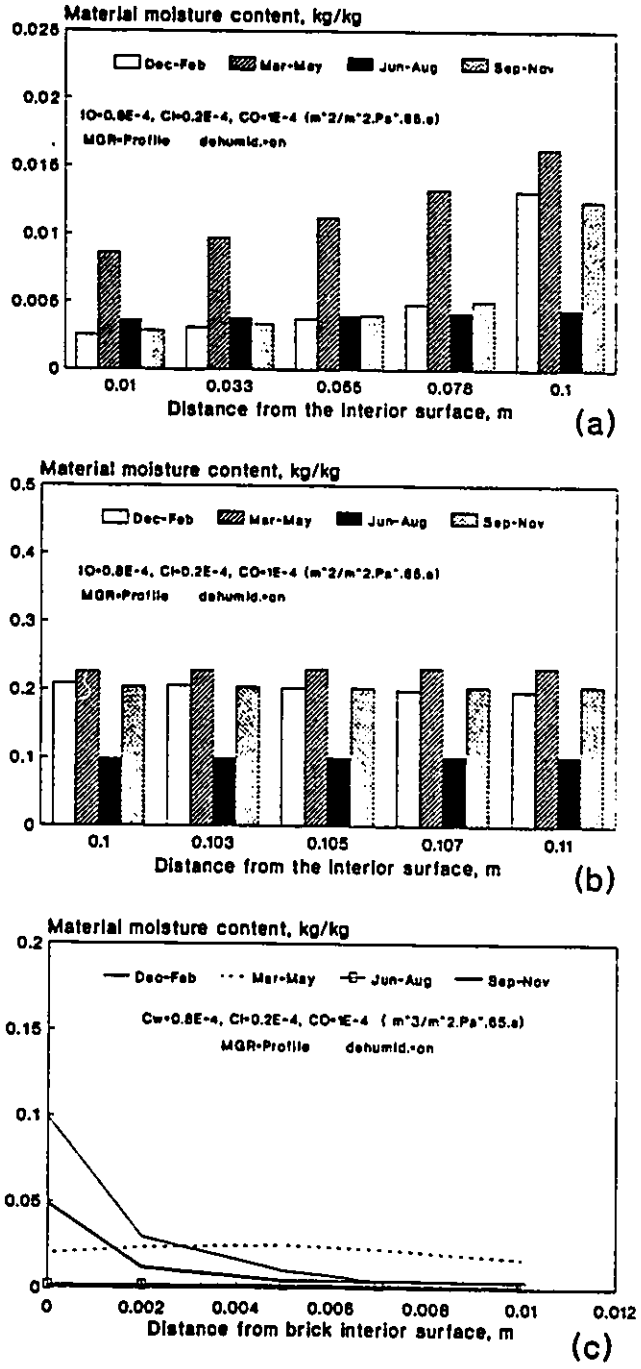

Fig. 7.77 Seasonal moisture content distribution across the west wall components in the absence of surface condensation. (a) insulation, (b) wood, (c) brick.

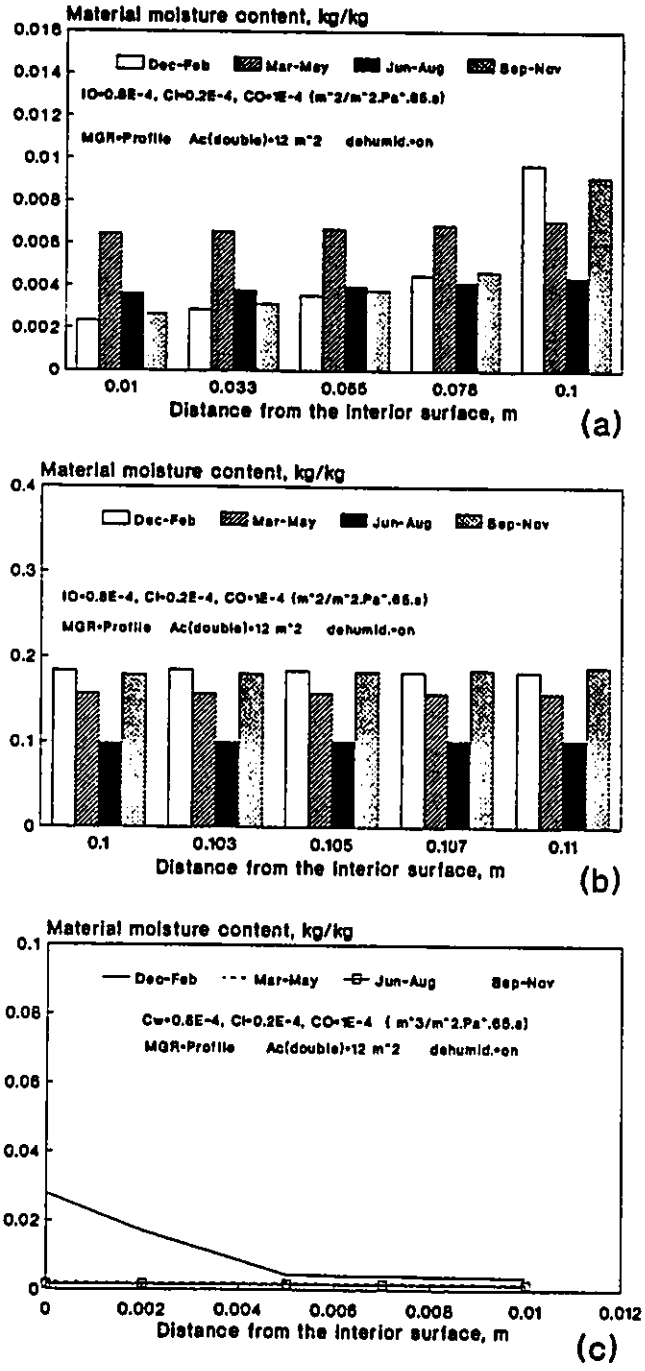

Fig. 7.78 Effect of surface condensation on the seasonal moisture content distribution of west wall components; (a) insulation, (b) wood, (c) brick.

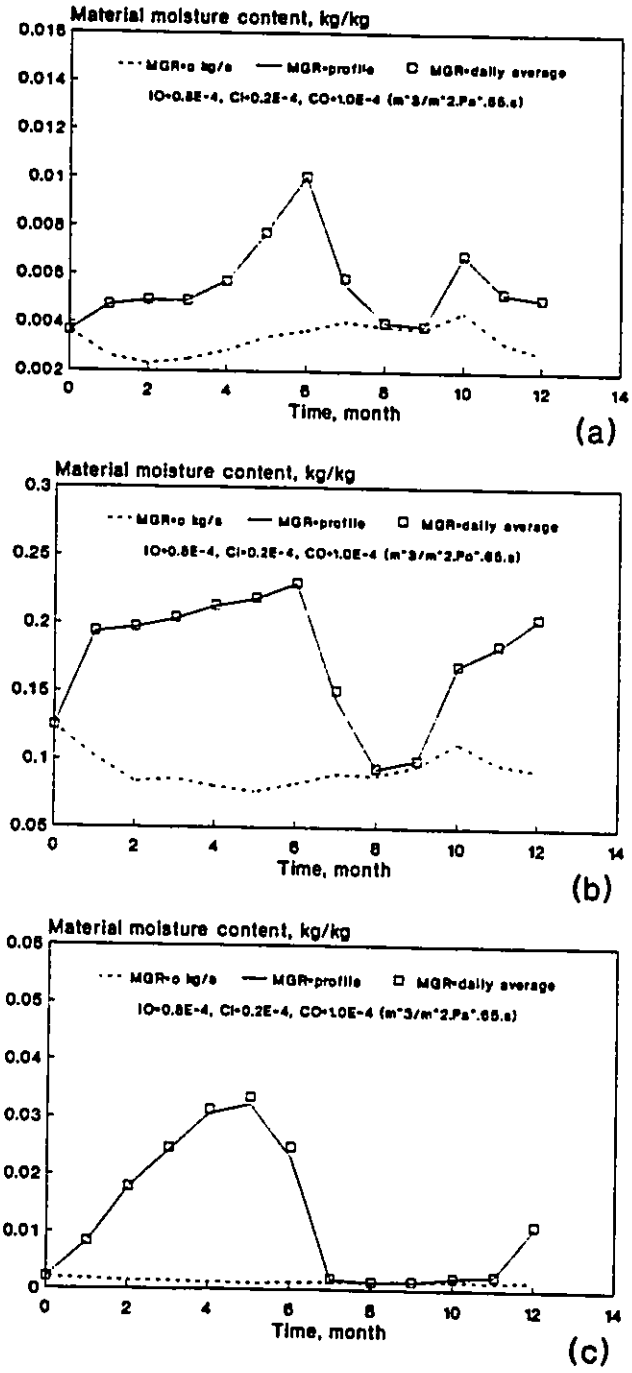

Fig. 7.79 Effect of indoor moisture generation on average moisture content variations of west wall components; (a) insulation, (b) wood, (c) brick.

accumulation within the insulation and the wood layers has been tripled during the wetting period. The brick layer experiences the greatest response with as much as 25 times more moisture accumulation when moisture is generated within the space. The pattern of the daily moisture generation seems to have some effect on moisture accumulation in the brick layer but no apparent influence on the other layers. This influence could be more pronounced for other walls which have better interaction with the indoor environment. For practical consideration, however, the use of the daily average moisture generation rate can be judged as accurate enough to be used in modelling long term moisture behaviour of cavity wall systems.

Depending on the level of interaction with the indoor environment during the dehumidification period, different walls are likely to respond differently to the summer dehumidification process. Fig. 7.80 illustrates the moisture behaviour of the west wall components with and without summer dehumidification. It can be seen that the absence of the dehumidification process has very little effect on the moisture behaviour of the brick layer but has some short term effect on the insulation and the wood layers. The insulation layer has experienced a noticeable increase in its moisture content during the seventh month while the wood layer experiences a reduced drying rate. The impact of the dehumidification process is much more pronounced for the east wall as shown in Fig. 7.81. In contrast with the west wall, the brick layer of the east wall exhibit a greater degree of dependence on the dehumidification process. The absence of dehumidification has considerably reduced the drying rate of the brick layer and resulted in as much as twice more moisture to be accumulated by the end of the twelfth month. On the other hand, the absence of dehumidification has resulted in a continuing increase in the moisture content of the insulation and the wood layers for two consecutive months. Such difference in

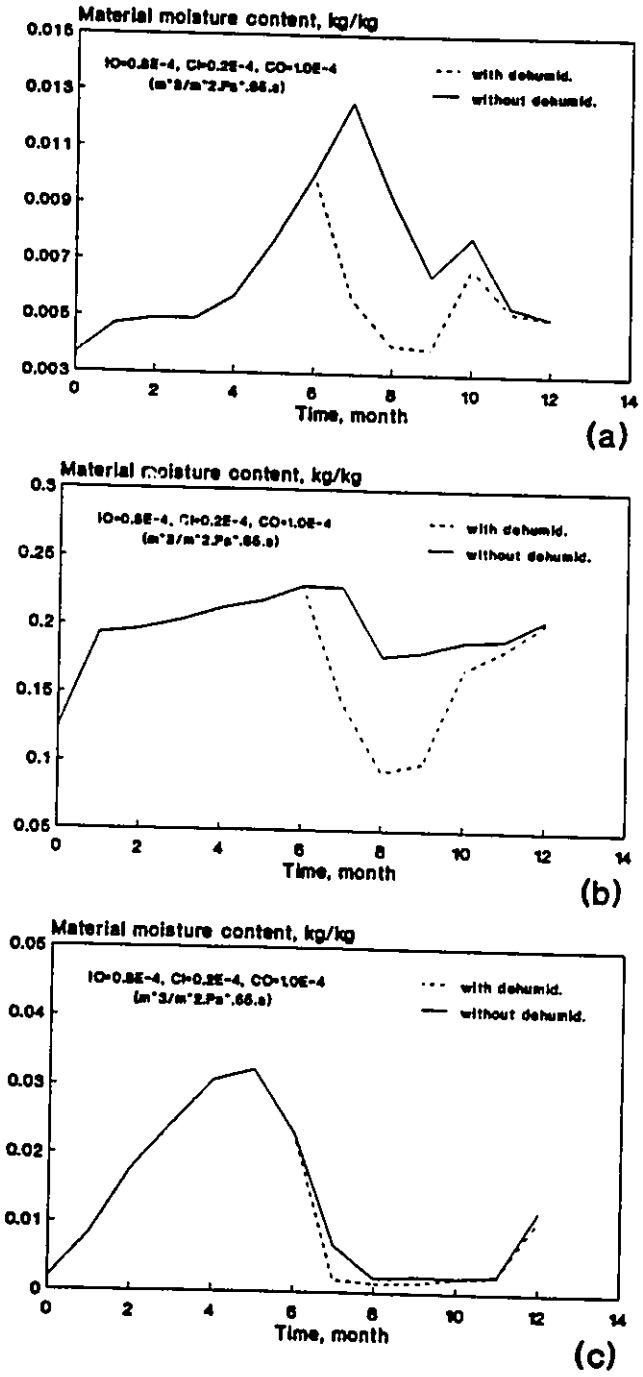

Fig. 7.80 Effect of summer dehumidification on variations of average moisture content of the west wall components; (a) insulation, (b) wood, (c) brick.

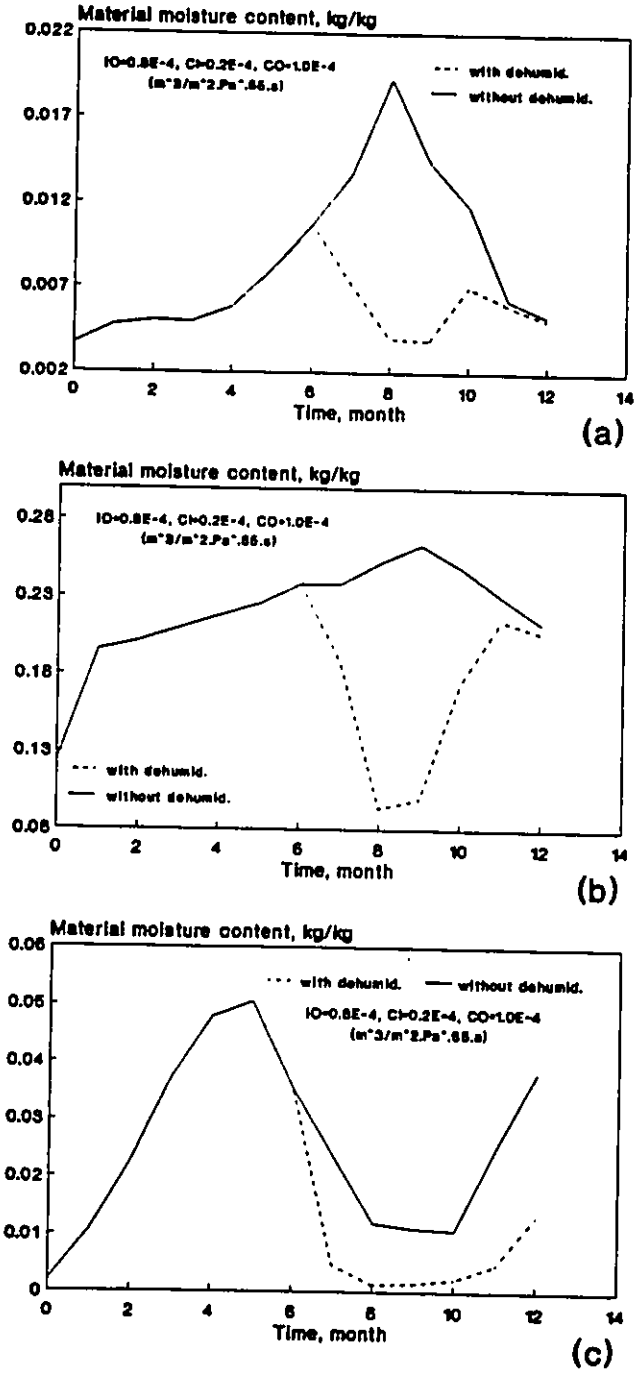

Fig. 7.81 Effect of summer dehumidification on variations of average moisture content of the east wall components; (a) insulation, (b) wood, (c) brick.

behaviour can only be explained by the different modes of interaction between the different walls and their surroundings.

7.4.5 Impact of wall interaction with indoor and outdoor environments on its moisture performance: Convective moisture transfer through exterior walls, which could be the dominant moisture transfer mechanism in cavity wall systems, is mainly determined by the wind speed and direction. Walls which are oriented differently with respect to wind direction, are expected to have different interaction with the indoor and outdoor environments, and hence different moisture performance is expected for the same indoor air humidity conditions. Fig. 7.82 compares the moisture accumulation patterns within the insulation, the wood and the brick layers of the different walls. It can be seen that the pattern of variations of material moisture content is essentially the same for all walls, but its relative magnitude is changing with time for all layers. The change in the relative magnitude can be attributed to variations in the interaction modes and the changing influence of the convective moisture transport process. For example, the outflow of air from the indoor space causes additional moisture accumulation during winter but enhances the drying process during the summer. Similarly, the inflow of outdoor air causes additional moisture accumulation in summer but discourages moisture deposition in winter. This behaviour can be best illustrated by comparing the wall's moisture behaviour in the presence and the absence of the convective moisture transport process. Fig. 7.83 compares the moisture behaviour of the east and west walls in the presence of convective moisture transfer with that when moisture transfer occurs only by diffusion. It is clear that the absence of the convective process has reduced the drying potential for all components during the summer period. The brick layer of both the east and the west walls is the most affected by the convective transport process. The presence of the

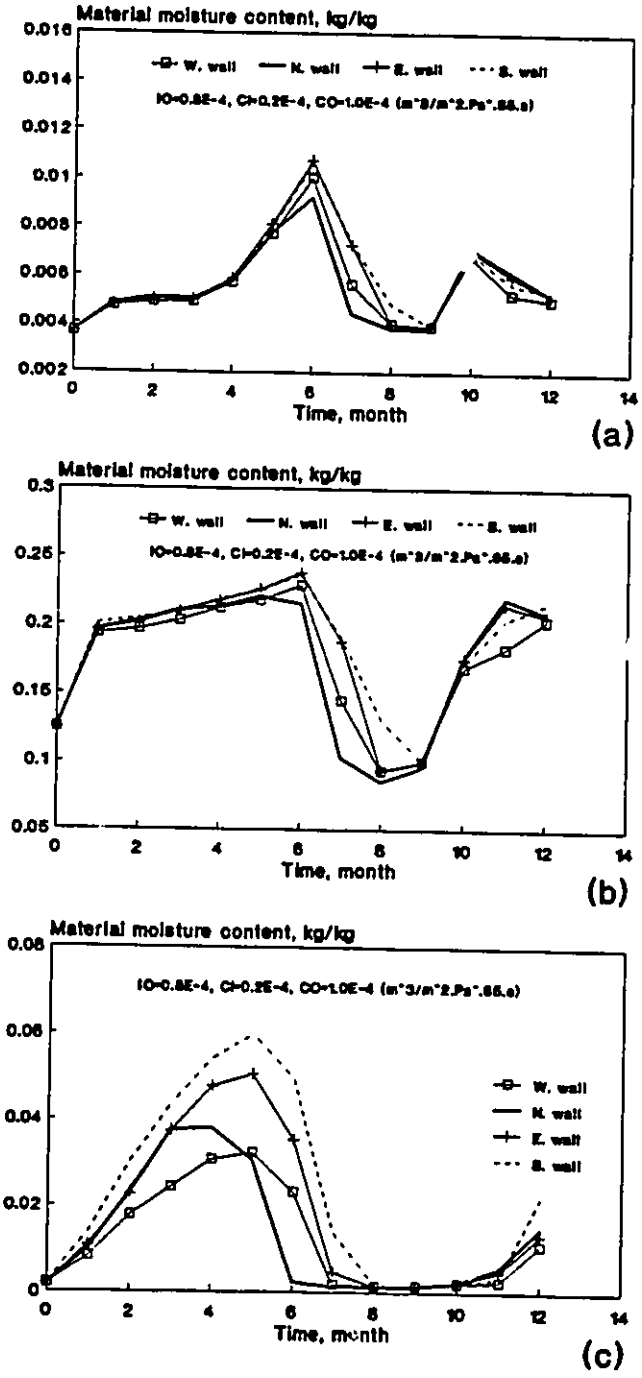

Fig. 7.82 Variations of the average moisture content of the different walls components; (a) insulation, (b) wood, (c) brick.

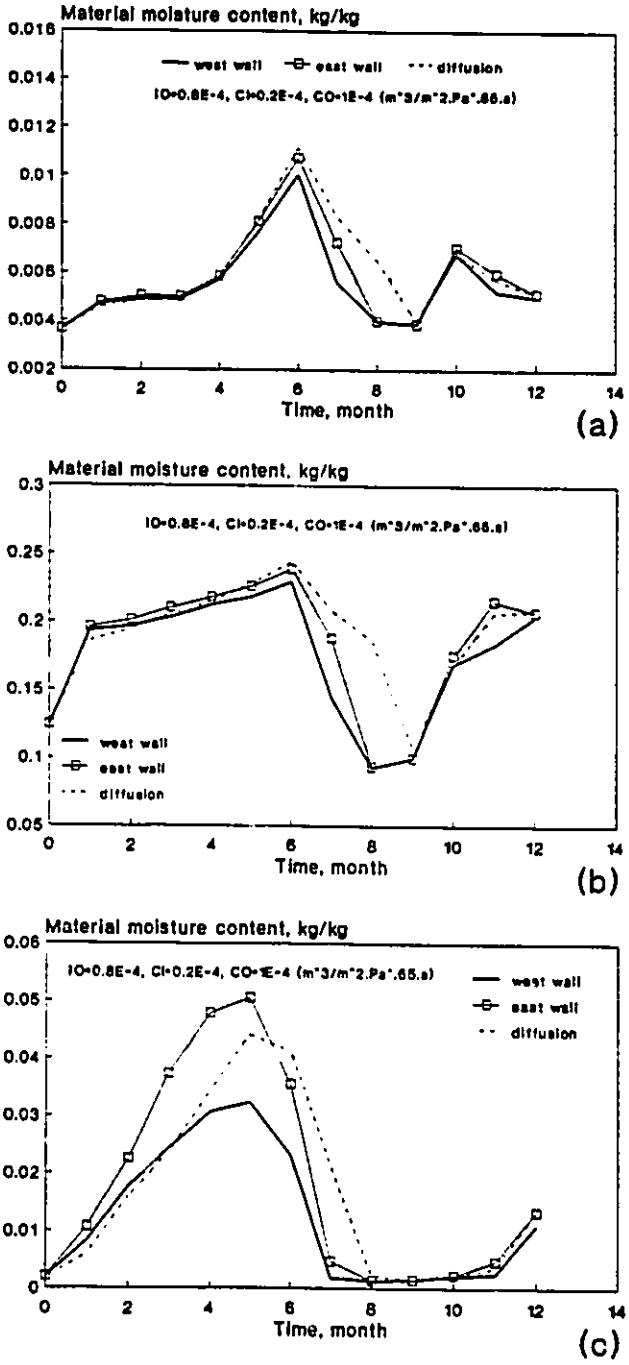

Fig. 7.83 Variations of the average moisture content of the wall components in the presence and absence of convective moisture transfer. (a) insulation, (b) wood, (c) brick.

convective process has resulted in less moisture accumulation in the brick layer of the west wall during the late winter-early spring period, but has resulted in more moisture accumulation in the brick layer of the east wall during the same period. This behaviour is an indication of the prevalence of the air inflow at the west wall and the air outflow at the east wall. In this case, moisture accumulation within the west wall, especially within its brick layer, will be more dependent on the air flow process through the interior wythe. Elimination of the air flow through the interior wythe of the west wall has resulted in a considerable reduction in the moisture accumulation in all layers as shown in Fig. 7.84. Moisture accumulation in the east wall, on the other hand, is less dependent on the air flow process through the inner wythe. Fig. 7.85 compares the moisture behaviour of the three layers of the east wall in the presence and the absence of air flow through the inner wythe. It can be seen that eliminating the air flow process through the inner wythe has also resulted in a reduced moisture accumulation in all layers. However, the resulting reduction in the east wall is proportionally less than that in the west wall since a good part of the accumulated moisture in the east wall is a by-product of the diffusion process.

The air leakage characteristics of the inner and the outer wythes of the wall system can affect its moisture performance by influencing the indoor air humidity behaviour and the degree of interaction between the wall and its surroundings. Fig. 7.86 illustrates the impact of increasing the air leakage coefficient of the inner wythe of the west wall by 100%. Increasing air flow through the inner wythe of the west wall has resulted in a decreased moisture accumulation for all layers during the late winter and early spring periods. The decrease in moisture accumulation is a result of increased air flow through the outer wythe which is necessary to balance the increased air flow through the inner wythe. Increasing the air leakage of the inner wythe of the east wall has resulted in a reduced moisture

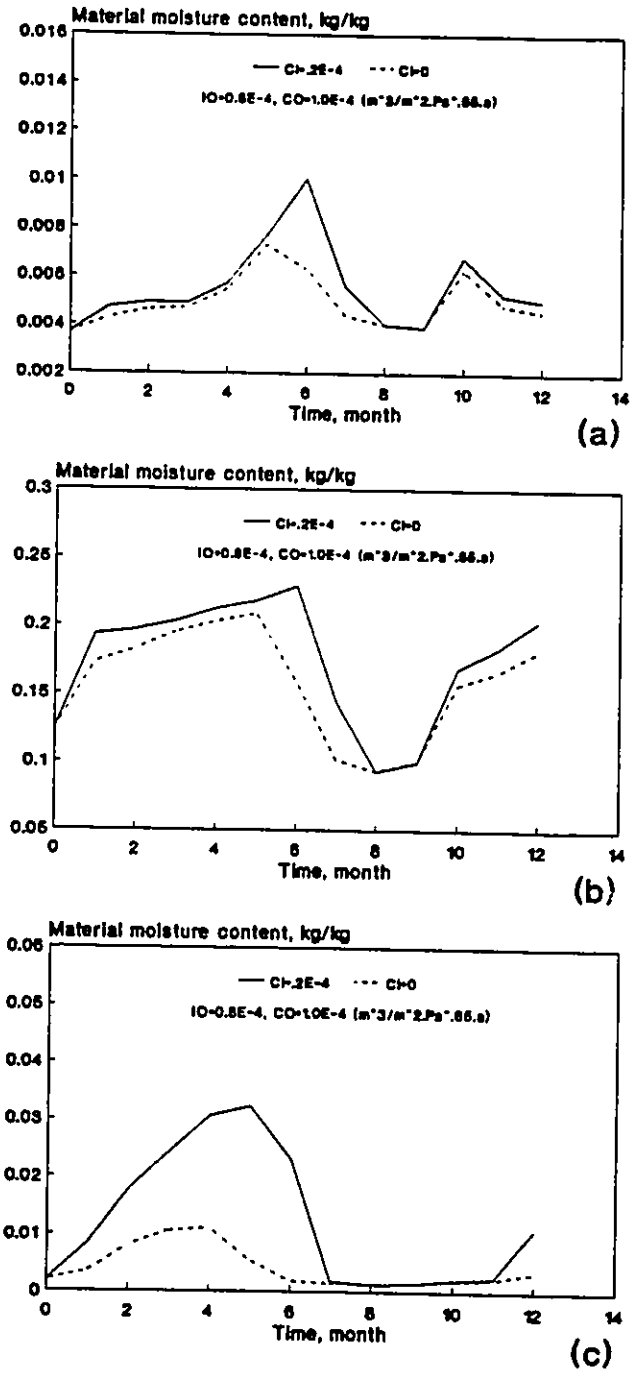

Fig. 7.84 Variation of average moisture content of west wall components in the presence and absence of air flow across the inner wythe. (a) insulation, (b) wood, (c) brick.

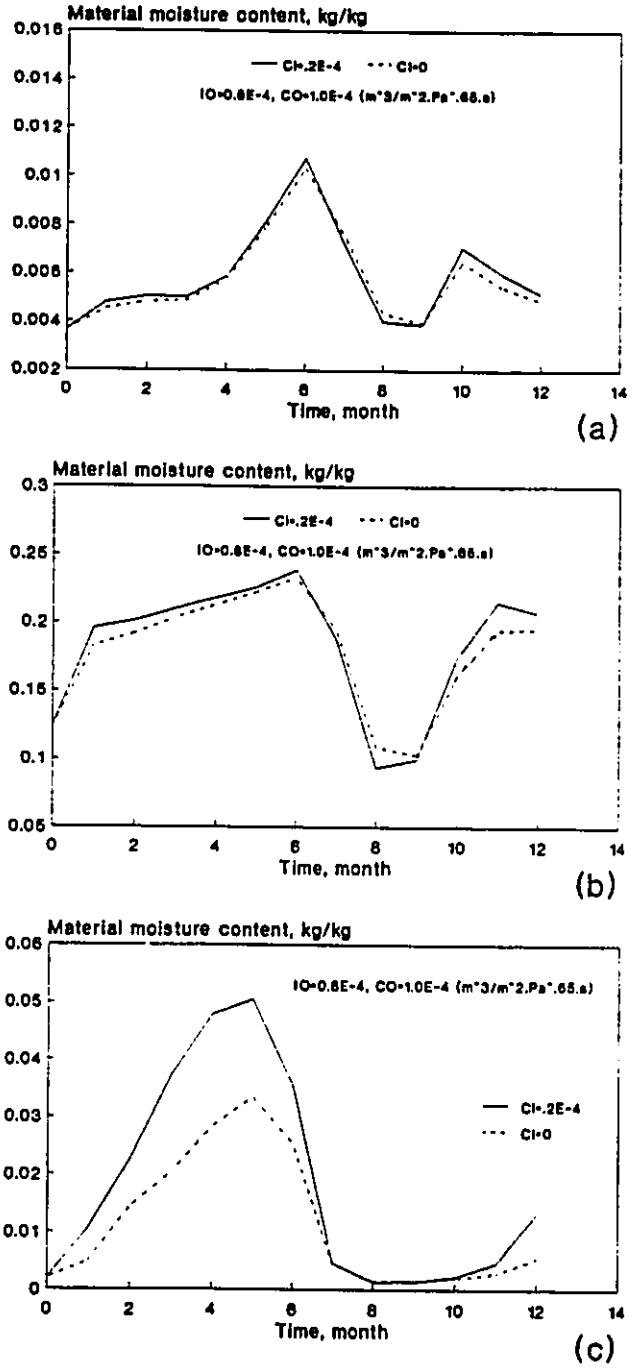

Fig. 7.85 Variations of average moisture content of east wall components in the presence and absence of air flow across the inner wythe. (a) insulation, (b) wood, (c) brick.

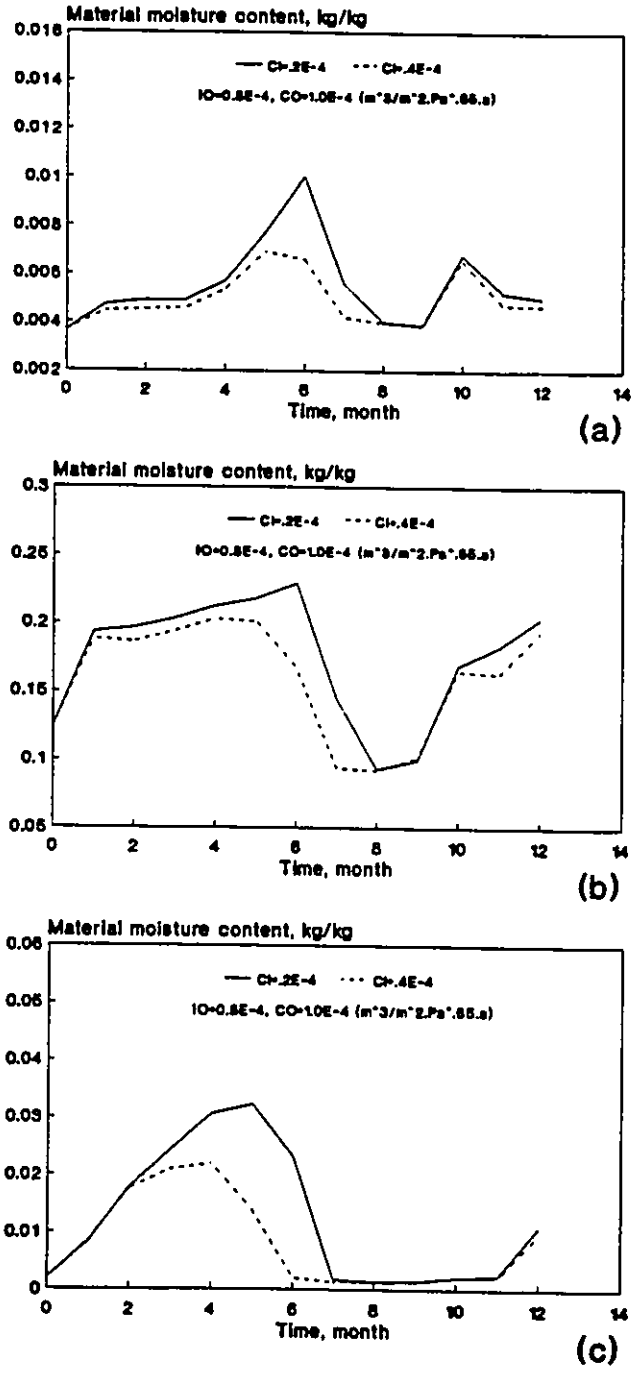

Fig. 7.86 Effect of inner wythe air leakage characteristics on the variations of the average moisture content of the west wall components. (a) insulation, (b) wood, (c) brick.

accumulation in the insulation and the wood layers, but has noticeably increased the moisture accumulation within the brick layer as shown in Fig. 7.87. The decrease in the insulation and the wood layers moisture accumulation is due to the reduced indoor humidity level which is a natural consequence of the increased air leakage rates through the inner wythe. In spite of the reduced indoor humidity level, the increase in air flow through the inner wythe of the east wall has resulted in a net increase in the brick layer moisture content during the winter months. Increasing the air flow through the outer wythe has generally resulted in less moisture accumulation in all layers for both the west wall as shown in Fig. 7.88, and the east wall as shown in Fig. 7.89. The most important modification in the moisture behaviour of both walls is the substantial increase in their drying potential which can be more clearly noticed during the fifth month in the brick layer of both walls. This change in behaviour is due to the reduced indoor air humidity level resulting from the increased air leakage rate through the exterior walls, as well as the increased air change rate within the cavity space which resulted in drier cavity air conditions.

7.5 Influence of Building Characteristics on Moisture Accumulation within Exterior Wall Components

Moisture Accumulation within the exterior wall components is dependent on the building physical and functional characteristics which directly or indirectly contribute to the moisture balance within the space. Through their influence on indoor air humidity behaviour, building physical characteristics, such as the air leakage coefficient of the exterior walls and functional characteristics, such as the rate of indoor moisture generation, can result in significant variations in the pattern and the amount of moisture accumulation in the wall components. The impact of a particular building physical characteristics on the wall

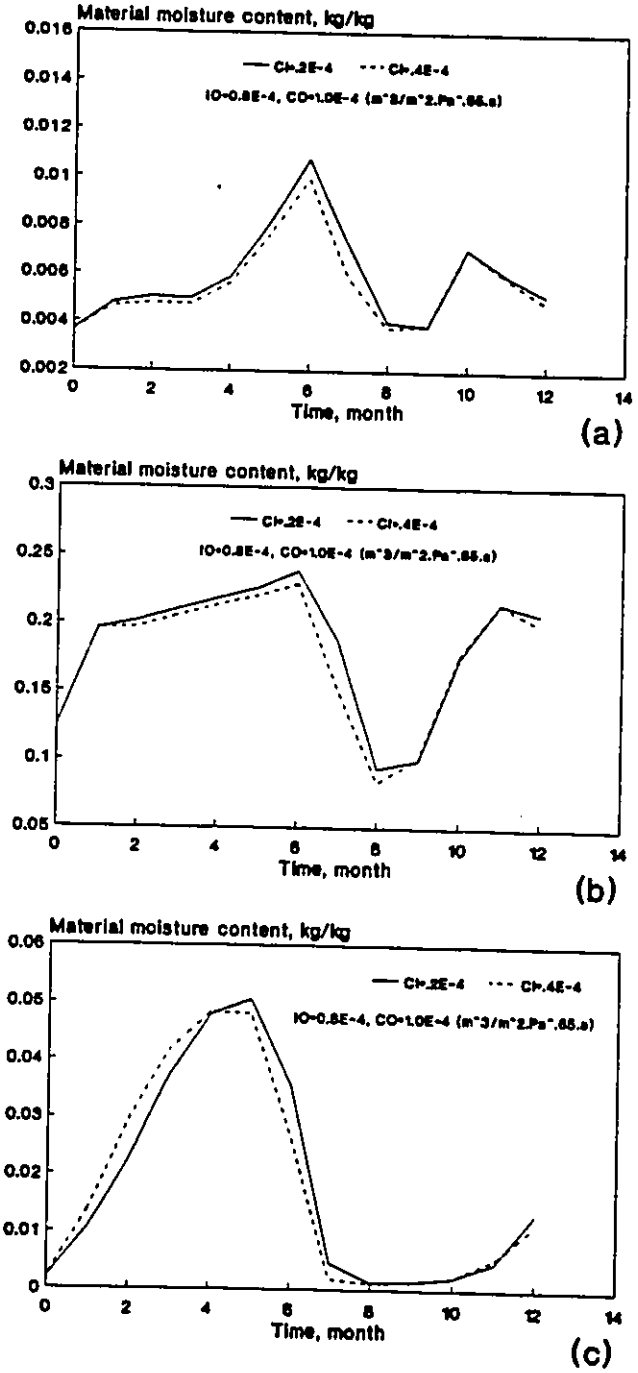

Fig. 7.87 Effect of inner wythe air leakage characteristics on the variations of the average moisture content of the east wall components. (a) insulation, (b) wood, (c) brick.

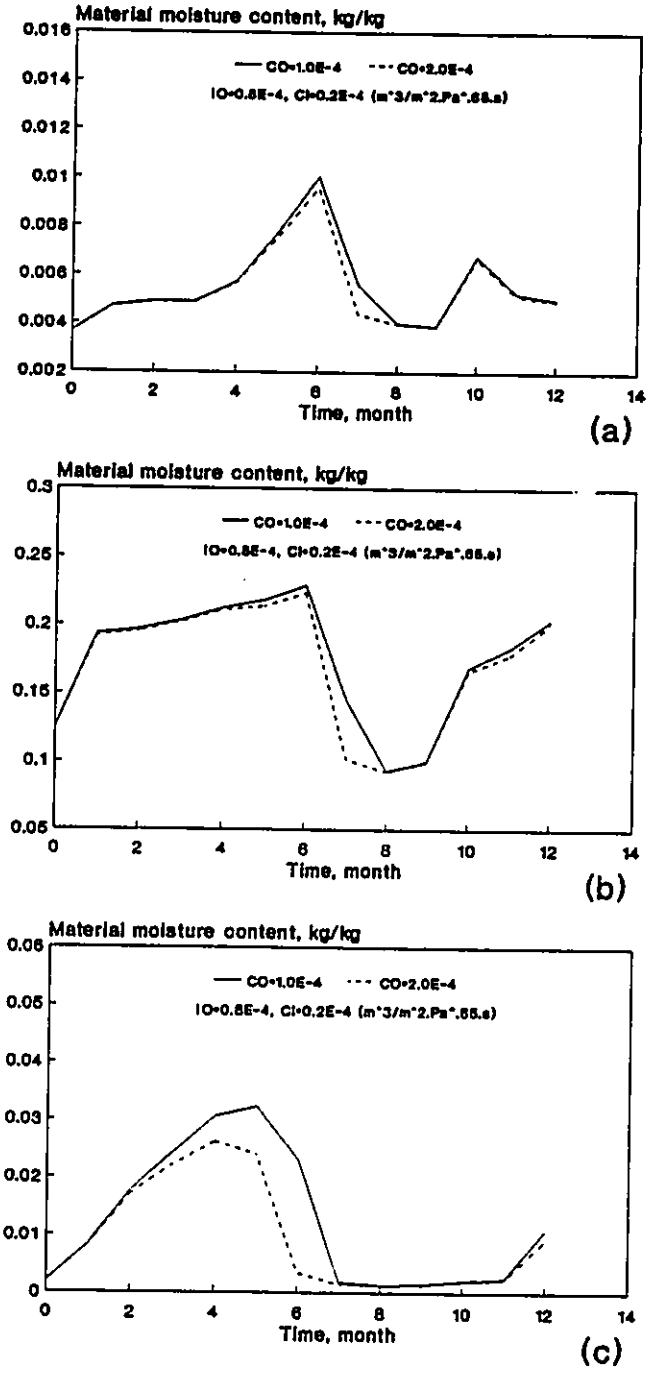

Fig. 7.88 Effect of outer wythe air leakage characteristics on the variations of the average moisture content of the west wall components. (a) insulation, (b) wood, (c) brick.

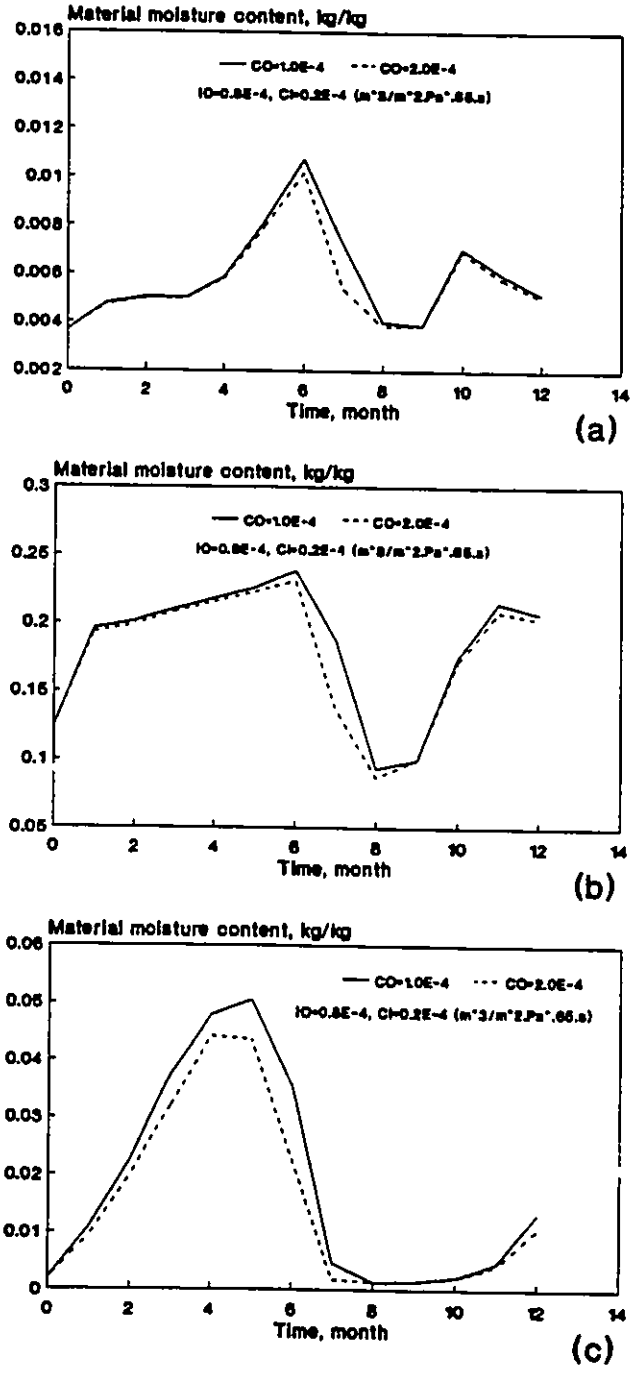

Fig. 7.89 Effect of outer wythe air leakage characteristics on the variations of the average moisture content of the east wall components. (a) insulation, (b) wood, (c) brick.

moisture behaviour is dependent on the contribution of the corresponding moisture transport process in determining the level and behaviour of indoor humidity. The contribution of a given process can be either enhanced or reduced by the presence of other moisture transport processes. For example, the presence of indoor moisture generation increases the risk of surface condensation and hence its role in determining indoor air humidity behaviour. On the other hand, the air leakage process can result in the reduction or even the elimination of the surface condensation process. The impact of the building physical characteristics on the wall moisture performance is also dependent on the moisture characteristics of the wall system and how it interacts with the indoor environment. Non-continuous moisture transport processes, such as surface condensation, are more dependent on the type and degree of moisture interaction, hence the presence of a fast mode of moisture transfer is likely to enhance the wall moisture response to the surface condensation process. In order to better appreciate the impact of the building physical and functional characteristics on wall moisture behaviour, a parametric study on the exterior wall air leakage coefficient, area of condensation surface, area of interior absorbing material as well as the rate of indoor moisture generation is carried out for the two different types of exterior walls described earlier in this chapter. These walls are modelled as part of a 600 m^3 space shown in Fig. 7.7, which is maintained at 21° C. and is exposed to the same outdoor environmental conditions used earlier. For the non-cavity wall system, seasonal variations of moisture accumulation in the insulation and the wood layers will be analyzed. Similarly, seasonal variations of moisture accumulation in the insulation, the wood as well as at the interior surface of the brick layer of the cavity wall system will be investigated. Differently located walls in terms of the space are likely to have different moisture response to a particular moisture transport process. Therefore, in evaluating the impact of building characteristics on cavity wall moisture performance,

different walls will be considered.

7.5.1 Exterior walls air leakage characteristics: In the presence of indoor moisture generation, higher air leakage rate is likely to result in a lower indoor air humidity level through out the year. Therefore, increasing the exterior walls air leakage coefficient will result in less moisture accumulation within the wall components. Fig. 7.90 shows the effect of the exterior wall air leakage characteristics on the seasonal moisture accumulation in the insulation layer of the non-cavity wall. It can be seen that for this layer, the air leakage coefficient has a significant impact on the moisture accumulation during spring while it has little or no effect during other seasons. During winter and fall months, larger temperature gradient across the insulation layer causes moisture to be transported and deposited near the wood layer exterior surface. In summer, indoor air humidity behaviour is mainly determined by the dehumidification process, hence increasing the air leakage coefficient will have almost no effect on moisture accumulation during summer. Variations in moisture accumulation during spring in response to increasing air leakage coefficient of exterior walls follow an exponential decay pattern with more than 60% reduction in moisture accumulation when the air leakage coefficient is increased from $0.5 \cdot 10^{-4}$ to $3.0 \cdot 10^{-4}$ $m^3/m^2 \cdot Pa^{.65} \cdot s$. Moisture accumulation in the wood layer is much more responsive than the insulation layer to changes in wall air leakage characteristics. Fig. 7.91 illustrates the seasonal variations in the wood layer average moisture content as a function of the wall air leakage coefficient. The largest change in material moisture content which is indicated by the slope of the moisture accumulation curve occurs within a narrow range of the air leakage coefficient. More than 25% less moisture has accumulated within the wood layer during winter when the air leakage coefficient is increased from $0.5 \cdot 10^{-4}$ to $0.8 \cdot 10^{-4}$ $m^3/m^2 \cdot Pa^{.65} \cdot s$. On the other hand, almost no change occurs in the material moisture

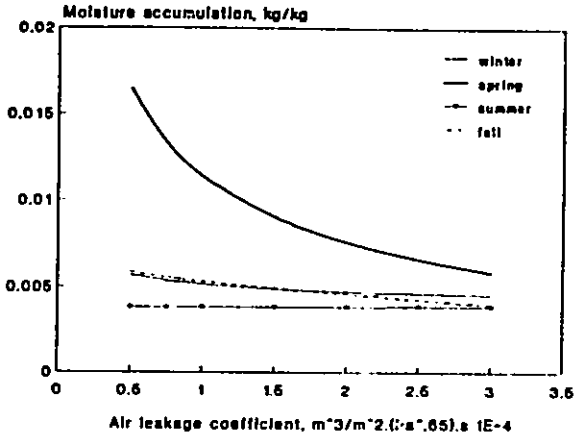

Fig.7.90 Effect of exterior wall air leakage characteristics on seasonal moisture accumulation in the insulation layer.

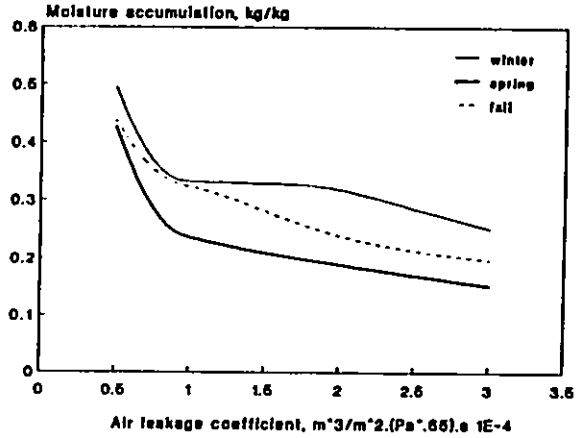

Fig.7.91 Effect of exterior wall air leakage characteristics on seasonal moisture accumulation in the wood layer.

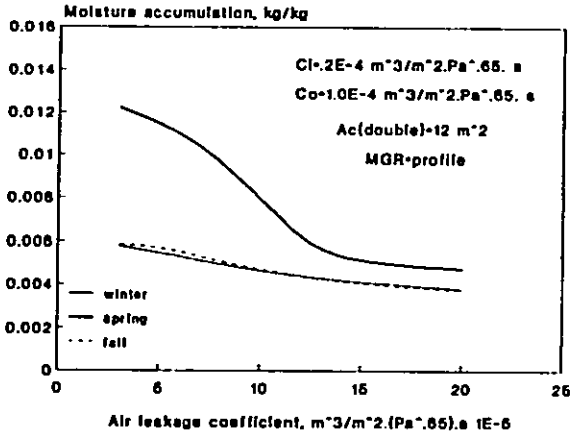

Fig.7.92 Effect of exterior wall air leakage characteristics on seasonal moisture accumulation in the insulation layer of the west wall.

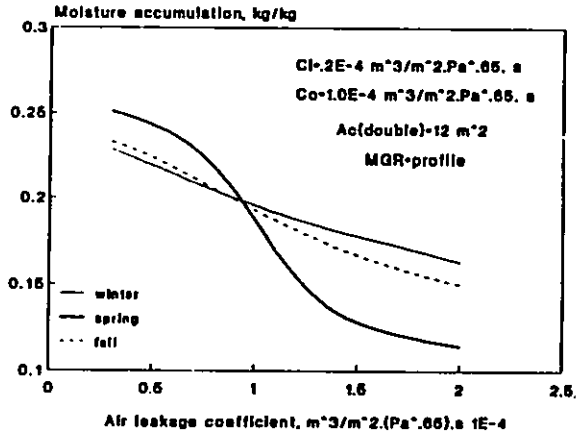

Fig.7.93 Effect of exterior wall air leakage characteristics on seasonal moisture accumulation in the wood layer of the west wall.

content as the air leakage coefficient is increased until it reaches a value of 2.0 10^{-4} $m^3/m^2 \cdot Pa^{.65} \cdot s$ beyond which the material moisture content starts to respond. Such behaviour of the moisture accumulation curve is a result of the transition in the occurrence of interstitial condensation within the wood layer. Similar, but less pronounced, moisture response due to wall air leakage characteristics is experienced by the wood layer during the fall period. During spring, which is mainly a drying period for the wood layer, the moisture content of the material is always less than that corresponding to the winter period. The difference between the winter and spring moisture accumulation curves represents the amount of moisture that has dried out of the material during the spring period which seems to get larger as the air leakage coefficient increases. This means that in the presence of indoor moisture generation, higher air leakage rate will result in an increased moisture drying rate during the spring period.

The impact of the exterior wall air leakage coefficient on its moisture behaviour is dependent on the type of the wall and its interaction with the indoor environment. Hence, a cavity wall system is expected to behave differently from the non-cavity wall system for the same indoor humidity conditions. Furthermore, for different moisture interaction modes, the same cavity wall system will respond differently to any changes in the air leakage characteristics of the exterior wall. In order to investigate these variations in behaviour, the impact of the air leakage characteristics on seasonal moisture accumulation in the west and the east walls will be studied. Figs. 7.92-7.94 illustrate the relationship between the wall air leakage characteristics and the seasonal moisture accumulation within its various components. It can be seen that higher air leakage coefficient will always result in a reduced material moisture content but with different degrees of influence determined mainly by the boundary conditions of the problem. Both the insulation and the wood layers

show more dependence on the air leakage characteristics during spring as compared to other seasons.On the other hand, moisture accumulation in the brick layer shows a similar degree of dependence on the air leakage characteristics for all seasons. The greatest impact on the moisture accumulation in the insulation layer occurs between an air leakage coefficient of $0.3 \cdot 10^{-4}$ to about $1.25 \cdot 10^{-4}$ $m^3/m^2 \cdot Pa^{.65} \cdot s$ beyond which no significant change in the material moisture content occurs. For the wood layer, however, the greatest response of the material moisture accumulation during the spring period occurs between an air leakage coefficient value of about $0.75 \cdot 10^{-4}$ to about $1.3 \cdot 10^{-4}$ $m^3/m^2 \cdot Pa^{.65} \cdot s$, with a relatively lower response below the lower limit and above the upper limit of this range. Variations in the slope of the moisture content curve are much less pronounced in the winter and fall periods for both layers where the material moisture content is almost linearly related with the air leakage coefficient. Seasonal moisture accumulation in the brick layer is generally more dependent on the air leakage characteristics than other layers. However, similar to the insulation and the wood layers, moisture accumulation in the spring period remains the most affected by the level of the air leakage coefficient. A sharp drop in material moisture content occurs during the spring between an air leakage coefficient value of $0.3 \cdot 10^{-4}$ and about $1.4 \cdot 10^{-4}$ $m^3/m^2 \cdot Pa^{.65} \cdot s$. More than 95% less moisture will be available in the material when the air leakage is increased from $0.3\ 10^{-4}$ (which is representing the direct air flow path) to $1.4 \cdot 10^{-4}$ $m^3/m^2 \cdot Pa^{.65} \cdot s$. A lower but still a significant reduction is obtained during other periods for the same increase in the air leakage coefficient. In the winter period, the moisture accumulation is reduced by about 70% while about 85% less moisture is accumulated in the fall period. Increasing the air leakage coefficient beyond that level will have no or little impact on the amount of moisture accumulation particularly in the spring and the fall months.

The relationship between moisture accumulation in the east wall components and the air leakage coefficient of the exterior walls is expected to be different from that corresponding to the west wall. Figs. 7.95-7.97 illustrate the impact of the air leakage characteristics on the seasonal moisture accumulation in the insulation, the wood and the brick layers of the east wall. The insulation layer being the least dependent on the cavity moisture conditions shows very little difference from the west wall component. On the other hand, the wood and the brick layer being directly influenced by the cavity conditions show different response to variations in the air leakage coefficient. The most noticeable change occurs in the wood layer during the spring period. Comparison between Fig. 7.93 and Fig. 7.96 shows that while the wood layer of the west wall experiences the greatest change in its moisture conditions within the air leakage coefficient range from $0.75 \cdot 10^{-4}$ to $1.3\ 10^{-4}$ $m^3/m^2 \cdot Pa^{.65} \cdot s$, the wood layer of the east wall shows little response within the same range. Instead, it is most responsive when the air leakage coefficient is higher than $1.5 \cdot 10^{-4}$ $m^3/m^2 \cdot Pa^{.65} \cdot s$, which is the range within which the wood layer of the west wall shows very little response. During the fall and winter periods, no major differences occur between the insulation and the wood layers in the two walls. The brick layer, however, exhibit greater seasonal variations in the relationship between moisture accumulation and the air leakage coefficient. This is due to the fact that moisture conditions at the brick interior surface is mainly determined by the cavity air conditions both in the drying and the wetting periods. Comparison between Fig. 7.94 and Fig. 7.97 reveals that the slope of the moisture accumulation curve of the east wall is smaller that of the west wall for the spring period, but the influencing range of the air leakage coefficient is increased. For the fall period, the slope of the moisture accumulation curve in the east wall is higher than that of the west wall particularly at low air leakage coefficient value, while it remains unaffected during winter. These variations in the seasonal moisture accumulation responses are clear

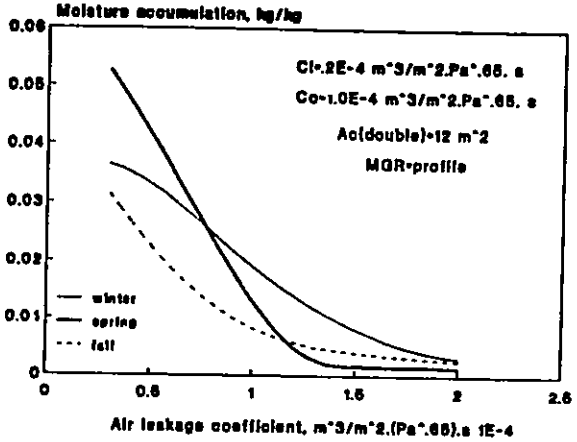

Fig.7.94 Effect of exterior wall leakage characteristics on seasonal moisture accumulation at the interior surface of the brick layer in the west wall.

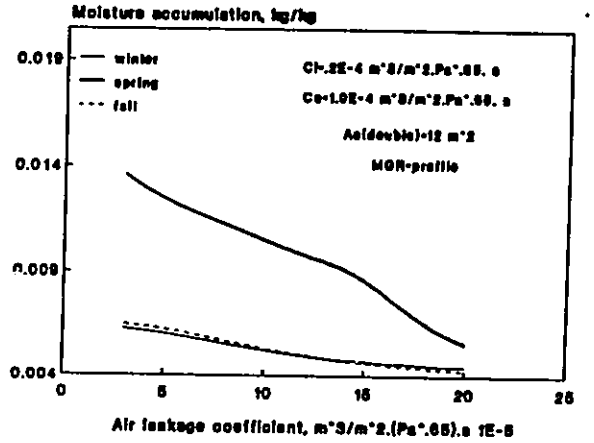

Fig. 7.95 Effect of exterior wall leakage characteristics on seasonal moisture accumulation in the insulation layer of the east wall.

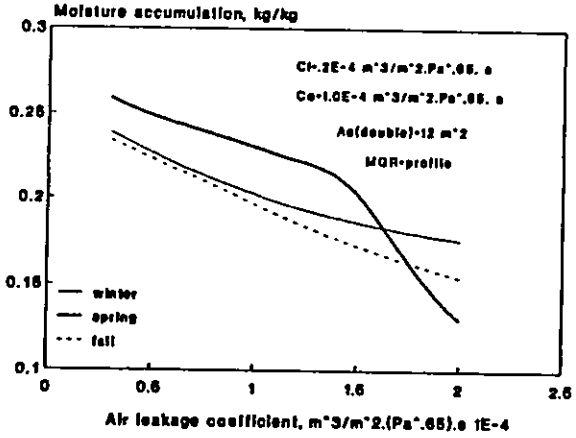

Fig. 7.96 Effect of exterior wall leakage characteristics on seasonal moisture accumulation in the wood layer of the east wall.

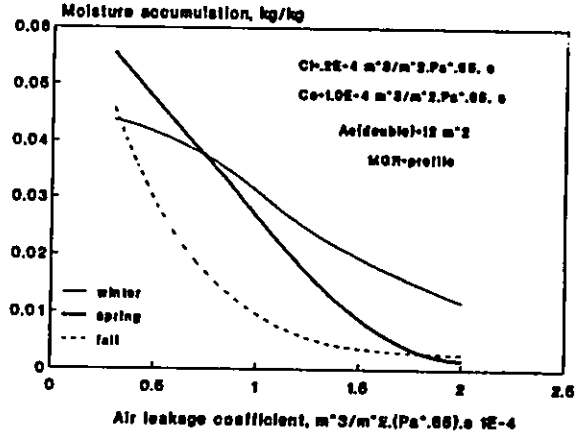

Fig. 7.97 Effect of exterior wall leakage characteristics on seasonal moisture accumulation at the interior surface of the brick layer in the east wall.

indications of the importance and the uniqueness of the influence of the interaction process between the wall system and its surrounding environments.

7.5.2 Surface area of interior absorbing/desorbing materials: Depending on their moisture hygroscopicity level, interior materials can considerably dampen the fluctuations in the level of air humidity within the space. At constant or slightly fluctuating indoor air humidity, the moisture absorption/desorption process will have no or very limited impact on indoor air humidity. On the other hand, its role will be significantly enhanced as the fluctuations in indoor humidity level increases. The pattern and the degree of fluctuations are mainly determined by the air leakage process because of the high variability level of its determining parameters (e.g., outdoor air moisture content, the air leakage rate), as well as its relatively faster mode of moisture transfer. Consequently, higher air leakage rate will result in more indoor air humidity fluctuations and hence increasing the role of the moisture absorption and desorption processes. In studying the impact of these processes on exterior wall moisture performance a relatively untight enclosure with an exterior wall air leakage coefficient of $2.0 \cdot 10^{-4}$ $m^3/m^2 \cdot Pa^{.65} \cdot s$ will be considered.

Because of its two-way impact on indoor air humidity, the accumulative effect of the absorption/desorption process on the long term exterior wall moisture performance may not be appreciable. However, its short term influence could be more pronounced following a period of continuous absorption or desorption. This influence can be further enhanced in the presence of a fast moisture transfer mechanism through the wall system. In a multi-layer non-cavity wall system, moisture can only be transferred by the diffusion process, hence the influence of the absorption/desorption process on the moisture accumulation within its components will be marginal. Figs. 7.98-7.99 illustrate the impact of the interior

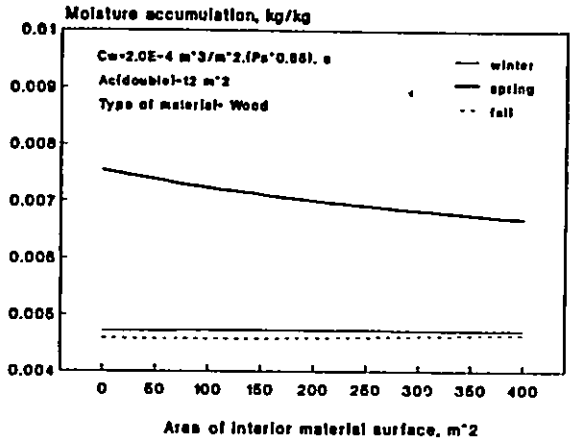

Fig. 7.98 Effect of absorbing/desorbing material surface area on seasonal moisture accumulation in the insulation layer.

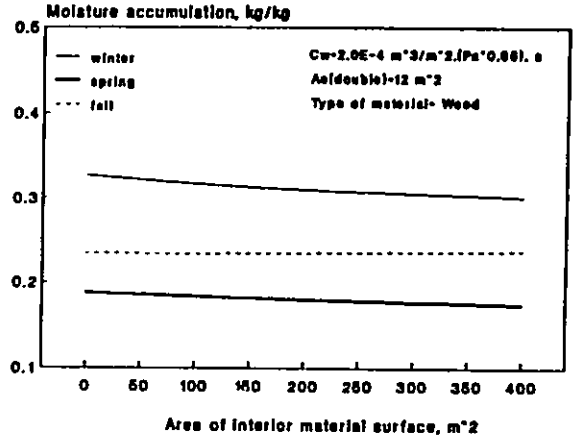

Fig. 7.99 Effect of absorbing/desorbing material surface area on seasonal moisture accumulation in the wood layer.

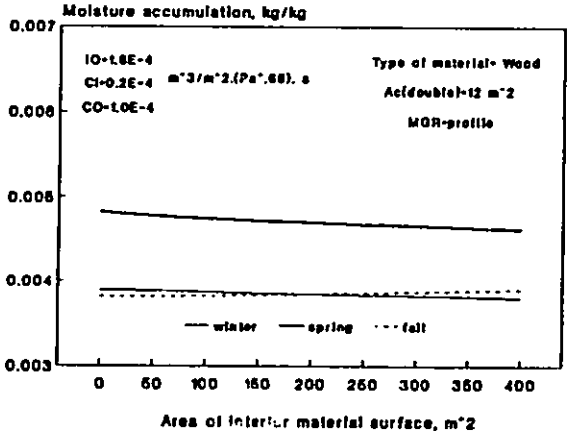

Fig. 7.100 Effect of absorbing/desorbing material surface area on seasonal moisture accumulation in the insulation layer of the west wall.

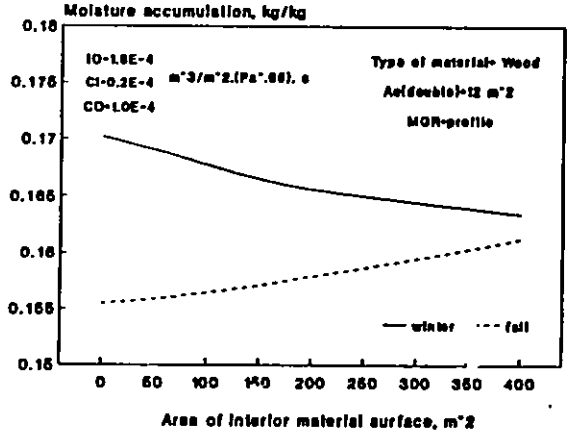

Fig. 7.101 Effect of absorbing/desorbing material surface area on seasonal moisture accumulation in the wood layer of the west wall.

absorbing material area on seasonal moisture accumulation in the insulation and the wood layers of the non-cavity wall. For the insulation layer, the most noticeable impact of the absorption/desorption process occurs during the spring period but less pronounced impact occurs for the wood layer during winter and spring periods. The presence of moisture absorbing material has resulted in a reduced moisture accumulation level for both periods indicating an overall reduction in the indoor air humidity level. In spite of the high hygroscopicity level of the absorbing material used, moisture absorption by 400 m^2 of the material surface has resulted in only 8% reduction in moisture accumulation within the wood layer during winter and about 12% reduction within the insulation layer during spring.

The influence of any moisture transport process within the space on exterior wall moisture behaviour is dependent on its role in determining the indoor humidity behaviour as well as the degree of dependence of wall moisture behaviour on indoor humidity. For example, placing a vapour retarder near the interior surface of the wall system will greatly reduce the influence of indoor air humidity. Similarly, the prevalence of inward convective moisture transfer in a cavity wall system (i.e., air flow occurs from the outdoor environment to the cavity space) will substantially decrease the role of indoor air humidity and consequently the role of any particular moisture transport process. The impact of the moisture absorption/desorption process on the seasonal moisture behaviour of the west wall components is shown in Fig. 7.100 through Fig. 7.104. It can be seen that moisture behaviour of both the insulation and the wood layers show very moderate response to the absorption/desorption process with as little as 3% change in material moisture content when 400 m^2 of absorbing material is used. Similar modest response is exhibited by the brick layer during spring, but a relatively more appreciable response is experienced during

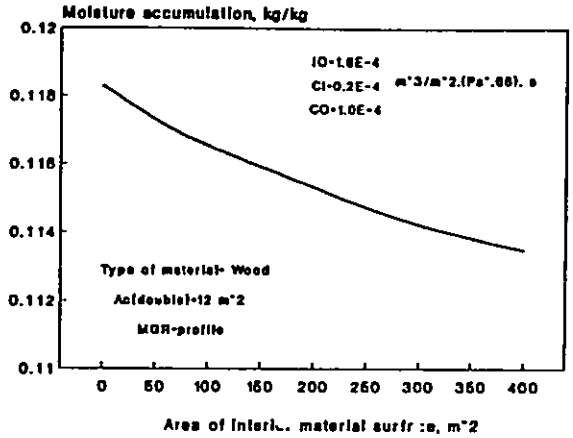

Fig. 7.102 Effect of absorbing/desorbing material surface area on moisture accumulation during spring in the wood layer of the west wall.

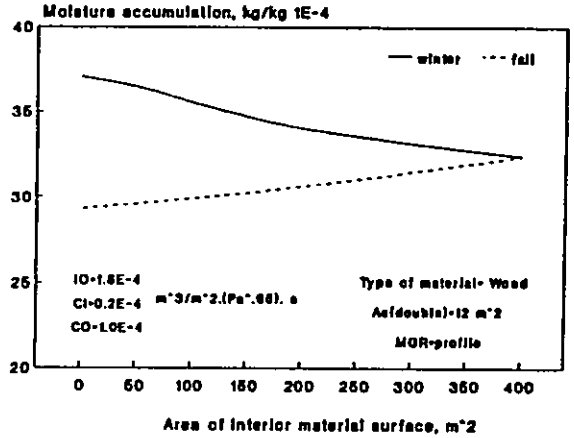

Fig. 7.103 Effect of absorbing/desorbing material surface area on seasonal moisture accumulation in the brick layer of the west wall.

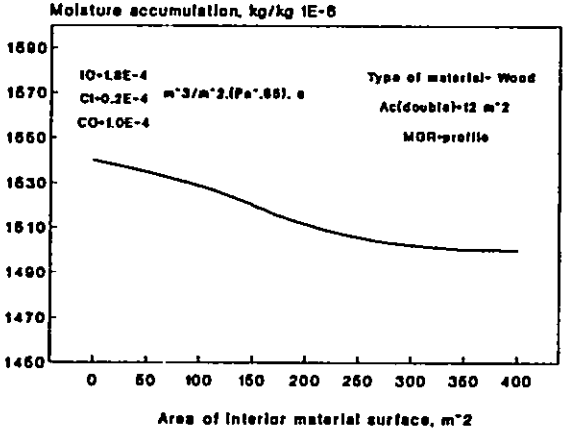

Fig. 7.104 Effect of absorbing/desorbing material surface area on moisture accumulation during spring in the brick layer of the west wall.

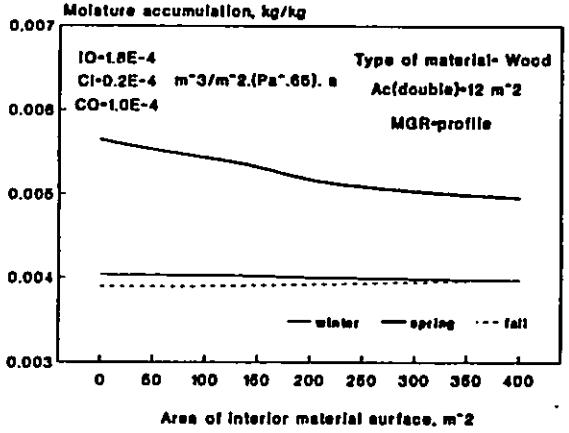

Fig. 7.105 Effect of absorbing/desorbing material surface area on seasonal moisture accumulation in the insulation layer of the east wall.

the winter and the fall periods with as much as 10% change in the material moisture content. Generally, it can be said that the impact of the absorption/desorption process on the west wall moisture behaviour is marginal which is an indication of the diminished role of indoor air humidity. An overall examination of the moisture response of the exterior wall components reveals that the moisture absorption process is the dominant during the winter and the spring pe iods, while the moisture desorption process is dominant during the fall.

The east wall has a better moisture interaction with the indoor environment, therefore, it is expected to be more responsive to variations in indoor air humidity behaviour. Variations in the seasonal moisture accumulation in the east wall components as a result of the moisture absorption/desorption process are shown in Fig. 7.105 through Fig. 7.108. As expected, comparison with the moisture behaviour of the west wall components shows that the east wall is generally more responsive. For example, while the presence of 400 m^2 surface area of absorbing material has resulted on in 4% reduction in the moisture content of the west wall insulation layer during spring, it has resulted in 12% reduction in the east wall component for the same period. The other seasonal moisture responses of the insulation layer of both walls remain essentially the same. Another major increase in the east wall response can be noticed in the moisture behaviour of the wood layer during the spring period when the reduction in moisture accumulation has increased from 3% to 14%. The brick layer of the east wall, on the other hand, shows a slightly decreased response during the winter and the fall periods, but greatly enhanced response during spring when the change in material moisture content has increased more than four folds.

For the same interior absorbing material (i.e. wood), the brick layer of the south wall

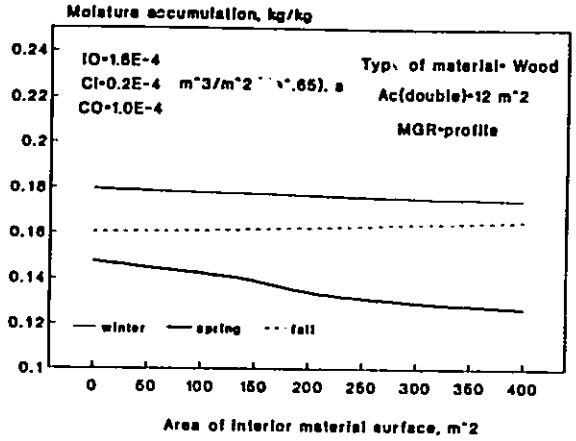

Fig. 7.106 Effect of absorbing/desorbing material surface area on seasonal moisture accumulation in the wood layer of the east wall.

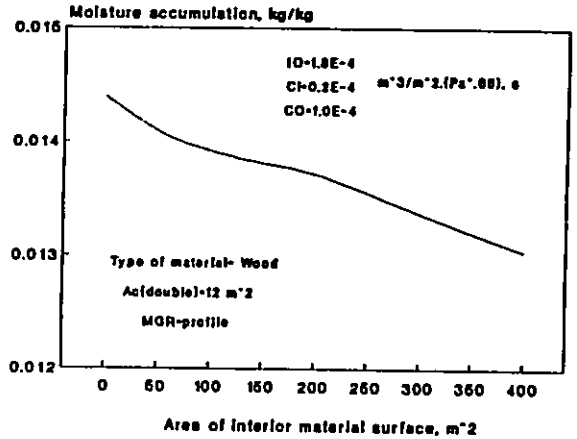

Fig. 7.107 Effect of absorbing/desorbing material surface area on seasonal moisture accumulation during winter at the interior surface of the brick layer in the east wall.

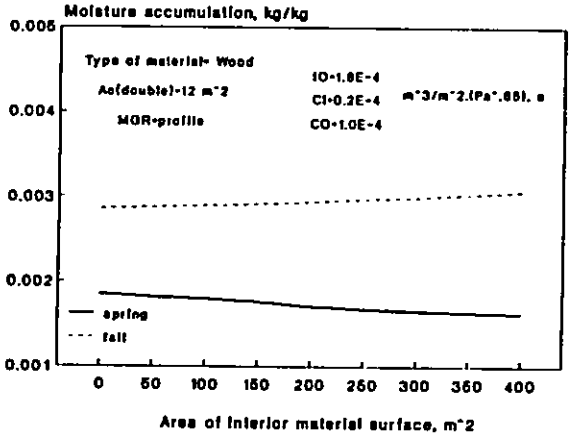

Fig. 7.108 Effect of absorbing/desorbing material surface area on seasonal moisture accumulation at the interior surface of the brick layer in the east wall.

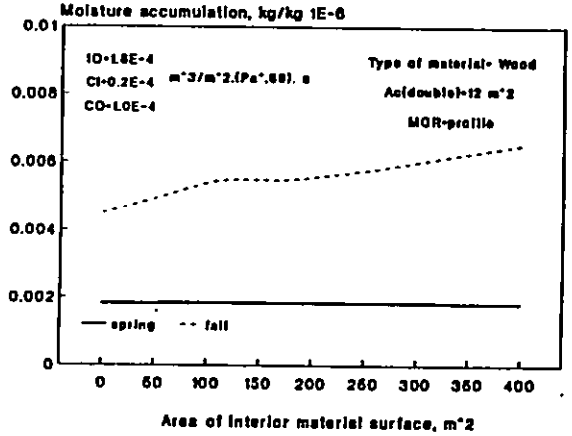

Fig. 7.109 Effect of absorbing/desorbing material surface area on seasonal moisture accumulation near the interior surface of the brick layer in the south wall.

shows more pronounced reaction to the moisture absorption process during the fall when as much as 45% less moisture has accumulated at its interior surface in the presence of 400 m^2 of absorbing material surface area as can be seen from Fig. 7.109. For the same layer, the absorption/desorption process has no or very little impact on material moisture content during spring and winter periods as shown in Figs. 7.109 to 7.110. The reduced influence for a certain period can be attributed to the balance effect of the absorption and the desorption processes over that period. Furthermore, when the material is at very high moisture content level (i.e., near saturation), as it could be the case in the winter period, the influence of indoor air humidity and hence all determining processes is greatly diminished since the material moisture content is no longer responding to fluctuations in indoor air humidity. So far, variations in the moisture behaviour of the different walls in response to the absorption/desorption process can only be attributed to the differences in their interaction with the indoor space. Nevertheless, different materials with different moisture and physical characteristics will result in a specific modification of indoor air humidity behaviour. When the resulting indoor air humidity profile is combined with a particular pattern of moisture interaction between the wall system and the indoor environment, the wall components will uniquely respond to the absorption/desorption process. Fig. 7.111 to Fig. 7.114 illustrate the impact of the absorption/desorption process on the seasonal moisture accumulation within the south wall components when the wood is replaced by the gypsum material. In this case, all layers experience a substantial increase in their moisture content during the spring period, but moderate or no change during other seasons. Both the insulation and the wood layers show no reaction during the fall and winter periods as can be seen from Figs. 7.111 to 7.112, while the brick layer experience moderate changes during winter similar to the east and west walls as shown in Fig. 7.113. Although the increase in the material moisture content is considerably

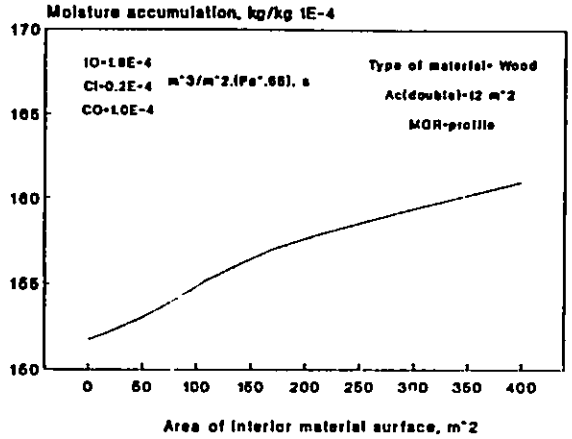

Fig. 7.110 Effect of absorbing/desorbing material surface area on seasonal moisture accumulation during winter near the interior surface of the brick layer in the south wall.

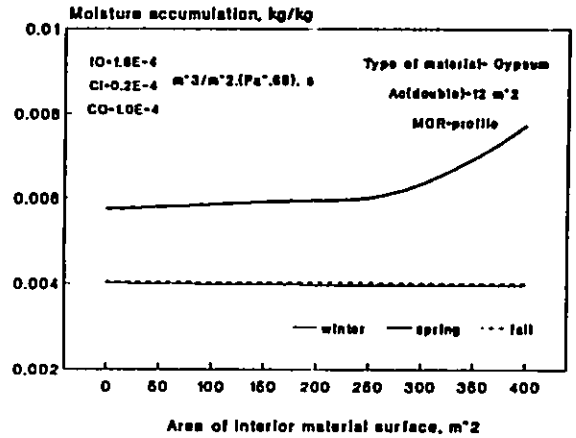

Fig. 7.111 Effect of absorbing/desorbing material surface area on seasonal moisture accumulation in the insulation layer of the south wall.

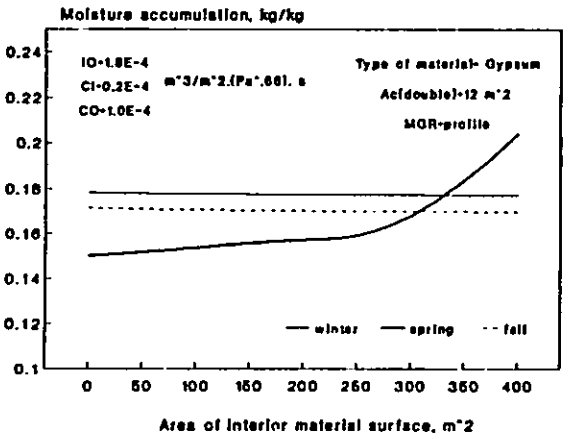

Fig. 7.112 Effect of absorbing/desorbing material surface area on seasonal moisture accumulation in the wood layer of the south wall.

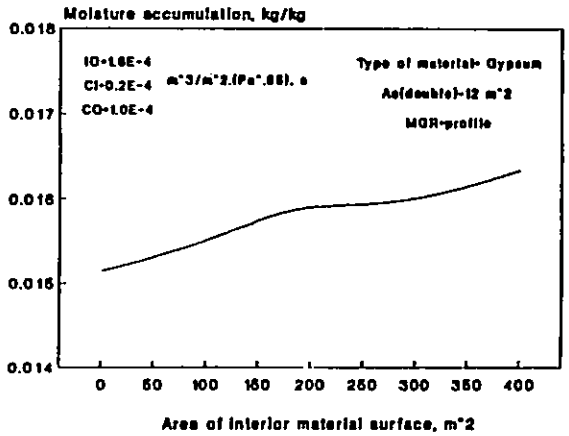

Fig. 7.113 Effect of absorbing/desorbing material surface area on seasonal moisture accumulation during winter near the interior surface of the brick layer in the south wall.

higher during the spring period, it is not consistently proportional to the area of absorbing material. The moisture accumulation curve for all layers can be seen to have very small slope when the surface area of the absorbing material is below about 250 m^2, while it is substantially larger at higher surface area. The presence of 400 m^2 of absorbing material surface area has resulted in about 35% additional moisture accumulation in the insulation and the wood layers, and has increased the moisture content at the brick layer interior surface by about three times for the same period as illustrated in Fig. 7.114. From the above discussion, it can be concluded that in spite of the low hygroscopicity level of the gypsum material, the corresponding absorption/desorption process has generally resulted in more modification in the wall moisture behaviour as compared to the wood material. This behaviour indicates the uniqueness of the wall moisture performance in response to the absorption/desorption process in the presence of the convective moisture transfer mechanism.

7.5.3 Area of condensation surface: Surface condensation process is a non-continuous process with its influence determined by the physical characteristics of the condensation surface, the outdoor conditions as well as the degree of participation of the other moisture transport processes within the space. At high air leakage rate, the indoor air is likely to be diluted and maintained at a relatively low moisture content even when indoor moisture is generated. As the air leakage rate is reduced, the potential of surface condensation as an influencing factor in determining the indoor air humidity is increased. For the modelled boundary conditions and the space characteristics, surface condensation has been found to have an appreciable influence on the wall moisture performance when an exterior wall air leakage coefficient of $0.5 \cdot 10^{-4}$ $m^3/m^2 \cdot Pa^{.65} \cdot s$, which represent a relatively tight enclosure, is used. In studying the impact of surface condensation, a double glazed

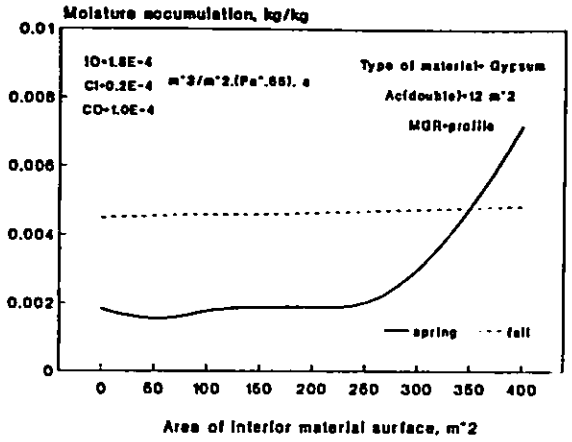

Fig. 7.114 Effect of interior material surface area on seasonal moisture accumulation near the interior surface of the brick layer in the south wall when gypsum material is used.

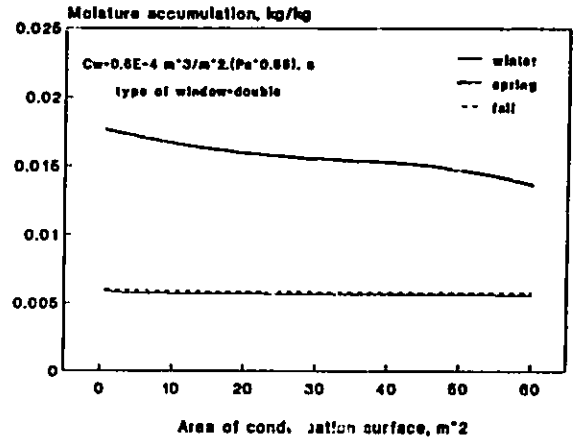

Fig. 7.115 Effect of condensation surface area on the seasonal moisture accumulation in the insulation layer.

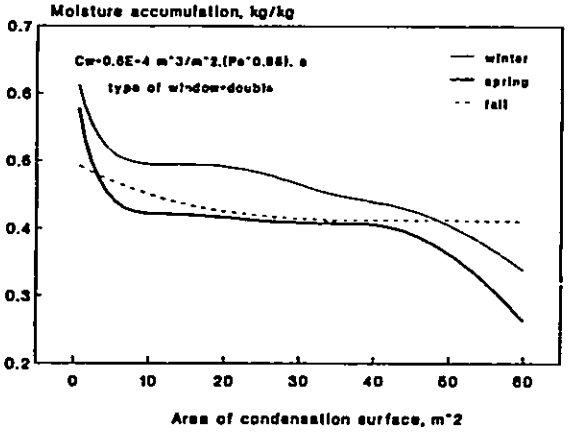

Fig. 7.116 Effect of condensation surface area on the seasonal moisture accumulation in the wood layer.

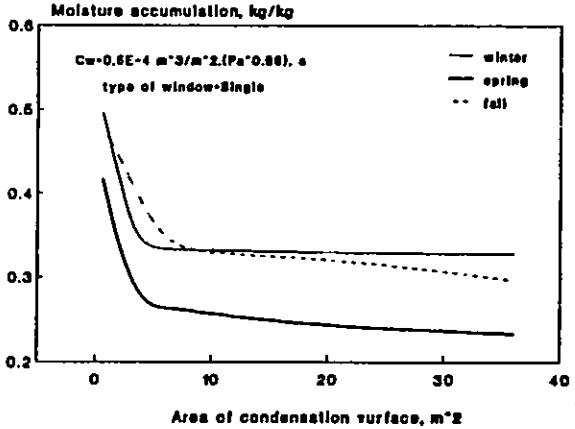

Fig. 7.117 Effect of condensation surface area of a single glazed window on the moisture accumulation in the wood layer.

window is mainly used to represent the condensation surface as part of the exterior vertical envelope of a tight enclosure.

The effectiveness of the surface condensation process in influencing indoor air humidity is a function of the area of the condensation surface as well as the boundary conditions of the condensation problem. Figs. 7.115 to 7.116 show the impact of condensation over a double glazed window on seasonal moisture accumulation within the components of the non-cavity wall system. During winter and fall periods, the condensation process has no effect on moisture accumulation in the insulation layer. However, by fully glazing the north wall (i.e., A_c=60 m^2), moisture accumulation during the spring period has been reduced by more than 20%. A much more pronounced response is shown by the wood layer since it is more dependent on indoor air humidity behaviour. The highest response occurs during winter when the material moisture content is reduced by more than 25% as a result of increasing the condensation surface area by 7 m^2. Major reductions in the wood layer moisture content occurs during winter and spring periods when the north wall is fully glazed. In this case, moisture accumulation has been reduced by more than 50% during spring and by more than 40% during winter. The least change in material moisture content occurs during the fall with only 17% reduction. Furthermore, by examining the moisture accumulation curve of the wood layer given in Fig. 7.116, it can be seen that increasing the condensation surface area from 10 m^2 to 50 m^2 has very little effect on the seasonal moisture accumulation within the material. This reduced response can be attributed to the fact that the resulting reduction in indoor air humidity is not enough to force a change in the interstitial condensation region within the layer. Increasing the condensation surface area from 50 m^2 to 60 m^2, has altered the pattern of interstitial condensation which is accompanied by major reduction in material moisture content. The influence of the

condensation surface area on moisture accumulation within the exterior wall components is dependent on the thermal characteristics of the condensation element. Fig. 7.117 illustrates the impact of surface condensation on seasonal moisture accumulation within the wood layer when a single glazed window is used. It can be seen that a significant drop in the material moisture content occurs during all seasons within a very small range of condensation surface area. However, no significant change in the material moisture content occurs over a condensation surface area of about 4 m^2 particularly during winter and spring periods. Comparison with Fig. 7.116 shows that in the case of a single glazed window, the material is generally less responsive to the condensation surface area. This is due to the considerable reduction in the moisture accumulation and the reduced potential of interstitial condensation even when a small area of a single glazed window is used.

The extent of influence of the surface condensation process varies according to the moisture characteristics of the wall system which determines the potential for moisture accumulation within its components. In spite of the presence of the convective moisture transport process, the modelled cavity wall system has less potential for moisture accumulation in the insulation and the wood layers relative to the non-cavity wall system. Consequently, moisture accumulation in these two layers will be less responsive to changes in indoor air humidity resulting from the surface condensation process. Figs. 7.118 to 7.119 illustrate the impact of the condensation surface area of a double glazed window on seasonal moisture accumulation in the insulation and the wood layers of the west wall. It is clear that the condensation surface area has a marginal effect on the moisture accumulation in both layers with a maximum reduction occurring during the spring period. When the north wall is fully glazed, about 10% less moisture is accumulated

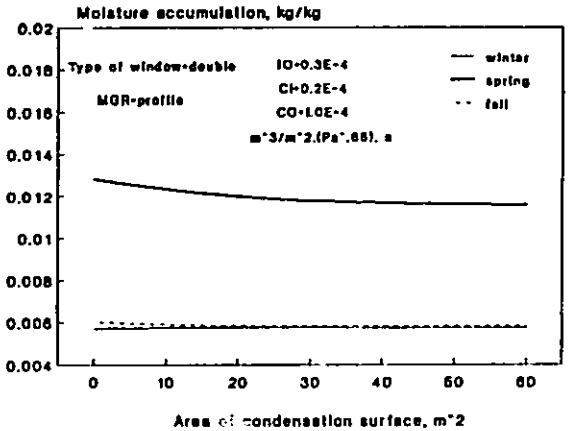

Fig. 7.118 Effect of condensation surface area on seasonal moisture accumulation in the insulation layer of the west wall.

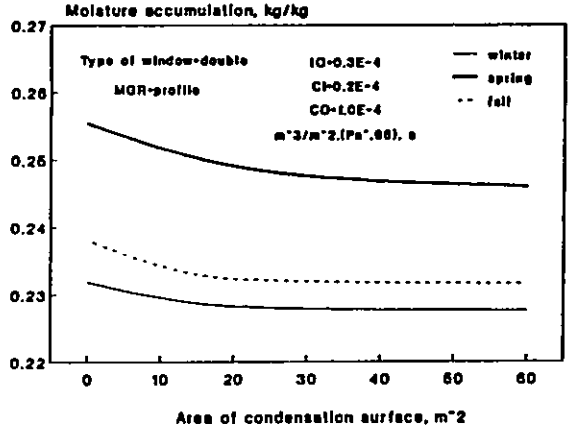

Fig. 7.119 Effect of condensation surface area on the seasonal moisture accumulation in the wood layer of the west wall.

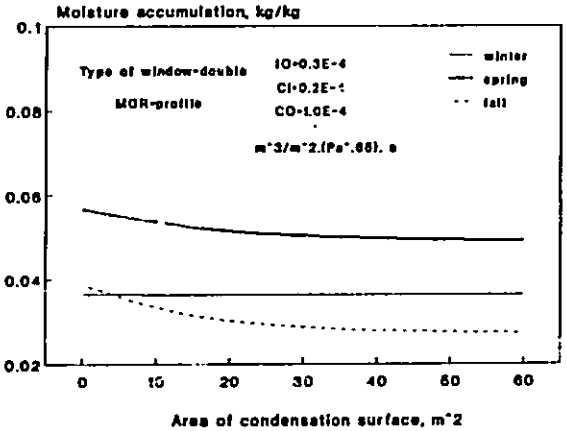

Fig. 7.120 Effect of condensation surface area on the seasonal moisture accumulation at the interior surface of the brick layer in the west wall.

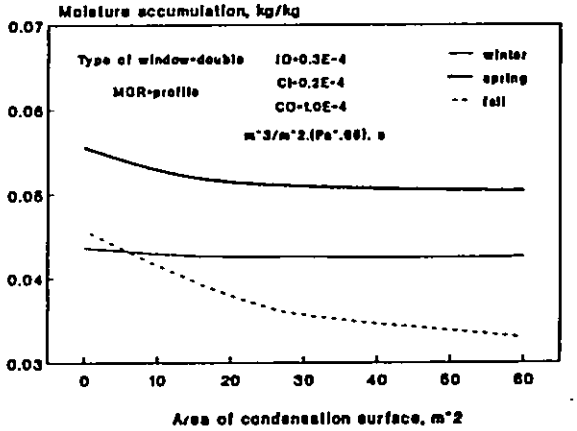

Fig. 7.121 Effect of condensation surface area on the seasonal moisture accumulation at the interior surface of the brick layer in the east wall.

in the insulation layer and only 4% less moisture is accumulated in the wood layer. This reduced response is due to relatively small moisture inertia of the inner wall as compared to the non-cavity wall system. In this case, the moisture conditions of the wall components are quickly modified in response to changes in indoor air humidity with very little accumulative effect of the surface condensation process. Similar moisture behaviour is exhibited by the inner wythe components of the east and south walls. However, because of the presence of the convective moisture transfer mode and the relatively high moisture capacity (above the hygroscopic level) of the brick material, the interior surfaces of the west, east and south walls experience a relatively considerable reaction to the condensation surface area as shown in Figs. 7.120 to 7.122. The most noticeable reduction in the moisture accumulation at the brick layer of the west and the east walls occurs during the spring and the fall periods, while the most noticeable reduction for the south wall occurs during spring. On the other hand, all layers show no response to increasing the condensation surface area during the winter period. During spring, the west and the east walls components show almost identical reaction to the surface condensation process while the brick layer of the east wall is more responsive for the same period. By fully glazing the north wall, the moisture content at the interior brick surface is reduced by 10% for both the east and the west walls during spring, but as much as 30% reduction is obtained during the fall. For the same glazing area, the brick layer of the south wall experiences about 23% reduction in its moisture content. In a percentage wise evaluation, the south wall is seen to be the least responsive to the surface condensation process, but in absolute terms, it is the most responsive with twice as much reduction for the same glazing area. Generally, these levels of reduction are obtained at smaller condensation surface area as can be detected from the corresponding Figure. However, for the purpose of comparison between the different walls, the case of fully glazed north wall is taken as

a reference. From the above discussion, it can be concluded that the influence of the condensation surface area on exterior wall moisture performance will be more appreciable through its accumulative effect since it has only a one-way impact on indoor air humidity. For the accumulative effect of the condensation process to be noticeable, the moisture inertia of the wall system has to be large enough so that moisture accumulation within its components will be a reflection of the variational pattern of indoor air humidity.

7.5.4 Indoor moisture generation rate: Indoor moisture generation represents the most important moisture transport process affecting the level and behaviour of indoor air humidity especially during winter when the outdoor air is relatively dry. The use of the daily average moisture generation rate, instead of the actual profile, has been found earlier in this study to provide sufficient accuracy when evaluating exterior walls moisture performance even in the presence of a fast moisture transfer mode. In evaluating the impact of indoor moisture generation rate on exterior wall moisture performance, a constant moisture generation rate representing the daily average value is used through out the modelled period. Figs. 7.123 to 7.124 show the effect of indoor moisture generation rate on the seasonal moisture accumulation within the insulation and the wood layers of the non-cavity wall system. As expected, the influence of indoor moisture generation on the moisture behaviour of the insulation layer is marginal during the cold periods as it is difficult for the material to attain moisture under large temperature gradients. As the temperature gradient is reduced during spring, the moisture behaviour of the insulation layer becomes more dependent on indoor air humidity and hence will be more responsive to any increase in the moisture generation rate. Below a moisture generation rate of $10 \cdot 10^{-5}$ kg/s, the moisture content of the insulation layer is almost linearly related to the rate of moisture generation with a corresponding curve slope of

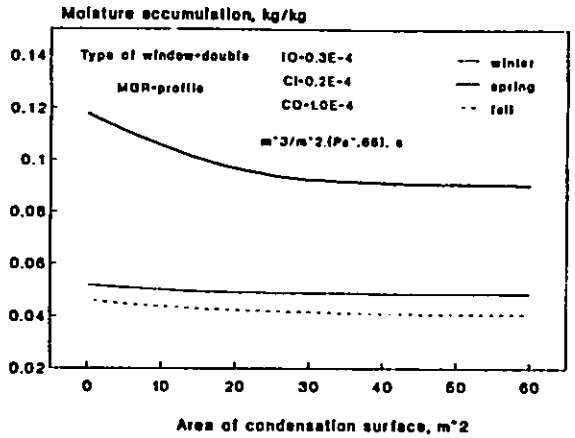

Fig. 7.122 Effect of condensation surface area on the seasonal moisture accumulation at the interior surface of the brick layer in the south wall.

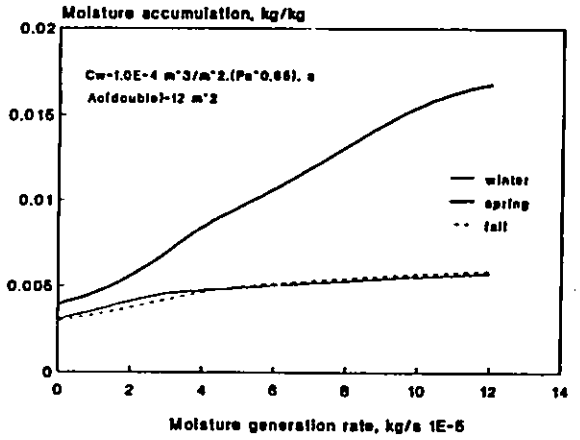

Fig. 7.123 Effect of indoor moisture generation on the seasonal moisture accumulation in the insulation layer.

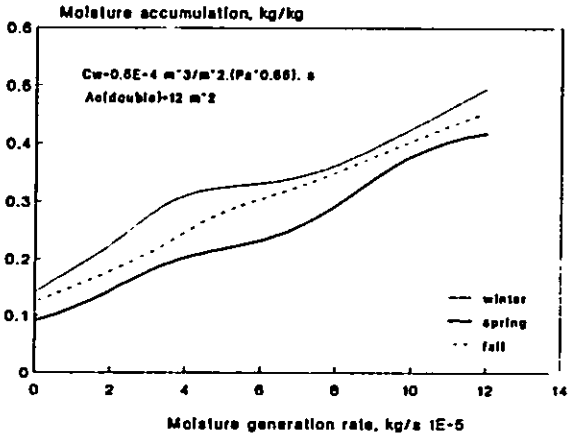

Fig. 7.124 Effect of indoor moisture generation on the seasonal moisture accumulation in the wood layer.

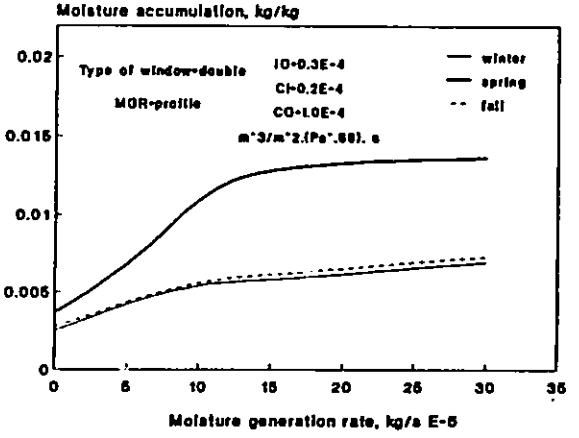

Fig. 7.125 Effect of indoor moisture generation on the seasonal moisture accumulation within the insulation layer of the west wall.

about 125 (kg/kg)/(kg/s). At higher moisture generation rate, the slope of the moisture accumulation curve is reduced since the material is no longer able to positively respond by accumulating more moisture. Such behaviour can be attributed to the fact that interstitial condensation region within the insulation layer did not advance inward form the wood layer interface, hence allowing no more moisture to be accumulated. The moisture response of the wood layer, on the other hand, is much more pronounced during all seasons. During winter the wood layer moisture accumulation curve experiences occasional changes in its slope as the moisture generation rate is increased. These changes in the slope are indications of either occurrence of interstitial condensation or that the material has reached the saturation level at a particular location. Increasing the moisture generation rate from 0 kg/s to $4 \cdot 10^{-4}$ kg/s has resulted in a constant rate of increase in the material moisture content. On the other hand, no significant change in the material moisture content occurs when the moisture generation rate is increased from $4 \cdot 10^{-5}$ to $7 \cdot 10^{-5}$ kg/s. This means that at a moisture generation rate of $4 \cdot 10^{-5}$ kg/s, the material moisture content has reached saturation at the location of condensation and increasing the rate of moisture generation to $7 \cdot 10^{-5}$ kg/s has not resulted in a significant increase in the indoor humidity level to advance the condensation region inward. By further increasing the moisture generation rate, the material experiences the original rate of increase in its moisture content indicating the advancement of the condensation region. The moisture behaviour of material during spring is similar to that during winter since the winter moisture conditions of the material represents the initial conditions for the spring period. During the fall, the moisture accumulation in the wood layer is almost linearly related to the indoor moisture generation rate with a characteristic slope of about $2.9 \cdot 10^{3}$ (kg/kg)/(kg/s). This linear relationship reflects the relative easiness of the advancement of interstitial condensation since indoor air humidity during fall is expected to be higher

than that during winter for the same moisture generation rate.

The impact of moisture generation rate on seasonal moisture accumulation within the components of the west cavity wall system is shown in Figs. 7.125 to 7.127. The insulation layer is still most responsive during the spring period with an initial linear behaviour below the moisture generation rate of $10 \cdot 10^{-5}$ kg/s. Comparison with Fig. 7.123 shows that the range of linear behaviour is almost the same as that of the non-cavity wall system, but is less responsive to changes in moisture generation rate with a characteristic slope of 83 (kg/kg)/(kg/s) as compared to 126 (kg/kg)/(kg/s) for the non-cavity wall component. Furthermore, the insulation of the cavity wall system has the same low moisture response to changes in moisture generation rate during the fall and the winter periods. The wood layer, on the other hand, is exhibiting an exponential decay behaviour in response to increased moisture generation rate with almost the same seasonal moisture accumulation patterns. The maximum moisture response occurs below the moisture generation level of $10 \cdot 10^{-5}$ kg/s with no major changes above it. Similar but more diverse seasonal moisture response is experienced at the interior surface of the brick layer as shown in Fig. 7.127. At high indoor moisture generation rate, more than 50% less moisture is accumulated during the fall and the winter period as compared to the spring period for the same indoor moisture generation rate. At low moisture generation rate (i.e., below $5 \cdot 10^{-5}$ kg/s), more moisture is accumulated during the winter period than other periods. This alternation in the amount of moisture accumulation with variations in the moisture generation rate is an indication of the uniqueness of the impact of the resulting air humidity behaviour especially because of the presence of convective moisture transfer. Variations in the material moisture content in response to increasing moisture generation rate can be generally seen to follow the S shape particularly during the spring and the fall

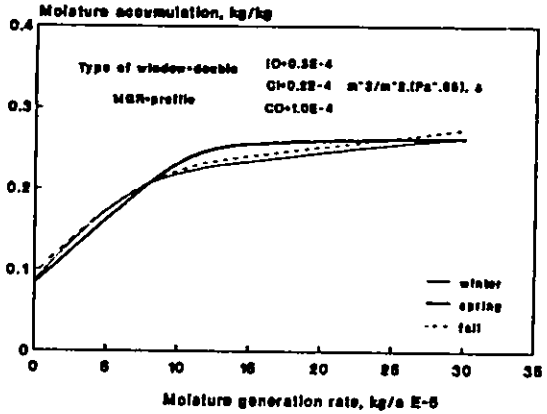

Fig. 7.126 Effect of indoor moisture generation on the seasonal moisture accumulation within the wood layer of the west wall.

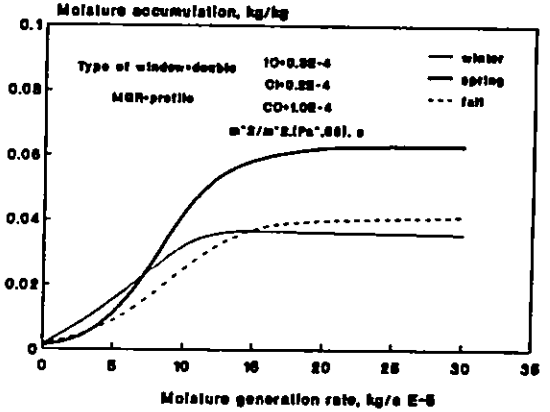

Fig. 7.127 Effect of indoor moisture generation on the seasonal moisture accumulation at the interior surface of the brick layer in the west wall.

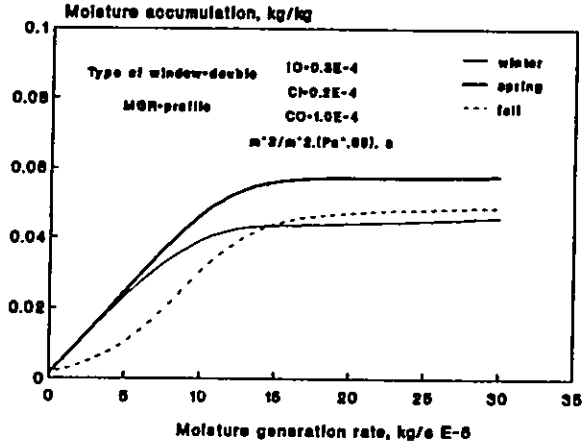

Fig. 7.128 Effect of indoor moisture generation on the seasonal moisture accumulation at the interior surface of the brick layer in the east wall.

periods. Besides variations in the magnitude and behaviour in the seasonal moisture accumulation, different seasonal responses have different critical moisture generation rate which is the level beyond which no significant change in the material moisture content occurs. For example, during the winter period, the critical moisture generation rate is about $14 \cdot 10^{-5}$ kg/s, while it is about $20 \cdot 10^{-5}$ kg/s for both the spring and the fall periods.

The insulation and the wood layers of the east wall show almost the same response to the moisture generation rate as the west wall components, while its brick layer experiences a different response both in magnitude and behaviour as can be seen from Fig. 7.128. Much less deviation in the material seasonal accumulation is obtained by an upward push to the winter and the fall periods curves and a downward push to the spring curve. For both the winter and the spring periods, relationship between the moisture accumulation and the indoor moisture generation can be seen to follow an exponential behaviour with a critical level of about $14 \cdot 10^{-5}$ kg/s, while it follows an S shape curve during the fall period with a critical moisture generation rate of about $20 \cdot 10^{-5}$ kg/s.

7.6 Summary

The impact of indoor air humidity behaviour on exterior wall moisture performance has been investigated by evaluating the mo[illegible]e behaviour of two different wall systems over a period of one year under different indoor air humidity variational patterns. The patterns of moisture accumulation within the layers of both wall systems have been found to follow the same variational trend as that of the indoor air humidity. A more complicated moisture behaviour is experienced by the cavity wall components due to the presence of the convective moisture transfer process.

The impact of the air leakage process on wall moisture performance has been examined by evaluating the wall moisture behaviour at different exterior walls air leakage characteristics. Three different air tightness levels were considered representing average, tight and loose enclosures. By increasing the exterior walls air leakage coefficient, moisture accumulation in all wall components can be substantially reduced due to reduced indoor air humidity level. The degree of reduction in the moisture accumulation within a particular component varies according to its thermal and moisture characteristics as well as the degree and type of interaction between the wall system and the indoor environment. The influence of the absorption/desorption process by interior materials on exterior walls moisture behaviour is mainly dependent on the level of fluctuation of indoor humidity, the hygroscopicity level of interior materials, and the characteristics of the wall system. In a cavity wall system, the presence of a faster mode of moisture transfer has generally enhanced the influence of the absorption/desorption process. However, its two-way impact on indoor humidity will be reflected on the moisture performance of the exterior wall by occasional increases and decreases in the moisture accumulation within the wall components. As a result, the accumulative effect of the absorption/desorption process will be marginalized.

In contrast with the absorption/desorption process, internal surface condensation on windows has a one-way effect on exterior wall moisture performance. However, since surface condensation is a non-continuous process, it will have an occasional negative impact on the level of moisture accumulation within the wall components. Generally, its impact will be more pronounced as the enclosure air tightness increases. At an average enclosure air tightness level, surface condensation over a double glazed window has very little effect on the moisture performance of both the cavity and the non-cavity wall

systems. A more appreciable reduction in the moisture accumulation at the same air tightness level can be experienced by the cavity wall system when a single glazed window is used.

Similar to the surface condensation process, indoor moisture generation has a one-way effect on the wall moisture performance. Higher indoor moisture generation rate will ultimately lead to higher indoor air humidity and consequently to more moisture accumulation. The impact of the indoor moisture generation process, at any given enclosure air tightness level, is limited to a particular range of moisture generation rate beyond which no significant change in the exterior wall moisture behaviour occurs. In the absence of indoor moisture generation, very little moisture accumulation is expected to occur during winter. Generally, the effect of indoor air humidity behaviour and the contributing moisture transport processes on wall moisture performance will be more pronounced as the moisture inertia of the exterior wall increases.

CHAPTER 8

CONCLUSIONS AND RECOMMENDATIONS FOR FUTURE STUDIES

Towards achieving the objectives of this research the following contributions and general findings are identified:

1) A practical theoretical model has been developed and validated for evaluating the rate of moisture absorption and desorption at interior materials surfaces. The model takes into account the following aspects:

   i) The diversity of the interior materials moisture behaviour has been defined using the dimensionless Biot number, which takes into account both the physical and moisture characteristics of the materials.

   ii) The alternating nature of the absorption/desorption process has been considered by incorporating the proposed model into a numerical formulation through which material moisture condition are updated at the end of each time interval used.

2) The transient behaviour of air humidity within a single space enclosure has been mathematically modelled using the mass balance concept. A linear differential equation is proposed to relate the rate of change in indoor air moisture content to the rate of moisture addition or removal from the space. As part of the modelling development, the following have been achieved:

i) Moisture coupling between the indoor air domain and the material domain has been mathematically expressed so that the diversity of the interior materials and the possibility of solution can be accommodated.

ii) Variations of the boundary conditions of the condensation process has been modelled and numerically evaluated by solving for the condensation surface temperature under transient conditions using the finite-difference approach. The unsteady state heat transfer through a single and double glazed windows has been modelled in the presence of condensation by taking into account the latent heat released at the condensation surface.

iii) Air leakage through the exterior walls has been modelled and evaluated under transient boundary conditions by considering the variability of both thermal and wind driving potentials. The resulting non-linear equation has been solved numerically using Newton's iterative method.

iv) Based on the by-pass factor, a cooling-coil dehumidification model has been suggested.

3) The mathematical developments and the suggested numerical techniques for solution have been coded into a computer program called "Single-Zone Humidity Variation Prediction Model (SHVPM)". The program has been utilized for simulating air humidity behaviour within a single zone space under different conditions.

4) Transient air humidity behaviour within a multi-zone space has been mathematically modelled via a system of coupled differential equations each representing the moisture balance in a particular zone. In addition to the developments carried out for the single space enclosure, the air leakage and the

inter-zone air flow rates, have been evaluated by incorporating the multi-cell air modelling approach. Solution of the resulting system of differential equations has been carried out numerically to evaluate the zonal air humidity response in multi-zone spaces.

5) A computer model named "Multi-Zone Humidity Variation Prediction Model (MHVPM)", has been developed to simulate zonal air humidity response under different boundary conditions and zonal physical and functional characteristics.

6) A case study has been carried out for investigating air humidity behaviour in a single space enclosure at different physical and functional characteristics. Based on hourly evaluation of indoor air humidity under transient outdoor conditions the following findings have been drawn:

   i) Indoor air humidity response to the air leakage process is mainly determined by the air infiltration rate.

   ii) At high air leakage rate, the overall indoor air humidity behaviour is determined by the air infiltration process even when other moisture transport processes are active.

   iii) In the presence of air leakage, the behaviour of indoor air humidity will generally follow the variational pattern of the outdoor air humidity conditions.

   iv) The influence of the surface condensation process is highly dependent on the air infiltration process. At average enclosure air tightness, surface condensation over a double glazed window will have a marginal impact on

indoor air humidity. On the other hand, at the same air tightness level, condensation over a single glazed window can still have a considerable impact.

v) Moisture absorption and desorption by interior materials can have significant dampening impact on indoor air humidity depending on the moisture and physical characteristics of the interior materials as well as the degree of fluctuations of air humidity.

vi) Depending on the enclosure air tightness level, the process of indoor moisture generation can have an appreciable role in defining the indoor air humidity behaviour according to the rate and the pattern of moisture generation. As a moisture source, it will always have a positive impact on the level of indoor humidity. However, at reduced air leakage rates, saturation of the indoor air can be quickly attained particularly at high moisture generation rates.

vii) When more than one moisture transport processes are active, the relative influence of a particular process is determined by its time constant, its continuity, and its interaction with other moisture transport processes.

viii) The relative influence of a particular moisture transport process on indoor air humidity behaviour is determined by the building physical and functional characteristics as well as the outdoor environmental conditions. For example, while surface condensation and indoor moisture generation processes are more active in cold climates, the air infiltration and the moisture absorption/desorption processes are likely to be more active in hot-humid climates.

ix) Prediction of indoor air humidity behaviour within buildings can significantly

help assessing the potential and the risk of surface condensation at different space physical and functional characteristics. Therefore, measures for modifying the indoor air humidity behaviour to reduce the risk of surface condensation can be identified.

x) Knowledge of indoor air humidity behaviour could also help in evaluating the humidification and the dehumidification requirements of the space over any particular period of time. By changing the space characteristics, the resulting modifications in indoor air humidity behaviour can result in a reduction in the humidification or dehumidification requirements and hence in the energy required to perform these processes.

7) A case study has been carried out for evaluating the impact of inter-zone air flow, zonal connectivity and zonal arrangement on air humidity behaviour in a multi-zone space. Based on hourly evaluation of zonal humidity responses under transient outdoor conditions the following findings have been deducted:

i) In a multi-zone space, each zone will have a unique air humidity behaviour determined by its own physical and functional characteristics as well as its interaction with the outdoor environment and other zones.

ii) At average enclosure air tightness, the air leakage process can have a significant impact on zonal air humidity behaviour particularly in zones which are located upstream relative to the air flow paths (i.e., the paths between the infiltrating and the exfiltrating air). Similar, but reduced response is obtained when enclosure air tightness increases while almost identical zonal responses are obtained at lower air tightness level.

iii) Dependent zones with only exfiltrating exterior walls are less affected by

the air leakage process.

iv) For a particular zonal arrangement, the degree of impact of the air leakage process is determined by the air leakage characteristics of the exterior walls as well as the type of inter-zonal connection. Moisture inter-dependence among different zones is generally enhanced when they are connected by large openings in the presence of air flow across the exterior boundaries.

v) Differently arranged zones within the same exterior space boundary will experience unique zonal air humidity response for the same air leakage characteristics. Such change in behaviour is a result of the varying degree and type of moisture interaction with the outdoor environment.

vi) The impact of local moisture transport processes such as surface condensation and indoor moisture generation on zonal air humidity behaviour is generally limited to the zone where they occur. However, when the source zone is located upstream in terms of the inter-zone air flow regime, local moisture transport processes could have an appreciable impact on air humidity behaviour in other dependent zones.

8) Simultaneous heat and moisture transfer in multi-layer non-cavity and cavity wall systems has been modelled under transient boundary conditions. Convective moisture transfer has been accommodated for by treating the cavity space as an intermediate layer which directly interacts with the indoor and outdoor environments.

9) The multi-cell air flow modelling approach has been utilized to evaluate the spacial

air pressures in the indoor and the cavity spaces so as to determine the air flow rate across the flow paths connecting the different spaces.

10) Moisture transfer, at all moisture content levels, has been considered by using the air moisture content and the temperature as the driving potentials in the hygroscopic range and utilizing the moisture equalization concept at higher moisture content levels.

11) Interstitial condensation occurrence criteria and finite-difference node distribution criteria for transient moisture transfer analysis have been suggested.

12) Using the implicit scheme of the finite-difference formulation technique, numerical formulations of the simultaneous heat and moisture transfer model for both the cavity and the non-cavity wall systems have been carried out.

13) Based on the above mathematical developments, a computer model called "Wall-MPM" has been developed for evaluating moisture behaviour of non-cavity and cavity multi-layer wall systems under transient boundary conditions.

14) A case study has been carried out to investigate the impact of indoor air humidity behaviour on the exterior wall moisture performance. In this case, moisture performance of a non-cavity and a cavity wall systems has been evaluated over a period of one year. Based on the evaluations and comparisons of moisture accumulation levels and distributions in the main components of both wall systems under different indoor air humidity variational patterns the following findings have

been drawn:

i) Indoor air humidity has an influential role in determining the exterior wall moisture performance. This role is greatly enhanced by the presence of a large temperature gradient across the wall system, and a fast moisture transfer mechanism.

ii) Short term and long term variations in indoor air humidity are uniquely reflected on the pattern and the level of moisture accumulation within the various wall components.

iii) In the presence of convective moisture transfer, walls with different orientation with respect to wind direction, will exhibit different moisture response to the same indoor air humidity variational pattern.

iv) The impact of a particular variational pattern of indoor air humidity on exterior wall moisture performance is largely dependent on the wall moisture characteristics as well as its interaction with the indoor environment.

v) High thermal resistance materials, such as insulation, are not likely to accumulate substantial amount of moisture in the presence of large temperature gradient which is likely to exist during the winter and fall periods.

vi) Interstitial condensation is likely to occur at the outer interface with the insulation layer when the outer adjacent layer has a relatively higher moisture resistance.

vii) In a cavity wall system, interstitial condensation is likely to occur at the interior surface of the outer wythe when convective moisture transfer takes place or when the overall moisture resistance of the inner wythe is

relatively low.

viii) Reducing the enclosure air tightness level has resulted in a decreased moisture accumulation in all components of the cavity and the non-cavity wall systems, but with variant levels of reduction determined by the variations in the outdoor air conditions and the thermal and moisture characteristics of the wall components.

ix) The maximum reduction in moisture accumulation due to decreased air tightness is obtained during winter when wall moisture behaviour is highly dependent on indoor air humidity and the air leakage process is a determining factor for the indoor air humidity behaviour.

x) As much as 100% difference in the average moisture accumulation can be obtained when the air tightness level is changed from one level to another (e.g. from low to average air tightness).

xi) Interstitial condensation and moisture contents distribution in the various components of the exterior wall can be significantly altered by changing the level of enclosure air tightness. Reducing the air tightness level can reduce or even eliminate condensation at certain locations within the wall system, and hence substantially decrease the local moisture accumulation. As much as twenty time more moisture can be locally accumulated when the air tightness level is changed from low (C_w=2.0 10^{-4} $m^3/m^2 \cdot Pa^{.65} \cdot s$) to average ($C_w$=1.0 10^{-4} $m^3/m^2 \cdot Pa^{.65} \cdot s$).

xii) Different wall systems will respond differently to changing the air tightness level depending on the wall moisture sensitivity to the resulting modification in indoor air humidity behaviour.

xiii) The influence of the absorption/desorption process on exterior wall

moisture performance is generally limited particularly when diffusion is the only moisture transfer mechanism across the wall system. However, the presence of the convective moisture transfer process together with a highly fluctuating indoor air humidity variational pattern can result in a more pronounced role for the absorption/desorption process.

xiv) Because of the two-way action of the absorption/desorption process, its net accumulation effect on exterior wall moisture performance is marginalized, yet occasional decreases and increases in the material moisture content occur.

xv) At average air tightness level, the surface condensation process over a double glazed window has limited occasional negative impact on the moisture accumulation within the exterior wall components.

xvi) For tight enclosures, surface condensation over a double glazed window can have an appreciable impact on the exterior wall moisture performance with more than 30% reduction in the material moisture content.

xvii) Surface condensation over a single glazed window, even in an average air tightness enclosure, can result in a substantial reduction in the moisture accumulation with more than 60% reduction in the moisture accumulation in some wall components as compared to a double glazed window with the same area

xviii) Since surface condensation process has a one-way action on indoor air humidity, its accumulative effect will be more pronounced as compared to the absorption/desorption process. Therefore, exterior walls with high moisture inertia (i.e., high potential for moisture storage) are likely to be more responsive to the surface condensation process.

xix) Indoor moisture generation will always have a positive impact on the indoor air humidity level, hence increasing the rate of moisture generation will result in more moisture accumulation. However, beyond a certain indoor moisture generation rate, determined mainly by the enclosure air tightness level, no significant additional moisture accumulation occurs.

xx) In the absence of indoor moisture generation, no significant moisture accumulation occurs in the exterior wall components during winter even when large temperature gradient exists.

xxi) When modelling the exterior wall long term moisture performance, the daily average moisture generation rate can be used with sufficient accuracy instead of the daily profile even in the presence of a fast moisture transfer mode.

xxii) When summer dehumidification is implemented, the moisture content of the exterior wall components at the end of the dehumidification period will be essentially unaffected by the physical and functional characteristics of the space.

xxiii) In the absence of summer dehumidification, the drying potential of the exterior wall will be substantially reduced leaving all wall components at higher moisture content by the end of summer.

xxiv) Depending on the mode of moisture transfer between the wall and the indoor space, implementation of summer dehumidification could result in as much as 80% reduction in the moisture accumulation by the end of summer and as much as 70% by the end of fall.

xxv) When diffusion is the only moisture transfer mechanism, implementation of scheduled dehumidification strategy (i.e., 8 hours daily) will have practically

the same impact on the exterior wall drying behaviour as the continuous dehumidification strategy. However, considerable differences between the two strategies are likely to be encountered when convective moisture transfer occurs.

xxvi) In cold climates with humid summer conditions, it is desirable to have some kind of summer dehumidification in order to sufficiently break the moisture accumulation trend within the wall components by allowing them to dry out through increasing the moisture capacity of the indoor air.

xxvii) Moisture accumulation within a non-cavity wall system components can be significantly reduced regardless of the behaviour of indoor humidity by reducing the influx of moisture into the wall by using the appropriate vapour retarder.

xxviii) Increasing the moisture outflux through the exterior surface of the wall can result in almost the same reduced level of moisture accumulation obtained by using the vapour retarder.

xxix) In a cavity wall system, moisture accumulation in the inner wythe components can be substantially reduced either by using a vapour retarder at the interior surface of the insulation layer, or by reducing the moisture resistance of the components adjacent to the insulation layer exterior surface. However, by implementing the later measure, the risk of moisture accumulation at the interior surface of the outer wythe is increased. Therefore, using a vapour retarder and reducing the convective currents from the indoor space seem to be the most effective measures.

xxx) As part of the case study, the indirect relationships between the building physical and functional characteristics and the moisture accumulation within

the exterior wall components have been investigated. This has been achieved by studying the variations of the seasonal moisture accumulation both in the cavity and the non-cavity wall components in response to varying exterior walls air leakage characteristics, type and area of interior moisture absorbing materials, type and area of condensation surface and finally, the rate of indoor moisture generation. This kind of study can serve as the base for formulating useful guidelines and recommendations to be used by the designer when evaluating the impact of building physical and functional characteristics on exterior wall moisture performance.

xxxi) Both the cavity and the non-cavity wall systems show considerable reaction to the changing air leakage characteristics of the exterior walls and the rate of indoor moisture generation, but a relatively much less pronounced reaction to the surface area of interior hygroscopic materials and the area of the condensation surface.

xxxii) The relationship between the moisture accumulation and the exterior wall air leakage coefficient can be generally described as a negative decaying trend, while the relationship with the moisture generation rate as a positive decaying trend.

xxiii) Finally, the importance of indoor air humidity behaviour in determining the exterior wall moisture performance can be recognized beyond any doubt. Therefore, for accurate assessment of exterior wall moisture performance, the transient nature of indoor air humidity must be accounted for.

As an enhancement and a continuation of the developments and findings of the present research work, the following research topics are recommended for future studies:

1) The indoor air humidity prediction model developed in this study can be further enhanced by incorporating different types of HVAC systems both in the air mass balance and the moisture mass balance models.

2) An extensive experimental program can be carried out for evaluating the moisture characteristics of interior construction and furnishing materials under transient ambient conditions. Moisture equilibrium curves and moisture diffusion coefficients are required for modelling the absorption/desorption process. However, when it is difficult to geometrically describe a particular material, a moisture time constant will be needed to describe its transient moisture behaviour.

3) Simultaneous heat and moisture transfer within the indoor air domain can be considered for better prediction of indoor air humidity behaviour when indoor air temperature is allowed to fluctuate.

4) The indoor air humidity prediction models suggested in this study can be used in conjunction with available energy evaluations models for better prediction of energy consumption.

5) Experimental evaluation of exterior wall moisture performance under transient indoor air moisture conditions needs to be carried out for different wall systems under different moisture interaction regimes with the indoor space, and compared with the theoretical predictions of this work.

6) Moisture transfer coefficients for the different building materials that could comprise

the exterior wall system are required to be experimentally evaluated under different ranges of temperatures and material moisture contents. In addition, more data about the material moisture characteristics such as the critical moisture content and the moisture equilibrium curves at different ambient temperatures are required for possible improvement in the evaluation of the moisture transport process.

7) Theoretical and experimental investigations are required for better and practical modelling approaches of the moisture transfer process at the interface between different layers of materials in a multi-layer wall system particularly at high material moisture content.

8) Further studies are needed in investigating the impact of zonal air humidity behaviour on exterior wall moisture performance at different zonal functional and physical characteristics.

9) A more comprehensive multi-dimensional model for simultaneous heat and moisture transfer through exterior walls can be developed and used in conjunction with the indoor humidity prediction and moisture interaction models for better representation of the wall system and possible enhancement of the accuracy in assessing its moisture performance.

10) Developed moisture transport models can be seen as part of a comprehensive building performance evaluation program for assessing the potential and the risk of surface condensation, humidification/dehumidification requirements as well as the quality of the indoor environment.

REFERENCES

[1] Hutcheon, N.B.,"Humidified Buildings", **Canadian Building Digest**, V. 137, No. 2, NRCC, Ottawa, Canada, 1963, pp. 42.1-42.4.

[2] Oxley, T.A.; Gobert, E.G., **Dampness in Buildings**, Page Bros Ltd., Norwich, Norfolk, 1983.

[3] Stewart, M.B.,"Annual Cycle Moisture Analysis", **Thermal Performance of the Exterior Envelopes of Buildings**, Proceedings of the ASHRAE/DOE-ORNL Conference, Orlando, Florida, 1979, pp. 887-896.

[4] Fanger, P. O., **Thermal Comfort Analysis and Applications in Environmental Engineering**, Mc-Graw Hill Book Company, 1970.

[5] Biswas, N.,"The Influence of Humidity on Thermal Comfort", **Int. Cons. Int. du Batim pour la Rech (CIB)/R12EM Symp. on Moisture Problems in Buildings**, 2nd, Programme, Rotterdam, Neth., sept. 10-12, 1974.

[6] Sterling, E.M.; Arundel; A.; Sterling, T.D.,"Criteria for Human Exposure to Humidity in Occupied Buildings", **ASHRAE Transaction**, V. 91, Part 1, 1985, pp. 611-621.

[7] Green, G.H.,"Indoor Relative Humidities in Winter and the Related Absenteeism", **ASHRAE Transaction**, V. 91, Part 1, 1985, pp.643-651.

[8] Kelly, K.M.,"Indoor Moisture Effects on Structure, Comfort, Energy, Consumption, and Health", **Thermal Performance of The Exterior Envelope of Buildings II**, Proceedings of the ASHRAE/DOE Conference, Las Vegas, Nevada, 1982, pp.1007-1032.

[9] Aslam, M.S.,"A Study of Humidity Requirements in 60 Homes", **ASHRAE Transaction**, V. 91, Part 1, 1985, pp.623-641.

[10] Hutcheon, N.B.,"Humidity in Canadian Buildings", **Canadian Building Digest**, V.137, No.2, NRCC, Ottawa, Canada, 1960, pp. 1.1-1.4.

[11] Hirning, H.J.; Vogal, L.P.; Handy, S.W.,"Energy Conservation in Homes Causes Excess Moisture Problems", **Winter Meeting of American Society of Agricultural Engineering**, Chicago, Illinois. 1982, pp. 1-8.

[12] Hanson, A.T.,"Moisture Problems in Houses' **Canadian Building Digest**, NRCC, Ottawa, Canada, 1984, CBD 231.

[13] Dfrek, J.; Croome, A.F.C., **Condensation in Buildings**, Sherratt, Applied Science Publishers Ltd., London, 1972.

[14] Gratwick, R.T., **Dampness in Buildings**, 2nd edition, John Wiley and Sons, New

York, 1974

[15] Decker, R.,"Condensation and Mould Growth in Dwellings-Parametric and Field Study", **Building and Environment**, V.19, No.4, 1984, pp. 243-250.

[16] Wilson, A.G.,"Condensation on Inside Window Surfaces", **Canadian Building Digest**, V. 137, No. 2, NRCC, Ottawa, Canada, 1973, pp. 4.1-4.4.

[17] Lombardi, C.; Aghemo, C.,"Surface Condensation and Moulds: A Case Study", **Thermal Performance of Exterior Envelopes of Buildings**, Proceedings of the ASHRAE/DOE/BTECC/CIBSE Conference IV Orlando Florida, 1989, pp. 543-555.

[18] Becker, R.; Jaegermann, C.,"The Influence of the Permeability of Materials and Absorption on Condensation in Dwellings", **Building and Environment**, V. 17, No. 2, 1982, pp.125-134.

[19] Jones, W.R.,"The Effect of an Improved Window on Condensation Potential" , **Symposium on Air Infiltration, Ventilation and Moisture Transfer**, Building Thermal Envelope Coordinating Council, FortWorth, Texas, 1986, pp.98-110.

[20] American Society of Heating Refrigeration and Air-Conditioning Engineers, **Handbook of Fundamental**, ASHRAE Inc., NEW YORK, 1981.

[21] Vos, B.H,"Internal Condensation in Structures", **Building Science**, V. 3, 1969, pp. 191-206.

[22] Davies, M.G.,"Computing the Rate of Superficial and Interstitial Condensation", **Building Science**, V. 8, 1973, pp.97-104.

[23] Shavit, G."Humidity Control and Energy Conservation", **ASHRAE Transaction**, V. 81, part 1, 1975, pp. 701-708.

[24] Miller, J.D.,"Development and Validation of a Moisture Mass Balance Model For Predicting Residential Cooling Energy Consumption", **ASHRAE Transaction**, V. 90, part 2, 1984, pp. 275-292.

[25] Martin, P.C.; Verchoor, J.D.,"Cyclical Moisture Desorption/Absorption by Building Construction and Furnishing Materials", **Symposium on Air Infiltration, Ventilation and Moisture Transfer**, Building Thermal Envelope Coordinating Council, FortWorth, Texas, 1986, pp.59-69.

[26] Fairey, P.W.; Keresteciogiue, A.A.,1985,"Dynamic Modelling of Combined Thermal and Moisture Transport in Buildings: Effect of Cooling Loads and Space Conditions", **ASHRAE Transactions**, V.91, part 2, 1985, pp.461-472.

[27] Isetti, C.;Laurenti, L.;Ponticiello, A.,"Predicting Vapour Content of Indoor Air and Latent Loads for Air-conditioned Environment: Effect of Moisture Storage Capacity of the Walls", **Energy and Buildings**, V.12, 1988, pp.141-148.

[28] Franssen, P.; Koppen, C.,"The Influence of Moisture Absorption and Desorption in Building Material on The Heating Load of Houses", Solar World Congress, **Proceedings of The 8th Biennial Congress of The International Solar Energy Society**, Perth, Aug. 1983, V.1, 1984, pp.466-470.

[29] Thomas, W.C.; Burch, D.M.,"Experimental Validation of a Mathematical Model for Predicting Water Vapour Sorption at Interior Building Surfaces", **ASHRAE Transaction**, V. 96, Part 1, 1990, pp. 487-496.

[30] Kent, D.; Handegord, O.;Robson, R.,"Study of Humidity Variations in Canadian Buildings", **ASHRAE Transactions**, V. 72, part 2, 1966, pp.1.1-1.7.

[31] Tsongas, G.A.,"The Effect of Building Air Leakage and Ventilation on Indoor Relative Humidity", **Symposium on Air Infiltration, Ventilation and Moisture Transfer**, Building Thermal Envelope Coordinating Council, FortWorth, Texas, 1986, pp. 286-291.

[32] Letherman, K.M.,"Room Air Moisture Content:Dynamic Effect of Ventilation and Vapour Generation", **Building Science Engineering Research and Technology**, V.9, No.2, 1988, pp.49-52.

[33] Achenback, P.R., "Moisture Management in Buildings", **Symposium on Air Infiltration, Ventilation and Moisture Transfer**, Building Thermal Envelope Coordinating Council, FortWorth, Texas, 1986, pp.73-81.

[34] Jennings, P.E.; Moody, T.L.,"Field Experiences Underscore the Importance of Moisture Control in Energy-Efficient Homes", **Thermal Performance of The Exterior Envelope of Buildings II**, Proceedings of the ASHRAE/DOE Conference, Las Vegas, Nevada, 1982, pp.1063-1077.

[35] Tamura, G.T.,"Measurements of Air Leakage Characteristics of House Enclosure", **ASHRAE Transaction**, V. 81, Part 1, 1975, pp. 202-211.

[36] Shaw, C.Y.; Sander, D.M; Tamura, G.T.,"Air Leakage Measurement of the Exterior Wall of Tall Buildings", **ASHRAE Transaction**, V. 79, Part 2, 1973, pp. 40-48.

[37] Liddament, M.W.,"Air Infiltration and Indoor Air Quality", **Symposium on Air Infiltration, Ventilation, and Moisture Transfer, Thermal Envelope Coordinating Council**, Fort Worth, Texas, 1986, pp.219-228.

[38] Shaw, C.Y.,"Wind And Temperature Induced Pressure Differentials and an Equivalent Pressure Difference Model for Predicting Air Infiltration in Schools", **ASHRAE Transaction**, V. 86, Part 2, 1980, pp.268-279.

[39] Janssen, J.E.; Pearman, A.N.; Hill,T.J.,"Calculating Infiltration: An Example of Handbook Models", **ASHRAE Transaction**, V. 86, Part 2, 1980, pp.751-764.

[40] Tamura, G.T.,"The Calculation of House Infiltration Rates', **ASHRAE Transaction**, V.85, Part 1, 1979, pp.58-71.

[41] Shaw, G.Y.; Tamura, G.T.,"The Calculation of Air Infiltration Rates Caused by Wind and Stack Action for Tall Buildings", **ASHRAE Transactions**, V. 83, Part 2, 1977, pp.145-158.

[42] Hutcheon, N.B.; Handegrod, G., **Building Science for Cold Climates**, NRC, John Wiley and Sons, New York, 1983.

[43] Air Infiltration Centre, **The Validation and Comparison of Mathematical Models of Air Infiltration**, Technical note AIC11, UK, 1983.

[44] Air Infiltration Centre, **The Validation and Comparison of Mathematical Models of Air Infiltration**, Technical note AIC9, UK, 1982.

[45] Swami, M.V.;Chandra, S.,"Correlation for Pressure Distribution on Buildings and Calculations of Natural-Ventilation Airflow", **ASHRAE Transactions**, V.94, Part 1, 1988, pp.243-266.

[46] Brown, W.G.;Solvason, K.R.,"Natural Convection Through Rectangular Openings in Partitions-1 Vertical Partitions", **International Journal for Heat and Mass Transfer**, V.5, 1963, pp.859-868.

[47] Brown, W.G,"Natural Convection Through Rectangular Openings in Partitions-2 Horizontal Partitions", **International Journal for Heat and Mass Transfer**, V.5, 1962, pp.869-878.

[48] Barakat, S.A.,"Inter-Zone Convective Heat Transfer in Buildings: A Review", **ASME Journal of Solar Engineering**, V.109, May, 1987, pp.71-78.

[49] Walton, G.N.,"A Computer Algorithm for Predicting Infiltration and Inter-room Airflows", **ASHRAE Transactions**, V. 90, Part 1, 1984, pp.601-610.

[50] Walton, G.A.,"Airflow and Multi-room Thermal Analysis", **ASHRAE Transactions**, V. 88, 1982, pp.78-90.

[51] Walton, G.A.,"Airflow Network Models for Element-Based Building Airflow Modelling", **ASHRAE Transactions**, V. 95, 1989, pp.611-620.

[52] Kurabuchi, T.;Kusuda, T.,"Numerical Predictions for Indoor Air Movement" , **ASHRAE Journal**, V.29, No.12, 1987, pp.26-29.

[53] Sander, D.M.; Tamura, G.T."Simulation of Air Movement in Multistorey Buildings", **Proceedings 2nd Symposium on Use of Computers for Thermal Environment Engineering**, V. 1, Paris, 1974, pp.165-171.

[54] Davies, M.G.,"Estimation of Loss of Water Vapour from an Enclosure", **Building Science**, V. 10, 1975, pp.185-188.

[55] Budaiwi, I, **Heat Gain and Loss Associated with Window's Surface Condensation**, M.Eng. Thesis, Concordia University, Montreal, Cananda, 1988.

[56] El-Diasty, R.; Budaiwi, I.,"External Condensation on Windows", **Construction and Building Materials**, V. 3, No. 3, 1989, pp.135-139.

[57] Sereda, P.J.; Hutcheon, N.B.,"Moisture Equilibrium and Migration in Building materials", American Society for Testing and Materials, **Special Technical Publication No. 385**, 1965, pp. 3-18.

[58] Quenard, D.; Sallee, H.," Water Vapour Adsorption and Transfer in Microporous Building Materials. A Network Simulation", **Building Simulation' 91 Conference Proceedings**, Nice, France, 1991, pp.31-36.

[59] Feldman, R.F.; Sereda, P.J.,"Moisture Content-its Significance and Interaction in a Porous Body", **International Symposium on Humidity and Moisture Proceedings**, Volume 4, Chapter 28, Washington, D.c., 1963, pp. 233-243.

[60] Fuzek, J.F.,"Absorption and Desorption of Water by Some Common Fibres", **Ind. Eng. Chem. Prod. Res. Dev.**, V. 24, 1985, pp. 140-144.

[61] Ahlgren, L.,"Moisture Sorption in Porous Materials", **Int. Cons. Int. du Batim pour la Rech (CIB)/R12EM Symp. on Moisture Problems in Buildings**, 2nd, Programme, Rotterdam, Neth., sept. 10-12, 1974.

[62] Harmathy, T.Z.,"Moisture Sorption of Building Materials", **Technical Paper No. 242 of the Division of Building research**, NRCC, Ottawa, 1967.

[63] Johansson, C.H.; Persson, G.,"Moisture Absorption Curves for Building Materials", National Research Council of Canada, **Technical Translation 747**, Ottawa, 1958.

[64] Kusuda, T.,"Indoor Humidity Calculations", **ASHRAE Transactions**, V. 89, part 2, 1983, pp.728-740.

[65] Kusuda, T.; Miki, M.,"Measurement of Moisture Content for Building Interior Surfaces", **Moisture and Humidity 1985: Measurement and Control in Science and Industry**, Proceedings of the 1985 International Symposium, 1985, pp. 297-311.

[66] Keresteciogiue, A.; Fairey, P.; Chandra, S.,"Algorithms to Predict Detailed Moisture Effects in Buildings", **Thermal Performance of The Exterior Envelopes of Buildings III**, Proceedings of The ASHRAE/DOE/BTECC Conference, Florida, Dec. 1985, pp. 606-619.

[67] Keresteciogiue, A.; Swami, M.; Kamel, A.,"Theoretical and Computational Investigation of Simultaneous Heat and Moisture Transfer in Buildings: 'Effective Penetration Depth Theory", **ASHRAE Transactions**, V. 96, Part 1, 1990, pp.447-454.

[68] Barringer, C.G.; McGugan, C.A.,"Development of a dynamic Model for Simulating Indoor Air Temperature And Humidity", **ASHRAE Transactions**, V.95, 1989, pp.449-460.

[69] Cunningham, M.J.,"A New Analytical Approach to the Long Term Behaviour of Moisture Concentration in Building Cavities-I. Non-Condensing Cavity", **Building and Environment**, V. 18, No. 3, 1983, pp.109-116.

[70] Cunningham, M.J.,"A New Analytical Approach to the Long Term Behaviour of Moisture Concentration in Building Cavities-II. Condensing Cavity", **Building and Environment**, V. 18, No. 3, 1983, pp.117-124.

[71] Cunningham, M.J.,"Further Analytical Study of Cavity Moisture Concentration", **Building and Environment**, V. 19, No. 1, 1984, pp.21-29.

[72] Cunningham, M.J.,"Effective Penetration Depth and Effective Resistance in Moisture Transfer", **Building and Environment**, V. 27, No. 3, 1992, pp. 379-386.

[73] Davies, M.G.,"The Environmental Temperature Procedure and Moisture Movement in an Enclosure", **Building Services Engineer**, V. 45, No. 6, 1977, pp. 83-92.

[74] Matsumoto, M; Fujihana, R.,"The Moisture Conductivity and Diffusivity of Wood for Estimation of Room Air Humidity Variation", **Int. Cons. Int. du Batim pour la Rech (CIB)/R12EM Symp. on Moisture Problems in Buildings**, 2nd, Programme, Rotterdam, Neth., sept. 10-12, 1974.

[75] Petzold, K.; Kunze, W.; Eisols, G.,"The Moisture Load of Domestic Kitchens Moisture Removal and Storage in the Structure", **Int. Cons. Int. du Batim pour la Rech (CIB)/R12EM Symp. on Moisture Problems in Buildings**, 2nd, Programme, Rotterdam, Neth., sept. 10-12, 1974.

[76] Yik, F.W.H.,"Dynamic Modelling of Indoor Air Humidity", **Building Simulation '91 conference Proceedings**, 1991, pp.42-48, Nice, France.

[77] Howell, R.H.,"Variation in Relative Humidity in a Conditioned Space Due to Coil Bypass Systems", **ASHRAE Transaction**, V. 92, part 1, 1986, pp.499-508.

[78] McQuistion, F.C.; Parker, J.D., **Heating Ventilation and Air Conditioning**, 2nd edition, John Wiley, N.Y., 1982.

[79] Shuttleworth, R., **Mechanical and Electrical Systems for Construction'**, McGraw Hill 'nc., 1983.

[80] TenWolde, A.,"A Mathematical Model for Indoor Humidity in Houses During Winter", **Symposium on Air Infiltration, Ventilation and Moisture Transfer**, Building Thermal Envelope Coordinating Council, FortWorth, Texas, 1986, pp.4-32.

[81] Spooner, D.C.,"The Practical Relevance of Mechanisms of Water Vapour Transport in Porous Building Materials", **Conference Proceedings of the Autoclaved aerated Concrete, Moisture and Properties**, Amsterdam, Netherlands, 1983. pp.27-41.

[82] Andesson, A.C., **Verification of Calculation Methods for Moisture Transport in**

Porous Building Materials, Swedish Council for Building Research, Document D6: 1985.

[83] Hall, C.,"Water Movement in Porous Building Materials-I Unsaturated Flow Theory and its Applications", **Building and Environment**, V. 12, 1977, pp. 117-125.

[84] Gummerson, R.J.; Hall, C.: Hoff, W.D.,"Water movement in porous Building Materials-II. A Sorptivity Test Procedure for Chemical Injection Damp Proofing", **Building and Environment**, V. 16, No. 3, 1981, pp.193-199.

[85] Gummerson, R.J.; Hall, C.: Hoff, W.D.,"Water movement in porous Building Materials-II. Hydraulic Suction and Sorptivity of Brick and other Masonry Materials", **Building and Environment**, V. 15, 1980, pp.101-108.

[86] Hall, C.; Hoff, W.D.; Nixon, N.R.,"Water Movement in Porous Building Materials-VI. Evaporation and Drying in Brick and Block Materials" **Building and Environment**, V. 19, No. 1, 1984, pp. 13-20.

[87] Hall, C.; Kalimeris, A.N.,"Water Movement in Porous Building Materials-V. Absorption and Shedding of Rain by Building Surfaces", **Building and Environment**, V. 17. No. 4, 1982, pp. 257-262.

[88] I'Anson, S.J.; Hoff, W.D.,"Water Movement in Porous Building Materials-VIII. Effect of Evaporative Drying on Hight of Capillary Rise Equilibrium in Walls", **Building and Environment**, V. 21, No. 3/4, 1986, pp. 195-200.

[89] Hall, E.,"Water Movement in Porous Building Materials-IV. The Initial Surface Absorption and the Sorptivity", **Building and Environment**, V. 16, No. 3, 1981, pp. 201-207.

[90] Hall, C.; Kam-Ming Tse, T.,"Water movement in Porous Building Materials-VII. The Sorptivity of Mortars", **Building and Environment**, V. 21, No. 2, 1986, pp. 113-118.

[91] Spolek, G.A.; Pircozmandi, F.,"Measurement of Unsaturated Wood Permeability by Transient Flow Methods"' **Water Vapour Transmission Through Building Materials and Systems: Mechanisms and Measurements**, ASTM STP 1039, Trechesel, H.; Bomberg, M., Eds., American Society for Testing and Materials, 1989, pp. 114-12[illegible].

[92] Cunningham, M.J.,"Modelling of Moisture Transfer in Structures-I. A Description of a Finite-Difference Nodal Model", **Building and Environment**, V. 25, No. 1, 1990, pp.55-61.

[93] Cvetkovic, M.Z.,"Water Vapour Diffusivity Measurements in Situ", **Int. Cons. Int. du Batim pour la Rech (CIB)/R12EM Symp. on Moisture Problems in Buildings**, 2nd, Programme, Rotterdam, Neth., sept. 10-12, 1974.

[94] Kumaran, M.K.,"Vapour Transport Characteristics of Mineral Fiber Insulation from

Heat Flow Meter Measurement", **Water Vapour Transmission Through Building Materials and Systems: Mechanisms and Measurements**, ASTM STP 1039, Trechesel, H.; Bomberg, M., Eds., American Society for Testing and Materials, 1989, pp. 19-27.

[95] Hansen, K.K.; Bertelsen, N.H.,"Results of a Water Vapour Transmission Round-Robin Test Using Cup Methods", **Water Vapour Transmission Through Building Materials and Systems: Mechanisms and Measurements**, ASTM STP 1039, Trechesel, H.; Bomberg, M., Eds., American Society for Testing and Materials, 1989, pp. 91-99.

[96] Pike, L.,"Review of Correlation of Infrared Detection Techniques for Water Vapour Transmission Rates (WVTR) with ASTM E 96-80 and Some approaches to Gravimetric Calibration", **Water Vapour Transmission Through Building Materials and Systems: Mechanisms and Measurements**, ASTM STP 1039, Trechesel, H.; Bomberg, M., Eds., American Society for Testing and Materials, 1989, pp. 134-138.

[97] Hoffee. A.R.,"Variability of Water Vapour Transmission Rates of Extruded Polystyrene Using ASTM E 96-80 (Desiccant Method)", **Water Vapour Transmission Through Building Materials and Systems: Mechanisms and Measurements**, ASTM STP 1039, Trechesel, H.; Bomberg, M., Eds., American Society for Testing and Materials, 1989, pp. 123-133.

[98] Hansen, K.K.,"Sorption Isotherms: A Catalog and a Data Base)", **Water Vapour Transmission Through Building Materials and Systems: Mechanisms and Measurements**, ASTM STP 1039, Trechesel, H.; Bomberg, M., Eds., American Society for Testing and Materials, 1989, pp. 28-32.

[99] Harmathy, T.Z.,"Simultaneous Moisture and Heat Transfer in Porous Systems with Particular Reference to Drying", **I& EC Fundamentals**, V. 8, No. 1, 1969, pp. 92-103.

[100] Luikov, A.V., **Heat and Mass Transfer in Capillary-Porous Bodies**, London, Pergaman Press, 1966.

[101] Luikov, A.V.,"Systems of Differential Equations of Heat and Mass Transfer in Capillary-Porous Bodies (Review), **International Journal of Heat and Mass Transfer**, V. 18, 1975, pp.1-14.

[102] Eckert, E.R.G.,"A General Analysis of Moisture Migration Caused by Temperature Differences in an Unsaturated Porous Medium", **International Journal of Heat and Mass Transfer**, V. 23, 1980, pp.1613-1623.

[103] De Vries, D.A.,"The Theory of Heat and Moisture Transfer in Porous Media Revisited", **International Journal of Heat and Mass Transfer**, V. 30, No. 7, 1987, pp. 1343-1350.

[104] Keresteciogiu, A.,"Detailed Simulation of Combined Heat and Moisture Transfer in

Building Components", **Thermal Performance of Exterior Envelopes of Buildings II** , Proceedings of the ASHRAE/DOE/BTECC/ CIBSE Conference, Orlando, Florida, 1989, pp. 477-491.

[105] Claesson, J.,"Fundamental of Moisture and Energy Flow in a Capillary-Porous Building Materials" **Energy Conservation in Heating, Cooling and Ventilating Buildings**, Volume 1, 1978, pp. 59-69.

[106] Matsumoto, M.,"Simultaneous Heat and Moisture Transfer in Porous Wall and Analysis of Internal Condensation" **Energy Conservation in Heating, Cooling and Ventilating Buildings**, Volume 1, 1978, pp. 45-58.

[107] Huang, C.L.D.; Siang, H.H.; Best, C.H.,"Heat and Moisture Transfer in Concrete Slabs", **J. Heat and Mass Transfer**, V. 22, 1979, pp. 257-266.

[108] Schwart, N.; Bomberg, M.; Kumaran, M.,"Vapour Transport Transmission and Moisture Accumulation in Polyurethane and Polyisocyanurate Foams" **Water Vapour Transmission Through Building Materials and Systems: Mechanisms and Measurements**, ASTM STP 1039, Trechesel, H.; Bomberg, M., Eds., American Society for Testing and Materials, 1989, pp. 63-72.

[109] Pierce, D.A.; Benner, S.M., 1986," Thermally Induced Hygroscopic Mass Transfer in a Fibrous Medium", **International Journal of Heat and Mass Transfer**, V. 29, No. 11, 1986, pp.1683-1693.

[110] Kumaran, M.K.; Mitalas, G.P.,"Analysis of Simultaneous Heat and Moisture Transport Through Glass Fibre Insulation", **ASME/AICHE, National Heat Transfer Conference**, Pittsburgh, PA, 1987, pp.1-6.

[111] Mitalas, G.P.; Kumaran, M.K.,"Simultaneous Heat and Moisture Transport Through Fibre Insulation, An Investigation of the Effect of Hygroscopicity", **ASME Winter Annual Meeting**, Boston, MA, 1987, pp.1-4.

[112] Kumaran, M.K.,"Moisture Transport Through Glass-Fibre Insulation in the Presence of a Thermal Gradient", **Journal of Thermal Insulation**, V. 10, 1987, pp. 243-255.

[113] Oqniewicz, Y.; Tien, C.,"Analysis of Canadian Porous Insulation", **International Journal of Heat and Mass Transfer**, V. 24, 1981, pp. 421-429.

[114] Benner, S.M.; Luu, D.V.,"The Thermal Mass-Transfer Coefficient and Equilibrium Moisture Content of Insulating Materials", **Thermal Performance of The Exterior Envelopes of Buildings II**, Proceedings of the ASHRAE/DOE Conference, Las Vagas, Nevada, 1982, pp. 1052-1062.

[115] Motakef, S.; El-Masri, M.,"Simultaneous Heat and Mass Transfer with Phase Change in Porous Slab", **International Journal of Heat and Mass Transfer**, V. 29, No. 10, 1986, pp. 1503-1512.

[116] Pierce, D.A.; Benner, S.M.,"Thermally Induced Hygroscopic Mass Transfer in a

Fibrous Medium", **J. Heat and Mass Transfer**, V. 29, 1986, pp. 1683-1694.

[117] Techsel, H.R.; Achenbach, P.R.; Ebbets, J.R.,"Effect of Exterior Air-Infiltration Barrier on Moisture Condensation and Accumulation within Insulated Frame wall Cavities', **ASHRAE Transaction**, V. 91, part 2, 1985, pp.545-559.

[118] Verschoor, J.D.,"Measurement of Water Vapour Migration and Storage in Composite Building Construction", **ASHRAE Transaction**, V. 91, part 2, 1985, pp. 390-403.

[119] Demars, Y.; Buck, Y.,"Water Vapour Diffusion Through Insulated Masonry Building Walls", **Moisture Migration in Buildings**, ASTM STP 779, M. Lieff and H.R. Trechsel, Eds., American Society for Testing and Materials, 1982, pp. 110-120.

[120] Stewert, M.B.,"An Experimental Approach to the Study of Moisture Dynamics in Walls", **Moisture Migration in Buildings**, ASTM STP 779, M. Lieff and H.R. Trechsel, Eds., American Society for Testing and Materials, 1982, pp. 92-101.

[121] Luft, F.J.,"A Study of Moisture Migration and Accumulation in Residential Stud Walls", **Thermal Performance of the Exterior Envelopes of Buildings II**, Proceedings of the ASHRAE/DOE Conference, Las Vagas, Nevada, 1982, pp. 1078-1089.

[122] TenWolde, A.; Mei, H.T.," Moisture Measurement in Walls in A Warm Humid Climate", **Thermal Performance of Exterior Envelopes of Buildings III**, Proceedings of the ASHRAE/DOE/BTECC/CIBSE Conference,Orlando, Florida, 1985, pp. 570-585.

[123] Forest, T.W.,"Moisture Transfer through Walls", **Thermal Performance of Exterior Envelopes of Buildings IV**, Proceedings of the ASHRAE/DOE/BTECC/CIBSE Conference, Orlando, Florida, 1989, pp. 532-542.

[124] Rao, K.R.,"Seasonal Variation of Moisture in Wall and Roof Sections Exposed to Natural Weather Conditions", **Int. Cons. Int. du Batim pour la Rech (C:B)/R12EM Symp. on Moisture Problems in Buildings**, 2nd, Programme, Rotterdam, Neth., sept. 10-12, 1974.

[125] Kohenen, R.,"Transient Analysis of the Thermal and Moisture Physical Behaviour of Building Constructions", **Building and Environment**, V. 19, No.1, 1984, pp. 1-11.

[126] TenWolde, A.,"The Kieper and Moist Wall Moisture Analysis Methods for Walls", **Thermal Performance of the Exterior Envelopes of Buildings II**, Proceedings of the ASHRAE/DOE Conference, Las Vagas, Nevada, 1982, pp. 1033-1051.

[127] TenWolde, A.,"Steady-State One-Dimensional Water Vapour Movement by Diffusion and Convection in a Multilayered Wall", **ASHRAE Transaction**, V. 91, 1982, pp. 322-342.

[128] Handegord, G.O.P.,"Prediction of the Moisture Performance of Walls", **ASHRAE Transaction**, V. 91, Part 2, 1985, pp. 1501-1508.

[129] Schuyler, G.; Swinton, M.; Smith, B.,"A Model of the Moisture Balance in the Outer Portion of Wood Frame Walls", **Symposium on Air Infiltration, Ventilation and Moisture Transfer**, Building Thermal Envelope Coordinating Council, FortWorth, Texas, 1986, pp.33-48.

[130] Schuyler, G.; Swinton, M.; Lankin, J.,"WALLDRY- A Computer Model that Simulates Moisture Migration Through Wood Frame Walls-Comparison to Field Data", **Thermal Performance of Exterior Envelopes of Buildings IV**, Proceedings of the ASHRAE/DOE/BTECC/CIBSE Conference, Orlando, Florida, 1989, pp. 492-505.

[131] Delsante, A.E.," A Response-Factor Method for Calculating Coupled Heat and Moisture Transfer in Buildings", **Building Simulation' 91 Conference Proceedings**, Nice, France, 1991, pp. 51-55.

[132] Spolek, G.A.; Osterhout, G.R.; Apfel, R.I.,"Transient Heat and Mass Transfer in Walls", **Thermal Performance of the Exterior Envelopes of Buildings**, Proceedings of the ASHRAE/DOE/BTECC/CIBSE Conference III, Orlando, Florida, 1985, pp. 634-647.

[133] Burch, D.M.; Thomas, W.C.; Mathene, L.R.; Licitra, B.A.; Ward, D.B.,"Transient Moisture and Heat Transfer in Multilayer Non-Isothermal Walls- Comparison of Predicted and Measured Results", **Thermal Performance of Exterior Envelopes of Buildings IV**, Proceedings of the ASHRAE/DOE/BTECC/CIBSE Conference, Orlando Florida, 1989, pp. 513-530.

[134] Spolek, G.A.," Computer Simulation of Moisture Transport in Walls of Residences", **Building Simulation' 91 Conference Proceedings**, Nice, France, 1991, pp. 37-41.

[135] Cunningham, M.J.,"The Moisture Performance of Framed Structures-A Mathematical Model", **Building and Environment**, V. 23, No. 2, 1988, pp. 123-135.

[136] Cunningham, M.J.,"Moisture Diffusion due to Periodic Moisture and Temperature Boundary Conditions-an Approximate Steady Analytical Solution with Non-Constant Diffusion Coefficients", **Building and Environment**, V. 27, No. 3, 1992, pp. 367-377.

[137] Ozisik, M.N., **Heat Conduction**, John Wiley & Sons, Inc., 1980.

[138] Brundrett, G.W., **Criteria for moisture control**, Butterworth & Co. Ltd., Great Britain, 1990

[139] Kreyszig, E., **Advanced Engineering Mathematics**, 5th edition, Wiley & Sons Inc.,New York, 1983.

[140] Duffie, J.A.; Beckman, W.A., **Solar Engineering of Thermal Processes**, John Wiley & Sons, New York, 1980.

[141] Brown, W.G.; Wilson, A.G.; Solvason, K.R.,"Heat and Moisture Flow Through Openings by Convection", **ASHRAE Journal**, V. 5, No. 9, 1963, pp. 49-54.

[142] Terry,E. Shoup, **Numerical Methods for the Personal Computer**, Prentice-Hall, Inc, New Jersy, 1983.

[143] Waters, J.R.; Wright, A.J.,"Criteria for the Distribution of Nodes in Multilayer Walls in Finite-Difference Thermal Modelling", **Building and Environment**, V. 20, No. 3, 1985, pp. 151-162.